Technische Universität München
TUM School of Medicine and Health

Functional Characterization of ACE2 Regulation in SARS-CoV-2-Infection-Associated Immune Response

Anna Erb

Vollständiger Abdruck der von der TUM School of Medicine and Health der Technischen Universität München zur Erlangung einer

Doktorin der Naturwissenschaften (Dr. rer. nat.)

genehmigten Dissertation.

Vorsitz: Prof. Percy A. Knolle

Prüfende der Dissertation:

1. Prof. Dr. Carsten Schmidt-Weber
2. Prof. Kathrin Schumann, Ph.D.

Die Dissertation wurde am 07.11.2023 bei der Technischen Universität München eingereicht und durch die TUM School of Medicine and Health am 13.03.2024 angenommen.

Table of Contents

List of Figures 4

List of Tables 6

Abbreviations 9

1 Introduction 14

1.1 The impact of the Corona Virus Disease 19 (COVID-19) 14

1.1.1 The pathogenesis of COVID-19 14

1.1.2 Asthma as a potential risk factor for SARS-CoV-2 infection and COVID-19 severity 14

1.1.3 SARS-CoV-2 infiltration, replication and activated pathways 15

1.1.4 The role of the RAAS and KKS system during SARS-CoV-2 infection 17

1.1.5 The regulation of ACE2 18

1.1.6 ACE2 isoform induced by interferons (IFNs) following SARS-CoV-2 infection. 19

1.2 The role of IFNs during viral infections 20

1.2.1 The IFN signaling pathway 20

1.2.2 The role of IFNs during SARS-CoV-2 infection 22

1.3 The transcription factor forkhead box protein 1 (FoxO1) and its pathways 23

1.3.1 The structure of FoxO1 and its binding sites 23

1.3.2 The post-translational regulation of FoxO1 24

1.3.3 The different roles of FoxO1 in the immune system 25

2 Aim of study 27

3 Materials and Methods 29

3.1 Materials 29

3.1.1 Chemicals 29

3.1.2 Reagents and recombinant proteins 31

3.1.3 Buffers 32

3.1.4 Media and Medium components 33

3.1.5 Buffer and Medium, house-made 34

3.1.6 Primary Antibodies 34

3.1.7 Secondary Antibodies 35

3.1.8 Consumables 35

3.1.9 Primers for RT-qPCR 36

3.1.10 Primers for PCR 37
3.1.11 Primers for competition experiments 37
3.1.12 Commercial kits and assays 38
3.1.13 Devices 39
3.1.14 Software 40
3.1.15 Plasmids 41
3.1.16 Consensus Sequence 42
3.1.17 Blocking Sequences 42
3.1.18 PCR Sequence 43
3.2 Methods 46
3.2.1 Cell culture conditions 46
3.2.2 IFN and inhibitor treatment 46
3.2.3 Quantitative expression analysis by Real Time PCR (RT-qPCR) 47
3.2.4 Immunoblotting 48
3.2.5 CRISPR/Cas9 knock-out 49
3.2.6 Plasmid amplification 49
3.2.7 Transfection for TF-ELISA 50
3.2.8 Cell lysis for TF-ELISA 50
3.2.9 Amplification of ACE2-(1119)-LUC promoter fragments for TF-ELISA 50
3.2.10 TF-ELISA 51
3.2.11 Air-liquid interface organoid cultures 52
3.2.12 Genome-wide microarray-based gene expression analysis 52
3.2.13 Study population and design 53
3.2.14 Statistical Analysis 54
4 Results 57
4.1 Differential effects on inflammation and epithelial integrity after IFN stimulation 57
4.1.1 Induction of similar ISGs by type-I, -II and -III IFNs 57
4.1.2 Pro-inflammatory pathways and homeostatic environment enhanced by IFNs 59
4.1.3 IFNs induce cell-cell adhesion, intercellular signaling and cell growth 63
4.1.4 Unique signalling pathways are induced by IFNs 65
4.2 Induction of ACE2 expression in primary human bronchial epithelial cells 67
4.2.1 Type-I, -II and -III IFNs induce ACE2 full-length and truncACE2 67
4.2.2 STAT1 and AKT play no role in IFN-dependent ACE2 regulation 70

4.3 ACE2 expression is regulated via transcription factor FoxO1 72
4.3.1 Characterization of FoxO1 binding sites within the ACE2 promoter 72
4.3.2 FoxO1 inhibition leads to ACE2 downregulation 74
4.3.3 FoxO1 knock-out cells exhibit low expression levels of ACE2 76
4.4 Genome expression patterns demonstrate advantages for asthmatics 79
4.4.1 ISG expression in high expressed *FOXO1* asthmatics and healthy individuals 79
4.4.2 SARS-CoV-2 infection related genes are downregulated in asthmatics 80
4.4.3 Reduced SARS-CoV-2-related genes correlate with elevated *IFN* levels in asthmatics 82
5 Discussion 85
5.1 IFN stimulation leads to enhanced epithelial integrity 85
5.2 IFNs induce ACE2 upregulation via the transcription factor FoxO1 86
5.3 Asthmatic patients demonstrate advantages towards SARS-CoV-2 infection 89
5.4 Conclusion and perspective 92
6 Scientific summary 94
6.1 English version 94
6.2 Deutsche Fassung 95
7 References 97
8 Publications 117
9 Supplementary Data 119

Acknowledgments 273

List of Figures

1.1 SARS-CoV-2 entry mechanisms. 16

1.2 The Renin-Angiotensin-Aldosterone (RAAS) and Kallikrein-Kinin (KKS) System. 18

1.3 ACE2 Promoter Sequence. 19

1.4 The IFN signaling pathways. 21

1.5 FoxO1 interaction with its DNA binding sequence. 24

1.6 Post-translational modifications of FoxO1..... 25

3.1 Plasmids used for TF-ELISA. 41

3.2 ACE2 full-length and truncACE2. 47

4.1 Whole genome analysis of IFN-stimulated ALIs. 57

4.2 IFNs induced similar ISG in ALIs..... 58

4.3 Differential expressed pro-inflammatory genes induced by type-I, -II and -III IFNs. 60

4.4 Differential expressed anti-inflammatory genes induced by type-I, -II and -III IFNs. 62

4.5 Overlapping genes associated with epithelial integrity induced by type-I, -II and -III IFNs..... 63

4.6 Differential expressed epithelial modulators induced in type-I, -II and -III IFN-stimulated ALIs..... 64

4.7 Gene network analysis of inflammatory pathways of IFN-stimulated ALIs..... 66

4.8 Gene network analysis of epithelial modulators pathways of IFN-stimulated ALIs. 66

4.9 Type-I, -II and -III IFNs induce ACE2 upregulation in ALIs. 67

4.10 IFN induce ACE2 full-length and truncACE2..... 68

4.11 ACE2 induction four hours post type-I, -II and -III IFN stimulation in NHBEs. 69

4.12 JAK inhibition leads to ACE2 downregulation in IFN co-stimulated NHBEs. 70

4.13 STAT and AKT inhibition has no impact on ACE2 expression in Calu3 cell line.... 71

4.14 FoxO1 affinity to the ACE2 proximal promoter..... 73

4.15 Inhibition of FoxO1 in NHBEs with the specific inhibitor AS..... 74

4.16 FoxO1 inhibition correlates with ACE2 downregulation on protein level. 74

4.17 FoxO1 inhibition correlates with ACE2 downregulation on a transcriptomic level. 75

4.18 Stable FoxO1 knock out in NHBEs. 76

4.19 Primary FoxO1-KO cells demonstrates downregulation of ACE2 full-length. 77

4.20 Primary FoxO1-KO cells demonstrates downregulation of truncACE2..... 78

4.21 ISG expression is associated dose-dependently with *FOXO1* expression in asthmatic patients and healthy control. 80

4.22 Asthmatic patients demonstrate differently expressed SARS-CoV-2 infection related genes compared to healthy individuals..... 81

4.23 Expressed genes associated with SARS-CoV-2 infection demonstrate a *IFNA2* dose-dependent correlation in asthmatic patients and healthy control. 83

9.1 Expressed genes associated with SARS-CoV-2 infection demonstrate a *IFNB1* dose-dependent correlation in asthmatics and healthy individuals. 119

9.2 Expressed genes associated with SARS-CoV-2 infection demonstrate a *IFNG* dose-dependent correlation in asthmatics and healthy individuals. 120

9.3 Expressed genes associated with SARS-CoV-2 infection demonstrate a *IFNL1* dose-dependent correlation in asthmatics and healthy individuals. 121

9.4 Expressed genes associated with SARS-CoV-2 infection demonstrate a *IFNL3* dose-dependent correlation in asthmatics and healthy individuals. 122

List of Tables

3.1 PCR program generating the promoter sequence 51

3.2 PCR program generating the blocking sequence 1-3 51

3.3 Subject characteristics..... 53

9.1 DEGs of overlapping induced ISGs by type-I, -II and -III IFNs (normalized) 123

9.2 DEGs of induced pro-inflammatory genes by IFN-α vs unstimulated.....126

9.3 DEGs of induced pro-inflammatory genes by IFN-β vs unstimulated.....139

9.4 DEGs of induced pro-inflammatory genes by IFN-λ1 vs unstimulated.....141

9.5 DEGs of induced pro-inflammatory genes by IFN-λ3 vs unstimulated.....147

9.6 DEGs of induced pro-inflammatory genes by IFN-γ vs unstimulated 152

9.7 DEGs of induced anti-inflammatory genes by IFN-α vs unstimulated 165

9.8 DEGs of induced anti-inflammatory genes by IFN-λ1 vs unstimulated 168

9.9 DEGs of induced anti-inflammatory genes by IFN-λ3 vs unstimulated 169

9.10 DEGs of induced anti-inflammatory genes by IFN-γ vs unstimulated.....170

9.11 DEGs of induced epithelial genes by IFN-α vs unstimulated 173

9.12 DEGs of induced epithelial genes by IFN-β vs unstimulated 186

9.13 DEGs of induced epithelial genes by IFN-λ1 vs unstimulated 188

9.14 DEGs of induced epithelial genes by IFN-λ3 vs unstimulated 194

9.15 DEGs of induced epithelial genes by IFN-γ vs unstimulated.....200

9.16 Cellular process enriched analysis output String network analysis of inflammatory and epithelial DEGs induced by type-I, -II and -III IFNs.....215

9.17 Significant gene expression changes of SARS-CoV-2 related genes comparing IFN-α-stimulated ALIs vs unstimulated ALIs 245

9.18 Significant gene expression changes of SARS-CoV-2 related genes comparing IFN-β-stimulated ALIs vs unstimulated ALIs 246

9.19 Significant gene expression changes of SARS-CoV-2 related genes comparing IFN-γ-stimulated ALIs vs unstimulated ALIs 247

9.20 Significant gene expression changes of SARS-CoV-2 related genes comparing IFN-λ1-stimulated ALIs vs unstimulated ALIs..... 248

9.21 Significant gene expression changes of SARS-CoV-2 related genes comparing IFN-λ3-stimulated ALIs vs unstimulated ALIs..... 249

9.22 Significant gene expression changes of IFN, SARS-CoV-2 related genes, KKS genes, acute phase genes, ISGs comparing asthma vs healthy control 250

9.23 Significant gene expression changes of ISGs comparing *FOXO1* high vs *FOXO1* low..... 253

9.24 Significant gene expression changes of IFN, SARS-CoV-2 related genes, KKS genes, acute phase genes, ISGs comparing *IFNA2* high vs *IFNA2* low of healthy individuals 254

9.25 Significant gene expression changes of IFN, SARS-CoV-2 related genes, KKS genes, acute phase genes, ISGs comparing *IFNA2* high vs *IFNA2* low of asthmatic patients..... 256

9.26 Significant gene expression changes of IFN, SARS-CoV-2 related genes, KKS genes, acute phase genes, ISGs comparing *IFNB1* high vs *IFNB1* low of healthy individuals 260

9.27 Significant gene expression changes of IFN, SARS-CoV-2 related genes, KKS genes, acute phase genes, ISGs comparing *IFNB1* high vs *IFNB1* low of asthmatic patients..... 261

9.28 Significant gene expression changes of IFN, SARS-CoV-2 related genes, KKS genes, acute phase genes, ISGs comparing *IFNG* high vs *IFNG* low of healthy individuals 264

9.29 Significant gene expression changes of IFN, SARS-CoV-2 related genes, KKS genes, acute phase genes, ISGs comparing *IFNG* high vs *IFNG* low of asthmatic patients 265

9.30 Significant gene expression changes of IFN, SARS-CoV-2 related genes, KKS genes, acute phase genes, ISGs comparing *IFNL1* high vs *IFNL1* low of asthmatic patients 268

9.31 Significant gene expression changes of IFN, SARS-CoV-2 related genes, KKS genes, acute phase genes, ISGs comparing *IFNL3* high vs *IFNL3* low of asthmatic patients 270

Abbreviations

ACE2	angiotensin converting enzyme 2
ADAM17	a disintegrin and metalloprotease 17
AMP	adenosine monophosphate
AngII	angiotensin II
APC	antigen presenting cell
ARDS	acute respiratory distress syndrom
AS1842856	5-amino-7-(cyclohexylamino)-1-ethyl-6-fluoro-4-oxo-1,4-dihydroquinoline-3-carboxylic acid
AT1R	angiotensin II type 1 receptor
ATR7	autophagy related 7
CBP	histone acetyltransferase cAMP-response element-binding protein (CREB)-binding protein
CCR7	C-C chemokine receptor type 7
COPD	chronic obstructive pulmonary disease
COVID-19	coronavirus disease 2019
DBE	Daf-16 binding element
DC	dentritic cells
DEG	differential expressed genes
DMEM	Dulbecco's Modified Eagle Medium
DMSO	dimethyl sulfoxide
DNA	deoxyribonucleic acid
dsRNA	double strand RNA

DTT	DL-Dithiothreitol
EDTA	ethylene diamine tetraacetic acid
ELISA	enzyme-linked immunosorbent assay
ER	endoplasmic reticulum
Fasl	Fas ligand
FBS	fetal bovine serum
FKH	Forkhead domain
FoxO1	forkhead Box transcription factor
G6PC	glucose-6-phosphatase
GO	GeneOntology
HNF	hepatocyte nuclear factors
HRP	horse-radish peroxidase
ICAM-1	intercellular adhesion molecule 1
ICS	inhaled corticosteroids
ICU	intensive care unit
IFN	interferon
IgG	immunoglobulin G
IL-6	interleukin 6
IRE	insulin-responsive sequence
IRF7	IFN regulatory factor 7
I/R injury	renal ischemia-reperfusion injury
ISG	IFN stimulated genes
ISGF3	IFN-stimulated gene factor 3

ISRE	IFN-stimulated response element
JNK	c-Jun N-terminal kinase
KCL	potassium chloride
KKS	Kinin-Kallikrein System
LB	lysogeny broth
mRNA	messenger ribonucleic acid
Mst1	macrophage-stimulating 1
NaCl	sodium chloride
NES	nuclear export signal
NK cells	natural killer cells
NLS	nuclear localization signal domain
NSP6	nonstructural protein 6
OAS	Oligoadenylatsynthetase
ORF6	open reading frame 6
PAK1	protein kinases p21-activated kinases 1
PAMP	pathogen associated molecular patterns
PBS	phosphate buffered saline
PCR	polymerase chain reaction
PEPCK	phosphoenolpyruvate carboxykinase
PI3K/PKB	Phosphoinositide 3-kinase/protein kinase B
PMSF	phenylmethylsulfonylfluorid
PRR	pathogen recognition receptors
RAAS	Renin-Angiotensin-Aldosterone System

RAG-1	recombination activating genes 1
RLRs	Restinoic acid-inducible gene (RIG)-1-like receptors
RNA	Ribonucleic Acid
RT	room temperature
RT-qPCR	real time quantitative polymerase chain reaction
S1	stalk fusion domain
S2	globular receptor domain
SARS-CoV-2	severe acute respiratory syndrom coronavirus type 2
Sir2	silent information regulator 2
SIRT1	histone deacetylase sirtuin 1
SH	SH-4-54
SKP21	S-phase kinase associated protein 2
SOP	standard operating procedures
STAT1	signal transducers and activators of transcription 1
TA	transactivation domain
TAE-Buffer	tris-acetate ethylenediaminetetraacetic acid buffer
TH cells	T helper cells
TLR	toll-like receptors
TMB	3,3´,5,5´-Tetramethylbenzidin
TMPRSS2	transmembrane serine protease 2
TNF-α	tumor necrosis factor alpha
Tofa	Tofacitinib citrate
truncACE2	truncated ACE2 isoform

Chapter 1

Introduction

1. Introduction

1.1. The impact of the Corona Virus Disease 19 (COVID-19)

1.1.1. The pathogenesis of COVID-19

The emergence of severe acute respiratory syndrome coronavirus type 2 (SARS-CoV-2), the virus causing the coronavirus disease 2019 (COVID-19) pandemic, has had a significant impact on global health, economies, and everyday life (*1–3*). The spectrum of patients symptoms varies from asymptomatic or mild cases to moderate or severe cases requiring intensive care unit admission and mechanical ventilation (*4*). Common symptoms include cough, taste disorder, myalgia, and fever (*5*). Studies revealed that the disease can progress quickly, often resulting in multiple organ failure and death (*4*). Non-survivors, tend to be older and have a higher risk of acute respiratory distress syndrome (ARDS), acute kidney injury, cardiac injury, and liver dysfunction (*6*). In addition, hyperinflammation and lung damage was associated with disease progression (*7*). SARS-CoV-2 predominantly infects alveolar epithelial cells and leads to an increased macrophage and neutrophil infiltration, resulting in a cytokine storm with high levels of pro-inflammatory cytokines such as interleukin 6 (IL-6), interferon gamma (IFN-γ) and tumor necrosis factor alpha (TNF-α) (*7*); (*8*); (*3*). COVID-19 patients show higher levels of SARS-CoV-2 antigen-specific T and B cells compared to healthy or recovered patients (*9*); (*10*). Patients generally demonstrate high levels of immunoglobulin G (IgG) antibodies, and even recovered patients maintain high levels of spike-protein-specific IgG antibodies (*11*); (*12*).

1.1.2. Asthma as a potential risk factor for SARS-CoV-2 infection and COVID-19 severity

During the pandemic several risk factors for potential SARS-CoV-2 infection and poor outcome were studied intensively. While factors like age, gender, and previously diagnosed health conditions such as chronic obstructive pulmonary disease (COPD) have been identified as risk factors for COVID-19, the role of asthma in the pathogenesis is controversial. Previous studies showed contradictory results, with some highlighting that asthma may increase the risk of severe illness (*13–15*), while others indicate advantages for asthmatics for viral infection and disease progression (*16–18*). Considering that asthma is one of the most common chronical respiratory diseases worldwide and is presented by symptoms such as coughing, wheezing, chronic airway inflammation and tissue remodeling (*19–21*) a broader understanding of the risk factors during viral infection has to be developed.

This complex disease is characterized by different types such as allergic or non-allergic asthma with unique set of triggers and activated cellular processes. Patients suffering from a substantial type-2 inflammation, such as allergic asthmatics, are characterized by eosinophilic airway inflammation and the presence of immunoglobulin E (IgE). Allergen-exposed lung epithelial cells release cytokines such as IL-25 and IL-33 that stimulate dendritic cells (DC). Combined with the activation by IL-4, T helper 2 (TH2) cell differentiation gets triggered and the differentiated TH2 cells migrate toward the lung (*22*). Additionally, IgE activates mast cells to release pro-inflammatory mediators such as histamine, leading to airway mucosal edema (*23*). Asthmatic patients, showing characteristics of low type-2 inflammation, demonstrate inflammasome activation, IL-1β, IL-6, IL-17 and neutrophilic inflammation (*24*); (*25*).

On the one hand, 13% of hospitalized COVID-19 patients in a US clinical cohort had previously diagnosed asthma and additionally patients showed a higher risk of subsequent bronchospasm, wheezing, and cough following the COVID-19 disease (*26*). Previous studies demonstrated the correlation between elevated levels of IL-4, IL-13, and IL-33 in serum samples and severe COVID-19 progression with the need for intensive care (*27*); (*28*). This implies a potential predisposition for asthmatic patients in terms of COVID-19 progression since these cytokines are abundant in allergic eosinophilic asthma with type 2 inflammation. Patients showed elevated levels of IL-13, IL-5, and eosinophils, suggesting an additionally burden for asthmatics (*29*). The reduced intrinsic IFN signaling in allergic asthma patients, which were shown in response to other viral infections, might further enhance the risk of severe COVID-19 development (*30–32*).

On the other hand, meta-analysis investigating 161,271 COVID-19 cases, demonstrated that 1.6% patients had previous diagnosed asthma, indicating advantages of asthmatic patient against viral infection (*33*). Studies have further revealed a reduced risk of SARS-CoV-2 infection among asthmatics compared to non-asthmatic patients, with no significant difference in hospitalization and intensive care unit (ICU) admissions (*34*). Higher number of eosinophils or overproduction of mucus and the inhaled corticosteroids (ICS) treatment, which are part of asthma pathogenesis, were associated with decreased virus susceptibility (*35*). In general, due to the resulting restrictions and lifestyle changes, such as social distancing, during the pandemic there were less reported cases of asthma admissions, severe asthma exacerbations, hospital admissions and lower prescriptions of ICS (*36–38*). Although the risks of prevalent respiratory diseases towards SARS-CoV-2 infection were studied in depth, the risk factors for asthmatic patients are still uncertain.

1.1.3. SARS-CoV-2 infiltration, replication and activated pathways

The SARS-CoV-2 virus, belonging to the virus family of the corona viruses, consists of spike, envelope, membrane and nucleocapsid proteins. The SARS-CoV-2 virus can enter the host cell via endocytosis or through direct fusion with the cell membrane (*39–41*). Therefore, the spike protein with its stalk fusion domain (S1) and the globular receptor domain (S2) plays an important role in interacting with the human receptor angiotensin-converting enzyme 2 (ACE2),

leading to virus infiltration (Figure 1.1); (*39*, *42*, *43*). Initially, S1 binds to ACE2 with its receptor binding domain, while host transmembrane serine protease 2 (TMPRSS2) sheds S1 to enable S2-mediated membrane fusion (*44*); (*45*). At the first site of infection in the upper airways, SARS-CoV-2 binds to ACE2 at the surface of airway cilia (*46*). Cilia promotes virus transport through the periciliary mucin layer. Within 24 hours post infection SARS-CoV-2 moves towards the elongated and highly branched microvilli with the support of protein kinases p21-activated kinases 1 and 4 (PAK1/4) involved.

The latest variant, when this study was conducted, Omicron, shows an enhanced spread via the "ciliary transport/microvilli reprogramming pathway" (*46*) compared to previous variants. To replicate its viral RNA and produce new virus particles, corona viruses utilize a replication-transcription complex and a vesicular network (*47*). Viral ribonucleic acid (RNA) replication occurs within double-membrane vesicles and convoluted membranes to evade detection by host innate immune sensors (*48*). A viral infection leads to degradation of cytosolic cellular messenger RNA (mRNA), enhancing the viral takeover of the mRNA pool in infected cells (*49*). It does not only interfere with the translation of proteins important in the antiviral cell state by blocking mRNA transport out of the nucleus, but also triggers an acute hyperinflammatory response known as a cytokine storm (*50*). This cytokine storm underlies several severe manifestations such as ARDS, myocardial infarction, and thromboembolic diseases. Activated T cells, macrophages and neutrophils release pro-inflammatory cytokines such as IL-1, IL-2, IL-6, TNF-α and IFN-γ and cause lung epithelial tissue damage (*51–53*). Not only pathways which SARS-CoV-2 uses directly for host infiltration and viral replication are important during infection. Thus SARS-CoV-2 utilizes ACE2 as an entry receptor, pathways such as the Renin–Angiotensin–Aldosterone System (RAAS) and the Kinin–Kallikrein System (KKS) are indirect impaired during viral infection.

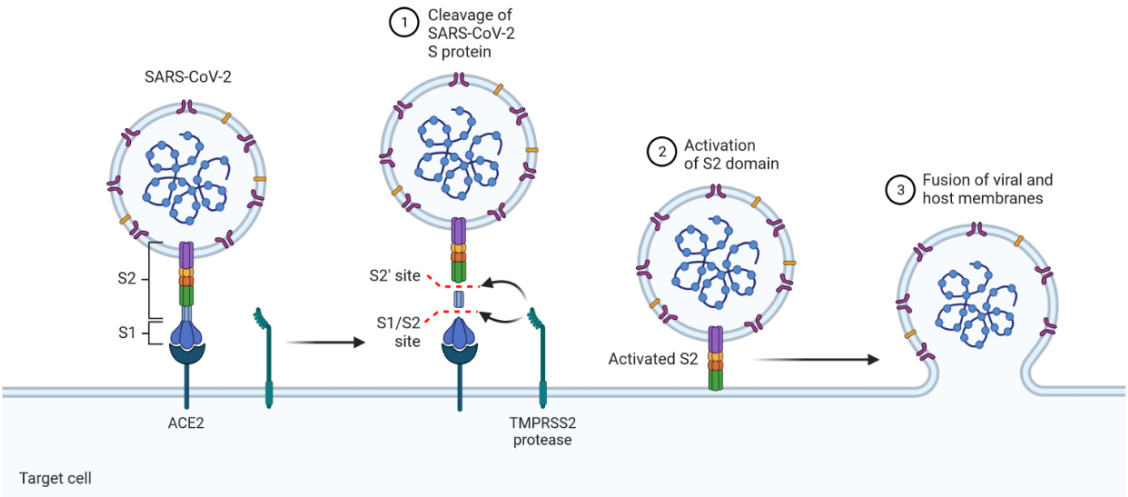

Figure 1.1 SARS-CoV-2 entry mechanisms.
The SARS-CoV-2 spike protein interacts with ACE2 on the cell surface of the target cell. TMPRSS2 protease cleaves subsequently S1/S2 and S2' sites which leads to activation of the S2 domain. Virus entries via cell fusion. Figure from Hartenian et al (*54*).

1.1.4. The role of the RAAS and KKS system during SARS-CoV-2 infection

ACE2 is a transmembrane protein which plays a crucial role in the RAAS and the KKS system by counterbalancing the action of angiotensin II (Ang II) and desArg9-bradykinin (*55*); (*56*). In normal physiology the RAAS is important for the homeostasis of blood pressure, fluids and salts in the human organism in various organs such as heart and lung (*57*). ACE2 plays a regulatory role in the homeostasis of RAAS (*58*); (*59*). However, under pathological circumstances, RAAS becomes dysregulated and leads to inflammation, cell proliferation and angiogenesis (*60*). RAAS functions via two axis: Ang II activates angiotensin II type 1 receptors (AT1R) leading to vasoconstriction, and the active angiotensin II type 2 receptors (AT2Rs) and Mas receptors leads to vasorelaxation (Figure 1.2); (*61*); (*62*). ACE2 sheds Ang I and Ang II to generate Ang(1–9) and Ang(1–7), which bind to AT2Rs and Mas receptors, activating the vasorelaxation axis of the RAAS (*63*). In COVID-19 the homeostasis of the RAAS is disrupted by the dysregulation of ACE2. Elevated Ang II levels, resulting from ACE2 occupancy and downregulation, in COVID-19 patients are associated with cytokine storm, inflammatory mediators and major vascular complications (*64–66*). Risk factors for COVID-19 such as obesity, cardiovascular disease and hypertension are associated with a dysregulated RAAS and increasing the risk of severe COVID-19 (*67*); (*68*). It has been shown that SARS-CoV-2 infection enhances cardiovascular comorbidities (*69*), and even young patients with low risk factors can suffer from organ impairment and long-term COVID-19 symptoms (*70*); (*71*).

There are regulatory links between the RAAS and the KKS. The two enzymes ACE and ACE2 degrade bradykinin, kallidin and des-Arg9-bradykinin into inactive metabolites and therefore inactivating KKS (*72*); (*73*). In contrast to RAAS, KKS is involved in arterial vasodilation, tissue repair and platelet aggregation (*74–76*). Within the KKS various kallikrein serine proteases cleave kininogens to activate vasoactive peptides such as bradykinin and kallidin (Figure 1.2). Further degradation leads to active des-Arg9-bradykinin and des-Arg10-kallidin, which are counterbalanced by ACE and ACE2 (*72*); (*74*). Dysregulation of the KKS also occurs during COVID-19. The accumulation of bradykinin and upregulation of KKS signaling contribute to symptoms such as dry cough, lung injury and inflammation (*73*); (*64*). It seems that also the indirect effect of dysregulated RAAS and KKS contributes to COVID-19 progression, highlighting the complexity of this disease.

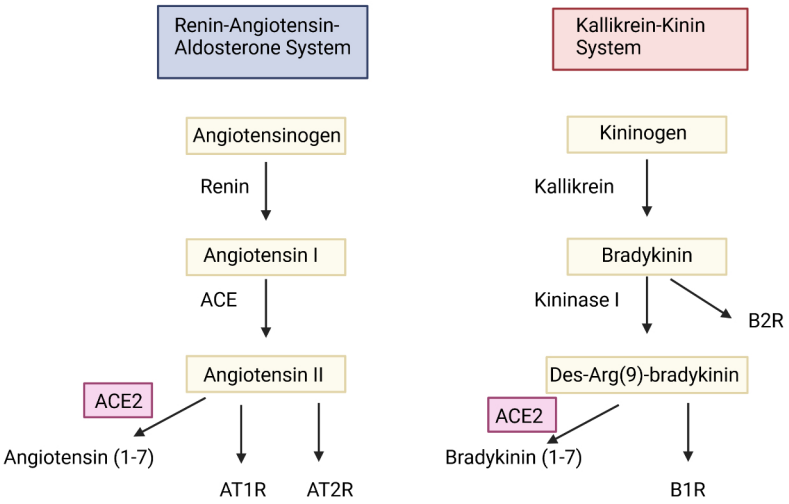

Figure 1.2 The Renin-Angiotensin-Aldoterone (RAAS) and Kallikrein-Kinin (KKS) System.
ACE2 (red) plays a crucial role in both RAAS and KKS system by converting Angiotensin II into Angiotensin(1-7) and Des-Arg(9)-bradykinin into Bradykinin(1-7). Created with Biorender.com

1.1.5. The regulation of ACE2

Expression and regulation of ACE2 differs between mice and humans with variations among different cell types and tissues within each species (*77*). Studies demonstrated the ubiquitous expression of human ACE2 in several tissues such as small intestine, testis, kidneys, heart, and lung without differences in expression levels between males and females and younger and older persons (*78*). The *ACE2* gene is located on chromosome Xp22 and consists of 18 exons (*59*). ACE2 is a zinc metallopeptidase, containing 805 amino acids and has a type I integral membrane glycoprotein. Post-translational regulation is mediated by glycosylation of several potential N-glycosylation sites (*79*). The regulation of the ACE2 protein includes processes such as Ang II induced shedding by a disintegrin and metalloprotease 17 (ADAM17) (*80*); (*81*). This results in a positive feedback loop in the RAAS system and influences cardiac remodeling through interactions with integrins and modulation of cell-extracellular matrix interactions (*82*). Despite extensive research during the SARS-CoV-2 pandemic, the transcriptional regulation of ACE2 remains incompletely understood. Previous studies have demonstrated that the expression of ACE2 is enhanced by hepatocyte nuclear factors (HNF) transcription factors, including HNF1-α, in pancreatic islets and HEK293 cells (*83*); (*84*). In addition, the histone deacetylase sirtuin 1 (SIRT1) contributes to the epigenetic regulation during cell energy stress such as hypoxia, exposure to cytokines, and adenosine monophosphate (AMP) kinase activation (*85*). ACE2 possesses one distal and one proximal promoter site, with distinct transcription factor binding sites found within the proximal promoter site (Figure 1.3) (*86*). Besides several HNF1 binding motifs, the proximal promoter site also contains FoxA and FoxO binding motifs. In addition, studies have shown that FoxO1 triggers SIRT1 expression in a positive feedback loop (*87*), suggesting a relation to ACE2 expression. In the context of asthma, studies revealed that IL-13 decreases the expression of ACE2 full-length on a transcriptomic and protein level on ciliated epithelial cells (*88*).

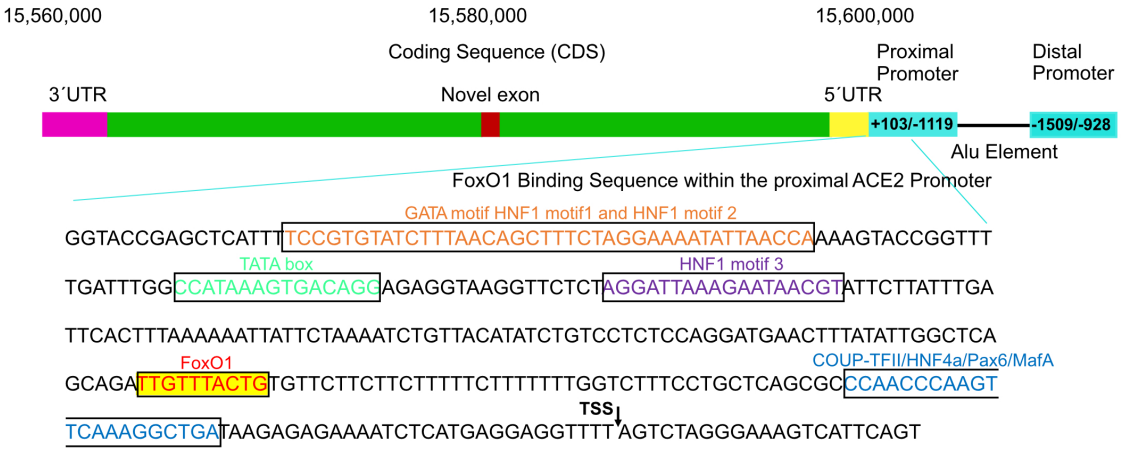

Figure 1.3 ACE2 Promoter Sequence.
Transcription factor binding sites are located within the proximal promoter site (GATA motif/HNF1 motif in orange, TATA box in green, HNF1 motif 3 in purple, COUP-TFII/HNF4a in blue). The FoxO1 binding site is highlighted in yellow and red.

1.1.6. ACE2 isoform induced by interferons (IFNs) following SARS-CoV-2 infection.

Early research during the pandemic demonstrated a potential ACE2 induction by IFNs (*89*). Cells treated with IFNs or infected by viruses such as influenza showed elevated ACE2 expression (*89*); (*90*). On the other hand, studies also showed that rather a truncated version (truncACE2) is induced by IFNs (*91*); (*92*). TruncACE2 lacks the SARS-CoV-2 spike protein binding domain, as well as the enzymatic domain. Furthermore, it could be shown that truncACE2 does not bind to SARS-CoV-2 spike binding domain, suggesting a lower virus susceptibility rate (*92*). The novel isoform initiates from a novel first exon in intron nine (*92*) and could be found in human nasal and bronchial respiratory epithelia as well as in asthmatic bronchial epithelia (*91*). In addition, it could be shown that truncACE2 had comparable baseline expression levels to ACE2 in primary bronchial respiratory cells (*92*). However, there is no evidence supporting its biological significance or necessity except a potential advantage during SARS-CoV-2 infection. In the following section, the IFN signaling pathway will be described in detail.

1.2. The role of IFNs during viral infections

1.2.1. The IFN signaling pathway

Following a viral infection, interferons (IFNs), which include type-I IFN (IFN-α, IFN-β), type-II IFN (IFN-γ), and type-III IFN (IFN-λ1- λ4), stimulate the transcription of IFN-stimulated genes (ISGs) to create an antiviral cell state. They are grouped according to their structural homology, chromosomal location, and the interaction with their specific receptor chains (*93*). While IFN-β is produced by many different cell types, plasmacytoid dentritic cells are the major source of IFN-α.

During a viral infection, pathogen associated molecular patterns (PAMPs) which consist of viral RNA, DNA or protein get recognized by intracellular pathogen recognition receptors (PRRs), inducing innate immune signaling cascades. Examples for PRR are Toll-like receptors (TLRs) and Retinoic acid-inducible gene (RIG)-1-like receptors (RLRs). Following viral RNA recognition via PRRs, cytoplasmic IFN regulatory factor 7 (IRF7) is phosphorylated and translocates to the nucleus, activating type-I IFN expression. Notably, type-I IFNs are able to induce components requiring for their own expression process such as IRF7, maintaining a positive feedback loop (*94*). Released IFNs bind to their IFN alpha receptor 1 and receptor 2 subunits which are connected with the kinases Tyk2 and JAK1 (Figure 1.4). Binding to their receptors leads to phosphorylation of tyrosine residues on the receptor tail (*95*), allowing Signal Transducers and Activators of Transcription 1 (STAT1) and STAT2 to bind to this tail and become phosphorylated themselves. Phosphorylation leads to a heterodimerization of STAT1 and STAT2 and additionally binding to cytoplasmic IRF9. This complex known as IFN-stimulated gene factor 3 (ISGF3) translocates to the nucleus and binds to a IFN-stimulated response element (ISRE) on a target DNA sequence and starts transcription of ISGs.

Prominent ISGs such as oligoadenylatsynthetase (OAS) degrade viral double strand RNA (dsRNA), but in general ISGs additionally disrupt viral replication by extinct protein assembly or inducing virus breakdown in infected or bystander cells (*96–98*). They are able to induce MHC class I expression and molecules such as CD86 on DC (*99*). This process leads to viral recognition and activation of TH1 cells, leading to key cytokines such as IL-2, IL-10 and TGF-β and triggering differentiation of CD8+ T cells (*100*). Type-I IFNs establish a paracrine action where infected cells secret IFNs to protect neighboring cells (*101*). Compared to type-I, type-III IFNs are prominent in the antiviral state in mucosal surfaces without enhancing damaging pro-inflammatory processes (*102*).

IFN-λs bind to IFNLR1 and IL10RB receptor subunits, which induce the transcription of ISGs also via the JAK/STAT signaling pathway. However, the IFN-λ receptors are located primarily on epithelial cells and activate an antiviral state at the site of infection and regulating tissue damage resulting from neutrophils in intestinal organs (*103*); (*104*).

On contrast to the other IFN family members, IFN-γ is produced by activated T and natural killer (NK) cells, but not by virus-infected cells (*105*). IFN-γ not only activates the transcription of ISG such as IRF-1 and IRF-9 via its IFNGR1/IFNGR2-JAK-STAT axis, but also plays a crucial role in isotype switching of B and TH1 cell differentiation (*106*); (*107*). In addition, CD4+ T helper type-1 and CD8+ cytotoxic T lymphocytes release IFN-γ in an antigen-dependent (*108*) and -independent way (*109*), leading the adaptive immune response towards the pathogen.

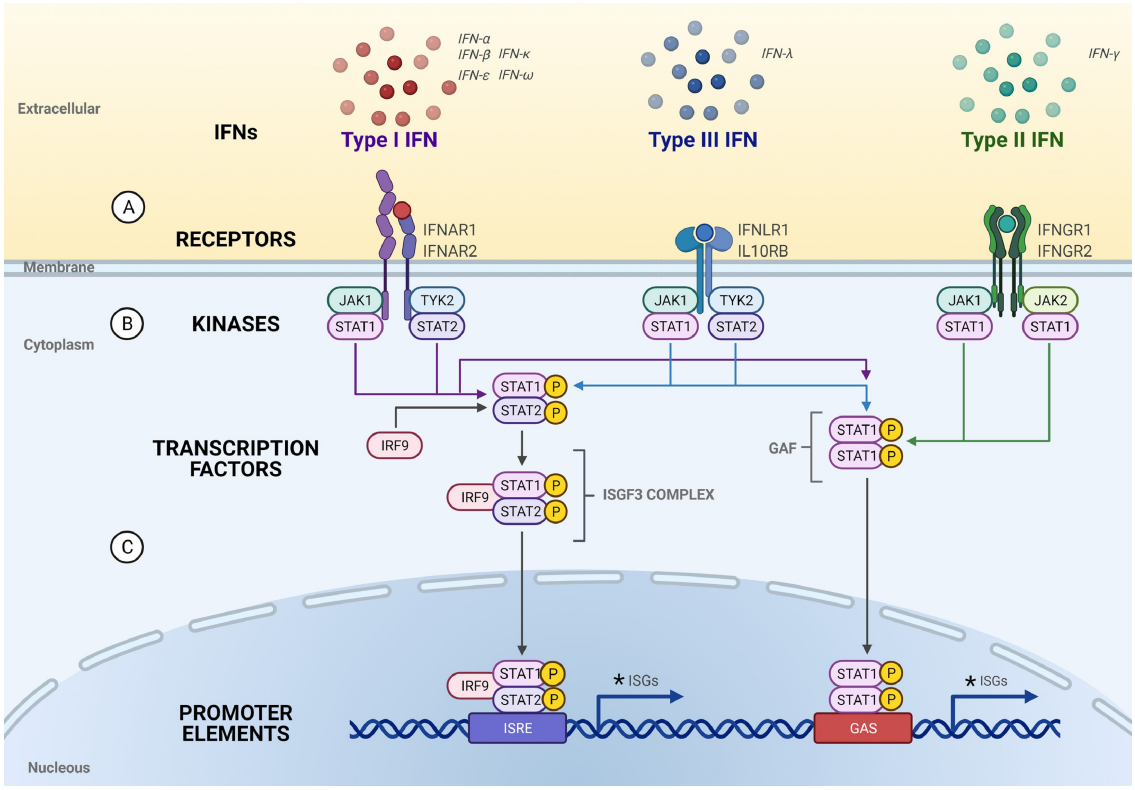

Figure 1.4 The IFN signaling pathways.
(A) Type-I, -III and -II IFNs bind to their specific receptors and (B) activate a JAK/STAT signaling cascade. (C) Following IFN binding STAT1 and STAT2 gets phosphorylated and generate the ISGF3 and GAF complex leading to translocation to the nucleus and the transcription of ISGs. Figure from Akamatsu et al (*110*).

1.2.2. The role of IFNs during SARS-CoV-2 infection

IFNs also play a crucial role during SARS-CoV-2 infection. Studies showed that in epithelial cell lines IFN dose-dependently inhibits SARS-CoV-2 (*111*). However, the action of IFNs following SARS-CoV-2 infection remains still uncertain. Although IFN response is present and interferes with SARS-CoV-2 viral replication, the response is delayed in primary human nasal epithelium differentiated air–liquid interface also compared to other respiratory viruses (*112*). In addition, severe COVID-19 patients demonstrated a weak and delayed IFN response and an activation of pro-inflammatory cytokines (*102*); (*113*); (*114*). These findings suggest, along with others (*102*), that type-I and -III IFN deficiency is a hallmark of severe COVID-19 and may contribute to the evolutionary success of SARS-CoV-2 (*115*). It has been postulated that viral proteins such as nonstructural protein 6 (NSP6), NSP13 and open reading frame 6 (ORF6) interferes with IRF3 and STAT1/STAT2 complex to inhibit IFN and ISG transcription (*115*). However, high levels of IFN-γ have been detected in peripheral blood of COVID-19 patients (*90*). In addition, severe COVID-19 patients developed high levels of nasal SARS-CoV-2 RNA together with inflammatory and type-II responsive macrophages compared to mild and moderate cases (*116*). Besides the pro-inflammatory effects of type-II, type-I IFNs co-existed with TNF and IL-1β-driven inflammation in severe COVID-19 patients compared to mild cases and severe influenza patients (*117*).Patients (2.6% female and 12.5% male) suffering from severe COVID-19 pneumonia have been associated with the presence of type-I IFN-blocking autoantibodies, which neutralize the IFN signaling (*118*). In conclusion, the role of IFNs following SARS-CoV-2 infection is diverse. Severe COVID-19 is characterized by deficiencies in type-I and type-III IFNs, along with an activation of pro-inflammatory cytokines. In addition, IFN might be involved in ACE2 regulation. The following section will focus on potential IFN downstream molecules involved in this ACE2 induction.

1.3. The transcription factor forkhead box protein 1 (FoxO1) and its pathways

1.3.1. The structure of FoxO1 and its binding sites

The FoxO1 transcription factor is part of the Fox transcription factor family and is known for its key role in maintaining homeostasis and responsiveness to environmental signals (*119*); (*120*). FoxO1 plays a critical role in various biological processes, including cancer development, gluconeogenesis, and glycogenolysis (*121–123*). The transcription factor acts primarily through binding to target DNA and activating transcription, following translocation to the nucleus. It is able to demonstrate “off target” effects by binding to other proteins in the nucleus and cytoplasm and acting as a co-regulator (*124*).

The FoxO1 protein consists of four functional domains including the nuclear localization signal domain (NLS), the nuclear export signal (NES), the transactivation domain (TA) and the Forkhead domain (FKH) (*125*); (*126*). The FKH domain is binding to the FoxO1 binding motif, with its H3 helices responsible for base-specific contact. In addition, the winged-loop W1 and the β strands S2 and S3 stabilize the protein-DNA binding complex and enhance the affinity to the DNA phosphate backbone (Figure 1.5). Crystal structures highlight two FoxO1 consensus sequences, one is the Daf-16 binding element (DBE) 5´-GTAAA(T/C) AA-3´ and second the insulin-responsive sequence (IRE) 5´-(C/A) (A/C) AAA(C/T) AA-3´ (Figure 1.5); (*127*) . All FoxO-family members recognize the DNA core sequence 5´-(A/C)AA(C/T)A-3´.

FoxO1 plays a crucial role in the regulation of hepatic gluconeogenesis and glycogenolysis (*128*). By binding to its target sequence and activating the transcription of glucose-6-phosphatase (G6PC) and phosphoenolpyruvate carboxykinase (PEPCK), FoxO1 enhances gluconeogenesis and glycogenolysis (*129*); (*130*). In contrast, elevated blood insulin levels, occurring after food consumption, decrease the glucose levels in the blood. This effect leads to glucose absorption and the inhibition of hepatic gluconeogenesis and glycogenolysis. The glucose production is thereby inhibited as well. This effect is mediated by insulin’s activation of the Phosphoinositide 3-kinase/protein kinase B (PI3K/PKB) signaling pathway in the liver, leading to the phosphorylation and subsequent degradation of FoxO1 (*131*). Therefore, FoxO1 regulation via post-translational modifications is beneficial for a fast insulin response and for glucose homeostasis. In addition, FoxO1 signaling is important during apoptosis and cell cycle arrest. FoxO1 mediates the transcription of its target genes such as Puma, Fas ligand (Fasl) (*132*), GADD45 (*133*), p27 (*134*), and Cyclin D1/2 (*135*), which are crucial for the inhibition of cell proliferation especially in malignant cells.

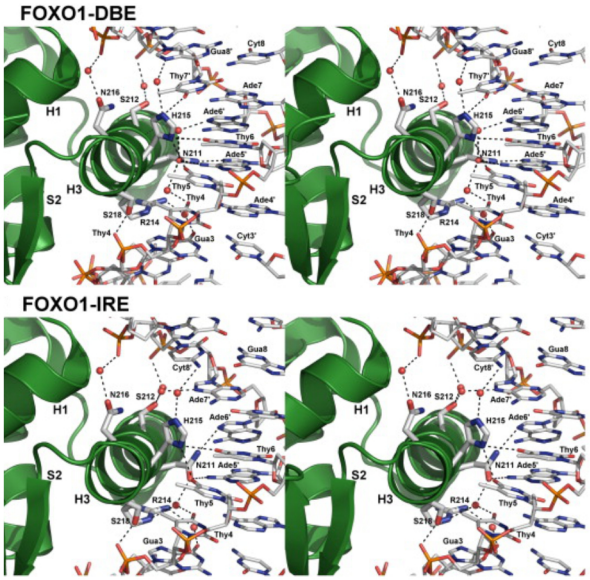

Figure 1.5 FoxO1 interaction with its DNA binding sequence.
FKH domain interacts via its H3 helix and the support of W1, S2 and H1 with either the DBE (5´-GTAAA(T/C) AA-3´) or the IRE (5´-(C/A) (A/C) AAA(C/T) AA-3´) binding motif. Figure from Obsil et al (*127*).

1.3.2. The post-translational regulation of FoxO1

To respond quickly to external signals, the expression of FoxO1 is tightly controlled by post-translational modifications such as acetylation, phosphorylation, and ubiquitination. Insulin and other growth factors mediate the phosphorylation of FoxO1 residues including threonine24, serine256, and serine319 by PI3K/PKB, thereby disrupting FoxO1 binding and leading to translocation to the cytoplasm (Figure 1.6); (*136*). In contrast, the phosphorylation by c-Jun N-terminal kinase (JNK) or macrophage-stimulating 1 (MST1) enhances the nuclear entry of FoxO1 and activates DNA binding (*137*); (*138*). FoxO1 is regulated by acetylation induced by histone acetyltransferase cAMP-response element-binding protein (CREB)-binding protein (CBP) and deacetylation by NAD-dependent histone deacetylase silent information regulator 2 (SIR2) at conserved residues such as lysine242, lysine245 and lysine262 (*139*); (*140*).

Positively charged lysine residues contribute to DNA binding. Acetylation at these amino acids on the other hand attenuates the FoxO1 affinity towards DNA and suppresses target gene transcription. Acetylation can enhance FoxO1 phosphorylation and supports FoxO1 translocation into the cytoplasm. This translocation exposes FoxO1 protein to a third possible post-translational regulation, the ubiquitination-dependent proteasomal degradation. FoxO1 gets polyubiquitinated by E3 ligases such as S-phase kinase associated protein 2 (SKP21) (*141*); (*142*), which is followed by degradation especially in human primary tumor cells and cancer cell lines (*143*).

Targeting FoxO1 has the potential to address metabolic disorders. Mass spectrometric affinity screening revealed the small molecule compound 5-amino-7-(cyclohexylamino)-1-ethyl-6-fluoro-4-oxo-1,4-dihydroquinoline-3-carboxylic acid (AS1842856), which binds to dephosphorylated and active FoxO1 protein (*144*); (*145*). It could be shown that AS1842856 inhibited the transcription activity with IC_{50} of 0.03μM. In addition, oral administration of AS1842856 led to decreased glucose levels after fasting and to suppression of genes associated with gluconeogenesis in a diabetic db/db mouse model (*144*).

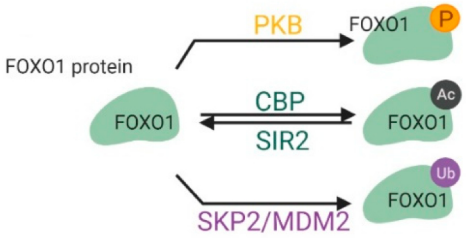

Figure 1.6 Post-translational modifications of FoxO1.
External stimuli lead to FoxO1 phosphorylation by PKB (yellow), acetylation by CBP and deacetylation by SIR2 (green) or ubiquitination by SKP2 or MDM2 (purple). FoxO1 thereby translocates from the nucleus to the cytoplasm and gets degraded. Figure from Peng et al (*128*).

1.3.3. The different roles of FoxO1 in the immune system

FoxO1 exhibits different roles in the innate and adaptive immune response. Although it is involved in regulating DCs (*146*), macrophages, neutrophils (*147*); (*148*) and TH cells (*149*) FoxO1 is also modulating cytokine production (*150*). Regarding the role of FoxO1 in the innate immune system previous studies reported that TLR4, which activates the intracellular NF-kB pathway, is downregulated by the PTEN/PI3K/Akt/FoxO1cascade in an acute lung injury model (*151*). FoxO1-mediated autophagy is essential for NK cell development and induced innate immunity, by the interaction of phosphorylated FoxO1 and Autophagy related 7 (Atg7) protein in immature NK cells (*152*). FoxO1 is involved in several DC functions such as DC phagocytosis of bacteria and binding to lymphocytes (*146*). C-C chemokine receptor type 7 (CCR7) and Intercellular Adhesion Molecule 1 (ICAM-1) both target genes of FoxO1, get upregulated via FoxO1 following bacteria recognition. CRR7 responds to chemokines, directing DC into the lymph node, whereas ICAM-1 is needed for DC-lymphocyte interaction and lymphocyte activation. FoxO1 overexpression in DC leads to elevated levels of IL-12, IL-6 and TNF-α *in vitro* (*153*). In adaptive immunity, FoxO1 plays a crucial role in lymphocyte development and cytokine expression (*154*). Previous studies showed that FoxO1 is crucial in regulatory T cell formation (*155*), (*156*). In addition, FoxO1 regulates the expression of recombination activating genes 1 (RAG-1) and RAG2, which are important for the vast repertoire of antigen receptors, in early B cell development (*157*). This effect is later in B cell development (pro-B cell and immature B cell) counterbalanced by Akt, which phosphorylates FoxO1 and thereby enhancing its degradation. Although FoxO1 plays a role in the innate and adaptive immune response, it remains largely unknown if FoxO1 is involved in the IFN signaling following SARS-CoV-2 infection.

Chapter 2

Aim of study

2. Aim of study

IFNs play a crucial role in the innate immune system and lead to an antiviral cell state following viral infection. This study aims to understand the impact of IFNs on the epithelial barrier by using whole-genome microarray analysis of type-I, -II and -III IFN-stimulated air liquid interface organotypic cultures. It is important to know if IFN stimulation is involved in a pro-inflammatory or homeostatic environment and in epithelial reconstruction or rather barrier disruption following viral infection.

Since ACE2 is the entry receptor for the SARS-CoV-2 virus its regulation is crucial for virus susceptibility. Anyway, its regulation still remains uncertain. To gain insights into the IFN-dependent ACE2 regulation, known key factors of the IFN pathway are inhibited. In addition, ACE2 expression is analyzed in FoxO1 knock-out primary human bronchial epithelial cells to gain insights into the IFN-ACE2 axis. This study demonstrates the risk factors for asthmatic patients during SARS-CoV-2 infection by analyzing the gene expression patterns of SARS-CoV-2 associated genes in an asthmatic adult cohort.

Chapter 3

Material and Methods

3. Materials and Methods

3.1. Materials

3.1.1. Chemicals

Name	**Manufacturer**
Dimethyl sulfoxide (DMSO) for cell culture	Applicam, Darmstadt, Germany
Ethanol absolute for RNA extraction	Merck, Darmstadt, Germany
UltraPure DEPC-Treated Water	Thermo Fisher Scientific, Waltham, MA, USA
Nonfat dried milk powder	Applicam, Darmstadt, Germany
Bovine Serum Albumin	Sigma-Aldrich, Merck, Darmstadt, Germany
Sodium chloride (NaCl)	Carl Roth, Karlsruhe, Germany
Trizma®hydrochloride	Sigma-Aldrich, Merck, Darmstadt, Germany
Tween®20	Merck, Darmstadt, Germany
Potassium chloride (KCl)	Merck, Darmstadt, Germany
HEPES (1M)	Thermo Fisher Scientific, Waltham, MA, USA
Magnesium chloride ($MgCl_2$)	Sigma-Aldrich, Merck, Darmstadt, Germany
IGEPAL CA-630	Sigma-Aldrich, Merck, Darmstadt, Germany
Glycine	Merck, Darmstadt, Germany
cOmplete Tablets, EDTA-free, EASYpack	Roche, Basel, Switzerland

Phenylmethylsulfonylfluorid (PMSF)	Merck, Darmstadt, Germany
DL-Dithiothreitol (DTT)	Sigma-Aldrich, Merck, Darmstadt, Germany
Ethylene diamine tetraacetic acid (EDTA)	Sigma-Aldrich, Merck, Darmstadt, Germany
Acetic acid	Merck, Darmstadt, Germany
Methanol	Merck, Darmstadt, Germany
Agarose	Thermo Fisher Scientific, Waltham, MA, USA
lysogeny broth (LB) Broth (Miller) Powder microbial growth medium	Sigma-Aldrich, Merck, Darmstadt, Germany
Agar-Agar, Kobe I	Carl Roth, Karlsruhe, Germany
Ampicillin sodium salt	Sigma-Aldrich, Merck, Darmstadt, Germany
Heparin	Stemcell Technologies, Vancouver, Canada
Sucrose	Sigma-Aldrich, Merck, Darmstadt, Germany
poly(deoxyinosinic-deoxycytidylic) acid	Sigma-Aldrich, Merck, Darmstadt, Germany
sulfuric acid (H_2SO_4)	Merck, Darmstadt, Germany
3,3´,5,5´-Tetramethylbenzidin (TMB)	Sigma-Aldrich, Merck, Darmstadt, Germany

3.1.2. Reagents and recombinant proteins

Name	**Manufacturer**
Trypan Blue solution, 0.4%	Thermo Fisher Scientific, Waltham, MA, USA
FastStart Universal SYBR Green Master (Rox)	Sigma-Aldrich, Merck, Darmstadt, Germany
GeneRuler 100 bp DNA Ladder	Thermo Fisher Scientific, Waltham, MA, USA
PeqGreen DNA/RNA Dye	VWR International GmbH, Darmstadt, Germany
SuperSignal^{TM} West Pico PLUS Chemilumineszenz-Substrat	Thermo Fisher Scientific, Waltham, MA, USA
SuperSignal^{TM} West Femto Maximum Sensitivity Substrat	Thermo Fisher Scientific, Waltham, MA, USA
NuPAGE^{TM} Probenreduktionsmittel (10x)	Thermo Fisher Scientific, Waltham, MA, USA
PageRuler^{TM} Plus Prestained Protein Ladder, 10 to 250 kDa	Thermo Fisher Scientific, Waltham, MA, USA
Roferon A	Roche, Basel, Switzerland
Human Interferon Alpha A (Alpha 2a)	Pbl assay Science, Piscataway, NJ, USA
Recombinant Human IFN-β	Peprotech, Rocky Hill, NJ, USA
Recombinant Human Interferon-gamma	PromoCell GmbH, Heidelberg, Germany
Recombinant Human IL-29/IFN-lambda 1 Protein	Biotechne, Minneapolis, MN, USA
Recombinant Human IL-28B/IFN-lambda 3 Protein	Biotechne, Minneapolis, MN, USA

AS1842856	Selleck Chemicals LLC, Houston, TX, USA
Tofacitinib Citrate	Sigma-Aldrich, Merck, Darmstadt, Germany
SH-4-54	Selleck Chemicals LLC, Houston, TX, USA
Capivasertip	Selleck Chemicals LLC, Houston, TX, USA
Alt-R S.p. HiFi Cas9 Nuclease V3, 500µg	Integrated DNA Technologies, Inc., Coralville, IA, USA
Alt-R Cas9 Electroporation Enhancer, 10nmol	Integrated DNA Technologies, Inc., Coralville, IA, USA
Alt-R CRISPR Cas9 Negative Control crRNA, 2nmol	Integrated DNA Technologies, Inc., Coralville, IA, USA
Alt-R CRISPR-Cas9 tracr RNA, 20nM	Integrated DNA Technologies, Inc., Coralville, IA, USA
Alt-R CRISPR-Cas9 crRNA XT, 10nmol	Integrated DNA Technologies, Inc., Coralville, IA, USA
Novex^{TM} NuPAGE^{TM} LDS-Probenpuffer (4X)	Thermo Fisher Scientific, Waltham, MA, USA
Collagen	Sigma-Aldrich, Merck, Darmstadt, Germany

3.1.3. Buffers

Name	**Manufacturer**
Novex^{TM} NuPAGE^{TM} MOPS SDS Laufpuffer (20X) (500ml)	Thermo Fisher Scientific, Waltham, MA, USA
NuPAGE^{TM} Transferpuffer (20x)	Thermo Fisher Scientific, Waltham, MA, USA

3.1.4. Media and Medium components

Name	**Manufacturer**
0.05% Trypsin-EDTA (1x)	Thermo Fisher Scientific, Waltham, MA, USA
Fetal Bovine Serum (FBS) SUPERIOR stabil	Bio&SELL GmbH, Nürnberg, Germany
Dulbecco´s Modified Eagle Medium (DMEM) (1x)	Thermo Fisher Scientific, Waltham, MA, USA
Dulbecco´s Phosphate Buffered Saline (PBS)	Thermo Fisher Scientific, Waltham, MA, USA
BEBM^{TM} Bronchial Epithelial Cell Growth Basal	Medium Lonza, Basel, Switzerland
BEGM^{TM} Bronchial Epithelial Cell Growth Medium BulletKit^{TM}	Lonza, Basel, Switzerland
Penicillin Streptomycin (Pen Strep)	Thermo Fisher Scientific, Waltham, MA, USA
PneumaCult^{TM}-Ex Plus Medium	Stemcell Technologies, Vancouver, Canada
PneumaCult^{TM}-ALI Medium	Stemcell Technologies, Vancouver, Canada
S.O.C Medium	Thermo Fisher Scientific, Waltham, MA, USA
MEM, without Glutamin	Thermo Fisher Scientific, Waltham, MA, USA
L-Glutamine 200mM (100x)	Thermo Fisher Scientific, Waltham, MA, USA

3.1.5. Buffer and Medium, house-made

Name	**Ingredients**
10x TBS	300mM Tris-HCl pH 7.4, 1.5M NaCl
Stripping Buffer	10% Methanol (100%), 10% Acedic Acid (100%)
Cytosolic extraction Buffer A	10mM HEPES pH 7.9, 10mM KCl, 300mM Sucrose, 1.5mM $MgCl_2$, 0.5mM DTT, 0.1% IGEPAL CA-630, 0.5mM PMSF, 1X cOmplete^{TM}, Mini protease inhibitor
Nuclear extraction Buffer B	20mM HEPES pH 7.9, 100mM KCl, 100mM NaCl, 0.5mM DTT, 20% Glycin, 0.5mM PMSF, 1X cOmplete^{TM}, Mini protease inhibitor
TF-ELISA washing Buffer PBS	0.05% Tween 20 in PBS
TF-ELISA blocking buffer	140mM NaCl, 1.5mM $MgCl_2$, 1mM DTT, 20mM HEPES pH 7.9, 0.2mM EDTA, 0.1% IGEPAL CA-630
TAE (Tris/Acetate/EDTA) electrophoresis buffer	40mM Tris, 1% glasial acetic acid, 2mM EDTA

3.1.6. Primary Antibodies

Antigen	**Host, Isotype**	**Dilution**	**Manufacturer**
ACE2 788-805 (C-term)	Rabbit, IgG	1:1000	Abcam, Cambridge, UK
FoxO1	Mouse, IgG1	1:1000	Cell Signaling Technology Inc, Danvers, MA, USA
GAPDH	Mouse, IgG1	1:3000	Cell Signaling Technology Inc, Danvers, MA, USA

3.1.7. Secondary Antibodies

Antigen	**Dilution**	**Manufacturer**
Anti-Rabbit IgG HRP-linked	1:5000 / 1:7000	Cell Signaling Technology Inc, Danvers, MA, USA
Anti-mouse IgG, HRP-linked	1:5000 / 1:7000	Cell Signaling Technology Inc, Danvers, MA, USA

3.1.8. Consumables

Name	**Manufacturer**
Immobilon-P Membran, PVDF, 0,45µm, 26,5cm x 3,75m-Rolle	Millipore, Merck, Darmstadt, Germany
SafeSeal tube 1.5/2ml	Sarstedt, Numbrecht, Germany
Cellstar Tubes 15/50ml	Greiner Bio-One, Frickenhausen, Germany
Serological Pipettes 5/10/25ml, graduated	Greiner Bio-One, Frickenhausen, Germany
SafeSeal SurPhob Tips 10/200/1250µl	Biozym Scientific, Hessisch Oldendorf, Germany
QIAshredder	Qiagen, Hilden, Germany
Pierce^{TM} Streptavidin Coated High Capacity Plates, 384-wells	Thermo Fisher Scientific, Waltham, MA, USA
Western-Blotting-Filter paper, extra thick, 20cm x 20cm	Thermo Fisher Scientific, Waltham, MA, USA
CELLSTAR® Filter Cap Cell Culture Flask, TCtreated, sterile, 25cm^2/75cm^2	Greiner Bio-One, Frickenhausen, Germany
TPP® tissue culture dishes	Sigma-Aldrich, Merck, Darmstadt, Germany
Falcon® Clear Flat Bottom TC-treated Multiwell Cell Culture Plate, with Lid, 6-well/12-well	Corning, Glendale, AZ, USA

NuPAGE^{TM} 10%, Bis-Tris, 1,0–1,5mm, Mini-Protein-Gele	Thermo Fisher Scientific, Waltham, MA, USA
Transwell Permeable Supports, 12mm Insert, 12-well plate, 0.4μm Polyester Membrane, Tissue Culture Treated, Polystyrene	Corning, Glendale, AZ, USA
Asi Rhino-Pro® cuvettes	Arlington Scientific, Springville, UT, USA

3.1.9. Primers for RT-qPCR

Name	**Sense/ Antisense**	**Sequence (5´→ 3´)**
bActin-Fwd	Sense	ATTGCCGACAGGATGCAGAA
bActin-Rev	Antisense	TCTTCATTGTGCTGGGTGCC
HPRT-Fwd	Sense	TGACACTGGCAAAACAATGCA
HPRT-Rev	Antisense	GGTCCTTTTCACCAGCAAGCT
ACE2-FL-Fwd	Sense	TGCCTATGTGAGGGCAAAGT
ACE2-FL-Rev	Antisense	ACCCCACATATCACCAAGCA
truncACE2-Fwd	Sense	GTGAGAGCCTTAGGTTGGATTC
truncACE2-Rev	Antisense	TAAGGATCCTCCCTCCTTTGT

3.1.10. Primers for PCR

Name	**Sense/ Antisense**	**Sequence (5´→ 3´)**
ACE2-1119-Fwd1	Sense	GCCACAGAACCAGTGTGAGA
ACE2-1119-Fwd2	Sense	TGGCCATAAAGTGACAGGAGAG
ACE2-1119-Fwd3	Sense	ACACCCGAGGGGGATGATAA
ACE2-1119-Fwd4	Sense	CAGTGCTGCAATGATACCGC
ACE2-1119-Rev-Bio	Antisense	Biotin-AATGTTCTGGCACCTGCACT

3.1.11. Primers for competition experiments

Name	**Sense/ Antisense**	**Sequence (5´→ 3´)**
Blocking-Fwd1	Sense	ACCATGTGGAGGCTTTCTTACT
Blocking-Rev1	Antisense	CCAGAAACTCTCTACTTGGGCA
Blocking-Fwd2	Sense	TGCCCAAGTAGAGAGTTTCTGG
Blocking-Rev2	Antisense	GGCCAAATCAAAACCGGTACTTT
Blocking-Fwd3	Sense	TCTGTCCTCTCCAGGATGAACT
Blocking-Rev3	Antisense	AGATCGCAGATCTCGTCCCC

3.1.12. Commercial kits and assays

Name	**Manufacturer**
RNeasy Mini Kit	Qiagen, Hilden, Germany
MinElute PCR Purification Kit	Qiagen, Hilden, Germany
AllPrep 96 DNA/RNA Kit	Qiagen, Hilden, Germany
QIAquick Gel Extraction Kit	Qiagen, Hilden, Germany
RNase-Free DNase Set	Qiagen, Hilden, Germany
High Sensitivity DNA Kit	Agilent Technologies, Santa Clara, CA, USA
Agilent RNA 6000 Nano Chip Kit	Agilent Technologies, Santa Clara, CA, USA
QIAprep Spin Miniprep Kit	Qiagen, Hilden, Germany
ONE-Glo Luciferase Assay System	Promega GmbH, Walldorf, Germany
Amaxa^{TM} P3 Primary cell 4D-Nucleofactor^{TM} X Kit L	Lonza, Basel, Switzerland
High-Capacity cDNA Reverse Transcription Kit	Thermo Fisher Scientific, Waltham, MA, USA
Pierce^{TM} Coomassie Plus (Bradford) Assay Kit	Thermo Fisher Scientific, Waltham, MA, USA
RIPA Lysis Buffer System	Santa Cruz Biotechnology, Dallas, TX, USA
Lipofectamine^{TM} 3000 Transfection Reagent	Thermo Fisher Scientific, Waltham, MA, USA
Platinum^{TM} II Hot-Start Green PCR Master Mix (2X)	Thermo Fisher Scientific, Waltham, MA, USA

3.1.13. Devices

Name	Manufacturer
Life Technologies PowerEase 90W Electrophoresis Power Supply	Thermo Fisher Scientific, Waltham, MA, USA
Mini Blot Module	Thermo Fisher Scientific, Waltham, MA, USA
Intas ECL Chemocam Imager	NTAS Science Imaging Instruments GmbH, Göttingen, Germany
Agilent 2100 BioAnalyzer	Agilent Technologies, Santa Clara, CA, USA
NanoDrop ND-1000	NanoDrop Technologies Inc., Wilmington, DE, USA
Thermomixer 5437	Eppendorf, Hamburg, Germany
NanoPhotometer® N60	Implen, Westlake Village, CA, USA
QuantStudio 5	Thermo Fisher Scientific, Waltham, MA, USA
Agilent G2545A Hybridization Oven	Agilent Technologies, Santa Clara, CA, USA
VANTAstar	BMG Labtech, Ortenberg, Germany
4D-Nucleofector Core and X Unit	Lonza, Basel, Switzerland
Vortex Genie2	Bender + Hobein, Bruchsal, Germany
Neubauer improved counting chamber	Marienfeld Superior, Lauda Konigshofen, Germany
Heracell^{TM} 150i CO2 Incubator	Heraeus, Hanau, Germany
Herasafe 2030i Safety Cabinets	Heraeus, Hanau, Germany
Megafuge 1.0R Centrifuge	Heraeus, Hanau, Germany

Centrifuge 5425 R	Eppendorf, Hamburg, Germany
Centrifuge 5420	Eppendorf, Hamburg, Germany
Eppendorf Research 0.5-10µl, 10-100µl, 20-200µl, 100-1000µl pipettes	Eppendorf, Hamburg, Germany
Voyager, 8 channels, 50µl	Integra Bioscience GmbH, Biebertal, Germany
Biometra P25 T	Analytikjena, Jena, Germany
S220 Focused-ultrasonicator	Covaris, Woburn, MA, USA
Infinite M200	Tecan Group Ltd, Männedorf, Switzerland

3.1.14. Software

Software	**Company / Accessibility**
Microsoft Office 365	Microsoft, Redmond, WA, USA
GraphPad Prism 6	GraphPad Software, La Jolla, CA, USA
GeneSpring GX 14.9	Agilent Technologies, Santa Clara, CA, USA
STRING 11.5	https://string-db.org
Affinity 1.10.4.1198	Serif(Europe)Ltd, Nottingham, UK
Biorender	BioRender.com

3.1.15. Plasmids

The plasmids pGL3-Basic-ACE2(-1119)-LUC and pCS2+N-flag-FoxO1 were provided from Addgene, Watertown, MA, USA (Gerhart Ryffel plasmid#3111053 (*83*) and Stefan Koch plasmid# 15314154 (*158*)) and were used for the transcription factor ELISA (TF-ELISA).

A

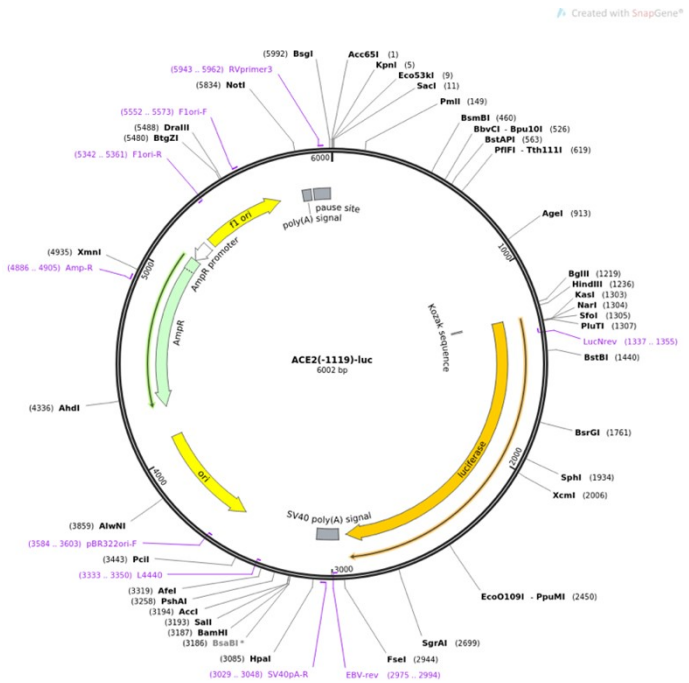

B

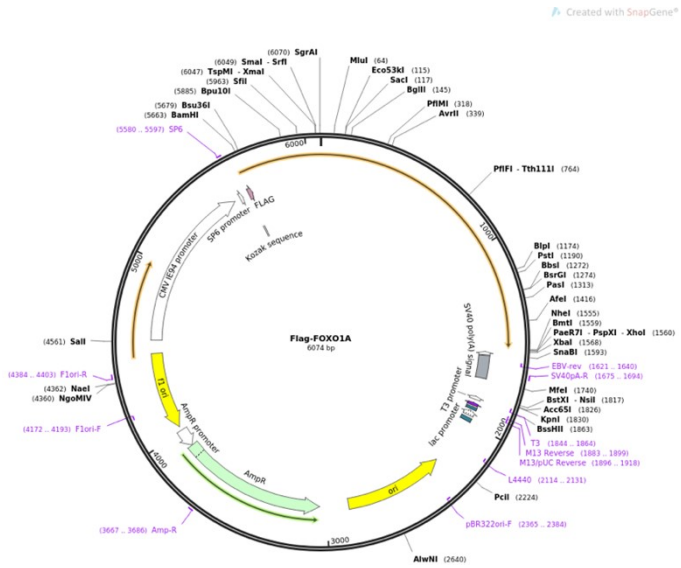

Figure 3.1 Plasmids used for TF-ELISA.
Plasmids (A) pGL3-Basic-ACE2(-1119)-LUC and (B) pCS2+N-flag-FoxO1 with their sites for restriction enzymes.

3.1.16. Consensus Sequence

The consensus sequence containing the FoxO1 binding site TTGTTTAC was designed in house and manufactured from Integrated DNA Technologies, Inc., Coralville, IA, USA.

5-BiosG/AGTGAAGTCCTAAATCAATCTGCAGTATCTGTGAGTGCGCGTGGTCTGACTTGTTTACACAGCCACA
GCTGCAGTCAGCTATGGCTCAGG

3.1.17. Blocking Sequences

For the competition experiments of the transcription factor ELISA the following Blocking sequences were generated by PCR (Table 3.2) with specific Primers (Table 3.1.10) and ACE2 Promoter Sequence as a template.

Blocking Sequence 1:

GGTACCGAGCTCGCTTCTGAAATTTGACAAGATAACCACTAAAATCTCTTTGAATTCTATGTTGTTGTGATCCC
ATGGCTACAGAGGATCAGGAGTTGACATAGATACTCTTTGGATTTCATACCATGTGGAGGCTTTCTTACTTCC
ACGTGACCTTGACTGAGTTTTGAATAGGTAAGTGAAGGAGAAGGAGGACTCAAAGAAGTCAGCCACAGAACC
AGTGTGAGAAATAGGAAATGAGCTTTTTTAAGTTTTGCAAAGGCAGATCAGGAGAGTTGACCTGTGGATGGA
GAGTAGTCATAATTTTAAAAAATGGCCATGGAAATTAAAACTGATCAGAAATGGCTGGGCACAGTGGCTCACG
CCTGTAATCCTAGCACTTTGGGAGGCCGAGTTGGGCAGATCACAAGGTCAGGAGATAGAGACCGTCCTGAC
TAACACGGTGAAACCCCGTCTCTATTAAAAATACAAAACTTAGCTGGGCGTGGTGGTGGGCACCTGTAGTCC
CAGCTACTCGGGAGGCTGAGGCAGGAGAATGGCGTGAACCTGGGAGGCAGAGCTTGCAGTGAGCCGAGAT
CGCGCCACTGTGCTCCAGCCTGGGCGACAGACCGAGACTCAGTCTCAAAAAAAAAAAAAAAAAAAAACTGA
TCAGAAATATGAATTCCATAAAGACAAGGGCA

Blocking Sequence 2:

TGCCCAAGTAGAGAGTTTCTGGGAATATGATCTTGAAATAAAAATAAATGTGAGATAACCTATTAATGAAATTG
TCTGAAAACCATACAAACACCAACATTATCTTCATGATCCCTAGTTCTAGACCTCTTTGGTCACTGTAAAATTA
TAACATTTTCCGTGTATCTTTAACAGCTTTCTAGGAAAATATTAACCAAAAGTACCGGTTTTGATTTGGCC

Blocking Sequence 3:

TCTGTCCTCTCCAGGATGAACTTTATATTGGCTCAGCAGATTGTTTACTGTGTTCTTCTTCTTTTTCTTTTTTTG
GTCTTTCCTGCTCAGCGCCCAACCCAAGTTCAAAGGCTGATAAGAGAGAAAATCTCATGAGGAGGTTTTAGT
CTAGGGAAAGTCATTCAGTGGATGTGATCTTGGCTCACAGGGGACGAGATCTGCGATCT

3.1.18. PCR Sequence

The sequence used for the transcription factor ELISA is listed below. The sequence was generated by PCR (Table 3.1) with a specific forward primer (Table 3.1.9) and pGL3-Basic-ACE2(-1119)-LUC as template. As a reverse Primer ACE2-1119-Rev-Bio was used, which contains a biotin tag.

GCCACAGAACCAGTGTGAGAAATAGGAAATGAGCTTTTTTAAGTTTTGCAAAGGCAGATCAGGAGAGTTGACCTGTGGATG
GAGAGTAGTCATAATTTTAAAAAATGGCCATGGAAATTAAAACTGATCAGAAATGGCTGGGCACAGTGGCTCACGCCTGTA
ATCCTAGCACTTTGGGAGGCCGAGTTGGGCAGATCACAAGGTCAGGAGATAGAGACCGTCCTGACTAACACGGTGAAACC
CCGTCTCTATTAAAAATACAAAAACTTAGCTGGGCGTGGTGGTGGGCACCTGTAGTCCCAGCTACTCGGGAGGCTGAGGC
AGGAGAATGGCGTGAACCTGGGAGGCAGAGCTTGCAGTGAGCCGAGATCGCGCCACTGTGCTCCAGCCTGGGCGACAG
ACCGAGACTCAGTCTCAAAAAAAAAAAAAAAAAAAAAACTGATCAGAAATATGAATTCCATAAAGACAAGGGCAAAGTCATG
TATTTGGAAGGGAAAATGTTGCCCAAGTAGAGAGTTTCTGGGAATATGATCTTGAAATAAAAATAAATGTGAGATAACCTATT
AATGAAATTGTCTGAAAACCATACAAACACCAACATTATCTTCATGATCCCTAGTTCTAGACCTCTTTGGTCACTGTAAAATT
ATAACATTTTCCGTGTATCTTTAACAGCTTTCTAGGAAAATATTAACCAAAAGTACCGGTTTTGATTTGGCCATAAAGTGACA
GGAGAGGTAAGGTTCTCTAGGATTAAAGAATAACGTATTCTTATTTGATTCACTTTAAAAAATTATTCTAAAATCTGTTACATA
TCTGTCCTCTCCAGGATGAACTTTATATTGGCTCAGCAGATTGTTTACTGTGTTCTTCTTCTTTTTCTTTTTTTGGTCTTTCCT
GCTCAGCGCCCAACCCAAGTTCAAAGGCTGATAAGAGAGAAAATCTCATGAGGAGGTTTTAGTCTAGGGAAAGTCATTCAG
TGGATGTGATCTTGGCTCACAGGGGACGAGATCTGCGATCTAAGTAAGCTTGGCATTCCGGTACTGTTGGTAAAGCCACCA
TGGAAGACGCCAAAAACATAAAGAAAGGCCCGGCGCCATTCTATCCGCTGGAAGATGGAACCGCTGGAGAGCAACTGCAT
AAGGCTATGAAGAGATACGCCCTGGTTCCTGGAACAATTGCTTTTACAGATGCACATATCGAGGTGGACATCACTTACGCT
GAGTACTTCGAAATGTCCGTTCGGTTGGCAGAAGCTATGAAACGATATGGGCTGAATACAAATCACAGAATCGTCGTATGC
AGTGAAAACTCTCTTCAATTCTTTATGCCGGTGTTGGGCGCGTTATTTATCGGAGTTGCAGTTGCGCCCGCGAACGACATT
TATAATGAACGTGAATTGCTCAACAGTATGGGCATTTCGCAGCCTACCGTGGTGTTCGTTTCCAAAAAGGGGTTGCAAAAAA
TTTTGAACGTGCAAAAAAAGCTCCCAATCATCCAAAAAATTATTATCATGGATTCTAAAACGGATTACCAGGGATTTCAGTCG
ATGTACACGTTCGTCACATCTCATCTACCTCCCGGTTTTAATGAATACGATTTTGTGCCAGAGTCCTTCGATAGGGACAAGA
CAATTGCACTGATCATGAACTCCTCTGGATCTACTGGTCTGCCTAAAGGTGTCGCTCTGCCTCATAGAACTGCCTGCGTGA
GATTCTCGCATGCCAGAGATCCTATTTTTGGCAATCAAATCATTCCGGATACTGCGATTTTAAGTGTTGTTCCATTCCATCAC
GGTTTTGGAATGTTTACTACACTCGGATATTTGATATGTGGATTTCGAGTCGTCTTAATGTATAGATTTGAAGAAGAGCTGTT
TCTGAGGAGCCTTCAGGATTACAAGATTCAAAGTGCGCTGCTGGTGCCAACCCTATTCTCCTTCTTCGCCAAAAGCACTCT
GATTGACAAATACGATTTATCTAATTTACACGAAATTGCTTCTGGTGGCGCTCCCCTCTCTAAGGAAGTCGGGGAAGCGGT
TGCCAAGAGGTTCCATCTGCCAGGTATCAGGCAAGGATATGGGCTCACTGAGACTACATCAGCTATTCTGATTACACCCGA
GGGGGATGATAAACCGGGCGCGGTCGGTAAAGTTGTTCCATTTTTTGAAGCGAAGGTTGTGGATCTGGATACCGGGAAAA
CGCTGGGCGTTAATCAAAGAGGCGAACTGTGTGTGAGAGGTCCTATGATTATGTCCGGTTATGTAAACAATCCGGAAGCG

ACCAACGCCTTGATTGACAAGGATGGATGGCTACATTCTGGAGACATAGCTTACTGGGACGAAGACGAACACTTCTTCATC

GTTGACCGCCTGAAGTCTCTGATTAAGTACAAAGGCTATCAGGTGGCTCCCGCTGAATTGGAATCCATCTTGCTCCAACAC

CCCAACATCTTCGACGCAGGTGTCGCAGGTCTTCCCGACGATGACGCCGGTGAACTTCCCGCCGCCGTTGTTGTTTTGGA

GCACGGAAAGACGATGACGGAAAAAGAGATCGTGGATTACGTCGCCAGTCAAGTAACAACCGCGAAAAAGTTGCGCGGAG

GAGTTGTGTTTGTGGACGAAGTACCGAAAGGTCTTACCGGAAAACTCGACGCAAGAAAAATCAGAGAGATCCTCATAAAGG

CCAAGAAGGGCGGAAAGATCGCCGTGTAATTCTAGAGTCGGGGCGGCCGGCCGCTTCGAGCAGACATGATAAGATACAT

TGATGAGTTTGGACAAACCACAACTAGAATGCAGTGAAAAAAATGCTTTATTTGTGAAATTTGTGATGCTATTGCTTTATTTG

TAACCATTATAAGCTGCAATAAACAAGTTAACAACAACAATTGCATTCATTTTATGTTTCAGGTTCAGGGGGAGGTGTGGGA

GGTTTTTTAAAGCAAGTAAAACCTCTACAAATGTGGTAAAATCGATAAGGATCCGTCGACCGATGCCCTTGAGAGCCTTCAA

CCCAGTCAGCTCCTTCCGGTGGGCGCGGGGCATGACTATCGTCGCCGCACTTATGACTGTCTTCTTTATCATGCAACTCGT

AGGACAGGTGCCGGCAGCGCTCTTCCGCTTCCTCGCTCACTGACTCGCTGCGCTCGGTCGTTCGGCTGCGGCGAGCGGT

ATCAGCTCACTCAAAGGCGGTAATACGGTTATCCACAGAATCAGGGGATAACGCAGGAAAGAACATGTGAGCAAAAGGCC

AGCAAAAGGCCAGGAACCGTAAAAAGGCCGCGTTGCTGGCGTTTTTCCATAGGCTCCGCCCCCCTGACGAGCATCACAAA

AATCGACGCTCAAGTCAGAGGTGGCGAAACCCGACAGGACTATAAAGATACCAGGCGTTTCCCCCTGGAAGCTCCCTCGT

GCGCTCTCCTGTTCCGACCCTGCCGCTTACCGGATACCTGTCCGCCTTTCTCCCTTCGGGAAGCGTGGCGCTTTCTCATAG

CTCACGCTGTAGGTATCTCAGTTCGGTGTAGGTCGTTCGCTCCAAGCTGGGCTGTGTGCACGAACCCCCCGTTCAGCCCG

ACCGCTGCGCCTTATCCGGTAACTATCGTCTTGAGTCCAACCCGGTAAGACACGACTTATCGCCACTGGCAGCAGCCACTG

GTAACAGGATTAGCAGAGCGAGGTATGTAGGCGGTGCTACAGAGTTCTTGAAGTGGTGGCCTAACTACGGCTACACTAGA

AGAACAGTATTTGGTATCTGCGCTCTGCTGAAGCCAGTTACCTTCGGAAAAAGAGTTGGTAGCTCTTGATCCGGCAAACAA

ACCACCGCTGGTAGCGGTGGTTTTTTTGTTTGCAAGCAGCAGATTACGCGCAGAAAAAAAGGATCTCAAGAAGATCCTTTG

ATCTTTTCTACGGGGTCTGACGCTCAGTGGAACGAAAACTCACGTTAAGGGATTTTGGTCATGAGATTATCAAAAAGGATCT

TCACCTAGATCCTTTTAAATTAAAAATGAAGTTTTAAATCAATCTAAAGTATATATGAGTAAACTTGGTCTGACAGTTACCAAT

GCTTAATCAGTGAGGCACCTATCTCAGCGATCTGTCTATTTCGTTCATCCATAGTTGCCTGACTCCCCGTCGTGTAGATAAC

TACGATACGGGAGGGCTTACCATCTGGCCCCAGTGCTGCAATGATACCGCGAGACCCACGCTCACCGGCTCCAGATTTAT

CAGCAATAAACCAGCCAGCCGGAAGGGCCGAGCGCAGAAGTGGTCCTGCAACTTTATCCGCCTCCATCCAGTCTATTAAT

TGTTGCCGGGAAGCTAGAGTAAGTAGTTCGCCAGTTAATAGTTTGCGCAACGTTGTTGCCATTGCTACAGGCATCGTGGTG

TCACGCTCGTCGTTTGGTATGGCTTCATTCAGCTCCGGTTCCCAACGATCAAGGCGAGTTACATGATCCCCCATGTTGTGC

AAAAAAGCGGTTAGCTCCTTCGGTCCTCCGATCGTTGTCAGAAGTAAGTTGGCCGCAGTGTTATCACTCATGGTTATGGCA

GCACTGCATAATTCTCTTACTGTCATGCCATCCGTAAGATGCTTTTCTGTGACTGGTGAGTACTCAACCAAGTCATTCTGAG

AATAGTGTATGCGGCGACCGAGTTGCTCTTGCCCGGCGTCAATACGGGATAATACCGCGCCACATAGCAGAACTTTAAAAG

TGCTCATCATTGGAAAACGTTCTTCGGGGCGAAAACTCTCAAGGATCTTACCGCTGTTGAGATCCAGTTCGATGTAACCCA

CTCGTGCACCCAACTGATCTTCAGCATCTTTTACTTTCACCAGCGTTTCTGGGTGAGCAAAAACAGGAAGGCAAAATGCCG

CAAAAAAGGGAATAAGGGCGACACGGAAATGTTGAATACTCATACTCTTCCTTTTTCAATATTATTGAAGCATTTATCAGGG

TTATTGTCTCATGAGCGGATACATATTTGAATGTATTTAGAAAAATAAACAAATAGGGGTTCCGCGCACATTTCCCCGAAAAG

TGCCACCTGACGCGCCCTGTAGCGGCGCATTAAGCGCGGCGGGTGTGGTGGTTACGCGCAGCGTGACCGCTACACTTGC

CAGCGCCCTAGCGCCCGCTCCTTTCGCTTTCTTCCCTTCCTTTCTCGCCACGTTCGCCGGCTTTCCCCGTCAAGCTCTAAA

TCGGGGGCTCCCTTTAGGGTTCCGATTTAGTGCTTTACGGCACCTCGACCCCAAAAAACTTGATTAGGGTGATGGTTCACG

TAGTGGGCCATCGCCCTGATAGACGGTTTTTCGCCCTTTGACGTTGGAGTCCACGTTCTTTAATAGTGGACTCTTGTTCCAA

ACTGGAACAACACTCAACCCTATCTCGGTCTATTCTTTTGATTTATAAGGGATTTTGCCGATTTCGGCCTATTGGTTAAAAAA

TGAGCTGATTTAACAAAAATTTAACGCGAATTTTAACAAAATATTAACGCTTACAATTTGCCATTCGCCATTCAGGCTGCGCA

ACTGTTGGGAAGGGCGATCGGTGCGGGCCTCTTCGCTATTACGCCAGCCCAAGCTACCATGATAAGTAAGTAATATTAAGG

TACGGGAGGTACTTGGAGCGGCCGCAATAAAATATCTTTATTTTCATTACATCTGTGTGTTGGTTTTTTGTGTGAATCGATAG

TACTAACATACGCTCTCCATCAAAACAAAACGAAACAAAACAAACTAGCAAAATAGGCTGTCCCCAGTGCAAGTGCAGGTG

CCAGAACATT-Biotin

3.2. Methods

3.2.1. Cell culture conditions

HEK293T cell line was cultured in Dulbecco´s Modified Eagle Medium (DMEM) (Thermo Fisher Scientific, Waltham, MA, USA) containing 10% Fetal Bovine Serum (FBS) (Bio&SELL GmbH, Nürnberg, Germany), and 1% Penicillin Streptomycin (Thermo Fisher Scientific, Waltham, MA, USA).Calu3 cell line was cultured with MEM Medium (Thermo Fisher Scientific, Waltham, MA, USA), 10% Fetal Bovine Serum (FBS) (Bio&SELL GmbH, Nürnberg, Germany), 1% Penicillin Streptomycin (Thermo Fisher Scientific, Waltham, MA, USA) and 1% L-Glutamine (Thermo Fisher Scientific, Waltham, MA, USA). Human primary bronchial epithelial cells (NHBEs, Lonza, Basel, Switzerland) originating from genetically independent donors were cultured with BEGM^{TM} Bronchial Epithelial Cell Growth Medium BulletKit^{TM} containing supplements (Lonza, Basel, Switzerland).

3.2.2. IFN and inhibitor treatment

Cells were seeded into 6-well plates (Corning, Glendale, AZ, USA) or 12-well plates for either immunoblotting or quantitative expression analysis by quantitative Real Time PCR (RT-qPCR). The cells were cultured until 90% confluence, incubated for 24 hours with their specific media without FBS or supplements (starving medium) and afterwards stimulated according to the individual treatments. Experiments using HEK293T and Calu3 cell lines were repeated at least three times. Cells were stimulated for two, four, or six hours for RT-qPCR readout with: IFN-α (Roche, Basel, Switzerland or Pbl assay Science, Piscataway, NJ, USA, 30IU/ml, 300IU/ml, 3000IU/ml), IFN-β (Peprotech, Rocky Hill, NJ, USA, 10IU/ml, 100IU/ml, 1000IU/ml), IFN-γ (PromoCell GmbH, Heidelberg, Germany, 20IU/ml, 200IU/ml, 2000IU/ml), IFN-λ1 (Biotechne, Minneapolis, MN, USA, 10ng/ml, 100ng/ml, 1000ng/ml) or IFN-λ3 (Biotechne, Minneapolis, MN, USA, 10ng/ml, 100ng/ml, 1000ng/ml). For the negative control cells were treated with starving medium. 30 minutes prior to IFN stimulation, cells were treated for inhibitor experiments with FoxO1 inhibitor AS1842856 (Selleck Chemicals LLC, Houston, TX, USA, 1μM), JAK inhibitor tofacitinib citrate (Sigma-Aldrich, Merck, Darmstadt, Germany, 1μM), STAT inhibitor SH-4-54 (Selleck Chemicals LLC, Houston, TX, USA, 0.01μM, 0.1μM, 1μM, 10μM) or AKT inhibitor Capivasertip (Selleck Chemicals LLC, Houston, TX, USA, 0.01μM, 0.1μM, 1μM, 10μM) and afterwards stimulated with IFNs (IFNα 300IU/ml, IFNβ 100IU/ml, IFNγ 200IU/ml, IFNλ1 100ng/ml or IFNλ3 100ng/ml) for two, four or six hours. Cells were treated with starving medium as a negative control. For immunoblotting readout, the cells were stimulated for 24 hours

with type-I and -III IFNs and AS1842856 was added 30 minutes prior to IFN treatment (IFNα 300IU/ml or IFNλ3 100ng/ml, 1μM AS1842856). For RT-qPCR readout, cells were harvested with RLT-Buffer (Qiagen, Hilden, Germany) and RNeasy Mini Kit was used for RNA extraction according to manufacturer's protocol (Qiagen, Hilden, Germany). For the immunoblotting harvest, cells were treated with 0.05% Trypsin-EDTA (1x) (5 minutes, Thermo Fisher Scientific, Waltham, MA, USA), washed with Dulbecco´s Phosphate Buffered Saline (Thermo Fisher Scientific, Waltham, MA, USA), the pellet was shock-frosted in liquid nitrogen and stored at -80℃ until further use.

3.2.3. Quantitative expression analysis by Real Time PCR (RT-qPCR)

First High-Capacity cDNA Reverse Transcription Kit (Thermo Fisher Scientific, Waltham, MA, USA) was used for reverse transcription of the extracted RNA into cDNA according to manufactures instructions. For each RT-qPCR reaction (total volume 10μl) the following reagents were mixed: 12ng cDNA, 64nM forward and reverse Primers specific for each target region (Metabion, Planegg, Germany) and 5μl FastStart Universal SYBR Green Master (Rox) (Sigma-Aldrich, Merck, Darmstadt, Germany), which incorporates into double-stranded DNA during amplification. The RT-qPCR readout was performed and analyzed using QuantStudio 5 (Thermo Fisher Scientific, Waltham, MA, USA) according to manufacturer's protocol. To detect ACE2 full-length or the truncated isoform (truncACE2), specific primers were designed binding to the specific sequence of the isoforms (Figure 3.2). The ΔΔCt Method and $2^{(-\Delta\Delta Ct)}$ after normalization to housekeeping genes *ACTINB* and *HPRT* were used to calculate fold changes (*159*); (*160*).

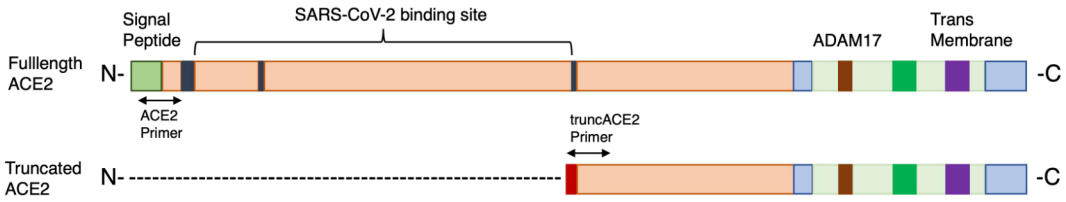

Figure 3.2 ACE2 full-length and truncACE2.
Trunc ACE2 lacks the SARS-CoV-2 spike protein interaction site and starts with a novel exon within intron 9. Specific primers were designed to detect ACE2 full-length and truncACE2.

3.2.4. Immunoblotting

Cells were lysed using 50µl RIPA Lysis Buffer System (Santa Cruz Biotechnology, Dallas, TX, USA) per sample according to manufacturer's protocol and protein concentration was determined using Pierce^{TM} Coomassie Plus (Bradford) Assay Kit (Thermo Fisher Scientific, Waltham, MA, USA) according to manufacturer's instructions. Samples containing Novex^{TM} NuPAGE^{TM} LDS-Probenpuffer (4X) (1:4 ratio, Thermo Fisher Scientific, Waltham, MA, USA), 1µl of NuPAGE^{TM} Probenreduktionsmittel (10x) (Thermo Fisher Scientific, Waltham, MA, USA) and 20µg cell lysate were heated to 95°C for 10 minutes. Protein solutions (10µl) were loaded onto NuPAGE^{TM} 10%, Bis-Tris, 1,0–1,5mm, Mini-Protein-Gele (Thermo Fisher Scientific, Waltham, MA, USA). To estimate correct protein molecular weight PageRuler^{TM} Plus Prestained Protein Ladder, 10 to 250kDa (5µl, Thermo Fisher Scientific, Waltham, MA, USA) was additionally loaded onto the gel. The proteins were separated for 30 minutes with 50V and 50 minutes with 150V with Life Technologies PowerEase 90W Electrophoresis Power Supply (Thermo Fisher Scientific, Waltham, MA, USA). Afterwards the gel was transferred onto Immobilon-P membrane, PVDF (Millipore, Merck, Darmstadt, Germany) for 90 minutes at 25V. Blocking was performed in Tris-Bis Buffer (1x) containing 1% Tween®20 (Merck, Darmstadt, Germany) and 5% non-fat dried milk powder (Applicam, Darmstadt, Germany) (TBS-T-Milk) for 1 hour at room temperature (RT). The membrane was incubated overnight at 4°C with a specific first antibody against the target protein in TBS-T-Milk, diluted at an antibody-specific dilution ratio (Table 3.1.6). Afterwards, the membrane was washed two times with TBS-T (20ml, 10 minutes, RT) and incubated with the according horse-radish peroxidase (HRP)-conjugated secondary antibody (Table 3.1.7) in 10ml TBS-T-Milk or TBS-T-BSA (1:5000 dilution) for 30 minutes. Following two washes with TBS-T (20ml, 10 minutes) and one wash with TBS (20ml, 10 minutes), membranes were incubated with detection mix SuperSignal^{TM} West Femto Maximum Sensitivity Substrat (Protein of interests, Thermo Fisher Scientific, Waltham, MA, USA) or SuperSignal^{TM} West Pico PLUS Chemilumineszenz-Substrat (Loading control, Thermo Fisher Scientific, Waltham, MA, USA). Intas ECL Chemocam Imager (NTAS Science Imaging Instruments GmbH, Göttingen, Germany) was used to visualize the protein bands. GAPDH was used as a loading control.

3.2.5. CRISPR/Cas9 knock-out

The whole CRISPR/Cas9 knock-out experimental set-up was adapted to a 100µl Nucleofaction Cuvette (total Volume 100µl, Lonza, Basel, Switzerland). A specific Alt-R CRISPR-Cas9 crRNA (4µl, CTCACCCATTATGACCGAAC, Integrated DNA Technologies, Inc., Coralville, IA, USA) binding to the FoxO1 sequence was added in a 1:1 ratio to Alt-R CRISPR-Cas9 tracrRNA (4µl, Integrated DNA Technologies, Inc., Coralville, IA, USA). An enzyme mix including the crRNA/tracrRNA-mix, Alt-R S.p. HiFi Cas9 Nuclease V3 (Integrated DNA Technologies, Inc., Coralville, IA, USA), Amaxa^{TM} P3 Primary cell 4D-Nucleofactor^{TM} X Kit mix (Lonza, Basel, Switzerland) and Alt-R Cas9 Electroporation Enhancer (Integrated DNA Technologies, Inc., Coralville, IA, USA) was mixed with a total volume of 26.25µl. Therefore, the crRNA/tracrRNA-mix (7.56µl) was added in a 3:1 ratio to Alt-R S.p. HiFi Cas9 Nuclease V3 (4.2µl). Additionally, Amaxa^{TM} P3 Primary cell 4D-Nucleofactor^{TM} X Kit mix (9.24µl) and Alt-R Cas9 Electroporation Enhancer (5.25µl) were added to the enzyme mix according to manufacturer's protocol. Low passaged NHBEs were treated with 0.05% Trypsin-EDTA (Thermo Fisher Scientific, Waltham, MA, USA) and at least 1 x 10^5 cells were added to the enzyme mix. As a negative control, the Alt-R CRISPR Cas9 negative control crRNA (Integrated DNA Technologies, Inc., Coralville, IA, USA) was used. Following the nucleofection with 4D-Nucleofector Core and X Unit (Pulse: DC-100), cells were incubated for 10 minutes at RT. Cells were incubated in warm BEGM media, containing supplements, and after recovery they were subsequently seeded into 12-well plates or 6-well plates for either RT-qPCR or immunoblotting readout. The successful knock-out was verified with immunoblotting.

3.2.6. Plasmid amplification

The transcription factor Enzyme-linked Immunosorbent Assay (TF-ELISA) and all steps necessary for these experiments were performed with the support of Dr. Soheila Asoudeh Moghanloo. One Shot TOP10 Chemically Competent E. coli (Thermo Fisher Scientific, Waltham, MA, USA) were transformed with 1µl containing 10-20ng of pCS2+N-flag-FoxO1 or pGL3-Basic-ACE2(-1119)-LUC plasmid (Addgene, Watertown, MA, USA, Gerhart Ryffel plasmid#3111053 (*83*) and Stefan Koch plasmid# 15314154 (*158*)) for 30 seconds at 42℃. Afterwards, 250µl of S.O.C medium (Thermo Fisher Scientific, Waltham, MA, USA) was added to each bacterial mix and was incubated at 37℃ for 1 hour at 225rpm according to manufacturer's instructions. The bacteria were plated onto lysogeny broth (LB) agar (Sigma-Aldrich, Merck, Darmstadt, Germany) containing ampicillin (100µg/ml, Sigma-Aldrich, Merck, Darmstadt, Germany). Grown colonies were picked and transferred in LB medium containing ampicillin (100µg/ml) and incu-

bated at 37℃ overnight. DNA vectors were purified from bacterial culture using the QIAprep Spin Miniprep Kit (Qiagen, Hilden, Germany) according to manufacturer's instructions. The vector sequences were verified using DNA sequencing (Eurofins, Ebersberg, Germany).

3.2.7. Transfection for TF-ELISA

HEK293T cells were transfected with pCS2+N-flag-FoxO1 or pGL3-Basic-ACE2(-1119)-LUC. For TF-ELISA the plasmid pCS2+N-flag-FoxO1 was transfected into the cell line and used for FoxO1 overexpression. Therefore, HEK293T cells (3 x 10^5 cells per well) were plated in 6-well dishes, incubated for 24 hours at 37℃ and were transfected with Lipofectamine^{TM} 3000 Transfection Reagent (Thermo Fisher Scientific, Waltham, MA, USA) according to the manufacturer's instructions (2.5µg plasmid per well). Afterwards, cells were harvested to gain protein lysate containing overexpressed FoxO1.

3.2.8. Cell lysis for TF-ELISA

Cell lysis was performed with HEK293T cells transfected with pCS2+N-flag-FoxO1 24 hours post-transfection. Therefore, cells were harvested with 0.05% Trypsin-EDTA (Thermo Fisher Scientific, Waltham, MA, USA) and the pellet was resuspended in 100µl buffer A and cytosolic protein suspension was collected after centrifugation (5 seconds at 13,200rpm). Additionally, the pellet was washed in buffer A and centrifuged for 5 seconds at 13,200rpm and resuspended in 130µl buffer B. To gain the nuclear fraction, the protein lysate was sonicated by S220 Focused-ultrasonicator (Tube: 130µl, PN520045, Holder: PN500114, PIP: 105, DF: 2, CPB: 200, Time-course: 3 minutes, Tempreture: 6 ℃, Covaris, Woburn, MA, USA). After centrifugation (5 seconds at 13,200rpm), the preserved supernatant, which contained nuclear proteins was collected and further used for TF-ELISA. The protein concentration of the nuclear and cytosolic fraction was measured using Pierce^{TM} Coomassie Plus (Bradford) Assay Kit (Thermo Fisher Scientific, Waltham, MA, USA) according to manufacturer's instructions.

3.2.9. Amplification of ACE2-(1119)-LUC promoter fragments for TF-ELISA

To gain a pGL3-Basic-ACE2(-1119)-LUC promoter fragment for TF-ELISA, the sequence of the proximal ACE2 promoter of the plasmid was amplified by polymerase chain reaction (PCR) using a specific forward primer and biotinylated reverse primer. Sequences generated for the competition experiment for the transcription factor ELISA were generated with PCR using specific primers and ACE2 promoter sequence as a template. Table 3.2 describes the program used to generate all blocking sequences. PCR reaction was adapted according to primer sequences and length of the PCR product (Table 3.1). The PCR was conducted using

Platinum^{TM} II Hot-Start Green PCR Master Mix (2X) (Thermo Fisher Scientific, Waltham, MA, USA) according to manufacturer's instructions. MinElute PCR Purification Kit (Qiagen, Hilden, Germany) was used to purify the PCR products, the sequence length was verified by 2% agarose gel electrophoresis and additionally confirmed by sequencing (Eurofins Genomics Germany GmbH, Ebersberg, Germany).

Table 3.1 PCR program generating the promoter sequence

Steps	**Temperature**	**Time**
Initial denaturation	94℃	2 minutes
Denaturate (35 cycles)	94℃	15 seconds
Annealing	60℃	15 seconds
Extension	68℃	5 minutes

Table 3.2 PCR program generating the blocking sequence 1-3

Steps	**Temperature**	**Time**
Initial denaturation	94℃	2 minutes
Denaturate (35 cycles)	94℃	15 seconds
Annealing	60℃	15 seconds
Extension	68℃	30 seconds

3.2.10. TF-ELISA

First, Pierce^{TM} Streptavidin Coated High-Capacity Plate, 384-wells (Thermo Fisher Scientific, Waltham, MA, USA) was washed three times with TF-ELISA washing buffer. Afterwards, biotinylated ACE2 promoter sequence and FoxO1-consensus sequence were added to the plate (1pmol/well) and incubated for one hour at RT. The plate was washed three times with TF-ELISA washing buffer and overexpressed FoxO1 nuclear protein lysate (1μg/μl) was added and incubated for one hour at room temperature. To block unspecific binding the nuclear extract was added in the presence of 5μg poly(deoxyinosinic-deoxycytidylic) acid (Sigma-Aldrich, Merck, Darmstadt, Germany). For the competition experiments, first FoxO1 protein lysate (1μg/μl) was incubated with blocking sequences 1, 2 or blocking sequence 3 (1pmol/well) and 5μg poly(deoxyinosinic-deoxycytidylic) acid (Sigma-Aldrich, Merck, Darmstadt, Germany) for

two hours at 4℃. Afterwards, the FoxO1-blocking sequences mix was added to the biotinylated ACE2 promoter sequence and the consensus sequence and was incubated at RT for one hour. As negative control, FoxO1 nuclear lysate was added without the ACE2 promoter sequence or consensus sequence and samples were incubated for one hour. After three wash cycles with TF-ELISA blocking buffer, the wells were incubated with the primary antibody FoxO1 (1:200 in TF-ELISA blocking buffer; Cell Signaling Technology Inc, Danvers, MA, USA) for two hours at 4℃. An HRP-conjugated secondary antibody anti-mouse (1:3000 in TF-ELISA blocking buffer; Cell Signaling Technology Inc, Danvers, MA, USA) was added after three additionally wash cycles with TF-ELISA blocking buffer and incubated for one hour at 4℃. Next, the plate was washed four times with TF-ELISA blocking buffer and 3,3´,5,5´-tetramethylbenzidin (TMB, Sigma-Aldrich, Merck, Darmstadt, Germany) was added to the wells. The reaction was stopped after five minutes by adding 2M H_2 SO_4 (Merck, Darmstadt, Germany). Absorbance at 450nm was measured using VANTAstar (BMG Labtech, Ortenberg, Germany).

3.2.11. Air-liquid interface organoid cultures

To generate air-liquid interface organoid cultures (ALI), six genetically independent NHBE donors were grown in PneumaCult-Ex Plus expansion medium (Stemcell Technologies, Vancouver, Canada) on Corning transwell polyester membrane cell culture inserts (precoated with 1% collagen, Merck, Darmstadt, Germany) as previously described (*161*). The differentiated ALIs were stimulated with IFN-α, IFN-β, IFN-γ, IFN-λ1, IFN-λ3 and starving medium as a negative control for 24 hours as described before (*161*).

3.2.12. Genome-wide microarray-based gene expression analysis

Extracted total RNA from ALI cultures (25ng) and from nasal scrapings (12ng) were hybridized and measured with SurePrint G3 Human gene exp v3 Array Kit (Agilent, Santa Clara, USA) according to manufacturer´s protocol. Cyanine-3 (Cy3) labeled sRNA was prepared using the One-Color Agilent Low Input Quick Amp Labeling Kit (Agilent, Santa Clara, USA). RNAeasy column purification (Qiagen, Hilden, Germany) was used for sample purification and dye incorporation and sRNA yield were analyzed with NanoDrop ND-1000 Spectrophotometer. 600ng Cy3-labelled cRNA with a specific activity above 6pmol (Cy3/μg cRNA) was processed and hybridized to Agilent Whole Human genme Oligo Microarrays (G4112A) by a rotating Agilent hybridization oven for 17 hours at 65℃. Agilent DNA Microarray Scanner (G2505B) with one color scan setting (8 x 60k array slides, 61 x 21.6mm scan area, 3μm scan resolution, green and 20 bit tiff dye channel) was used to scan the slides.

3.2.13. Study population and design

In the adult arm of the ALL Age Asthma Cohort (ALLIANCE) of the German Center for Lung Research, 255 genetically independent adults with age ≥ 18 years were recruited at the study centers Grosshandsdorf and Borstel, Germany between 2013 and 2016. The comparability between study centers and cohort arms were ensured using standard operating procedures (SOPs) for each procedure (*162*). 208 patients demonstrated an established diagnosis of asthma according to current guidelines of the Global Initiative for Asthma (GINA) (*163*); (*164*) and 47 patients were part of the healthy control group. The study was approved by local ethic committees and is registered at clinicaltrials.gov (pediatric arm: NCT02419274). 2-3mg samples were collected using Asi Rhino-Pro® cuvettes (Arlington Scientific, Springville, UT, USA). Total RNA was extracted from 238 nasal samples (27 samples from *N*=27 healthy individuals, 211 samples from *N*=150 asthmatics including follow up samples) by AllPrep 96 DNA/RNA Kit (Qiagen, Hilden, Germany) according to manufacture´s instructions and genome-wide microarray-based gene expression analysis was performed with extracted RNA. RNA concentration and quality was analyzed using Nano Bioanalyzer (Agilent, Santa Clara, USA). Patient characteristics are listed in Table 3.3. Detailed description of the study design, inclusion and exclusion criteria were highlighted in previous publications (*162*); (*165*).

Table 3.3 Subject characteristics.
ATS/ERS Severity describes the severity classification according to ERS/ATS guideline 2014 and based on ICS dosage and/or oral corticosteroid use and asthma control (ACT or ACQ), frequency of exacerbations, and lung function (FEV1). Eosinophilic Asthma describes the classification for severity and type of inflammation according to ERS/ATS guideline 2014. Eosinophilia was defined according to >= or < 300 Eosinophils absolute per μl blood. Current smoking or former smoking was defined with >= 10 pack years (PY). Data depict the frequencies of the two subject groups healthy and asthma and are presented as *N*, *N* (%). Age is depicted as median with range.

	Healthy	**Asthma**
Included Subjects *N*=177	*N*=27	*N*=150
Male	13 (48.1%)	65 (43.3%)
Age	61.00 [26.00-79.00]	59.50 [21.00-88.00]
ATS/ERS Severity		
Mild-moderate Asthma	n.a.	67 (44.7%)
Severe Asthma	n.a.	74 (49.3%)
Eosinophilic Asthma		

Smoking asthmatic	n.a.	17 (11.3%)
Severe, eosinophilic asthmatic	n.a.	24 (16.0%)
Severe, non-eosinophilic asthmatic	n.a.	16 (10.7%)
Mild/moderate, eosinophilic asthmatic	n.a.	21 (14.0%)
Mild/moderate, non-eosinophilic asthmatic	n.a.	28 (18.7%)

3.2.14. Statistical Analysis

GraphPad Prism 6 (GraphPad Software, La Jolla, CA, USA) was used to statistically analyze the transcriptomic experiments. The two-tailed Mann-Whitney U test were employed to assess the statistical significance with samples from NHBEs, whereas the Student's t-test were used for samples from Calu3 cell lines and TF- ELISA. A significance level of $^{*}P \leq .05$, $^{**}P \leq .01$, $^{***}P \leq .001$ was considered statistically significant. The statistically analysis of the gene expression of IFN-stimulated air liquid interface organoid cultures was performed with GeneSpring GX 14.9 (Agilent Technologies, Santa Clara, CA, USA) as described in Erb et al (*161*). Significantly regulated genes were concluded in GeneOntology (GO) terms and entity lists (Supplementary Table 9.1-9.21). To segregate specific genes the following GO-terms were used: ISGs: "0070254", "0097072", "0001730", "0035394" and the gene symbols IFITM and IFIT; pro- and anti-inflammatory genes: "0033209", "0032640", "0034612", "0006954", "0050727", "0002526", "0032611", "0070555", "2000661", "0032635", "0004915", "0070741", "0070103", "0036363", "0071604", "0004920", "0032613", "0050728", "0140105", "0032733"; epithelial factors: "0060429", "0060428", "0030054", "0016049", "0098609", "0090136", "0034103", "0070160", "0030057", "0070160", "0120193","0005923", "0005915" and "0005921". Genes associated with SARS-CoV-2 infection were segregated with the following GO-terms: "0097011", "0097012", "1990661", "1990662", "0032635", "0070741", "0098609", "0085033", "0006954", "0050727", "0002526", "0008236" and "0098594". Significantly differential expressed hits were genes with $FC \geq 1.5$ (fold change) and $P \leq 0.05$, classified by moderated t-test and were marked with asterisks within each of the associated heat maps. Extracted mRNA from nasal scrapings of *N*=238 asthmatic patients and healthy individuals were statistically analyzed using GeneSpring GX 14.9 (Agilent Technologies, Santa Clara, CA, USA) as previously described (*161*). Genes demonstrating a $FC \geq 1.5$ (fold change) and $P \leq 0.05$ by using moderated t-test were considered as significantly differential expressed hits and are marked with asterisks

in the heatmaps. Benjamin Hochberg (FDR) correction was applied to the gene expression analysis to correct multiple testing. The significantly regulated genes related to IFN expression, SARS-CoV-2 infection, KKS system, acute phase of inflammation and ISGs were summarized in entity lists (Supplementary Table 9.22-9.31). To gain gene clusters, Manhattan cityblock on entities (Ward's linkage) was performed. Affinity 1.10.4.1198 (Serif(Europe)Ltd, Nottingham, UK) and Biorender (BioRender.com) was used to visualize graphs and figures.

Chapter 4

Results

4. Results

4.1. Differential effects on inflammation and epithelial integrity after IFN stimulation

4.1.1. Induction of similar ISGs by type-I, -II and -III IFNs

IFNs are the first line of the innate immune system and the induction of ISGs is crucial for the antiviral cell state. To investigate the impact of IFNs on airway epithelium regarding ISG expression and epithelial composition, primary organotypic 3D air-liquid interface airway cultures (ALIs) were stimulated for 24 hours with type-I, -II and -III IFNs to simulate the early IFN release after viral infection as previously described in Erb et al (*161*). The transcriptome of ALIs was analyzed using whole-genome microarray. The data were grouped according to IFN treatment and 5,107 upregulated genes and 2,208 downregulated genes for IFN-α, 888 upregulated genes and 152 downregulated genes for IFN-β, 3,454 upregulated genes and 2,475 downregulated genes for IFN-γ, 1,920 upregulated genes and 909 downregulated genes for IFN-λ1 and 2,882 upregulated genes and 700 downregulated genes for IFN-λ3 ($P \leq .05$; $FC \geq 1.5$) were identified in comparison to unstimulated cultures (Figure 4.1). The regulation of differential expressed genes (DEGs) highlighted that among the IFN family members, IFN-α demonstrated the most significant effect on upregulating ALI expression patterns. On the other hand IFN-β induced least genes in comparison to other IFNs. All IFNs upregulated DEGs rather than downregulated DEGs.

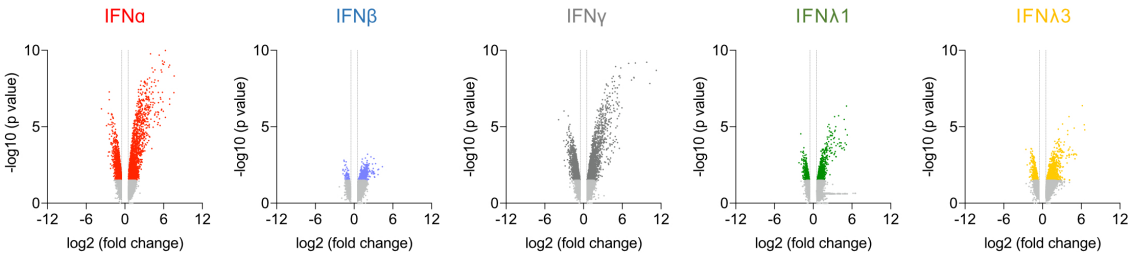

Figure 4.1 Whole genome analysis of IFN-stimulated ALIs.
ALIs were stimulated with type-I, -II and -III IFNs. Extracted RNA was analyzed with whole transcriptome microarray approach (n=8). Volcano blot of statistically significant entities ($P \leq .05$; $FC \geq 1.5$) comparing IFN-α (red), IFN-β (blue), IFN-γ (grey), IFN-λ1 (green), IFN-λ3 (yellow)- stimulated and unstimulated cultures (*161*).

GeneOntology (GO) annotation of induced genes confirmed the validity of ALI cultures and revealed a high overlap in the induction of known ISGs by different IFN family members (Figure 4.2). In general, up to 19 entities were regulated by IFNs, and among them, type-I IFNs shared 16 upregulated genes with type-II and -III IFNs ($P \leq .05$; Figure 4.2A). Furthermore, type-II IFNs induced 17 ISGs similar to type-III IFN. Notably, among these upregulated ISGs *OAS1, OAS2, OAS3, OASL, IFITM1*, and *IFIT2* were the most prominent and strongly upregulated by IFN-α and type-III IFNs (Figure 4.2B). Specifically, IFN-α and IFN-γ each uniquely upregulated one (*IFIT1B*) or two genes (*VAMP2* and *VAMP8*), respectively.

Overall, whole-genome expression analysis was used to investigate the impact of IFN stimulation on ALIs. The analysis revealed the induction of similar ISGs by all IFN family members and demonstrated the overlapping role of IFNs regarding the antiviral cell state. As a next step the impact of IFNs on other pathways associated with viral infection has been analyzed.

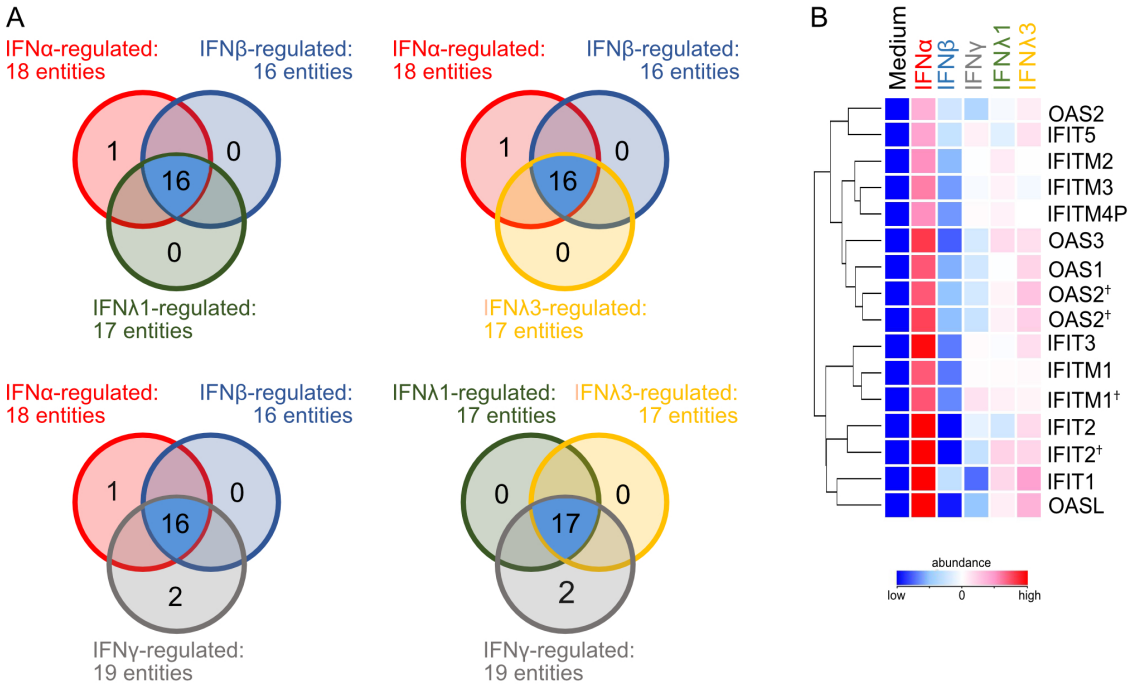

Figure 4.2 IFNs induced similar ISG in ALIs.
(A) Venn blot of overlapping regulated ISGs by type-I, -II, and -III IFNs stimulation (IFN-α (red), IFN-β (blue), IFN-γ (grey), IFN-λ1 (green), IFN-λ3 (yellow)). Blue area indicates the overlapping regulated ISGs. T-test of IFN-stimulated vs unstimulated cultures ($P \leq .05$; $FC \geq 1.5$). (B) Heat map of overlapping upregulated ISGs by type-I, -II, and -III IFN. Duplicate gene names are marked with a cross and indicate the occurrence of two or more transcripts of the same gene in the analysis. Grouped genes are represented by similar expression patterns and hierarchical clustering. Their connection was described by dendrograms to the left and each row represents, indicated by the color, the intensity of their abundance across each group (*161*).

4.1.2. Pro-inflammatory pathways and homeostatic environment enhanced by IFNs

To assess the induction of pro- or homeostatic state in the airway epithelium, ALI cultures were examined for pro- and anti-inflammatory factors using the GO annotation. IFN family members induced more pro-inflammatory genes compared to ISGs (Figure 4.3A). Especially, IFN-α and IFN-γ-stimulated cultures showed an upregulation of over 140 pro-inflammatory genes, whereas IFN-β and type-III IFNs induced up to 60 genes. Importantly, there was limited overlap in pro-inflammatory genes among the analyzed IFNs. Type-I IFNs shared up to eight similar pro-inflammatory genes with type-III IFNs, whereas type-II IFNs shared 23 regulated genes common with type-III IFNs. Genes such as *IL36RN, STAT1, USP18*, and *CXCL10* were induced in all type-I, -II, and -III IFN-stimulated ALI cultures compared to unstimulated cultures. Moreover, IFN-α and IFN-γ enhanced the expression of pro-inflammatory genes, such as *CXCL9, CXCL11, GBP5, CD38, JAK2*, and *APOL3* compared to unstimulated cultures (Figure 4.3C,E). In contrast, IFN-β induced pro-inflammatory DEGs, such as *AOC3, H2BC1*, and *CD70*, while IFN-λ3 upregulated *AKNA* and the chemokine *CXCL13*. IFN-λ1 stimulation, on the other hand, demonstrated an attenuated regulation of pro-inflammatory DEGs (*CXCL10* and *IL36RN*) compared to unstimulated cultures and the other IFNs.

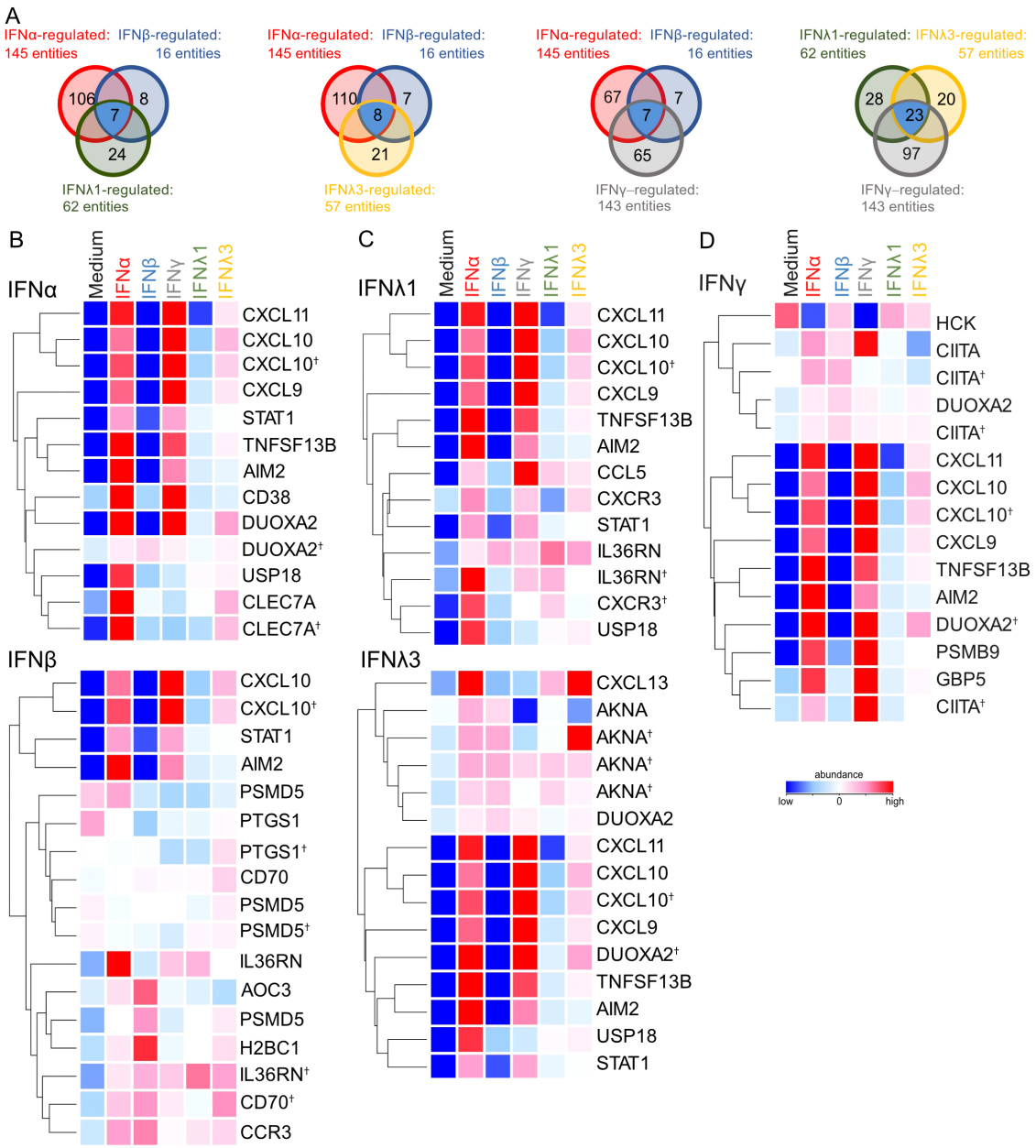

Figure 4.3 Differential expressed pro-inflammatory genes induced by type-I, -II and -III IFNs.
(A) Venn blot of overlapping regulated pro-inflammatory genes by type-I, -II, and -III IFNs stimulation (IFN-α (red), IFN-β (blue), IFN-γ (grey), IFN-λ1 (green), IFN-λ3 (yellow)). Blue area indicates the overlapping regulated pro-inflammatory genes. T-test of IFN-stimulated vs unstimulated cultures ($P \leq .05$; $FC \geq 1.5$). (B) Heat map of induced pro-inflammatory genes by type-I IFNs (t-test IFN-α-stimulated; t-test IFN-β-stimulated vs unstimulated cultures), (C) by type-III IFNs (t-test IFN-λ1-stimulated; IFN-λ3-stimulated vs unstimulated cultures) and (D) type-II IFNs (t-test IFN-γ-stimulated vs unstimulated cultures). Duplicate gene names are marked with a cross and indicate the occurrence of two or more transcripts of the same gene in the analysis. Grouped genes are represented by similar expression patterns and hierarchical clustering. Their connection was described by dendrograms to the left and each row represents, indicated by the color, the intensity of their abundance across each group (*161*).

In contrast, IFN-α, IFN-γ and type-III IFNs additionally regulated anti-inflammatory genes (Figure 4.4A, B). Notably, only one anti-inflammatory gene (*METRNL*) was induced by IFN-β. *METRNL* was also regulated by IFN-α and IFN-γ, while type-III IFNs did not show any overlapping anti-inflammatory genes with the other IFNs.

IFN-α-stimulated cultures showed downregulated anti-inflammatory genes such as *BCR*, whereas genes such as *CNR2* and *NT5E* were upregulated compared to unstimulated samples. IFN-γ downregulated pro-inflammatory genes in ALI cultures, such as *TSLP* and *PBK* compared to unstimulated cultures, while genes associated with cell proliferation and differentiation, such as *ACP5, CALCRL*, and *PTPN2*, were also upregulated by type-II IFN (Figure 4.4D). The microarray data revealed that all analysed IFNs upregulated anti-inflammatory genes, such as *IL12B* and *IL22RA2*, with IFN-λ3 showing the strongest impact on anti-inflammatory DEG expression by uniquely upregulating the regulatory cytokine *IL10* (Figure 4.4B-D).

Taken together, type-I, -II, and -III IFN stimulation resulted in differential chemokine expression. IFN-α and IFN-γ in particular enhanced the expression of pro-inflammatory genes. Simultaneously, IFNs, but especially IFN-λ3 stimulation, led to the induction of homeostatic, anti-inflammatory factors such as *IL10*. To further examine the impact of IFNs on the epithelial composition, the 3D model was used to analyze epithelial integrity following IFN stimulation.

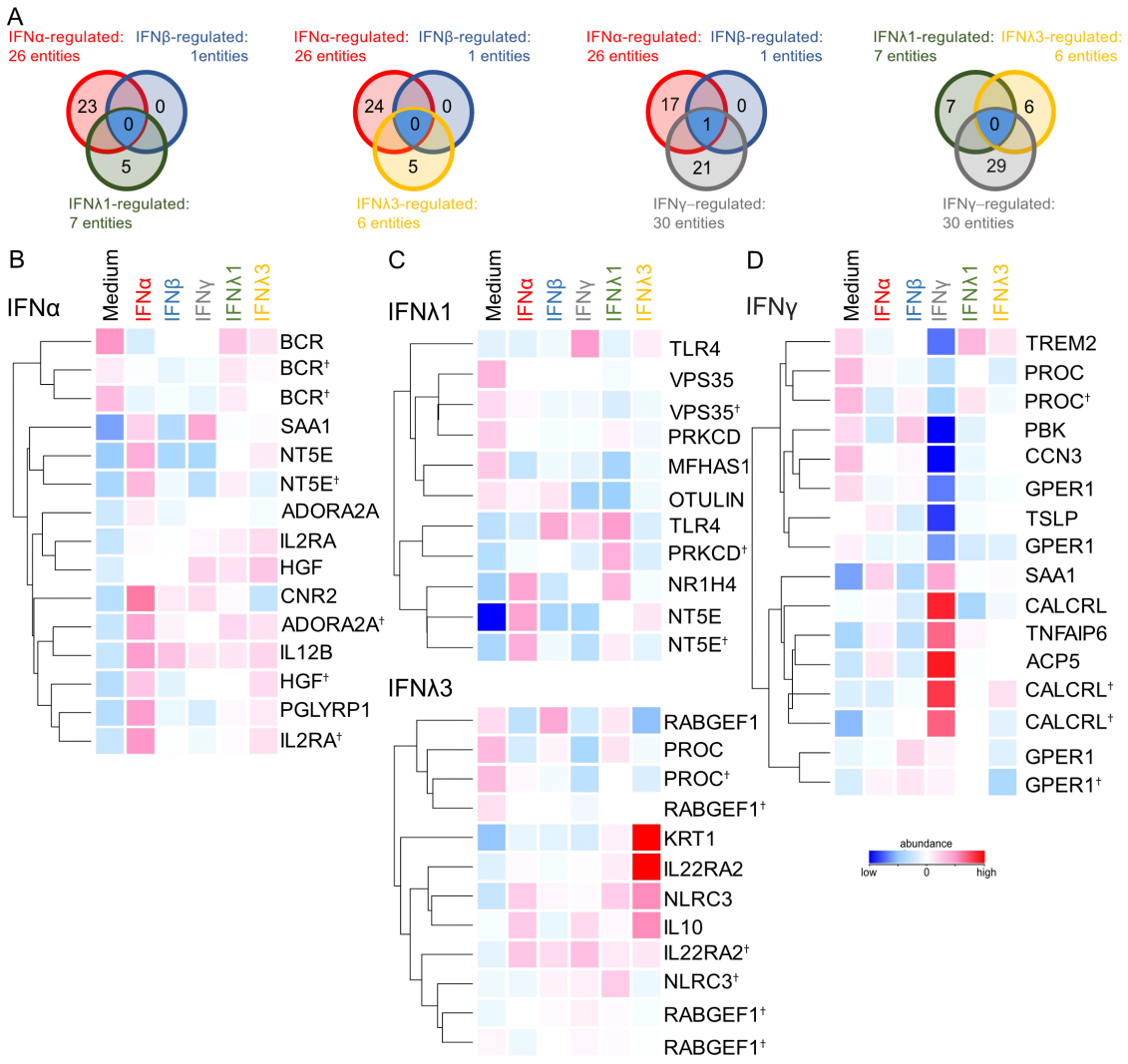

Figure 4.4 Differential expressed anti-inflammatory genes induced by type-I, -II and -III IFNs.
(A) Venn blot of overlapping regulated anti-inflammatory genes by type-I, -II, and -III IFNs stimulation (IFN-α (red), IFN-β (blue), IFN-γ (grey), IFN-λ1 (green), IFN-λ3 (yellow)). Blue area indicates the overlapping regulated anti-inflammatory genes. T-test of IFN-stimulated vs unstimulated cultures ($P \leq .05$; $FC \geq 1.5$). (B) Heat map of induced pro-inflammatory genes by type-I IFNs (t-test IFN-α-stimulated; t-test IFN-β-stimulated vs unstimulated cultures), (C) by type-III IFNs (t-test IFN-λ1-stimulated; IFN-λ3-stimulated vs unstimulated cultures) and (D) by type-II IFNs (t-test IFN-γ-stimulated vs unstimulated cultures). Duplicate gene names are marked with a cross and indicate the occurrence of two or more transcripts of the same gene in the analysis. Grouped genes are represented by similar expression patterns and hierarchical clustering. Their connection was described by dendrograms to the left and each row represents, indicated by the color, the intensity of their abundance across each group (*161*).

4.1.3. IFNs induce cell-cell adhesion, intercellular signaling and cell growth

IFNs play a crucial role in the defence against viral infection and enhance pro-inflammatory pathways. In order to examine the effects of IFNs on airway epithelial structure after viral invasion, specific GO-terms were used to identify structural epithelial genes. Also in this analysis, IFN-α (145 entities) and IFN-γ (160 entities) demonstrated the highest number of induced entities compared to IFN-β (18 entities) and type-III IFNs (65 and 66 entities) (Figure 4.5). Notably, type-I IFNs shared with type-II and -III IFNs one regulated gene associated with epithelial integrity. In contrast, type-II IFNs induced seven genes similar to type-III IFN-stimulated cultures. Among these overlapping induced genes, type-I and type-II IFNs both upregulated *CBLL1*, while type-I and type-III IFNs similarly induced *PECAM1*.

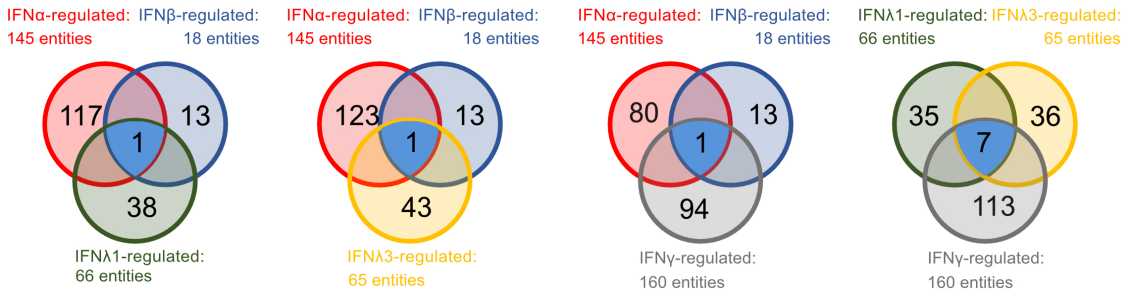

Figure 4.5 Overlapping genes associated with epithelial integrity induced by type-I, -II and -III IFNs. Venn blot of overlapping regulated epithelial modulators by type-I, -II, and -III IFNs stimulation (IFN-α (red), IFN-β (blue), IFN-γ (grey), IFN-λ1 (green), IFN-λ3 (yellow)). Blue area indicates the overlapping regulated epithelial modulators. T-test of IFN-stimulated vs unstimulated cultures ($P \leq .05$; $FC \geq 1.5$).

In general, type-I IFNs stimulation displayed a different expression pattern compared to other IFNs, in which they induced genes crucial for epithelial integrity, including cell-cell adhesion and tight junctions (*ICAM2, PECAM1, CDH10, TJP2, JAML, CLDN25, CBLL1*) compared to unstimulated cultures (Figure 4.6A). Moreover, type-III IFNs induced genes linked to intercellular signalling through ion channels and receptors, such as *CTNNA2, GABRR1, GABRA2, GLRA3, SYT9*, and *GABRG3* (Figure 4.6C). Conversely, genes such as *DUOX2, PTPRR, C4A, C4B*, and *HTR20*, which are associated with cell growth, inflammation, and the complement system were induced by IFN-γ (Figure 4.6D).

Altogether, the three IFN types demonstrated a differential effect on epithelial integrity concerning cell-cell adhesion, tight junctions, ion channels, and cell growth. These findings indicates the importance of IFNs on epithelial remodelling after viral infection. A further investigation regarding connecting pathways is necessary to show this.

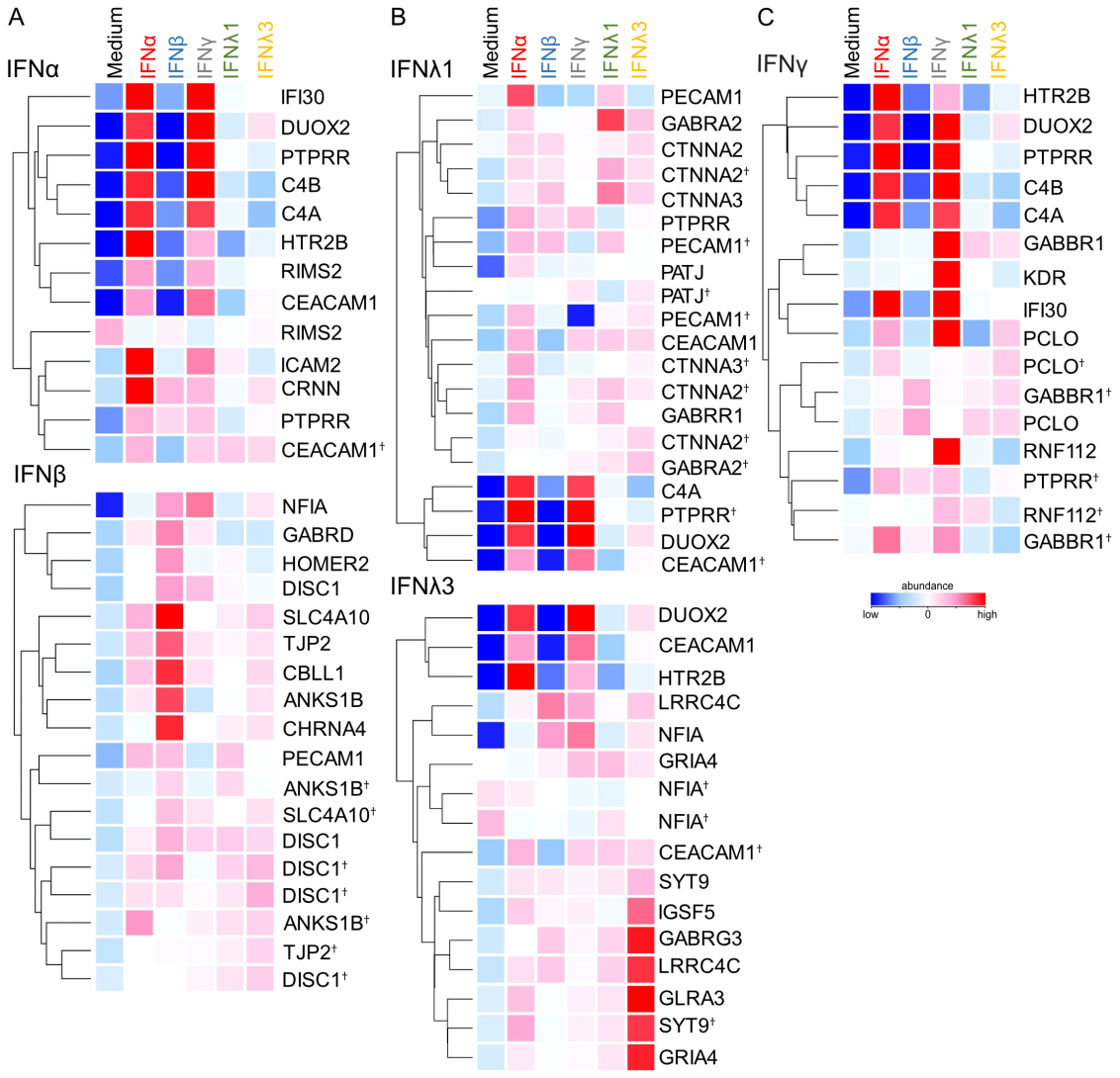

Figure 4.6 Differential expressed epithelial modulators induced in type-I, -II and -III IFN-stimulated ALIs. (A) Heat map of induced epithelial modulators by type-I IFNs (t-test IFN-α-stimulated vs unstimulated cultures), (B) by type-III IFNs (t-test IFN-λ1-stimulated; IFN-λ3-stimulated vs unstimulated cultures) and (C) by type-II IFNs (t-test IFN-γ-stimulated vs unstimulated cultures). Duplicate gene names are marked with a cross and indicate the occurrence of two or more transcripts of the same gene in the analysis. Grouped genes are represented by similar expression patterns and hierarchical clustering. Their connection was described by dendrograms to the left and each row represents, indicated by the color, the intensity of their abundance across each group (*161*).

4.1.4. Unique signalling pathways are induced by IFNs

To gain broader insight into potential activated mechanisms after IFN stimulation, the „STRING“ database was used to identify enriched cellular gene networks induced by type-I, -II, and –III IFNs. The analysis included genes associated with inflammatory pathways, epithelial integrity, and cell proliferation. In consistence with the microarray data, pro-inflammatory genes (*CXCL10, STAT1, PSMB8*, and *USP18*) were induced by all IFNs (Figure 4.7A, grey). Nevertheless, pathway analysis revealed unique regulation by each member of the IFN family (Figure 4.7B-D). Type-I IFN (red) induced *TGFB1* and its regulator, Latent TGF Beta Binding Protein 3 (*LTBP3*), as well as IL-6 and IL-18 receptors (*IL18R1* and *IL18RAP*) (Figure 4.7B), while type-II IFN (purple) induced chemotactic factors such as *CCL7, CCL8, CCL19, CCL25*, and *IL1B* (Figure 4.7C). The last cluster (yellow) consisted of interleukins such as *IL-9, IL-10*, and receptors TNF-α receptor *TNFRSF1B* and IL-6 receptor *IL6R*, which were only induced by type-III IFN (Figure 4.7D).

The gene network analysis revealed no overlapping pathways associated with epithelial remodelling or integrity among any of the IFNs induced genes (Figure 4.8). Three distinct groups associated to each IFN family member could be shown: cluster 1 (red) mainly comprised cell-cell adhesion and tight junction-associated genes induced by type-I IFNs, such as *JAM2, VCL*, and *PECAM1* (Figure 4.8A); cluster 2 (purple) contained various growth factors and genes associated with cytoskeletal organization (*KDR, ARHGEF5*), mainly induced by type-II IFN (Figure 4.8B); and cluster 3 (yellow) specifically connected tight junctions, cell-cell adhesion molecules, and intercellular signalling molecules induced by type-III IFNs (*TJP1, IGSF5, CTNNA1-3, NRXN1*); (Figure 4.8C).

Overall, these data demonstrated the induction of pro-inflammatory and epithelial remodelling pathways in ALIs following IFN stimulation. While some pathways that contain *CXCL10* and *STAT1* were induced by all IFN family members, type-I, -II and -III IFNs exhibited differential effects on pathways associated with epithelial integrity and cell proliferation. These findings demonstrate the role of IFNs in many complex pathways and highlight the unique role of each IFN family member after viral infection. To gain more insights in the role of IFNs in mechanisms associated with SARS-CoV-2 infection, ACE2 expression was analyzed in the context of IFN stimulation.

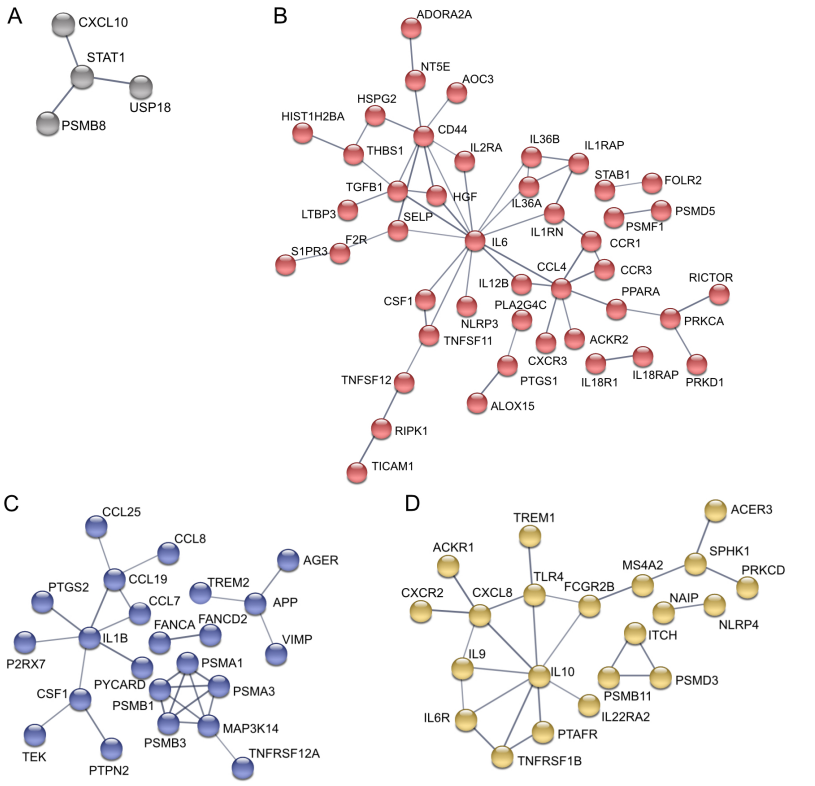

Figure 4.7 Gene network analysis of inflammatory pathways of IFN-stimulated ALIs.
Pro-inflammatory gene network analysis of (A) overlapping induced inflammatory genes by type-I, -II and -III IFNs (grey), of (B) type-I IFNs-induced inflammatory genes (red), of (C) type-II IFN-induced inflammatory genes (purple) and (D) type-III IFNs-induced inflammatory genes (yellow) (*161*).

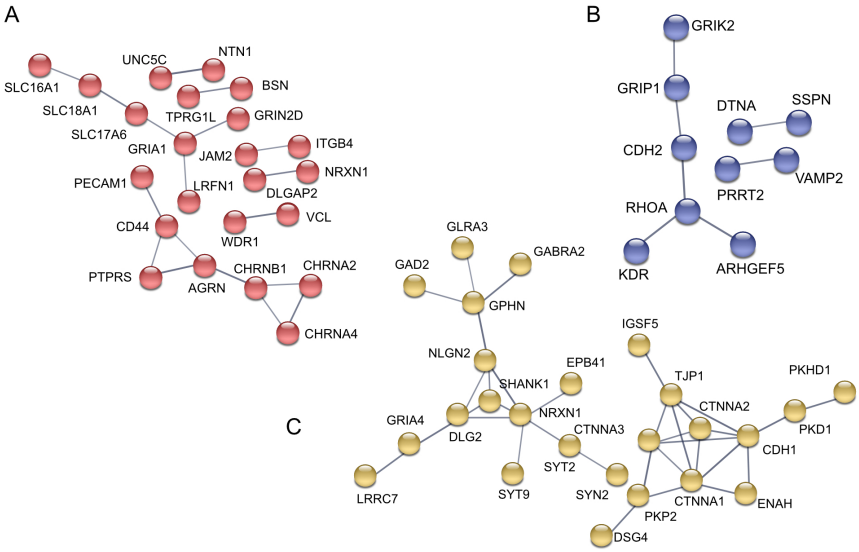

Figure 4.8 Gene network analysis of epithelial modulators pathways of IFN-stimulated ALIs.
Epithelial gene network analysis of (A) type-I IFNs-induced epithelial modulators (red), of (B) type-II IFN-induced epithelial modulators (purple) and (C) type-III IFNs-induced epithelial modulators (yellow) (*161*).

4.2. Induction of ACE2 expression in primary human bronchial epithelial cells

4.2.1. Type-I, -II and -III IFNs induce ACE2 full-length and truncACE2

As a next step, the role of IFNs in ACE2 regulation was analyzed in depth. Since IFNs induced differential expression patterns in ALIs associated with pro-inflammatory genes and epithelial composition, the transcriptome of type-I, -II and -III IFNs-stimulated ALIs was further analyzed using GO-terms associated with SARS-CoV-2 infection related genes. As described before genes such as *CXCL10* and *IL36RN* were all significantly upregulated in type-I, -II and -III IFN-stimulated compared to unstimulated cultures ($P \leq .05$; $FC \geq 1.5$) (Figure 4.9). *ACE2* was induced by IFN-α, type-II and type-III IFNs in ALI cultures. IFN-α upregulated genes such as *TMPRSS11E, CXCR3* and *IL36A* and therefore demonstrated augmented expression of SARS-CoV-2 related genes.

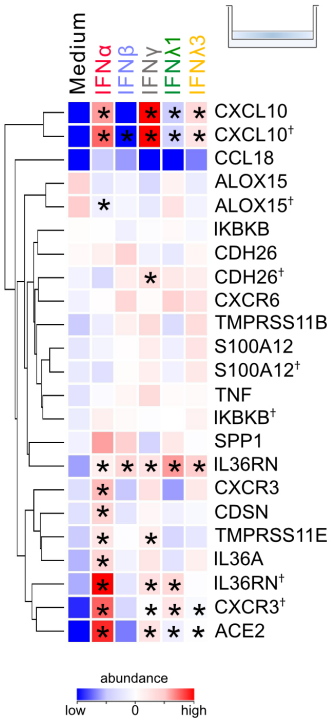

Figure 4.9 Type-I, -II and -III IFNs induce ACE2 upregulation in ALIs.
Expression profile of 24 hours IFN-stimulated ALIS. Heat map of SARS-CoV-2 infection related genes induced by type-I, -II and -III IFNs. Significantly regulated genes are highlighted with an asterisk (t-test IFN-stimulated vs unstimulated cultures ($P \leq .05$; $FC \geq 1.5$)). Duplicate gene names are marked with a cross and indicate the occurrence of two or more transcripts of the same gene in the analysis. Grouped genes are represented by similar expression patterns and hierarchical clustering. Their connection was described by dendrograms to the left and each row represents, indicated by the color, the intensity of their abundance across each group.

Next, the IFN-dependent expression of ACE2 was analyzed in submerged NHBEs. To assess the two main isoforms important during SARS-CoV-2 infection, two specific primer pairs were designed to bind specifically either to ACE2 full-length or to the truncated ACE2 (truncACE2) isoform (Figure 3.2). NHBEs were stimulated with type-I, -II and -III IFNs for six hours. ACE2 showed a dose-dependent upregulation in type-I and type-III IFN stimulated compared to unstimulated samples with a more significant effect on truncACE2 expression ($P \leq .05$, $P \leq .01$, and $P \leq .001$) (Figure 4.10). IFN-γ induced truncACE2 rather than ACE2 full-length.

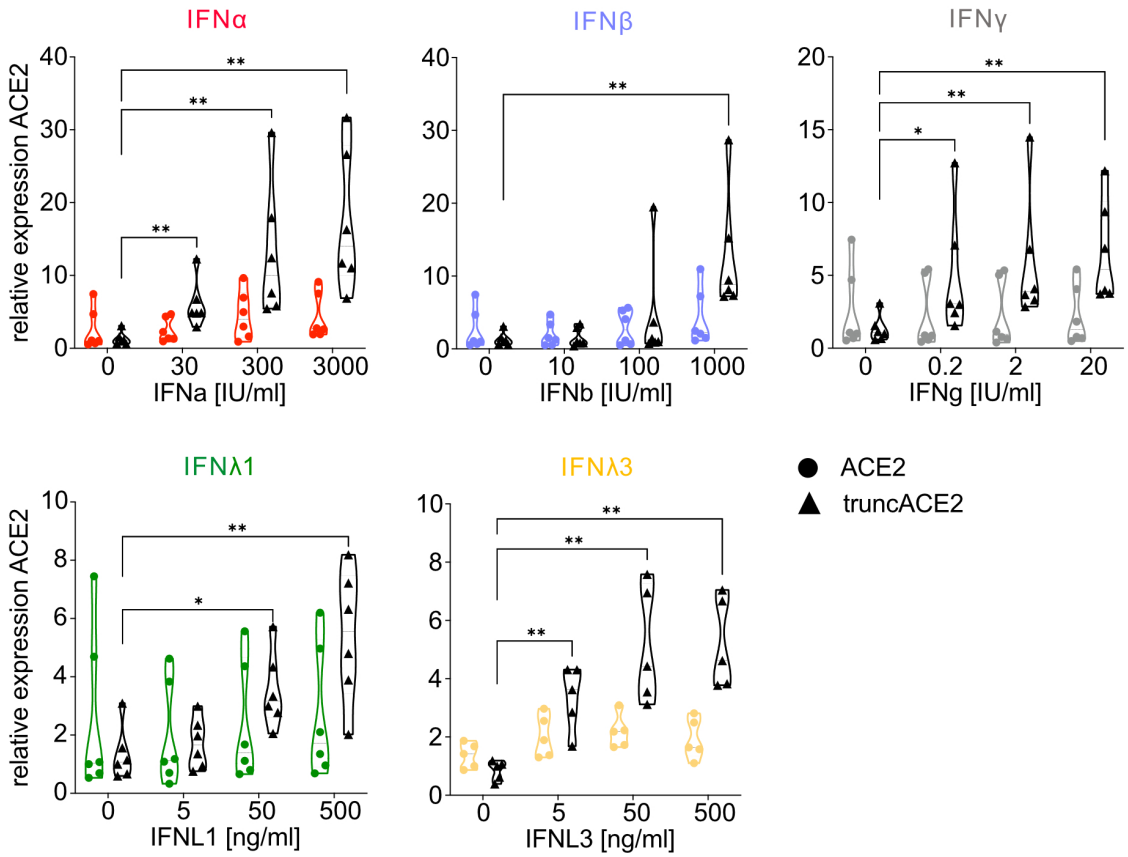

Figure 4.10 IFNs induce ACE2 full-length and truncACE2.
Analysis of human ACE2 full-length and truncACE2 gene expression using RT-qPCR of NHBEs treated with different type-I, -II, -III IFNs concentrations for six hours (IFN-α: red; IFN-β: blue; IFN-γ: grey; IFN-λ1: green; IFN-λ3: yellow). Circles represents ACE2 full-length expression, triangle truncACE2 expression. Symbols represent individual NHBE donors (n=6 per condition). Graphs show means ±SEM. $^{*}P \leq .05$, $^{**}P \leq .01$, $^{***}P \leq .001$ by Mann-Whitney *U* test.

In order to analyze the time-course of ACE2 induction in NHBEs, RT-qPCR readout was performed with cells stimulated either for two, four or six hours with type-I, -II and -III IFNs. Cells stimulated with IFN-α exhibited the strongest ACE2 full-length upregulation within six hours (1.77±0.326 vs. 0.8193±0.1716; $P \leq .01$) and truncACE2 induction within four (2.627±0.7112 vs 0.5183±0.1392; $P \leq .01$) and six hours (2.7±0.6820 vs 0.5183±0.1392; $P \leq .05$) compared

to untreated cells (Figure 4.11). While IFN-β showed no impact on neither ACE2 full-length nor on truncACE2 after six hours, type-II and type-III IFNs induced truncACE2 significantly after six hours stimulation ($P \leq .05$ and $P \leq .01$) (Figure 4.11). Nevertheless, ACE2 full-length showed an increased expression after four hours of IFN stimulation. For future experiments NHBEs were treated for four hours with the IFN family members.

Taken together, type-I, -II and -III IFN stimulation of air liquid interface organotypic cultures and submerged NHBEs induced ACE2 full-length and truncACE2 and strengthens the hypothesis of IFN-dependent ACE2 regulation. Further analysis of potential downstream molecules will be performed to demonstrate a potential IFN-ACE2 axis.

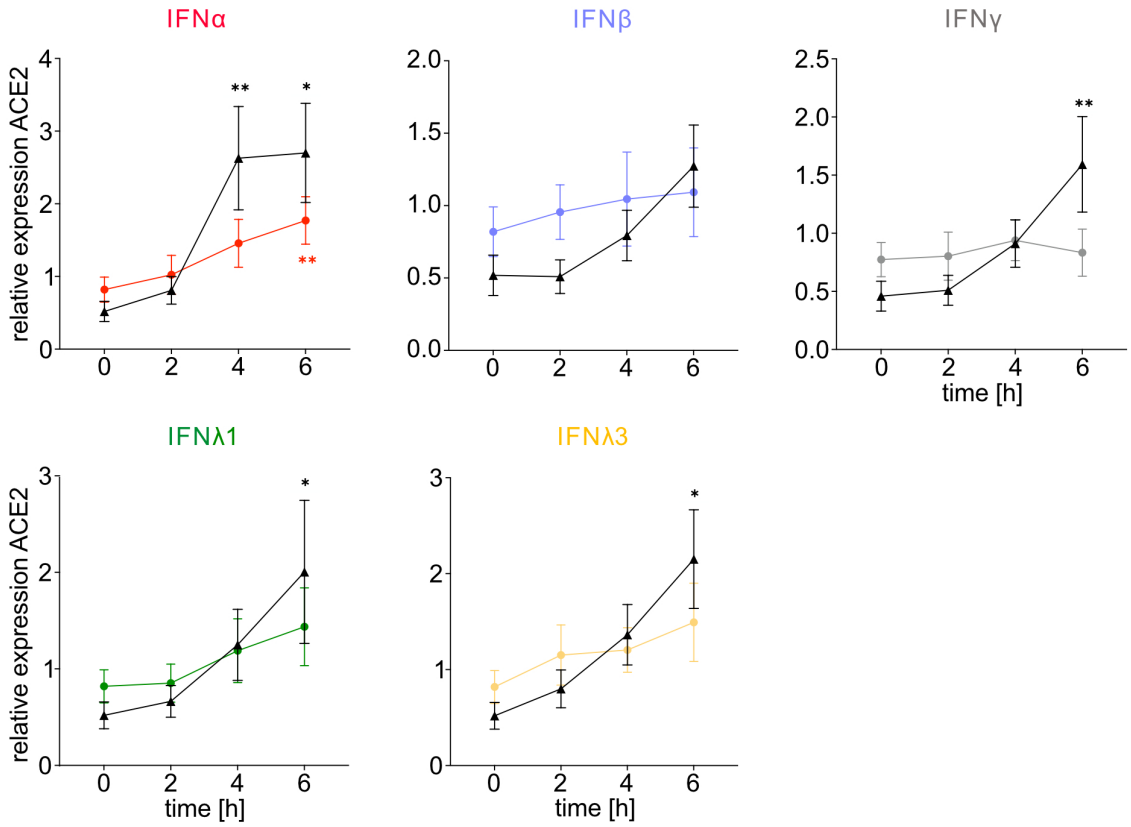

Figure 4.11 ACE2 induction after four hours type-I, -II and -III IFN stimulation in NHBEs.
Time kinetic analysis of human ACE2 full-length and truncACE2 gene expression using RT-qPCR after 2h, 4h, and 6h treatment of NHBEs with type-I, -II, -III IFNs (IFN-α: 300IU/ml, red; IFN-β: 100IU/ml, blue; IFN-γ: 200IU/ml, grey; IFN-λ1: 100ng/ml, green; IFN-λ3: 100ng/ml, yellow). Circles represents ACE2 full-length expression, triangle truncACE2 expression. Graphs show means ±SEM (n=5 per condition). $^{*}P \leq .05$, $^{**}P \leq .01$, $^{***}P \leq .001$ by Mann-Whitney *U* test.

4.2.2. STAT1 and AKT play no role in IFN-dependent ACE2 regulation

The IFN signaling pathways are well understood and the intracellular key factors JAK, STAT1 and AKT enhances IFN signalling. To investigate the impact of these key factors which might be involved in the IFN-induced ACE2 regulation, NHBE cells were treated with specific inhibitors and co-stimulated with type-I, -II and -III IFNs. First, JAKs were inhibited with a pan-JAK inhibitor Tofacitinib (Tofa). Samples inhibited with Tofa and co-stimulated with IFN-α showed a decrease in ACE2 full-length expression compared to samples stimulated with IFN-α alone (1.17±0.2 vs 2.166±0.1135; $P \leq .05$) (Figure 4.12). IFN-β, IFN-γ and type-III IFN co-stimulated samples exhibited a downregulation of truncACE2 compared to samples stimulated with IFN alone ($P \leq .05$ and $P \leq .01$). ACE2 full-length expression was comparable for these two groups.

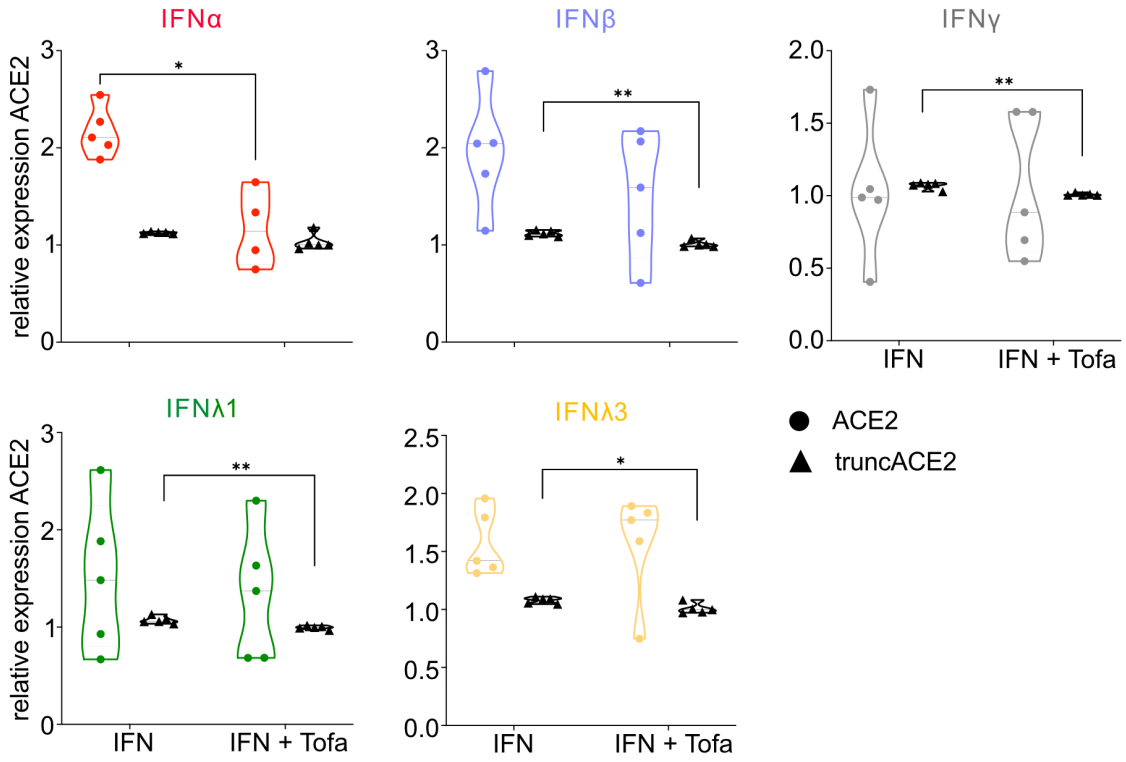

Figure 4.12 JAK inhibition leads to ACE2 downregulation in IFN co-stimulated NHBEs.
Analysis of human ACE2 full-length and truncACE2 gene expression using RT-qPCR after 30min pre-treatment of NHBEs with 1μM Tofa, followed by type-I, -II and -III IFN stimulation for 4h (IFN-α: 300IU/ml, red; IFN-β: 100IU/ml, blue; IFN-γ: 200IU/ml, grey; IFN-λ1: 100ng/ml, green; IFN-λ3: 100ng/ml, yellow). Circles represents ACE2 full-length expression, triangle truncACE2 expression. Symbols represent individual NHBE donors (n=5 per condition). Graphs show means ±SEM. $^{*}P \leq .05$, $^{**}P \leq .01$, $^{***}P \leq .001$ by Mann-Whitney *U* test.

As a next step, downstream molecules of the IFN/JAK pathway, which are important for ISG expression such as STAT1 and AKT were inhibited with their specific inhibitors SH-4-54 (SH) and Capivasertip in Calu3 cell line (Figure 4.13). Cells stimulated with SH and Capivasertip and co-stimulated with IFN-β and IFN-λ1 did not show any dose-dependent change neither in ACE2 full-length nor in truncACE2 expression. In general, the expression level of truncACE2 was lower than ACE2 full-length.

Overall, while JAK was involved in IFN-dependent ACE2 regulation the two downstream molecules STAT and AKT did not demonstrate a significant impact on ACE2 regulation. These data highlight the involvement of other potential factors in the IFN-dependent ACE2 regulation.

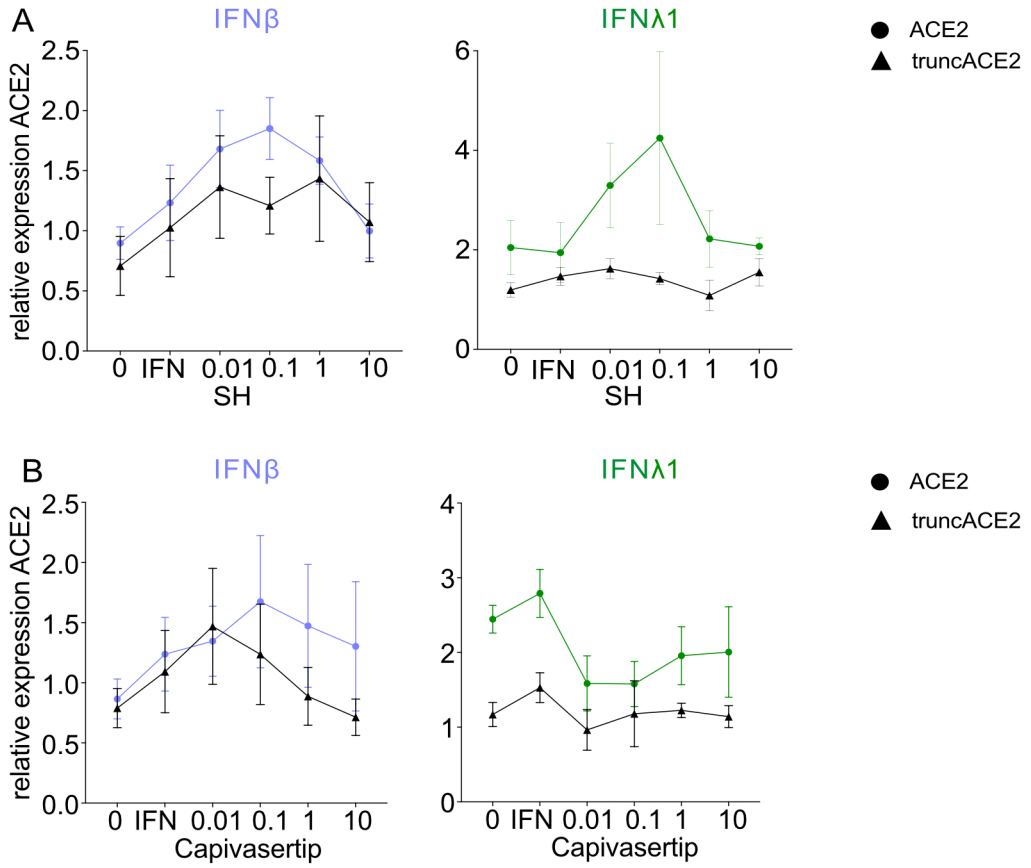

Figure 4.13 STAT and AKT inhibition has no impact on ACE2 expression in Calu3 cell line.
Analysis of human ACE2 full-length and truncACE2 gene expression using RT-qPCR after 30min pre-treatment of Calu3 cell line with 1μM (A) SH4-54 or (B) Capivasertip, followed by type-I, -II and -III IFN stimulation for 4h (IFN-β: 100IU/ml, blue; IFN-λ1:100 ng/ml, green). Circles represents ACE2 full-length expression, triangle truncACE2 expression. Graphs show means ±SEM (n=3 per condition). $^{*}P \leq .05$, $^{**}P \leq .01$, $^{***}P \leq .001$ by Student's t-test.

4.3. ACE2 expression is regulated via transcription factor FoxO1

4.3.1. Characterization of FoxO1 binding sites within the ACE2 promoter

In order to further examine the transcriptional regulation of ACE2, TF-ELISA was used to analyze the binding affinity of potential transcription factors binding to the ACE2 promoter. Within the ACE2 proximal promoter site (Figure 1.3), different transcription factor binding sites are situated upstream of the transcription start site (TSS) (+63) including FoxO1 binding sequence (TTGTTTACTG) (-42/-32). To test FoxO1 binding to the ACE2 promoter, a proximal ACE2 promoter sequence (-1119/+103) was used as previously described (*166*).

The ACE2 promoter sequence demonstrated significantly higher absorbance compared to samples of FoxO1 nuclear extract without the ACE2 promoter sequence (negative control) (0.51±0.15 vs 2.48±0.17; $P \leq .001$) (Figure 4.14A). In competition experiments, in which the FoxO1-ACE2 promoter sequence interaction was blocked by specific blocking sequences, the precise FoxO1 binding site was validated. A decreased absorbance compared to the unblocked promoter sequence was observed, suggesting the binding of FoxO1 within the ACE2 proximal promoter site upstream of TSS (-42/-32; Figure 4.14A). Significant reduction in absorbance could be demonstrated in samples incubated with blocking sequence 3 (-83/+124) compared to the ACE2 promoter sequence (1.21±0.04 vs 2.48±0.169; $P \leq .05$) and the consensus sequence 0.23±0.028 vs 0.84±0.201; $P \leq .01$) alone, indicating its potential significance as a key binding site for FoxO1 (Figure 4.14).

Altogether, these results demonstrate binding of FoxO1 to the ACE2 promoter sequence and its role in activating downstream ACE2 gene expression. To further validate the role of FoxO1 in ACE2 regulation, the inhibition of the transcription factor was necessary.

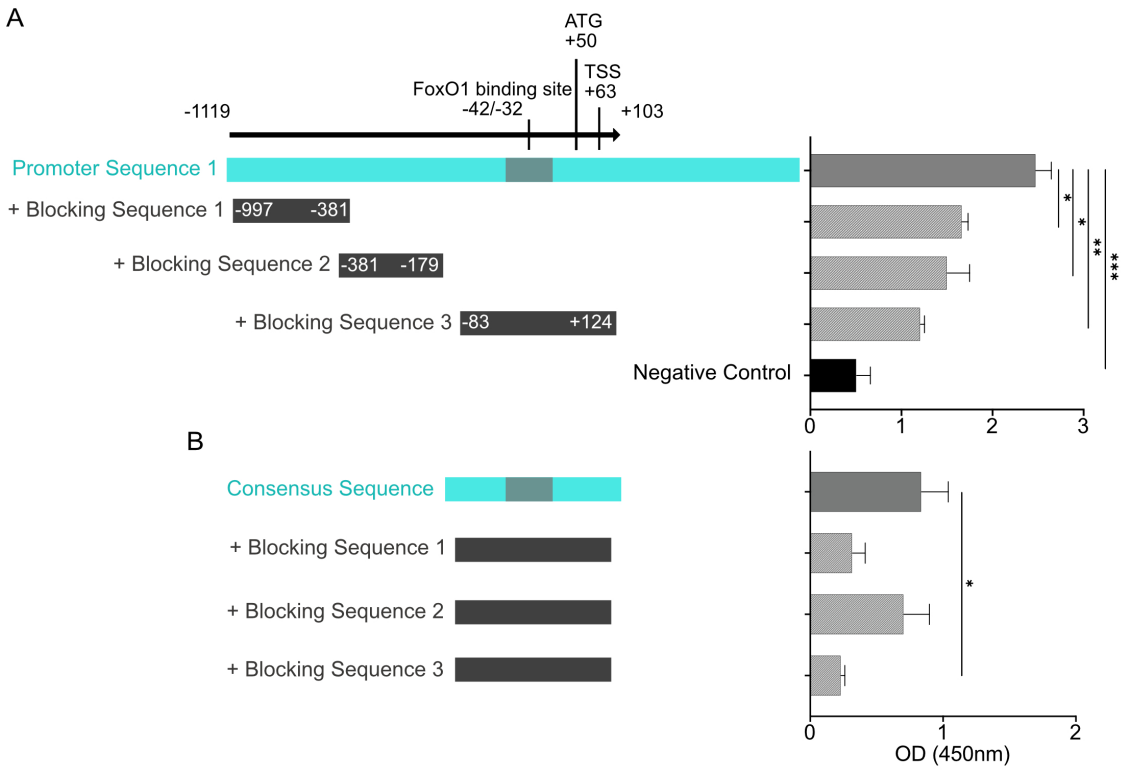

Figure 4.14 FoxO1 binds within the ACE2 proximal promoter.
Nuclear extracts of HEK cells transfected with FoxO1 vector were incubated with (A) ACE2 promoter sequence in the presence or absence of competitor oligonucleotides or (B) a designed ACE2 promoter consensus sequence. Binding of FoxO1 was quantified using FoxO1 TF-ELISA. Position of potential FoxO1, ATG and transcription start site (TSS) are described accordingly. Graphs show means ±SEM. $^{*}P \leq .05$, $^{**}P \leq .01$, $^{***}P \leq .001$ by Student's t-test.

4.3.2. FoxO1 inhibition leads to ACE2 downregulation

To further investigate the role of FoxO1 in IFN-dependent ACE2 regulation, NHBEs were treated with the specific FoxO1 inhibitor AS1842856 (AS), prior and during IFN stimulation. Although, NHBE cells treated with AS alone did not demonstrate an effect on ACE2 full-length expression compared to baseline, truncACE2 expression was downregulated after six hours of AS stimulation (Figure 4.15). However, on protein level FoxO1 inhibition led to ACE2 full-length downregulation compared to control samples (Figure 4.16).

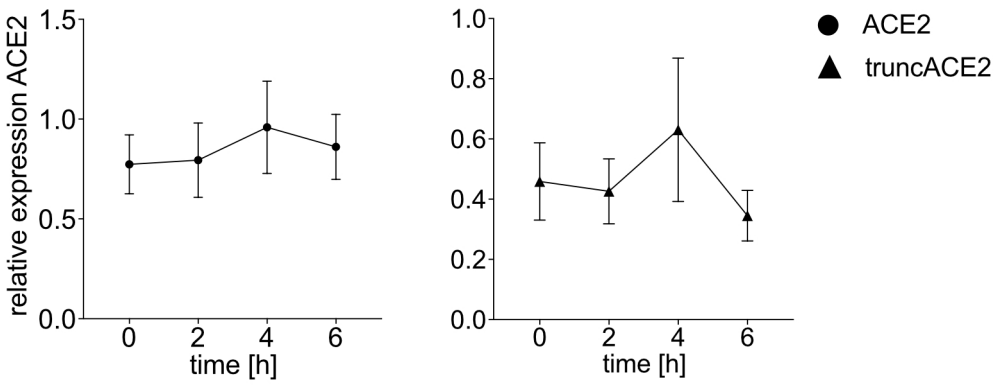

Figure 4.15 Inhibition of FoxO1 in NHBEs with the specific inhibitor AS.
Analysis of human ACE2 full-length and truncACE2 gene expression using RT-qPCR. NHBEs were stimulated with 1μM AS for 4h. Circles represents ACE2 full-length expression, triangle truncACE2 expression. Graphs show means ±SEM (n= 5 per condition). $^{*}P \leq .05$, $^{**}P \leq .01$, $^{***}P \leq .001$ by Mann-Whitney *U* test.

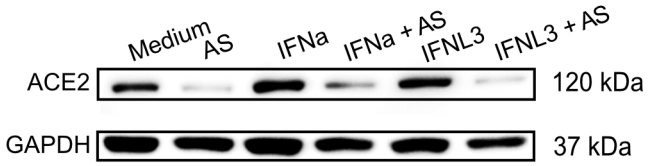

Figure 4.16 FoxO1 inhibition correlates with ACE2 downregulation on protein level.
Immunoblot analysis of one representative NHBE donor (n=6) which was inhibited with 1μM AS (-30´) and stimulated with IFN-α (300IU/ml) and IFN-λ3 (100ng/ml) for 24h. GAPDH was used as loading control.

Next, the transcriptomic and protein ACE2 expression was analyzed in AS and IFN co-stimulated NHBEs after four hours of treatment (Figure 4.16 and 4.17). In general, samples stimulated with IFN family members and incubated with AS demonstrated a downregulation of ACE2 full-length trancript at both the mRNA and protein level compared to samples stimulated with IFNs alone (Figure 4.16 and 4.17). No significant changes were observed of truncACE2 between AS and IFN treated samples (Figure 4.17). Especially IFN-α (1.040±0.1 vs 1.786±0.12; $P \leq .01$) and IFN-λ3 (0.94±0.09 vs 1.52±0.092; $P \leq .01$) showed a significant downregulation of ACE2 full-length in samples co-treated with AS (Figure 4.16 and 4.17).

Overall, this data further supports the hypothesis that active FoxO1 leads to ACE2 upregulation. Particularly IFN-α and IFN-λ3-stimulated NHBEs showed a significant effect on ACE2 expression following FoxO1 inhibition. The following experiments of FoxO1 knock-out cells were used to further analyze the functional role of FoxO1 during ACE2 regulation.

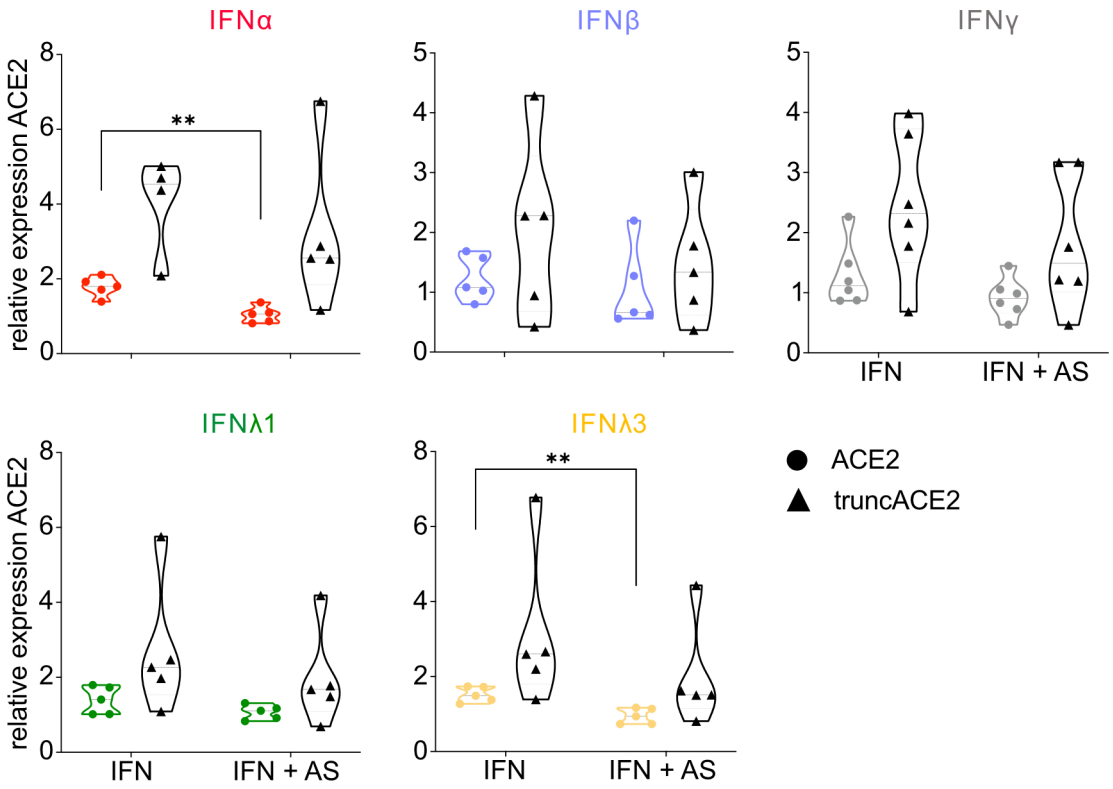

Figure 4.17 FoxO1 inhibition correlates with ACE2 downregulation on a transcriptomic level.
Analysis of human ACE2 full-length and truncACE2 gene expression using RT-qPCR. NHBEs were pre-treated with 1μM AS, followed by type-I, -II and -III IFN stimulation for 4h (IFN-α: 300IU/ml, red; IFN-β: 100IU/ml, blue; IFN-γ: 200IU/ml, grey; IFN-λ1: 100ng/ml, green; IFN-λ3: 100ng/ml, yellow). Symbols represent individual NHBE donors (n=6 per condition). Circles represents ACE2 full-length expression, triangle truncACE2 expression. Graphs show means ±SEM. $^{*}P \leq .05$, $^{**}P \leq .01$, $^{***}P \leq .001$ by Mann-Whitney *U* test.

4.3.3. FoxO1 knock-out cells exhibit low expression levels of ACE2

In order to validate the previous findings regarding ACE2 regulation via FoxO1, the transcription factor was knocked out in six genetically independent NHBE donors (FoxO1-KO). Immunoblotting was used for validation of the reduced FoxO1 protein expression. As a first step, the stability of FoxO1 knock out was confirmed on a protein level over a time course of 240 hours post nucleofection (Figure 4.18A). Notably, the protein expression of ACE2 full-length was reduced in FoxO1-KO cells compared to non-targeting control (NTC) cells after 240h post nucleofection (Figure 4.18). In addition, ACE2 full-length expression level was reduced on transcriptomic level in FoxO1-KO compared to NTC cells.

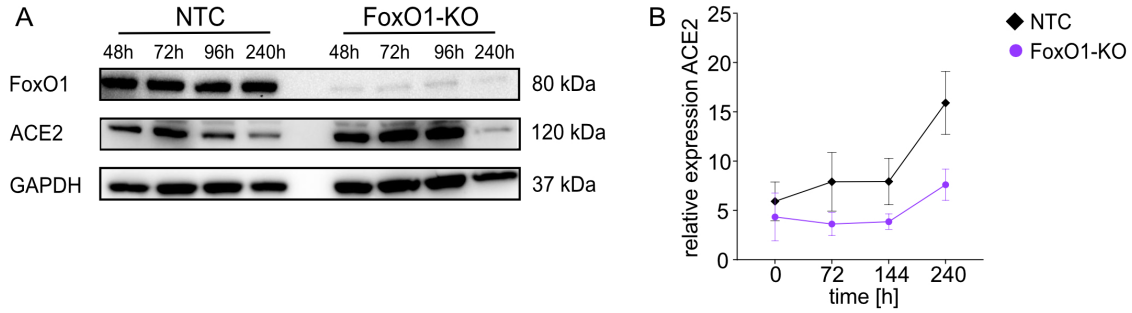

Figure 4.18 Stable FoxO1 knock out in NHBEs.
(A) The FoxO1-KO primary NHBE cells were transfected with specific FoxO1 crRNA using CRISPR/Cas9 system. Cells were cultured in a time course of 240h after transfection. Immunoblot analysis of NTC and FoxO1-KO cells of one representative NHBE donor (n=6). (B) Analysis of human ACE2 full-length gene expression using RT-qPCR of FoxO1-KO NHBEs in a time course of 240h post-nucleofection. Circles represents ACE2 full-length expression in FoxO1-KO cells, rhombus ACE2 full-length expression in NTC cells. Graphs show means ±SEM (n=6 per condition). $^{*}P \leq .05$, $^{**}P \leq .01$, $^{***}P \leq .001$ by Mann-Whitney *U* test.

Next, FoxO1-KO cells were stimulated with IFNs. ACE2 full-length expression level was significantly reduced in IFN-stimulated FoxO1-KO cells compared to NTC cells at a transcriptomic level (Figure 4.19). Especially IFN-stimulated FoxO1-KO cells treated with higher concentrations of IFN-λ1 (1.24±0.13 vs 2.16±0.24; $P \leq .05$) and IFN-λ3 (1.334±0.1138 vs 2.738±0.5813; $P \leq .05$) exhibited a significantly downregulation of ACE2 full-length compared to NTC cells. In contrast, truncACE2 expression was not affected by IFN treatment, except for IFN-β which induced truncACE2 in FoxO1-KO cells compared to NTC cells (1.537±0.1291 vs 0.4585±0.1068; $P \leq .05$) (Figure 4.20).

These results supported the data from the TF-ELISA regarding the IFN-dependent ACE2 regulation. Especially type-III IFNs might induce ACE2 expression via FoxO1. Investigating the impact of FoxO1 on ISG expression is crucial for the role of the transcription factor during the antiviral state.

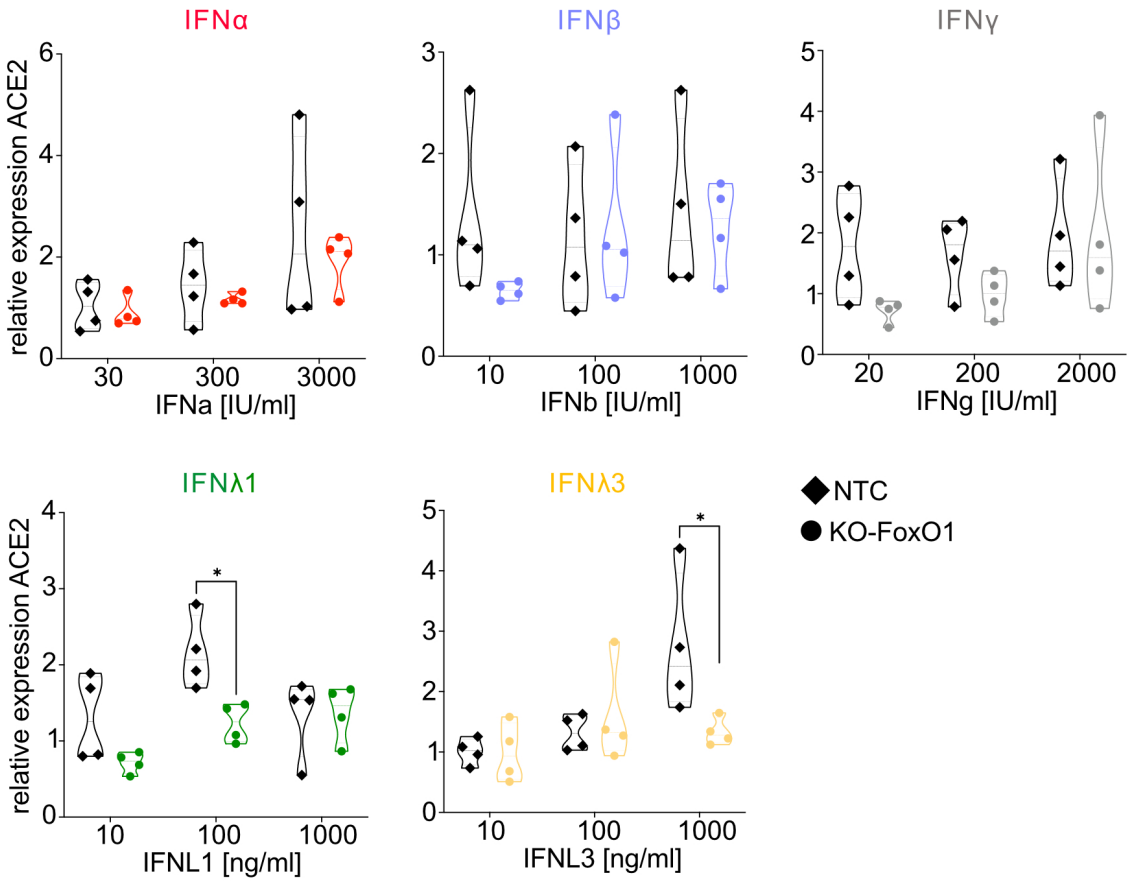

Figure 4.19 Primary FoxO1-KO cells demonstrates downregulation of ACE2 full-length.
Analysis of human ACE2 full-length gene expression using RT-qPCR of FoxO1-KO NHBEs followed by type-I, -II and -III IFN stimulation for 4h (IFN-α: 300IU/ml, red; IFN-β: 100IU/ml, blue; IFN-γ: 200IU/ml, grey; IFN-λ1: 100ng/ml, green; IFN-λ3: 100ng/ml, yellow). Symbols represent individual NHBE donors (n=4 per condition). Circles represents ACE2 full-length expression in FoxO1-KO cells, rhombus ACE2 full-length expression in NTC cells. Graphs show means ±SEM. $^{*}P \leq .05$, $^{**}P \leq .01$, $^{***}P \leq .001$ by Mann-Whitney *U* test.

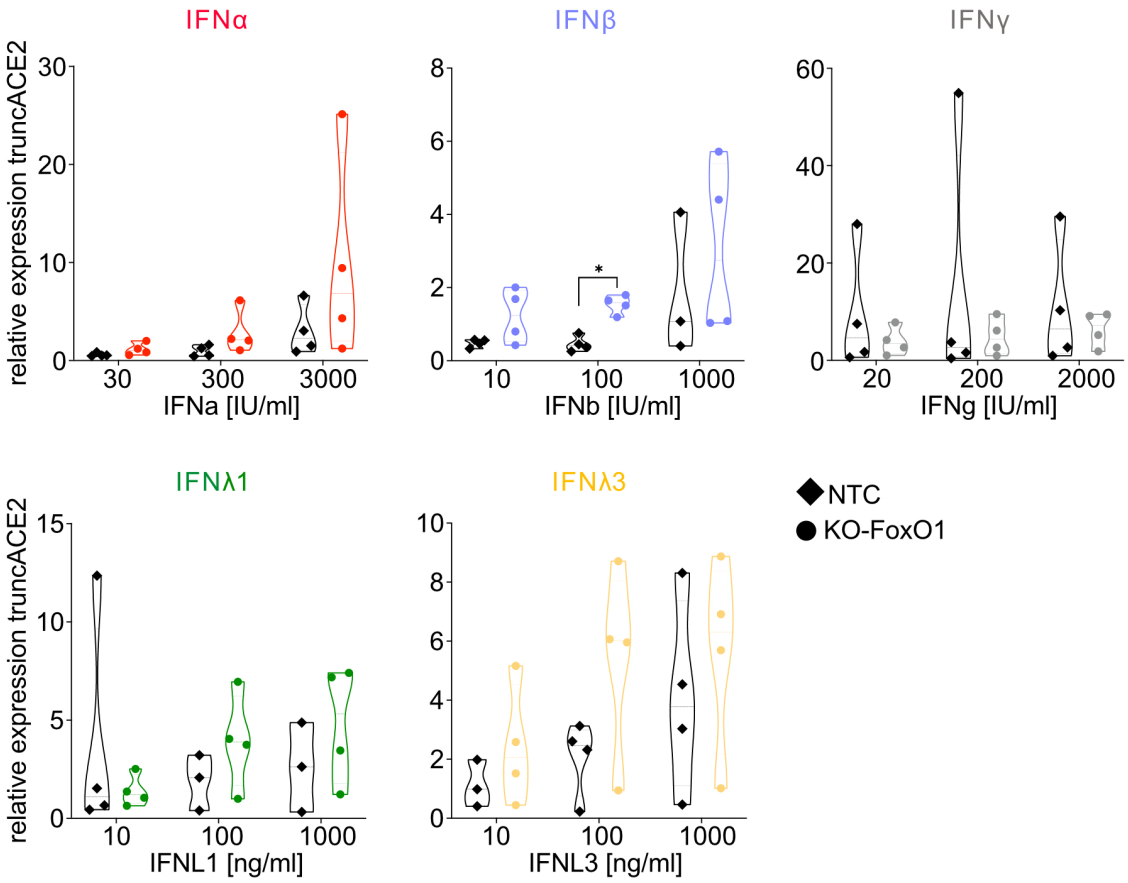

Figure 4.20 Primary FoxO1-KO cells demonstrates downregulation of truncACE2.
Analysis of human truncACE2 gene expression using RT-qPCR of FoxO1-KO NHBEs followed by type-I, -II and -III IFN stimulation for 4h (IFN-α: 300IU/ml, red; IFN-β: 100IU/ml, blue; IFN-γ: 200IU/ml, grey; IFN-λ1: 100ng/ml, green; IFN-λ3: 100ng/ml, yellow). Symbols represent individual NHBE donors (n=4 per condition). Circles represents truncACE2 expression in FoxO1-KO cells, rhombus truncACE2 expression in NTC cells. Graphs show means ±SEM. $^{*}P \leq .05$, $^{**}P \leq .01$, $^{***}P \leq .001$ by Mann-Whitney *U* test.

4.4. Genome expression patterns demonstrate advantages for asthmatics

4.4.1. ISG expression in high expressed *FOXO1* asthmatics and healthy individuals

To gain insights into the expression patterns of asthmatics and healthy individuals at the first site of infection in the upper airways, whole-genome microarray approach was used to analyze genes associated with virus infection and the antiviral cell state of nasal scrapings obtained from a cohort of healthy and asthmatic adults (*N*=238). The data was first stratified by different health conditions (asthma patients and healthy controls) and 98 upregulated genes and 494 downregulated genes were identified in asthmatic compared to healthy control ($P \leq$.05; $FC \geq$ 1.5). In order to further examine the role of FoxO1 in the IFN pathway, *FOXO1* dose-dependent gene expression patterns were analyzed by grouping each sample according to their low, intermediate, or high *FOXO1* expression levels using the 20^{th} and 80^{th} percentile in this nasal transcriptome analysis as limits. Although *FOXO1* high expressed asthmatic samples showed an induction of ISGs such as *OAS1, IFITM1* and *OASL* compared to low *FOXO1* samples, in general the induction of the majority of ISGs did not correlate with high levels of *FOXO1* in asthmatic patients nor healthy individuals (Figure 4.21).

Altogether, while FoxO1 seems to be involved in IFN-dependent *ACE2* regulation, the transcription factor did not have any effect on ISG expression in asthmatic patients or healthy individuals. This is in alignment with the hypothesis that FoxO1 might be a potential target, which could be addressed to interfere SARS-CoV-2 infiltration without disturbing the antiviral cell state induced by IFNs.

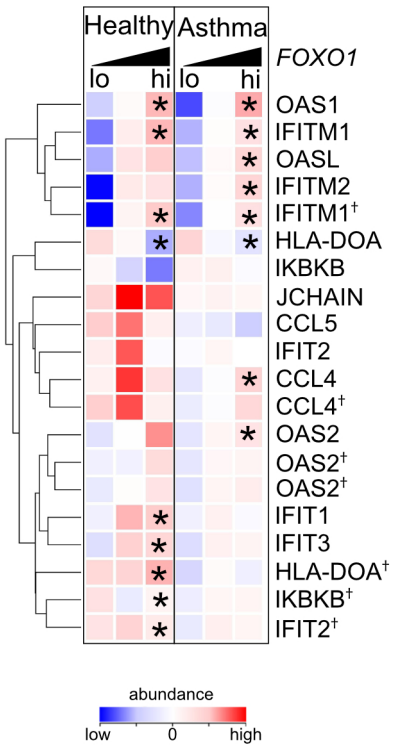

Figure 4.21 ISG expression is associated dose-dependently with *FOXO1* expression in asthmatic patients and healthy control.
Transcriptional analysis of ISGs in relation to the expression levels of *FOXO1*, categorized as high, intermediate, and low groups of nasal scrapings (*N*=238) of healthy individuals and asthmatic patients. Significantly regulated genes are indicated with an asterisk ($P \leq .05$; $FC \geq 1.5$) in *FOXO1* high expressed samples compared to low in asthmatic patients and healthy control respectively and Benjamin Hochberg (FDR) correction was applied. Duplicate gene names are marked with a cross and indicate the occurrence of two or more transcripts of the same gene in the analysis. Grouped genes are represented by similar expression patterns and hierarchical clustering. Their connection was described by dendrograms to the left and each row represents, indicated by the color, the intensity of their abundance across each group.

4.4.2. SARS-CoV-2 infection related genes are downregulated in asthmatics

The next question was whether asthmatics exhibit potential risk factors towards SARS-CoV-2 infection. The nasal transcriptome data revealed distinct differences in the gene expression patterns between asthmatic patients and healthy individuals (Figure 4.22). While the expression of SARS-CoV-2 related genes such as *CDH26* and *SPP1* were upregulated in asthmatic patients, the expression of *ACE2, TMPRSS11B, CXCR3* and *CXCL10* showed significantly lower expression levels in asthmatic patients in comparison with the healthy control group ($P \leq .05$; $FC \geq 1.5$); (Figure 4.22A). In addition, genes associated with the KKS exhibited a significant downregulation in asthmatics compared to non-asthmatics (*KLK6, KLK13* and *ACE2*); (Figure 4.22B). Genes prominent in a pro-inflammatory environment, summarized in the acute phase gene set, showed different expression patterns in asthmatic patients (Figure 4.22C). While genes such as *IL36RN, CXCL10* and *TNF* were significantly downregulated in asthmatics compared to healthy individuals, there were no significant effects observed

for genes such as *IL10, STAT1* and *IL6* in neither asthmatic patients nor in the healthy control group.

Although, these findings support that asthmatics might have an advantage during SARS-CoV-2 infection, further analysis is required to determine the role of IFNs. Asthmatic patients demonstrated lower levels of genes associated with SARS-CoV-2 infection, KKS and the acute phase highlighting asthma as a protecting factor against viral infection. The dependency of IFNs regrading SARS-CoV-2 infection related gene expression is described in the following paragraph.

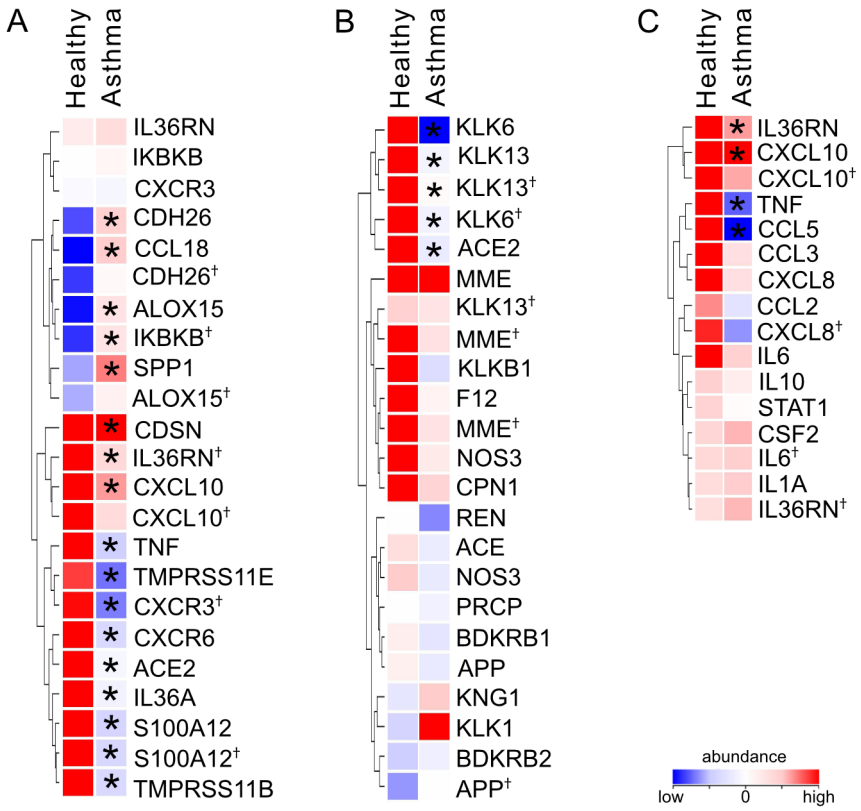

Figure 4.22 Asthmatic patients demonstrate differently expressed SARS-CoV-2 infection related genes compared to healthy individuals.
(A) Transcriptional analysis of SARS-CoV-2 infection related genes of asthmatic and healthy nasal scrapings. Significantly regulated genes are indicated with an asterisk of asthma samples compared to healthy samples ($P \leq .05$; $FC \geq 1.5$) and Benjamin Hochberg (FDR) correction was applied. (B) Heat map of KKS genes of asthmatic compared to healthy nasal scrapings and (C) of acute phase genes of asthmatic compared healthy nasal scrapings. Duplicate gene names are marked with a cross and indicate the occurrence of two or more transcripts of the same gene in the analysis. Grouped genes are represented by similar expression patterns and hierarchical clustering. Their connection was described by dendrograms to the left and each row represents, indicated by the color, the intensity of their abundance across each group.

4.4.3. Reduced SARS-CoV-2-related genes correlate with elevated *IFN* levels in asthmatics

Since SARS-CoV-2 related genes were differential expressed, the relation between type-I, -II and -III *IFN* expression and genes associated with viral infection was further analyzed. Therefore, each sample was grouped as described earlier according to their low, intermediate, or high *IFN* expression levels using the 20^{th} and 80^{th} percentile in this nasal transcriptome analysis as limits. Type-I and -II *IFN*s expression significantly associated with the induction of type-I and -II *IFN*s, whereas type-III *IFN*s were not significantly altered in nasal scrapings of healthy or asthmatic subjects ($P \leq$.05; $FC \leq$1.5); (Figure 4.23A, 9.1A, 9.2A, 9.3A, 9.4A). Notably, an IFN-dose dependent correlation could be seen between all members of the IFN family and the upregulation of *ACE2* in healthy subjects, whereas this effect could not be observed in asthmatic patients. Especially a significantly elevated expression of *IFNL3* is co-expressed with *ACE2* in healthy individuals compared to asthmatic patients (Figure 9.4A). In addition, upregulated genes, which are associated with the KKS such as *KLK1, KNG1, KLK13*, and *MME*, showed a dose-dependent association with *IFN* levels (Figure 4.23B, 9.1B, 9.2B, 9.3B, 9.4B). Genes related to SARS-CoV-2 infection (*TMPRSS11E, TMPRSS11B, S100A12, ACE2*) did not show any significant upregulation in nasal scrapings of asthmatic patients in association with high *IFN* levels (Figure 4.23C, 9.1C, 9.2C, 9.3C, 9.4C). All IFN family members affected similar dose-dependent expression patterns of genes associated with the acute phase after viral infection (Figure 4.23D, 9.1D, 9.2D, 9.3D, 9.4D). High levels of IFN expression in nasal scrapings of asthmatic patients associated with the upregulation of acute phase genes such as *IL36RN, IL6*, and *IL10*, compared to samples with lower levels of *IFN* expression. Notably, high type-I *IFN* expression was associated with lower ISG expression such as *OAS1, OAS2, IFIT1, IFIT2*, whereas the expression of type-II and -III did not correlate with the induction of ISGs in asthmatic patients (Figure 4.23E, 9.1E, 9.2E, 9.3E, 9.4E).

In conclusion, the data demonstrated distinct expression patterns between asthmatic patients and healthy control in the upper airways for genes associated with the KKS, SARS-CoV-2 infection, and antiviral defence mechanisms in an IFN dependency. These findings highlight the differential antiviral responses between asthmatic and healthy individuals and showing the potential implications for immune responses in the context of asthma.

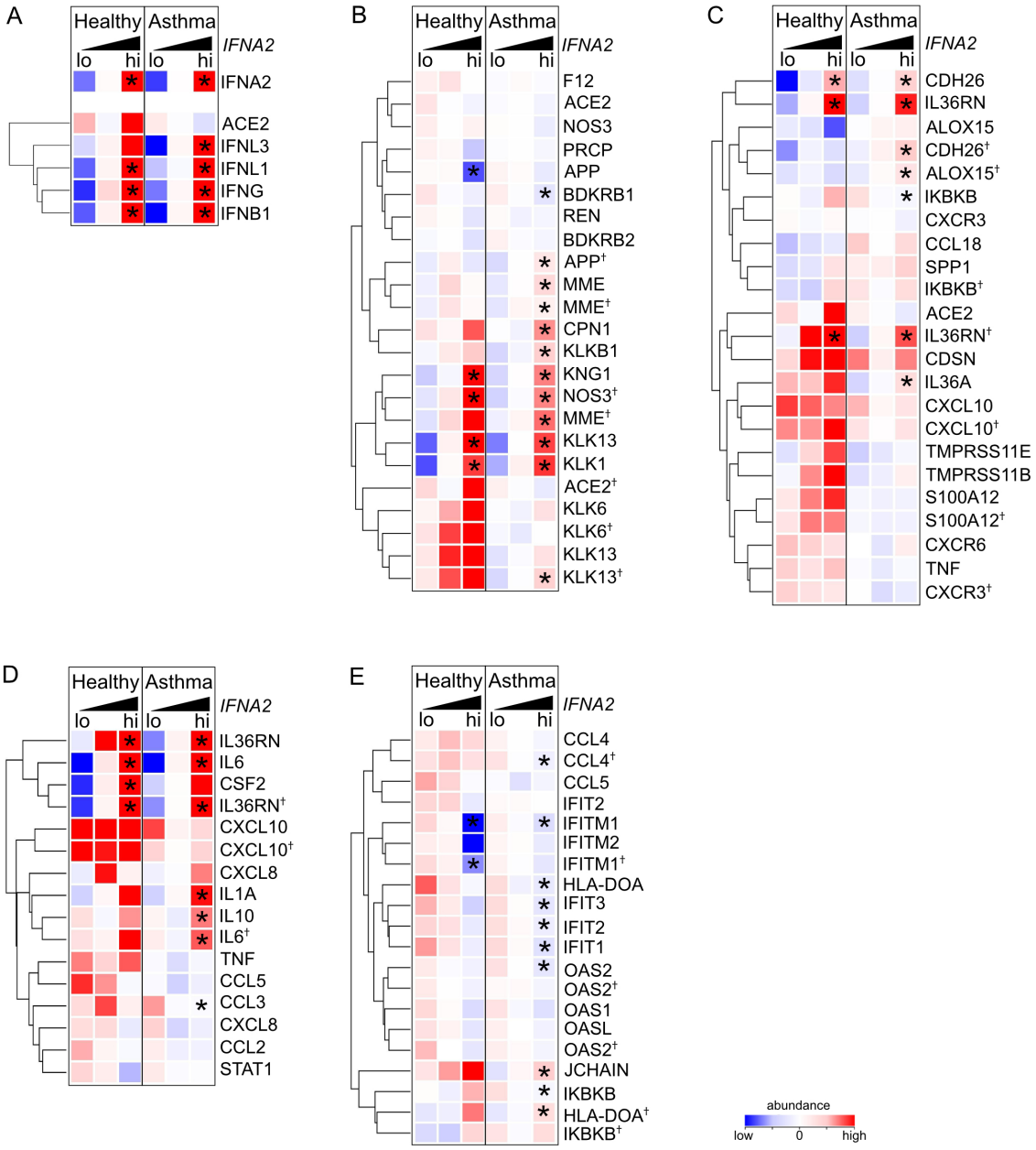

Figure 4.23 Expressed genes associated with SARS-CoV-2 infection demonstrate a *IFNA2* dose-dependent correlation in asthmatic patients and healthy control.
(A) Heat map of induced *IFNs* and *ACE2* in relation to the expression levels of *IFNA2*, categorized as high, intermediate, and low groups of healthy individuals and asthmatic patients. Significantly regulated genes ($P \leq .05$; $FC \geq 1.5$) are indicated with an asterisk in *IFNA2* high expressed samples compared to low in asthmatic patients and healthy control respectively. Benjamin Hochberg (FDR) correction was additionally applied. (B) Heat map of KKS genes in relation to the expression levels of *IFNA2*, categorized as high, intermediate, and low groups of healthy individuals and asthmatic patients. (C) Heat map of induced SARS-CoV-2 infection associated genes in relation to the expression levels of *IFNA2*, categorized as high, intermediate, and low groups of healthy individuals and asthmatic patients. (D) Heat map of acute phase genes in relation to the expression levels of *IFNA2*, categorized as high, intermediate, and low groups of healthy individuals and asthmatic patients. (E) Heat map of induced ISGs in relation to the expression levels of *IFNA2*, categorized as high, intermediate, and low groups of healthy individuals and asthmatic patients. Duplicate gene names are marked with a cross and indicate the occurrence of two or more transcripts of the same gene in the analysis. Grouped genes are represented by similar expression patterns and hierarchical clustering. Their connection was described by dendrograms to the left and each row represents, indicated by the color, the intensity of their abundance across each group.

Chapter 5

Discussion

5. Discussion

5.1. IFN stimulation leads to enhanced epithelial integrity

Even though it is known that the IFN pathway leads to an antiviral cell state, its impact on epithelial processes is less well investigated. Using whole-genome analysis of IFN-stimulated ALIs, this thesis shows the impact of type-I, -II and -III IFNs on the airway epithelium by analyzing ISG expression, inflammatory processes and epithelial integrity. The upregulation of overlapping ISGs by the IFN family members was subject of our initial study (*161*). However, organotypic airway cultures stimulated with type-I, -II and -III IFNs induced differential expressed pro-inflammatory genes and epithelial modulators. All IFN family members induced 16 similar ISGs. Even though type-I, -II, and -III originate from different cell types such as plasmacytoid dendritic cells (IFN-α) or NK cells (IFN-γ) and enhance different cellular processes such as TH1 cell differentiation (IFN-γ), in this study they all induced ISGs associated with viral entry blockage (*IFITM*), interfering viral mRNA synthesis (*APOBEC*s), protein synthesis (*IFIT1*) and viral replication (*APOBECs, OAS*); (*98*).

Although IFNs induced overlapping ISGs this thesis revealed the differential expression of pro-inflammatory molecules unique to each IFN family member. In general type-I, -II and -III IFNs stimulated distinct the pro-inflammatory environment. In particular, IFN-α upregulated the pro-inflammatory gene *IL18R1*, which correlates with severe asthma in bronchial alveolar lavage and in human bronchial epithelial biopsy (*167*). The common upregulation of pro-inflammatory genes such as *CXCL9, CXCL11, GBP5, CD38, JAK2* and *APOL3* by IFN-α and IFN-γ is in line with previous findings of overlapping mechanisms of these two IFNs in acute influenza A virus infection (*168*) and HSV-2 virus infection (*169*). These orchestrated IFN stimulation leads to antigen presenting cell (APC) and TH1 activation. Type-II IFN plays also a role in the cytokine storm in COVID-19 patients (*170*) and could lead to cytokine dysfunction of secondary organs (*171*). This data suggests that despite their induction of an antiviral cell state via ISGs expression, IFN family members enhance a pro-inflammatory environment. Elevated levels of chemokines such as *CXCL9* and *CXCL11* can enhance the immune response by recruiting leukocytes via their corresponding receptors on the cell surface (*172*). Since IFN-λs are the first IFNs interfering with viral spread of influenza at the epithelial barrier without enhancing a pro-inflammatory environment (*103*), this study furthermore demonstrated the unique upregulation of *IL10* by IFN-λ3. In contrast, previous studies revealed the IL-10 activation in DCs and macrophages were restricted to type-I IFN stimulation (*173*). IFN-λ3 might thereby counterbalance pro-inflammatory processes to maintain the homeostasis and to prevent an overreaction of the immune system.

IFN stimulation led to three distinct epithelial mechanisms in the airway epithelium. While type-I IFNs upregulated cell-cell adhesion molecules and tight junctions, type-II IFN stimulation led to gene induction associated with cell proliferation and type-III IFNs induced intercellular signaling by upregulating ion channels. This data is in line with previous studies showing that IFN-activated epithelial resistance to influenza infection (*174*), exhibited a barrier to bacterial dissemination (*175*) and induced a blood–brain barrier in *in vivo* models (*176*). Especially tight junctions which were upregulated by type-I IFNs such as the JAM gene family and cell-cell adhesion molecules (*PECAM1*), are downregulated by SARS-CoV-2, resulting in disruption of the alveolar–capillary barrier (*177*). Type-I IFN release following a virus infection might counterbalance viral mediated epithelial disruption and prevent virus susceptibility and thereby enhance recovery after virus infection. By upregulating several ion channels, receptors, and adhesion molecules (*GABRR1, GABRA2, GLRA3, SYT9, GABRG3* and *CTNNA1-3*), type-III IFNs stimulate intracellular signaling processes and ion transport across the epithelial barrier (*178*). However, IFN-λs might increase cell permeability via NF-kB signaling upregulating the TNF-α receptor *NFRSF1B* (*179*), which inhibits lung repair during influenza recovery by inducing p53 and thereby decreases epithelial proliferation and differentiation (*180*). In addition, IFN-γ uniquely induced genes such as *IL1B, CCL7, KDR* and *ARHGEF5* suggesting a pro-inflammatory environment and cell proliferation. In neutrophilic asthma IL-1β activation is associated with epithelial barrier dysregulation, increased mucin production and neutrophilic infiltration (*181*). Genes (*KDR, VEGFA, ARHGEF5*) upregulated by IFN-γ were associated with shorter survival time in lung cancer patients due to their impact on cell-proliferation (*182*), cell invasion and tumor growth (*183*). This IFN-γ dependent effect on cell proliferation after viral infection might be beneficial, as it might promote rebuilding processes after epithelium damage. Future studies have to confirm the role of these IFN-induced inflammatory genes and epithelial modulators in the antiviral cell state after viral infection.

5.2. IFNs induce ACE2 upregulation via the transcription factor FoxO1

In addition, this study reveals aspects of the molecular mechanisms underlying IFN-dependent ACE2 regulation in primary human bronchial epithelial cells. IFN expression is triggered during SARS-CoV-2 infection by PAMPs in infected airway epithelial cells and activate the first line of antiviral host defense (*96*); (*119*). Unfortunately, ACE2 is induced by IFNs as part of the IFN-induced antiviral cell state, providing a strategy for SARS-CoV-2 to evade immune response, as known from other viruses (*89*). This SARS-CoV-2-induced vicious cycle utilizes the IFN signaling pathways to increase viral spread via high ACE2 expression, thereby leading to enhanced virus susceptibility. However, with the progression of the pandemic, research demonstrated that not the functional ACE2 full-length is upregulated by IFN release, but rather truncACE2 (*92*); (*120*). The isoform starts with a novel exon within intron nine and lacks the N-terminus including the enzymatic and SARS-CoV-2 spike protein binding domains (*92*). In this study, type-I, -II and -III IFNs upregulated both the full-length and truncated isoform,

with a more significant effect on truncACE2. Especially IFN-γ-induced truncACE2 rather than the full-length isoform, suggesting that type-II release might be beneficial to counterbalance viral susceptibility. Anyway, type-I, -II and -III IFNs-stimulated airway epithelium demonstrated the induction of *ACE2*, which comfirms the findings observed in submerged NHBE cultures. This data is in line with previous findings of IFN-dependent induction of ACE2 full-length and truncACE2 (*91*). In addition, COVID-19 patients demonstrated elevated levels of ISGs correlated with viral load, including ACE2 (*121*). Even though, according to the Cancer Genome Atlas truncACE2 occurs in squamous cell carcinomas of the respiratory, gastrointestinal, and urogenital tract (*92*), the biological relevance is still uncertain. Anyway, this study along with others (*91*); (*92*) postulates a potential advantage during SARS virus infection, since the interaction between the virus and truncACE2 is prevented, and thereby diminishs virus susceptibility. Future studies have to address the biological relevance of truncACE2 for the RAAS and KKS and their homeostasis during COVID-19.

As the pandemic revealed the importance of investigating the dynamics between SARS-CoV-2 infection, antiviral immunity, and viral susceptibility, in this study potential involved factors in the IFN-dependent ACE2 regulation were analyzed. Inhibition of JAK, which is important in the IFN pathway, led to ACE2 downregulation in NHBEs. However, the inhibition of downstream molecules of the canonical and non-canonical IFN pathway such as STAT1 and AKT (*184*) did not show any impact on neither ACE2 full-length nor truncACE2, suggesting other involved transcription factors. In contrast, studies using the AKT inhibitor triciribine and human lung alveolar epithelial cell lines (A549) demonstrated the downregulation of ACE2 on transcriptomic and protein level (*185*). Although, triciribine showed excellent safety profiles and excellent pharmacokinetics (*186*); (*187*), it was also declared as “a weak AKT inhibitor” (*188*). Studies analyzing the time course of AKT inhibition and ACE2 regulation might be necessary to distinguish the role of AKT in the IFN-ACE2 axis. Its role is still unclear and this data suggests other involved molecules beyond the canonical and non-canonical IFN pathways.

Since the SARS-CoV-2 induced vicious cycle utilizes the otherwise beneficial IFN-dependent antiviral defense mechanisms for virus susceptibility, targeting transcription factors could be a promising strategy to interrupt the vicious cycle without disturbing the antiviral cell state. Although the IFN-JAK axis plays a role in ACE2 upregulation and tofacitinib, an anti-JAK drug, is clinically available, it would also consequently inhibit the beneficial IFN-dependent ISG activation. Therefore, the transcription factor FoxO1 might be a suitable target due to its positive role in ACE2 induction. FoxO1 is part of the Forkhead box transcription factor family with its conserved DNA-binding domain FKH (*122*); (*123*), regulating target genes depending on environmental signals (*119*); (*120*). In this study, a putative FoxO1 binding sequence (-42/-32) located within the ACE2 proximal promoter site was identified and was further validated by competition experiments. This data is in line with previous findings showing FoxA and FoxO binding sites within the same ACE2 promoter sequences (*86*).

This study demonstrates that the inhibition and knock out of FoxO1 leads to the downregulation of ACE2 full-length at mRNA and protein level in IFN co-stimulated NHBEs. Especially type-I and type-III IFN-stimulated cells showed a significant downregulation of ACE2, highlighting the importance of FoxO1 as these IFNs also induced the highest expression of ACE2 full-length and thereby enhancing viral susceptibility. So far studies primarily focused on targeting FoxO1 via AS1842856 in the context of metabolic diseases and biogenesis. In addition, the complex regulation and diverse roles of FoxO1 have to be considered, as it demonstrates specific effects under normal conditions but exhibits opposite effects in diseases such as diabetes (*189*); (*123*). Previous studies demonstrated the positive effects of AS1842856 treatment in type 2 diabetic db/db mice leading to decreased levels of plasma glucose levels and the downregulation of phosphoenolpyruvate carboxykinase and glucose-6 phosphatase mRNA levels, which are important during glucose production (*144*). However, this effect was not observed in the control group. Mice suffering from non-alcoholic steatohepatitis, which was induced by a high fat diet, demonstrated reduced endoplasmic reticulum (ER) stress and necroptosis following AS1842856 treatment (*190*).

Apparently, the timing of FoxO1 inhibition is also crucial, as mice treated with AS1842856 prior to renal ischemia-reperfusion (I/R) injury led to lower serum levels of urea nitrogen and creatinine, followed by decreased tubular damage score after injury in mice (*191*). In contrast, post I/R injury AS1842856 treatment enhanced the survival rate following injury. Notably, FoxO1 kinetics follow sigmoid curves containing phases crucial for the regulation of mitochondrial proteins, clonal expansion and cell cycle arrest (*145*). In the terminal stage of adipocyte differentiation, FoxO1 demonstrated several cycles of activation and inactivation. While persistent inhibition by AS1842856 suppressed adipocyte differentiation, the inhibition in selective stages had controversial effects on adipogenesis (*145*). In addition, it appears that ACE2 has a prolonged half-life in NHBEs, remaining detectable on a protein level more than 96 hours following CRISPR/Cas9-mediated FOXO1 knock-out. Future studies have to determine the time-course of FoxO1-mediated ACE2 regulation and its impact on virus susceptibility during the initial days of infection in the context of FoxO1 inhibition.

Considering the diverse roles of FoxO1 in metabolism and cell cycle regulation is crucial in targeting FoxO1 during SARS-CoV-2 infection. Inhibition of FoxO1 may not only downregulate ACE2 expression, potentially interfering with virus susceptibility, but might also affect other pathways, leading to disease progression. Anyway, if the timing of FoxO1 inhibition will be appropriately selected, targeting FoxO1 might be a useful strategy to interfere with the SARS-CoV-2 induced vicious cycle. The timing of FoxO1 inhibition might be important due to the dynamic phases of FoxO1 activation, as also observed here in the prolonged cell growth of FoxO1-KO NHBE cells, and the disruption of ACE2's homeostatic role in the RAAS and KKS, leading to typical COVID-19 symptoms (*64*).

5.3. Asthmatic patients demonstrate advantages towards SARS-CoV-2 infection

In addition, this study provides insights into potential risk factors of asthmatic patients during SARS-CoV-2 infection. In this study, *ACE2* expression along with other SARS-CoV-2 infection-related genes were investigated in the genome-wide nasal expression analysis of the asthma ALLIANCE cohort. In this study, asthmatics showed significantly lower expression of genes associated with SARS-CoV-2 infection (*ACE2, S100A12, CXCR6, CXCR3*) compared to healthy controls. These findings suggest a potential shift in the host-virus interaction within the upper airways of asthmatics, suggesting a protective state against virus susceptibility. Furthermore, in healthy individuals high nasal *IFN* expression correlated with high *ACE2* expression, whereas in asthmatics high *IFN* expression was correlated with low *ACE2* expression. Especially high *IFNL3* expression in healthy individuals demonstrated significantly higher levels of *ACE2* compared to samples with high *IFNL3* levels of asthmatic samples. In asthmatics, the SARS-CoV-2 induced vicious cycle might be dysfunctional, not only due the general downregulation of ACE2 but also due to the reduced IFN-ACE2 signaling. These findings are in line with previous studies showing a downregulation of ACE2 transcripts in nasal and bronchial epithelial cells of asthmatic and allergic patients (*35*).

This study highlights potential intervention elements of the vicious cycle, in particular genes associated with the KKS and acute phase of infection. High nasal expression levels of *KLK1, KLK13*, and *NOS3* were associated with high type-I, -II, and -III IFN levels both in asthmatics and healthy individuals. Under normal conditions the KKS system with its involved kallikrein serine proteases, is crucial for tissue repair and platelet aggregation (*75*); (*76*). This study is consistent with previous findings showing upregulated kallikreins in COVID-19 patients admitted to intensive care (*192*). In addition, it has been postulated that a bradykinin storm combined with a cytokine storm is associated with severe COVID-19 symptoms and major vascular complications (*193*). SARS-CoV-2 occupies ACE2 and thereby enhancing the bradykinin storm and leading to the progression of severe COVID-19 (*194*); (*195*). But also as demonstrated in this study, the elevated levels of KKS genes in healthy individuals and asthmatic patients might further enhance this effect. Drugs, such as the approved molecule icatibant, that targets components of the KKS were suggested to be beneficial in COVID-19 patients (*196*); (*197*), particularly for cardiovascular complications (*69*) and counterbalance KKS dysregulation (*195*); (*197*).

The vicious cycle in which SARS-CoV-2 utilizes the IFN pathway is also related to acute phase proteins. These proteins play a crucial role in the cytokine storm and are relevant to later stages of COVID-19. High nasal expression of type-I, -II, and -III IFNs were associated with genes of the cytokine storm (*IL6, IL36RN, IL1A, IL10, CXCL10, STAT1*) in asthmatics and non-asthmatics. Previous studies reported a delayed secretion of type-I and -III IFNs following SARS-CoV-2 infection, which correlated with the release of pro-inflammatory cytokines from

mononuclear macrophages (*113*). In addition, low levels of IFN activity and ISG transcription together with high cytokine levels such as IL-6 and TNF-α were demonstrated in COVID-19 patients (*102*). This study highlightes the relationship between IFN release and acute phase genes in the upper airways, suggesting that targeting these acute phase factors could be an additional possibility to reduce COVID-19 severity. Tocilizumab a humanized anti-IL-6 receptor antibody, which is used in rheumatic diseases (*198*) and cytokine storm treatment (*199*), might be a potential drug against the progression of a cytokine storm. Studies provided evidence for the successful treatment in severe COVID-19 patients suffering from cytokine storm and ARDS (*200–202*).

Several studies highlighted the potential risk factors for asthmatic patients during the SARS-CoV-2 pandemic (*13–15*). Pre-existing airway damage as occurring in asthma was characterized enhancing severe SARS-CoV-2 infections. Asthma patients are characterized by low IFN levels (*102*). Type-I and -III IFNs induction is reduced in allergic asthmatic children after rhinovirus infection by an high-affinity IgE receptor (*203*). On the one hand, reduced IFN levels might be helpfull during SARS-CoV-2 infection by inherently lower ACE2 expression levels due to the diminished vicious cycle. On the other hand, low ISG expression levels and inactivation of the antiviral cell state might be disadvantageous. This study demonstrates the low induction of ISGs especially in high *IFNA2* asthmatic samples, suggesting additionally disadvantages for asthmatic patients. This results are in line with previous studies showing that asthmatics did not demonstrate a greater susceptibility to rhinovirus infection compared to healthy individuals, but were more likely to develop severer symptoms and lower respiratory tract disruption (*204*). Although only 0.87% of SARS-CoV-2 infected children showed prevalence of asthma, severe symptoms such as cough, shortness of breath and diarrhea were significantly higher in asthmatics compared to non-asthmatics (*205*). In addition, studies showed that the infection with respiratory viruses early on in life increases asthma development by inducing a TH2-like effector phenotype in T regulatory cells (*206*). The diminished vicious cycle in asthmatics might lead to COVID-19 disease progression and severe symptoms. Anyway, disease progression and the correlation of severe COVID-19 to asthma and elevated IFN and ISG levels in asthmatics have to be further analyzed.

In contrast, several studies reported no significant differences in hospitalizations and ICU between asthmatics and non-asthmatics along with lower risk of SARS-CoV-2 infection in asthmatics (*207*). In addition, in pediatric cohort studies asthmatic children also demonstrated similar viral infection risks compared to non-asthmatic children (*208*). Since several meta-analysis highlighted the low levels of pre-diagnosed asthma in COVID-19 patients (*207*), current studies suggest that asthma may exhibit advantages rather than being considered as a risk factor for SARS-CoV-2 infection. ACE2 expression was further inversely correlated with positive allergen-specific IgE levels and IL-13 expression in nasal epithelial cells of asthmatic patients (*35*). ICS treatment, a common drug for type 2 asthma, might be beneficial for asthmatics thus it was associated with lower ACE2 and TMPRSS2 levels in sputum cells (*209*). However, previous studies showed that glucocorticoids did not decrease ACE2 expression and

affect viral host response in NHBEs (*197*). The diminished SARS-CoV-2 induced vicious cycle in asthmatics might be an indication for the protective effects of asthma, with ICS treatment enhancing the protective state of asthmatics towards SARS-CoV-2 infection. This study not only highlightes that in healthy individuals potential targets such as FoxO1 could be addressed to counteract the SARS-CoV-2 induced vicious cycle without disrupting the beneficial ISG induction by IFNs, but also provides evidence of the role of the KKS and potential targets of the acute phase in asthmatics and non-asthmatics. This study provides evidence that asthma might not increase the risk of SARS-CoV-2 infection, due to reduced *ACE2* and *TMPRSS2* expression levels in asthmatics, preventing virus susceptibility. SARS-CoV-2 infection might not activate the vicious cycle in asthmatics to increase viral susceptibility, although the mechanisms behind the diminished vicious cycle have to be further investigated.

5.4. Conclusion and perspective

In conclusion, type-I, -II and -III IFNs induce similar ISGs while having unique effects on pro-inflammatory environment and airway epithelial barrier integrity. This study not only highlights the relevance of genome-wide gene expression analysis using differentiated organotypic 3D air-liquid interface cultures but also demonstrates the unique roles of the different IFNs. IFN stimulation contributes to epithelial reconstruction after viral infection by inducing cell-cell adhesion molecules, tight junctions, cell proliferation and intercellular signaling. Thus, it can be postulated that personalized inhaled therapies may target IFN-type-specific dysregulation of epithelial integrity and enhance intrinsic anti-viral immunity. However, to counterbalance the epithelial disruption, as observed in Long COVID, the long-term effect of IFNs on airway epithelium also post-infection remains to be addressed by future studies.

This study provides evidence for a SARS-CoV-2-induced vicious cycle, in which especially type-I and type-III IFNs upregulate full-length ACE2, thereby supporting the viral evasion mechanism of first-line anti-viral immune defense. The transcription factor FoxO1 plays a crucial role in the signaling pathway of the vicious cycle, where it contributes to the IFN-dependent ACE2 induction. Addressing FoxO1 with specific inhibitors might evade the vicious cycle by downregulating ACE2 without disrupting intrinsic antiviral immune response. Future studies are needed to evaluate the impact of FoxO1 inhibition during SARS-CoV-2 infection and COVID-19 progression on metabolic pathways, the RAAS and KKS. The IFN-dependent *ACE2* regulation is inactive in asthmatics, which might be explained by the inoperative vicious cycle. Due to decreased *ACE2* and *TMPRSS2* levels, asthmatics might have benefits against viral susceptibility at early stages of infection. However, future studies have to address the risk factors of asthma hallmarks such as lung epithelial barrier disruption in the context of severe COVID-19 disease progression.

Chapter 6

Scientific Summary

6. Scientific summary

6.1. English version

Interferons (IFNs) are important for the antiviral defense mechanisms following viral infection. Although the IFN pathway is mainly understood and leads to the expression of IFN stimulated genes (ISGs), the impact of type-I, -II and -III IFNs on epithelial integrity remains elusive. In addition, the SARS-CoV-2 pandemic highlighted the need to address the relation between viral infiltration, virus-host cell interaction and immune response in the context of IFN release. This thesis addresses this relation by analyzing the IFN-dependent ACE2 regulation.

This study shows that besides the expression of similar ISGs, type-I, -II and -III IFNs induce different epithelial modulators in primary organotypic 3D air-liquid interface airway cultures. While type-I IFNs upregulate cell-cell adhesion molecules, type-II induces cell proliferation and mainly pro-inflammatory genes, and type-III IFNs enhance intercellular signalling. In addition, ACE2 was upregulated in 3D cultures and submerged primary human bronchial epithelial cells following IFN stimulation. Different known molecules of the IFN pathway such as JAK, but also the transcription factor FoxO1 could be identified to play a role in the IFN-dependent ACE2 regulation, by establishing FoxO1 knock out cells. Whole-genome analysis of nasal scrapings of asthmatic patients and healthy control group revealed the downregulation of SARS-CoV-2 infection related genes such as *ACE2* and *TMPRSS2* in asthmatics compared to healthy individuals.

In conclusion, this study focuses on the complex IFN-mediated pathways including epithelial modulation and ACE2 induction. It suggests the involvement of transcription factor FoxO1 in ACE2 regulation as a potential target to address virus susceptibility without disrupting ISG expression. Asthmatic patients demonstrate potential advantages against the first phase of SARS-CoV-2 infection by lacking the IFN-dependent induction of ACE2.

6.2. Deutsche Fassung

Interferone (IFNs) sind essenziell für die antiviralen Abwehrmechanismen nach einer Virusinfektion. Obwohl der IFN-Signalweg weitgehend verstanden ist und zur Expression von IFN-stimulierten Genen (ISGs) führt, ist die Auswirkung von Typ-I-, -II- und -III-IFNs auf die Integrität des Epithels nach wie vor unklar. Darüber hinaus hat die SARS-CoV-2-Pandemie gezeigt, dass die Beziehung zwischen viraler Infektion, Virus-Wirtszell-Interaktion und Immunantwort im Zusammenhang mit den IFN Wirkmechanismen noch genauer untersucht werden muss. Die vorliegende Arbeit befasst sich mit diesem Zusammenhang, indem sie die IFN-abhängige ACE2-Regulation analysiert.

Diese Studie zeigt, dass Typ-I-, -II- und -III-IFNs neben der Expression von gleichen IFN stimulierten Genen (ISGs), unterschiedliche epitheliale Modulatoren in primären organotypischen 3D-Atemwegs-Kulturen induzieren. Während Typ-I-IFNs Zell-Zell-Adhäsionsmoleküle hochregulieren, induzieren Typ-II-IFNs die Zellproliferation und hauptsächlich pro-inflammatorische Gene, und Typ-III-IFNs verstärken die interzelluläre Signalübertragung. Darüber hinaus wurde ACE2 in 3D-Kulturen und primären menschlichen Bronchialepithelzellen nach IFN-Stimulation hochreguliert. Indem FoxO1-Knock-out-Zellen etabliert wurden, konnten verschiedene bekannte Moleküle des IFN-Signalwegs wie JAK, aber auch der Transkriptionsfaktor FoxO1, die eine Rolle bei der IFN-abhängigen ACE2-Regulierung spielen, identifiziert werden. Die Analyse des gesamten Genoms von nasalen Probem asthmatischer und gesunder Patienten ergab, dass Gene, die mit der SARS-CoV-2-Infektion zusammenhängen, wie *ACE2* und *TMPRSS2*, bei Asthmatikern im Vergleich zu Gesunden herunterreguliert sind.

Diese Studie arbeitet die komplexen IFN-vermittelten Signalwege heraus, zu denen die Modulation des Epithels und die Induktion von ACE2 gehören. Die Arbeit legt durch die Beteiligung des Transkriptionsfaktors FoxO1 an der ACE2-Regulierung, den TRanskriptionsfaktor als potenzielles Ziel für die Behandlung der Virusanfälligkeit ohne Störung der ISG-Expression nahe. Asthmapatienten zeigen potenzielle Vorteile gegen die erste Phase der SARS-CoV-2-Infektion, da ihnen die IFN-abhängige Induktion von ACE2 fehlt.

Chapter 7

References

7. References

(*1*) Azkur, A. K., Akdis, M., Azkur, D., Sokolowska, M., van de Veen, W., Bruggen, M. C., O'Mahony, L., Gao, Y., Nadeau, K., and Akdis, C. A. (2020). Immune response to SARS-CoV-2 and mechanisms of immunopathological changes in COVID-19. *Allergy 75*, 1564–1581.

(*2*) Chen, G. et al. (2020). Clinical and immunological features of severe and moderate coronavirus disease 2019. *J Clin Invest 130*, 2620–2629.

(*3*) Huang, C. et al. (2020). Clinical features of patients infected with 2019 novel coronavirus in Wuhan, China. *Lancet 395*, 497–506.

(*4*) Xu, Z. et al. (2020). Pathological findings of COVID-19 associated with acute respiratory distress syndrome. *Lancet Respir Med 8*, 420–422.

(*5*) Calica Utku, A., Budak, G., Karabay, O., Guclu, E., Okan, H. D., and Vatan, A. (2020). Main symptoms in patients presenting in the COVID-19 period. *Scott Med J 65*, 127–132.

(*6*) Yang, X. et al. (2020). Clinical course and outcomes of critically ill patients with SARS-CoV-2 pneumonia in Wuhan, China: a single-centered, retrospective, observational study. *Lancet Respir Med 8*, 475–481.

(*7*) Rendeiro, A. F. et al. (2021). The spatial landscape of lung pathology during COVID-19 progression. *Nature 593*, 564–569.

(*8*) Hussman, J. P. (2020). Cellular and Molecular Pathways of COVID-19 and Potential Points of Therapeutic Intervention. *Front Pharmacol 11*, 1169.

(*9*) Mathew, D. et al. (2020). Deep immune profiling of COVID-19 patients reveals distinct immunotypes with therapeutic implications. *Science 369*, DOI: 10.1126/science.abc8511.

(*10*) Weiskopf, D. et al. (2020). Phenotype and kinetics of SARS-CoV-2-specific T cells in COVID-19 patients with acute respiratory distress syndrome. *Sci Immunol 5*, DOI: 10.1126/sciimmunol.abd2071.

(*11*) Ni, L. et al. (2020). Detection of SARS-CoV-2-Specific Humoral and Cellular Immunity in COVID-19 Convalescent Individuals. *Immunity 52*, 971–977 e3.

(*12*) Grifoni, A. et al. (2020). Targets of T Cell Responses to SARS-CoV-2 Coronavirus in Humans with COVID-19 Disease and Unexposed Individuals. *Cell 181*, 1489–1501 e15.

(*13*) Schultze, A. et al. (2020). Risk of COVID-19-related death among patients with chronic obstructive pulmonary disease or asthma prescribed inhaled corticosteroids: an observational cohort study using the OpenSAFELY platform. *Lancet Respir Med 8*, 1106–1120.

(*14*) Bloom, C. I. et al. (2021). Risk of adverse outcomes in patients with underlying respiratory conditions admitted to hospital with COVID-19: a national, multicentre prospective cohort study using the ISARIC WHO Clinical Characterisation Protocol UK. *Lancet Respir Med 9*, 699–711.

(*15*) Zhu, Z., Hasegawa, K., Ma, B., Fujiogi, M., Camargo, C. A., and Liang, L. (2020). Association of asthma and its genetic predisposition with the risk of severe COVID-19. *J Allergy Clin Immunol 146*, 327–329 e4.

(*16*) Ssentongo, P., Ssentongo, A. E., Heilbrunn, E. S., Ba, D. M., and Chinchilli, V. M. (2020). Association of cardiovascular disease and 10 other pre-existing comorbidities with COVID-19 mortality: A systematic review and meta-analysis. *PLoS One 15*, e0238215.

(*17*) Ren, J. et al. (2022). Impact of Allergic Rhinitis and Asthma on COVID-19 Infection, Hospitalization, and Mortality. *J Allergy Clin Immunol Pract 10*, 124–133.

(*18*) Terry, P. D., Heidel, R. E., and Dhand, R. (2021). Asthma in Adult Patients with COVID-19. Prevalence and Risk of Severe Disease. *Am J Respir Crit Care Med 203*, 893–905.

(*19*) Stikker, B. S., Hendriks, R. W., and Stadhouders, R. (2023). Decoding the genetic and epigenetic basis of asthma. *Allergy 78*, 940–956.

(*20*) Erle, D. J., and Sheppard, D. (2014). The cell biology of asthma. *J Cell Biol 205*, 621–31.

(*21*) Lambrecht, B. N., and Hammad, H. (2015). The immunology of asthma. *Nat Immunol 16*, 45–56.

(*22*) Ballesteros-Tato, A., Randall, T. D., Lund, F. E., Spolski, R., Leonard, W. J., and Leon, B. (2016). T Follicular Helper Cell Plasticity Shapes Pathogenic T Helper 2 Cell-Mediated Immunity to Inhaled House Dust Mite. *Immunity 44*, 259–73.

(*23*) Yamauchi, K., and Ogasawara, M. (2019). The Role of Histamine in the Pathophysiology of Asthma and the Clinical Efficacy of Antihistamines in Asthma Therapy. *Int J Mol Sci 20*, DOI: 10.3390/ijms20071733.

(*24*) Hammad, H., and Lambrecht, B. N. (2021). The basic immunology of asthma. *Cell 184*, 1469–1485.

(*25*) Lambrecht, B. N., Hammad, H., and Fahy, J. V. (2019). The Cytokines of Asthma. *Immunity 50*, 975–991.

(*26*) Wang, L., Foer, D., Zhang, Y., Karlson, E. W., Bates, D. W., and Zhou, L. (2023). Post-Acute COVID-19 Respiratory Symptoms in Patients With Asthma: An Electronic Health Records-Based Study. *J Allergy Clin Immunol Pract 11*, 825–835 e3.

(*27*) Gibellini, L. et al. (2022). Plasma Cytokine Atlas Reveals the Importance of TH2 Polarization and Interferons in Predicting COVID-19 Severity and Survival. *Front Immunol 13*, 842150.

(*28*) Carapito, R. et al. (2022). Identification of driver genes for critical forms of COVID-19 in a deeply phenotyped young patient cohort. *Sci Transl Med 14*, eabj7521.

(*29*) Lucas, C. et al. (2020). Longitudinal analyses reveal immunological misfiring in severe COVID-19. *Nature 584*, 463–469.

(*30*) Zhu, J. et al. (2019). Bronchial mucosal IFN-alpha/beta and pattern recognition receptor expression in patients with experimental rhinovirus-induced asthma exacerbations. *J Allergy Clin Immunol 143*, 114–125 e4.

(*31*) Contoli, M. et al. (2006). Role of deficient type III interferon-lambda production in asthma exacerbations. *Nat Med 12*, 1023–6.

(*32*) Skevaki, C., Karsonova, A., Karaulov, A., Xie, M., and Renz, H. (2020). Asthma-associated risk for COVID-19 development. *J Allergy Clin Immunol 146*, 1295–1301.

(*33*) Mendes, N. F., Jara, C. P., Mansour, E., Araujo, E. P., and Velloso, L. A. (2021). Asthma and COVID-19: a systematic review. *Allergy Asthma Clin Immunol 17*, 5.

(*34*) Sunjaya, A. P., Allida, S. M., Di Tanna, G. L., and Jenkins, C. R. (2022). Asthma and COVID-19 risk: a systematic review and meta-analysis. *Eur Respir J 59*, DOI: 10.1183/13993003.01209-2021.

(*35*) Jackson, D. J. et al. (2020). Association of respiratory allergy, asthma, and expression of the SARS-CoV-2 receptor ACE2. *J Allergy Clin Immunol 146*, 203–206 e3.

(*36*) Davies, G. A., Alsallakh, M. A., Sivakumaran, S., Vasileiou, E., Lyons, R. A., Robertson, C., Sheikh, A., and Collaborators, E. I. (2021). Impact of COVID-19 lockdown on emergency asthma admissions and deaths: national interrupted time series analyses for Scotland and Wales. *Thorax 76*, 867–873.

(*37*) To, T., Zhang, K., Terebessy, E., Zhu, J., and Licskai, C. (2023). Healthcare utilization in Canadian children and young adults with asthma during the COVID-19 pandemic. *PLoS One 18*, e0280362.

(*38*) Feldman, J. M., Serebrisky, D., Starr, S., Castano, K., Greenfield, N., Silverstein, G., Fruchter, N., Mammen, J., McGovern, C., and Arcoleo, K. (2023). Reduced asthma morbidity during COVID-19 in minority children: is medication adherence a reason? *J Asthma 60*, 468–478.

(*39*) Shang, J., Ye, G., Shi, K., Wan, Y., Luo, C., Aihara, H., Geng, Q., Auerbach, A., and Li, F. (2020). Structural basis of receptor recognition by SARS-CoV-2. *Nature 581*, 221–224.

(*40*) Bayati, A., Kumar, R., Francis, V., and McPherson, P. S. (2021). SARS-CoV-2 infects cells after viral entry via clathrin-mediated endocytosis. *J Biol Chem 296*, 100306.

(*41*) Inoue, Y., Tanaka, N., Tanaka, Y., Inoue, S., Morita, K., Zhuang, M., Hattori, T., and Sugamura, K. (2007). Clathrin-dependent entry of severe acute respiratory syndrome coronavirus into target cells expressing ACE2 with the cytoplasmic tail deleted. *J Virol 81*, 8722–9.

(*42*) Hoffmann, M., Kleine-Weber, H., and Pohlmann, S. (2020). A Multibasic Cleavage Site in the Spike Protein of SARS-CoV-2 Is Essential for Infection of Human Lung Cells. *Mol Cell 78*, 779–784 e5.

(*43*) Shang, J., Wan, Y., Luo, C., Ye, G., Geng, Q., Auerbach, A., and Li, F. (2020). Cell entry mechanisms of SARS-CoV-2. *Proc Natl Acad Sci U S A 117*, 11727–11734.

(*44*) Hoffmann, M. et al. (2020). SARS-CoV-2 Cell Entry Depends on ACE2 and TMPRSS2 and Is Blocked by a Clinically Proven Protease Inhibitor. *Cell 181*, 271–280 e8.

(*45*) Cai, Y., Zhang, J., Xiao, T., Peng, H., Sterling, S. M., Walsh, R. M., Rawson, S., Rits-Volloch, S., and Chen, B. (2020). Distinct conformational states of SARS-CoV-2 spike protein. *Science 369*, 1586–1592.

(*46*) Wu, C. T. et al. (2023). SARS-CoV-2 replication in airway epithelia requires motile cilia and microvillar reprogramming. *Cell 186*, 112–130 e20.

(*47*) Sola, I., Almazan, F., Zuniga, S., and Enjuanes, L. (2015). Continuous and Discontinuous RNA Synthesis in Coronaviruses. *Annu Rev Virol 2*, 265–88.

(*48*) Knoops, K., Kikkert, M., Worm, S. H., Zevenhoven-Dobbe, J. C., van der Meer, Y., Koster, A. J., Mommaas, A. M., and Snijder, E. J. (2008). SARS-coronavirus replication is supported by a reticulovesicular network of modified endoplasmic reticulum. *PLoS Biol 6*, e226.

(*49*) Finkel, Y. et al. (2021). SARS-CoV-2 uses a multipronged strategy to impede host protein synthesis. *Nature 594*, 240–245.

(*50*) Bhaskar, S., Sinha, A., Banach, M., Mittoo, S., Weissert, R., Kass, J. S., Rajagopal, S., Pai, A. R., and Kutty, S. (2020). Cytokine Storm in COVID-19-Immunopathological Mechanisms, Clinical Considerations, and Therapeutic Approaches: The REPROGRAM Consortium Position Paper. *Front Immunol 11*, 1648.

(*51*) Ruan, Q., Yang, K., Wang, W., Jiang, L., and Song, J. (2020). Clinical predictors of mortality due to COVID-19 based on an analysis of data of 150 patients from Wuhan, China. *Intensive Care Med 46*, 846–848.

(*52*) Chen, J., and Subbarao, K. (2007). The Immunobiology of SARS*. *Annu Rev Immunol 25*, 443–72.

(*53*) Qin, C. et al. (2020). Dysregulation of Immune Response in Patients With Coronavirus 2019 (COVID-19) in Wuhan, China. *Clin Infect Dis 71*, 762–768.

(*54*) Hartenian, E., Nandakumar, D., Lari, A., Ly, M., Tucker, J. M., and Glaunsinger, B. A. (2020). The molecular virology of coronaviruses. *J Biol Chem 295*, 12910–12934.

(*55*) Tipnis, S. R., Hooper, N. M., Hyde, R., Karran, E., Christie, G., and Turner, A. J. (2000). A human homolog of angiotensin-converting enzyme. Cloning and functional expression as a captopril-insensitive carboxypeptidase. *J Biol Chem 275*, 33238–43.

(*56*) Rice, G. I., Thomas, D. A., Grant, P. J., Turner, A. J., and Hooper, N. M. (2004). Evaluation of angiotensin-converting enzyme (ACE), its homologue ACE2 and neprilysin in angiotensin peptide metabolism. *Biochem J 383*, 45–51.

(*57*) Patel, S., Rauf, A., Khan, H., and Abu-Izneid, T. (2017). Renin-angiotensin-aldosterone (RAAS): The ubiquitous system for homeostasis and pathologies. *Biomed Pharmacother 94*, 317–325.

(*58*) Kuba, K., Imai, Y., Ohto-Nakanishi, T., and Penninger, J. M. (2010). Trilogy of ACE2: a peptidase in the renin-angiotensin system, a SARS receptor, and a partner for amino acid transporters. *Pharmacol Ther 128*, 119–28.

(*59*) Hamming, I., Cooper, M. E., Haagmans, B. L., Hooper, N. M., Korstanje, R., Osterhaus, A. D., Timens, W., Turner, A. J., Navis, G., and van Goor, H. (2007). The emerging role of ACE2 in physiology and disease. *J Pathol 212*, 1–11.

(*60*) Paz Ocaranza, M., Riquelme, J. A., Garcia, L., Jalil, J. E., Chiong, M., Santos, R. A. S., and Lavandero, S. (2020). Counter-regulatory renin-angiotensin system in cardiovascular disease. *Nat Rev Cardiol 17*, 116–129.

(*61*) Crajoinas, R. O., Polidoro, J. Z., Carneiro de Morais, C. P., Castelo-Branco, R. C., and Girardi, A. C. (2016). Angiotensin II counteracts the effects of cAMP/PKA on NHE3 activity and phosphorylation in proximal tubule cells. *Am J Physiol Cell Physiol 311*, C768–C776.

(*62*) Hunyady, L., and Catt, K. J. (2006). Pleiotropic AT1 receptor signaling pathways mediating physiological and pathogenic actions of angiotensin II. *Mol Endocrinol 20*, 953–70.

(*63*) Cure, E., Ilcol, T. B., and Cumhur Cure, M. (2020). Angiotensin II, III, and IV may be important in the progression of COVID-19. *J Renin Angiotensin Aldosterone Syst 21*, 1470320320972019.

(*64*) Chung, M. K. et al. (2020). SARS-CoV-2 and ACE2: The biology and clinical data settling the ARB and ACEI controversy. *EBioMedicine 58*, 102907.

(*65*) Chatterjee, B., and Thakur, S. S. (2020). ACE2 as a potential therapeutic target for pandemic COVID-19. *RSC Adv 10*, 39808–39813.

(*66*) Wu, Z., Hu, R., Zhang, C., Ren, W., Yu, A., and Zhou, X. (2020). Elevation of plasma angiotensin II level is a potential pathogenesis for the critically ill COVID-19 patients. *Crit Care 24*, 290.

(*67*) Esakandari, H., Nabi-Afjadi, M., Fakkari-Afjadi, J., Farahmandian, N., Miresmaeili, S. M., and Bahreini, E. (2020). A comprehensive review of COVID-19 characteristics. *Biol Proced Online 22*, 19.

(*68*) Vellas, C., Delobel, P., de Souto Barreto, P., and Izopet, J. (2020). COVID-19, Virology and Geroscience: A Perspective. *J Nutr Health Aging 24*, 685–691.

(*69*) Shi, S. et al. (2020). Association of Cardiac Injury With Mortality in Hospitalized Patients With COVID-19 in Wuhan, China. *JAMA Cardiol 5*, 802–810.

(*70*) Venkatesan, P. (2021). NICE guideline on long COVID. *Lancet Respir Med 9*, 129.

(*71*) Dennis, A. et al. (2021). Multiorgan impairment in low-risk individuals with post-COVID-19 syndrome: a prospective, community-based study. *BMJ Open 11*, e048391.

(*72*) Vickers, C. et al. (2002). Hydrolysis of biological peptides by human angiotensin-converting enzyme-related carboxypeptidase. *J Biol Chem 277*, 14838–43.

(*73*) Sodhi, C. P., Wohlford-Lenane, C., Yamaguchi, Y., Prindle, T., Fulton, W. B., Wang, S., McCray, P. B., Chappell, M., Hackam, D. J., and Jia, H. (2018). Attenuation of pulmonary ACE2 activity impairs inactivation of des-Arg(9) bradykinin/BKB1R axis and facilitates LPS-induced neutrophil infiltration. *Am J Physiol Lung Cell Mol Physiol 314*, L17–L31.

(*74*) Ancion, A., Tridetti, J., Nguyen Trung, M. L., Oury, C., and Lancellotti, P. (2019). A Review of the Role of Bradykinin and Nitric Oxide in the Cardioprotective Action of Angiotensin-Converting Enzyme Inhibitors: Focus on Perindopril. *Cardiol Ther 8*, 179–191.

(*75*) Michael, I. P., Pampalakis, G., Mikolajczyk, S. D., Malm, J., Sotiropoulou, G., and Diamandis, E. P. (2006). Human tissue kallikrein 5 is a member of a proteolytic cascade pathway involved in seminal clot liquefaction and potentially in prostate cancer progression. *J Biol Chem 281*, 12743–50.

(*76*) Raspi, G. (1996). Kallikrein and kallikrein-like proteinases: purification and determination by chromatographic and electrophoretic methods. *J Chromatogr B Biomed Appl 684*, 265–87.

(*77*) Snouwaert, J. N. et al. (2023). Human ACE2 expression, a major tropism determinant for SARS-CoV-2, is regulated by upstream and intragenic elements. *PLoS Pathog 19*, e1011168.

(*78*) Li, M. Y., Li, L., Zhang, Y., and Wang, X. S. (2020). Expression of the SARS-CoV-2 cell receptor gene ACE2 in a wide variety of human tissues. *Infect Dis Poverty 9*, 45.

(*79*) Shajahan, A., Archer-Hartmann, S., Supekar, N. T., Gleinich, A. S., Heiss, C., and Azadi, P. (2021). Comprehensive characterization of N- and O- glycosylation of SARS-CoV-2 human receptor angiotensin converting enzyme 2. *Glycobiology 31*, 410–424.

(*80*) Lambert, D. W., Yarski, M., Warner, F. J., Thornhill, P., Parkin, E. T., Smith, A. I., Hooper, N. M., and Turner, A. J. (2005). Tumor necrosis factor-alpha convertase (ADAM17) mediates regulated ectodomain shedding of the severe-acute respiratory syndrome-coronavirus (SARS-CoV) receptor, angiotensin-converting enzyme-2 (ACE2). *J Biol Chem 280*, 30113–9.

(*81*) Patel, V. B., Clarke, N., Wang, Z., Fan, D., Parajuli, N., Basu, R., Putko, B., Kassiri, Z., Turner, A. J., and Oudit, G. Y. (2014). Angiotensin II induced proteolytic cleavage of myocardial ACE2 is mediated by TACE/ADAM-17: a positive feedback mechanism in the RAS. *J Mol Cell Cardiol 66*, 167–76.

(*82*) Clarke, N. E., Fisher, M. J., Porter, K. E., Lambert, D. W., and Turner, A. J. (2012). Angiotensin converting enzyme (ACE) and ACE2 bind integrins and ACE2 regulates integrin signalling. *PLoS One 7*, e34747.

(*83*) Senkel, S., Lucas, B., Klein-Hitpass, L., and Ryffel, G. U. (2005). Identification of target genes of the transcription factor HNF1beta and HNF1alpha in a human embryonic kidney cell line. *Biochim Biophys Acta 1731*, 179–90.

(*84*) Pedersen, K. B., Chhabra, K. H., Nguyen, V. K., Xia, H., and Lazartigues, E. (2013). The transcription factor HNF1alpha induces expression of angiotensin-converting enzyme 2 (ACE2) in pancreatic islets from evolutionarily conserved promoter motifs. *Biochim Biophys Acta 1829*, 1225–35.

(*85*) Clarke, N. E., Belyaev, N. D., Lambert, D. W., and Turner, A. J. (2014). Epigenetic regulation of angiotensin-converting enzyme 2 (ACE2) by SIRT1 under conditions of cell energy stress. *Clin Sci (Lond) 126*, 507–16.

(*86*) Pedersen, K. B., Chodavarapu, H., and Lazartigues, E. (2017). Forkhead Box Transcription Factors of the FOXA Class Are Required for Basal Transcription of Angiotensin-Converting Enzyme 2. *J Endocr Soc 1*, 370–384.

(*87*) Xiong, S., Salazar, G., Patrushev, N., and Alexander, R. W. (2011). FoxO1 mediates an autofeedback loop regulating SIRT1 expression. *J Biol Chem 286*, 5289–99.

(*88*) Stocker, N., Radzikowska, U., Wawrzyniak, P., Tan, G., Huang, M., Ding, M., Akdis, C. A., and Sokolowska, M. (2023). Regulation of angiotensin-converting enzyme 2 isoforms by type 2 inflammation and viral infection in human airway epithelium. *Mucosal Immunol 16*, 5–16.

(*89*) Ziegler, C. G. K. et al. (2020). SARS-CoV-2 Receptor ACE2 Is an Interferon-Stimulated Gene in Human Airway Epithelial Cells and Is Detected in Specific Cell Subsets across Tissues. *Cell 181*, 1016–1035 e19.

(*90*) Chua, R. L. et al. (2020). COVID-19 severity correlates with airway epithelium-immune cell interactions identified by single-cell analysis. *Nat Biotechnol 38*, 970–979.

(*91*) Blume, C. et al. (2021). A novel ACE2 isoform is expressed in human respiratory epithelia and is upregulated in response to interferons and RNA respiratory virus infection. *Nat Genet 53*, 205–214.

(*92*) Onabajo, O. O. et al. (2020). Interferons and viruses induce a novel truncated ACE2 isoform and not the full-length SARS-CoV-2 receptor. *Nat Genet 52*, 1283–1293.

(*93*) Raftery, N., and Stevenson, N. J. (2017). Advances in anti-viral immune defence: revealing the importance of the IFN JAK/STAT pathway. *Cell Mol Life Sci 74*, 2525–2535.

(*94*) Levy, D. E., Marie, I., Smith, E., and Prakash, A. (2002). Enhancement and diversification of IFN induction by IRF-7-mediated positive feedback. *J Interferon Cytokine Res 22*, 87–93.

(*95*) Brooks, A. J. et al. (2014). Mechanism of activation of protein kinase JAK2 by the growth hormone receptor. *Science 344*, 1249783.

(*96*) Gao, S., von der Malsburg, A., Paeschke, S., Behlke, J., Haller, O., Kochs, G., and Daumke, O. (2010). Structural basis of oligomerization in the stalk region of dynamin-like MxA. *Nature 465*, 502–6.

(*97*) Diamond, M. S., and Farzan, M. (2013). The broad-spectrum antiviral functions of IFIT and IFITM proteins. *Nat Rev Immunol 13*, 46–57.

(*98*) Schoggins, J. W. (2019). Interferon-Stimulated Genes: What Do They All Do? *Annu Rev Virol 6*, 567–584.

(*99*) Simmons, D. P., Wearsch, P. A., Canaday, D. H., Meyerson, H. J., Liu, Y. C., Wang, Y., Boom, W. H., and Harding, C. V. (2012). Type I IFN drives a distinctive dendritic cell maturation phenotype that allows continued class II MHC synthesis and antigen processing. *J Immunol 188*, 3116–26.

(*100*) Cella, M., Salio, M., Sakakibara, Y., Langen, H., Julkunen, I., and Lanzavecchia, A. (1999). Maturation, activation, and protection of dendritic cells induced by double-stranded RNA. *J Exp Med 189*, 821–9.

(*101*) Ivashkiv, L. B., and Donlin, L. T. (2014). Regulation of type I interferon responses. *Nat Rev Immunol 14*, 36–49.

(*102*) Hadjadj, J. et al. (2020). Impaired type I interferon activity and inflammatory responses in severe COVID-19 patients. *Science 369*, 718–724.

(*103*) Galani, I. E. et al. (2017). Interferon-lambda Mediates Non-redundant Front-Line Antiviral Protection against Influenza Virus Infection without Compromising Host Fitness. *Immunity 46*, 875–890 e6.

(*104*) Henden, A. S. et al. (2021). IFN-lambda therapy prevents severe gastrointestinal graft-versus-host disease. *Blood 138*, 722–737.

(*105*) Wheelock, E. F. (1965). Interferon-Like Virus-Inhibitor Induced in Human Leukocytes by Phytohemagglutinin. *Science 149*, 310–1.

(*106*) Takaoka, A., and Yanai, H. (2006). Interferon signalling network in innate defence. *Cell Microbiol 8*, 907–22.

(*107*) Zissler, U. M. et al. (2016). Interleukin-4 and interferon-gamma orchestrate an epithelial polarization in the airways. *Mucosal Immunol 9*, 917–26.

(*108*) Szabo, S. J., Kim, S. T., Costa, G. L., Zhang, X., Fathman, C. G., and Glimcher, L. H. (2000). A novel transcription factor, T-bet, directs Th1 lineage commitment. *Cell 100*, 655–69.

(*109*) Bou Ghanem, E. N., Nelson, C. C., and D'Orazio, S. E. (2011). T cell-intrinsic factors contribute to the differential ability of CD8+ T cells to rapidly secrete IFN-gamma in the absence of antigen. *J Immunol 186*, 1703–12.

(*110*) Akamatsu, M. A., de Castro, J. T., Takano, C. Y., and Ho, P. L. (2021). Off balance: Interferons in COVID-19 lung infections. *EBioMedicine 73*, 103642.

(*111*) Felgenhauer, U., Schoen, A., Gad, H. H., Hartmann, R., Schaubmar, A. R., Failing, K., Drosten, C., and Weber, F. (2020). Inhibition of SARS-CoV-2 by type I and type III interferons. *J Biol Chem 295*, 13958–13964.

(*112*) Hatton, C. F. et al. (2021). Delayed induction of type I and III interferons mediates nasal epithelial cell permissiveness to SARS-CoV-2. *Nat Commun 12*, 7092.

(*113*) Blanco-Melo, D. et al. (2020). Imbalanced Host Response to SARS-CoV-2 Drives Development of COVID-19. *Cell 181*, 1036–1045 e9.

(*114*) Galani, I. E. et al. (2021). Untuned antiviral immunity in COVID-19 revealed by temporal type I/III interferon patterns and flu comparison. *Nat Immunol 22*, 32–40.

(*115*) Xia, H., Cao, Z., Xie, X., Zhang, X., Chen, J. Y., Wang, H., Menachery, V. D., Rajsbaum, R., and Shi, P. Y. (2020). Evasion of Type I Interferon by SARS-CoV-2. *Cell Rep 33*, 108234.

(*116*) Ziegler, C. G. K. et al. (2021). Impaired local intrinsic immunity to SARS-CoV-2 infection in severe COVID-19. *Cell 184*, 4713–4733 e22.

(*117*) Lee, J. S. et al. (2020). Immunophenotyping of COVID-19 and influenza highlights the role of type I interferons in development of severe COVID-19. *Sci Immunol 5*, DOI: 10.1126/sciimmunol.abd1554.

(*118*) Bastard, P. et al. (2020). Autoantibodies against type I IFNs in patients with life-threatening COVID-19. *Science 370*, DOI: 10.1126/science.abd4585.

(*119*) Brent, M. M., Anand, R., and Marmorstein, R. (2008). Structural basis for DNA recognition by FoxO1 and its regulation by posttranslational modification. *Structure 16*, 1407–16.

(*120*) Psenakova, K., Kohoutova, K., Obsilova, V., Ausserlechner, M. J., Veverka, V., and Obsil, T. (2019). Forkhead Domains of FOXO Transcription Factors Differ in both Overall Conformation and Dynamics. *Cells 8*, DOI: 10.3390/cells8090966.

(*121*) Xing, Y. Q., Li, A., Yang, Y., Li, X. X., Zhang, L. N., and Guo, H. C. (2018). The regulation of FOXO1 and its role in disease progression. *Life Sci 193*, 124–131.

(*122*) Dong, X. C. (2017). FOXO transcription factors in non-alcoholic fatty liver disease. *Liver Res 1*, 168–173.

(*123*) Eijkelenboom, A., and Burgering, B. M. (2013). FOXOs: signalling integrators for homeostasis maintenance. *Nat Rev Mol Cell Biol 14*, 83–97.

(*124*) Iyer, S. et al. (2013). FOXOs attenuate bone formation by suppressing Wnt signaling. *J Clin Invest 123*, 3409–19.

(*125*) Zanella, F., Dos Santos, N. R., and Link, W. (2013). Moving to the core: spatiotemporal analysis of Forkhead box O (FOXO) and nuclear factor-kappaB (NF-kappaB) nuclear translocation. *Traffic 14*, 247–58.

(*126*) Clark, K. L., Halay, E. D., Lai, E., and Burley, S. K. (1993). Co-crystal structure of the HNF-3/fork head DNA-recognition motif resembles histone H5. *Nature 364*, 412–20.

(*127*) Obsil, T., and Obsilova, V. (2011). Structural basis for DNA recognition by FOXO proteins. *Biochim Biophys Acta 1813*, 1946–53.

(*128*) Peng, S., Li, W., Hou, N., and Huang, N. (2020). A Review of FoxO1-Regulated Metabolic Diseases and Related Drug Discoveries. *Cells 9*, DOI: 10.3390/cells9010184.

(*129*) Matsumoto, M., Pocai, A., Rossetti, L., Depinho, R. A., and Accili, D. (2007). Impaired regulation of hepatic glucose production in mice lacking the forkhead transcription factor Foxo1 in liver. *Cell Metab 6*, 208–16.

(*130*) Wu, Y. et al. (2018). Novel Mechanism of Foxo1 Phosphorylation in Glucagon Signaling in Control of Glucose Homeostasis. *Diabetes 67*, 2167–2182.

(*131*) Altomonte, J., Richter, A., Harbaran, S., Suriawinata, J., Nakae, J., Thung, S. N., Meseck, M., Accili, D., and Dong, H. (2003). Inhibition of Foxo1 function is associated with improved fasting glycemia in diabetic mice. *Am J Physiol Endocrinol Metab 285*, E718–28.

(*132*) Matsuzaki, H., Lee, S., Maeda, M., Kumagai-Takei, N., Nishimura, Y., and Otsuki, T. (2016). FoxO1 regulates apoptosis induced by asbestos in the MT-2 human T-cell line. *J Immunotoxicol 13*, 620–7.

(*133*) Ju, Y., Xu, T., Zhang, H., and Yu, A. (2014). FOXO1-dependent DNA damage repair is regulated by JNK in lung cancer cells. *Int J Oncol 44*, 1284–92.

(*134*) Chang, Y. W., Zhao, Y. F., Cao, Y. L., Gu, X. F., Li, Z. Q., Wang, S. Q., Miao, J. H., and Zhan, H. S. (2013). Liver X receptor alpha inhibits osteosarcoma cell proliferation through up-regulation of FoxO1. *Cell Physiol Biochem 32*, 180–6.

(*135*) Jeong, O. S., Chae, Y. C., Jung, H., Park, S. C., Cho, S. J., Kook, H., and Seo, S. (2016). Long noncoding RNA linc00598 regulates CCND2 transcription and modulates the G1 checkpoint. *Sci Rep 6*, 32172.

(*136*) Biggs, W. H., Meisenhelder, J., Hunter, T., Cavenee, W. K., and Arden, K. C. (1999). Protein kinase B/Akt-mediated phosphorylation promotes nuclear exclusion of the winged helix transcription factor FKHR1. *Proc Natl Acad Sci U S A 96*, 7421–6.

(*137*) Grabiec, A. M., Angiolilli, C., Hartkamp, L. M., van Baarsen, L. G., Tak, P. P., and Reedquist, K. A. (2015). JNK-dependent downregulation of FoxO1 is required to promote the survival of fibroblast-like synoviocytes in rheumatoid arthritis. *Ann Rheum Dis 74*, 1763–71.

(*138*) Yuan, Z., Lehtinen, M. K., Merlo, P., Villen, J., Gygi, S., and Bonni, A. (2009). Regulation of neuronal cell death by MST1-FOXO1 signaling. *J Biol Chem 284*, 11285–92.

(*139*) Pramanik, K. C., Fofaria, N. M., Gupta, P., and Srivastava, S. K. (2014). CBP-mediated FOXO-1 acetylation inhibits pancreatic tumor growth by targeting SirT. *Mol Cancer Ther 13*, 687–98.

(*140*) van der Heide, L. P., and Smidt, M. P. (2005). Regulation of FoxO activity by CBP/p300-mediated acetylation. *Trends Biochem Sci 30*, 81–6.

(*141*) Carpenter, W. E. (1966). Tolnaftate, its effectiveness in pedal mycosis. A preliminary report. *J Am Podiatry Assoc 56*, 541–6.

(*142*) Matsuzaki, H., Daitoku, H., Hatta, M., Tanaka, K., and Fukamizu, A. (2003). Insulin-induced phosphorylation of FKHR (Foxo1) targets to proteasomal degradation. *Proc Natl Acad Sci U S A 100*, 11285–90.

(*143*) Fu, W. et al. (2009). MDM2 acts downstream of p53 as an E3 ligase to promote FOXO ubiquitination and degradation. *J Biol Chem 284*, 13987–4000.

(*144*) Nagashima, T., Shigematsu, N., Maruki, R., Urano, Y., Tanaka, H., Shimaya, A., Shimokawa, T., and Shibasaki, M. (2010). Discovery of novel forkhead box O1 inhibitors for treating type 2 diabetes: improvement of fasting glycemia in diabetic db/db mice. *Mol Pharmacol 78*, 961–70.

(*145*) Zou, P., Liu, L., Zheng, L., Liu, L., Stoneman, R. E., Cho, A., Emery, A., Gilbert, E. R., and Cheng, Z. (2014). Targeting FoxO1 with AS1842856 suppresses adipogenesis. *Cell Cycle 13*, 3759–67.

(*146*) Dong, G., Wang, Y., Xiao, W., Pacios Pujado, S., Xu, F., Tian, C., Xiao, E., Choi, Y., and Graves, D. T. (2015). FOXO1 regulates dendritic cell activity through ICAM-1 and CCR7. *J Immunol 194*, 3745–55.

(*147*) Chung, S., Ranjan, R., Lee, Y. G., Park, G. Y., Karpurapu, M., Deng, J., Xiao, L., Kim, J. Y., Unterman, T. G., and Christman, J. W. (2015). Distinct role of FoxO1 in M-CSF- and GM-CSF-differentiated macrophages contributes LPS-mediated IL-10: implication in hyperglycemia. *J Leukoc Biol 97*, 327–39.

(*148*) Dong, G., Song, L., Tian, C., Wang, Y., Miao, F., Zheng, J., Lu, C., Alsadun, S., and Graves, D. T. (2017). FOXO1 Regulates Bacteria-Induced Neutrophil Activity. *Front Immunol 8*, 1088.

(*149*) Kerdiles, Y. M., Stone, E. L., Beisner, D. R., McGargill, M. A., Ch'en, I. L., Stockmann, C., Katayama, C. D., and Hedrick, S. M. (2010). Foxo transcription factors control regulatory T cell development and function. *Immunity 33*, 890–904.

(*150*) Behl, Y., Siqueira, M., Ortiz, J., Li, J., Desta, T., Faibish, D., and Graves, D. T. (2008). Activation of the acquired immune response reduces coupled bone formation in response to a periodontal pathogen. *J Immunol 181*, 8711–8.

(*151*) Zhou, M., Zhang, Y., Chen, X., Zhu, J., Du, M., Zhou, L., Zhang, L., Wang, W., and Sun, G. (2015). PTEN-Foxo1 signaling triggers HMGB1-mediated innate immune responses in acute lung injury. *Immunol Res 62*, 95–105.

(*152*) Wang, S., Xia, P., Huang, G., Zhu, P., Liu, J., Ye, B., Du, Y., and Fan, Z. (2016). FoxO1-mediated autophagy is required for NK cell development and innate immunity. *Nat Commun 7*, 11023.

(*153*) Xiao, W., Dong, G., Pacios, S., Alnammary, M., Barger, L. A., Wang, Y., Wu, Y., and Graves, D. T. (2015). FOXO1 deletion reduces dendritic cell function and enhances susceptibility to periodontitis. *Am J Pathol 185*, 1085–93.

(*154*) Ouyang, W. et al. (2012). Novel Foxo1-dependent transcriptional programs control T(reg) cell function. *Nature 491*, 554–9.

(*155*) Bothur, E. et al. (2015). Antigen receptor-mediated depletion of FOXP3 in induced regulatory T-lymphocytes via PTPN2 and FOXO1. *Nat Commun 6*, 8576.

(*156*) Hawse, W. F., Sheehan, R. P., Miskov-Zivanov, N., Menk, A. V., Kane, L. P., Faeder, J. R., and Morel, P. A. (2015). Cutting Edge: Differential Regulation of PTEN by TCR, Akt, and FoxO1 Controls CD4+ T Cell Fate Decisions. *J Immunol 194*, 4615–9.

(*157*) Amin, R. H., and Schlissel, M. S. (2008). Foxo1 directly regulates the transcription of recombination-activating genes during B cell development. *Nat Immunol 9*, 613–22.

(*158*) Moparthi, L., and Koch, S. (2020). A uniform expression library for the exploration of FOX transcription factor biology. *Differentiation 115*, 30–36.

(*159*) Livak, K. J., and Schmittgen, T. D. (2001). Analysis of relative gene expression data using real-time quantitative PCR and the 2(-Delta Delta C(T)) Method. *Methods 25*, 402–8.

(*160*) Svec, D., Tichopad, A., Novosadova, V., Pfaffl, M. W., and Kubista, M. (2015). How good is a PCR efficiency estimate: Recommendations for precise and robust qPCR efficiency assessments. *Biomol Detect Quantif 3*, 9–16.

(*161*) Erb, A., Zissler, U. M., Oelsner, M., Chaker, A. M., Schmidt-Weber, C. B., and Jakwerth, C. A. (2022). Genome-Wide Gene Expression Analysis Reveals Unique Genes Signatures of Epithelial Reorganization in Primary Airway Epithelium Induced by Type-I, -II and -III Interferons. *Biosensors (Basel) 12*, DOI: 10.3390/bios12110929.

(*162*) Fuchs, O. et al. (2018). The all age asthma cohort (ALLIANCE) - from early beginnings to chronic disease: a longitudinal cohort study. *BMC Pulm Med 18*, 140.

(*163*) Bateman, E. D. et al. (2008). Global strategy for asthma management and prevention: GINA executive summary. *Eur Respir J 31*, 143–78.

(*164*) German Medical Association (BÄK) NAoSHIPK, W. G. o. S. M. S. (, *Nationale VersorgungsLeitlinie Asthma*; [National Asthma Care Guideline – Long Version]. Version 1., (2020).: 2020; Vol. 4. Auflage.

(*165*) Maison, N. et al. (2022). T2-high asthma phenotypes across lifespan. *Eur Respir J 60*, DOI: 10.1183/13993003.02288-2021.

(*166*) Burgler, S., Mantel, P. Y., Bassin, C., Ouaked, N., Akdis, C. A., and Schmidt-Weber, C. B. (2010). RORC2 is involved in T cell polarization through interaction with the FOXP3 promoter. *J Immunol 184*, 6161–9.

(*167*) Li, X. et al. (2016). Expression of asthma susceptibility genes in bronchial epithelial cells and bronchial alveolar lavage in the Severe Asthma Research Program (SARP) cohort. *J Asthma 53*, 775–82.

(*168*) Stifter, S. A., Bhattacharyya, N., Pillay, R., Florido, M., Triccas, J. A., Britton, W. J., and Feng, C. G. (2016). Functional Interplay between Type I and II Interferons Is Essential to Limit Influenza A Virus-Induced Tissue Inflammation. *PLoS Pathog 12*, e1005378.

(*169*) Lee, A. J. et al. (2017). Inflammatory monocytes require type I interferon receptor signaling to activate NK cells via IL-18 during a mucosal viral infection. *J Exp Med 214*, 1153–1167.

(*170*) Conti, P., Ronconi, G., Caraffa, A., Gallenga, C. E., Ross, R., Frydas, I., and Kritas, S. K. (2020). Induction of pro-inflammatory cytokines (IL-1 and IL-6) and lung inflammation by Coronavirus-19 (COVI-19 or SARS-CoV-2): anti-inflammatory strategies. *J Biol Regul Homeost Agents 34*, 327–331.

(*171*) Mohseni Afshar, Z. et al. (2023). The role of cytokines and their antagonists in the treatment of COVID-19 patients. *Rev Med Virol 33*, e2372.

(*172*) Miller, M. C., and Mayo, K. H. (2017). Chemokines from a Structural Perspective. *Int J Mol Sci 18*, DOI: 10.3390/ijms18102088.

(*173*) Ng, C. T., and Oldstone, M. B. (2012). Infected CD8alpha- dendritic cells are the predominant source of IL-10 during establishment of persistent viral infection. *Proc Natl Acad Sci U S A 109*, 14116–21.

(*174*) Hebert, K. D., McLaughlin, N., Galeas-Pena, M., Zhang, Z., Eddens, T., Govero, A., Pilewski, J. M., Kolls, J. K., and Pociask, D. A. (2020). Targeting the IL-22/IL-22BP axis enhances tight junctions and reduces inflammation during influenza infection. *Mucosal Immunol 13*, 64–74.

(*175*) Odendall, C., Voak, A. A., and Kagan, J. C. (2017). Type III IFNs Are Commonly Induced by Bacteria-Sensing TLRs and Reinforce Epithelial Barriers during Infection. *J Immunol 199*, 3270–3279.

(*176*) Lazear, H. M., Daniels, B. P., Pinto, A. K., Huang, A. C., Vick, S. C., Doyle, S. E., Gale, M., Klein, R. S., and Diamond, M. S. (2015). Interferon-lambda restricts West Nile virus neuroinvasion by tightening the blood-brain barrier. *Sci Transl Med 7*, 284ra59.

(*177*) D'Agnillo, F. et al. (2021). Lung epithelial and endothelial damage, loss of tissue repair, inhibition of fibrinolysis, and cellular senescence in fatal COVID-19. *Sci Transl Med 13*, eabj7790.

(*178*) Ewart, S. L., Kuperman, D., Schadt, E., Tankersley, C., Grupe, A., Shubitowski, D. M., Peltz, G., and Wills-Karp, M. (2000). Quantitative trait loci controlling allergen-induced airway hyperresponsiveness in inbred mice. *Am J Respir Cell Mol Biol 23*, 537–45.

(*179*) Ma, T. Y., Iwamoto, G. K., Hoa, N. T., Akotia, V., Pedram, A., Boivin, M. A., and Said, H. M. (2004). TNF-alpha-induced increase in intestinal epithelial tight junction permeability requires NF-kappa B activation. *Am J Physiol Gastrointest Liver Physiol 286*, G367–76.

(*180*) Major, J., Crotta, S., Llorian, M., McCabe, T. M., Gad, H. H., Priestnall, S. L., Hartmann, R., and Wack, A. (2020). Type I and III interferons disrupt lung epithelial repair during recovery from viral infection. *Science 369*, 712–717.

(*181*) Tan, H. T. et al. (2019). Tight junction, mucin, and inflammasome-related molecules are differentially expressed in eosinophilic, mixed, and neutrophilic experimental asthma in mice. *Allergy 74*, 294–307.

(*182*) Zhang, S. D., McCrudden, C. M., and Kwok, H. F. (2015). Prognostic significance of combining VEGFA, FLT1 and KDR mRNA expression in lung cancer. *Oncol Lett 10*, 1893–1901.

(*183*) Komiya, Y. et al. (2016). The Rho guanine nucleotide exchange factor ARHGEF5 promotes tumor malignancy via epithelial-mesenchymal transition. *Oncogenesis 5*, e258.

(*184*) Kaur, S., Sassano, A., Dolniak, B., Joshi, S., Majchrzak-Kita, B., Baker, D. P., Hay, N., Fish, E. N., and Platanias, L. C. (2008). Role of the Akt pathway in mRNA translation of interferon-stimulated genes. *Proc Natl Acad Sci U S A 105*, 4808–13.

(*185*) Adil, M. S., Verma, A., Rudraraju, M., Narayanan, S. P., and Somanath, P. R. (2021). Akt-independent effects of triciribine on ACE2 expression in human lung epithelial cells: Potential benefits in restricting SARS-CoV2 infection. *J Cell Physiol 236*, 6597–6606.

(*186*) Garrett, C. R., Coppola, D., Wenham, R. M., Cubitt, C. L., Neuger, A. M., Frost, T. J., Lush, R. M., Sullivan, D. M., Cheng, J. Q., and Sebti, S. M. (2011). Phase I pharmacokinetic and pharmacodynamic study of triciribine phosphate monohydrate, a small-molecule inhibitor of AKT phosphorylation, in adult subjects with solid tumors containing activated AKT. *Invest New Drugs 29*, 1381–9.

(*187*) Sampath, D. et al. (2013). Phase I clinical, pharmacokinetic, and pharmacodynamic study of the Akt-inhibitor triciribine phosphate monohydrate in patients with advanced hematologic malignancies. *Leuk Res 37*, 1461–7.

(*188*) Shan, S., Liu, F., Ford, E., Caldwell, R. B., Narayanan, S. P., and Somanath, P. R. (2023). Triciribine attenuates pathological neovascularization and vascular permeability in a mouse model of proliferative retinopathy. *Biomed Pharmacother 162*, 114714.

(*189*) Xiao, E., and Graves, D. T. (2015). Impact of Diabetes on the Protective Role of FOXO1 in Wound Healing. *J Dent Res 94*, 1025–6.

(*190*) Ding, H. R. et al. (2020). Protective Properties of FOXO1 Inhibition in a Murine Model of Non-alcoholic Fatty Liver Disease Are Associated With Attenuation of ER Stress and Necroptosis. *Front Physiol 11*, 177.

(*191*) Wang, D. et al. (2020). FOXO1 inhibition prevents renal ischemia-reperfusion injury via cAMP-response element binding protein/PPAR-gamma coactivator-1alpha-mediated mitochondrial biogenesis. *Br J Pharmacol 177*, 432–448.

(*192*) Lipcsey, M., Persson, B., Eriksson, O., Blom, A. M., Fromell, K., Hultstrom, M., Huber-Lang, M., Ekdahl, K. N., Frithiof, R., and Nilsson, B. (2021). The Outcome of Critically Ill COVID-19 Patients Is Linked to Thromboinflammation Dominated by the Kallikrein/Kinin System. *Front Immunol 12*, 627579.

(*193*) Garvin, M. R., Alvarez, C., Miller, J. I., Prates, E. T., Walker, A. M., Amos, B. K., Mast, A. E., Justice, A., Aronow, B., and Jacobson, D. (2020). A mechanistic model and therapeutic interventions for COVID-19 involving a RAS-mediated bradykinin storm. *Elife 9*, DOI: 10.7554/eLife.59177.

(*194*) Hu, B., Huang, S., and Yin, L. (2021). The cytokine storm and COVID-19. *J Med Virol 93*, 250–256.

(*195*) Roche, J. A., and Roche, R. (2020). A hypothesized role for dysregulated bradykinin signaling in COVID-19 respiratory complications. *FASEB J 34*, 7265–7269.

(*196*) Mansour, E. et al. (2021). Safety and Outcomes Associated with the Pharmacological Inhibition of the Kinin-Kallikrein System in Severe COVID-19. *Viruses 13*, DOI: 10.3390/v13020309.

(*197*) Jakwerth, C. A. et al. (2022). Early reduction of SARS-CoV-2-replication in bronchial epithelium by kinin B(2) receptor antagonism. *J Mol Med (Berl) 100*, 613–627.

(*198*) Ding, C., and Jones, G. (2006). Anti-interleukin-6 receptor antibody treatment in inflammatory autoimmune diseases. *Rev Recent Clin Trials 1*, 193–200.

(*199*) Dholaria, B. R., Bachmeier, C. A., and Locke, F. (2019). Mechanisms and Management of Chimeric Antigen Receptor T-Cell Therapy-Related Toxicities. *BioDrugs 33*, 45–60.

(*200*) Stebbing, J., Phelan, A., Griffin, I., Tucker, C., Oechsle, O., Smith, D., and Richardson, P. (2020). COVID-19: combining antiviral and anti-inflammatory treatments. *Lancet Infect Dis 20*, 400–402.

(*201*) Bhimraj, A. et al. (2020). Infectious Diseases Society of America Guidelines on the Treatment and Management of Patients with COVID-19. *Clin Infect Dis*, DOI: 10.1093/cid/ciaa478.

(*202*) Xu, X. et al. (2020). Effective treatment of severe COVID-19 patients with tocilizumab. *Proc Natl Acad Sci U S A 117*, 10970–10975.

(*203*) Durrani, S. R. et al. (2012). Innate immune responses to rhinovirus are reduced by the high-affinity IgE receptor in allergic asthmatic children. *J Allergy Clin Immunol 130*, 489–95.

(*204*) Corne, J. M., Marshall, C., Smith, S., Schreiber, J., Sanderson, G., Holgate, S. T., and Johnston, S. L. (2002). Frequency, severity, and duration of rhinovirus infections in asthmatic and non-asthmatic individuals: a longitudinal cohort study. *Lancet 359*, 831–4.

(*205*) Metbulut, A. P., Mustafaoglu, O., Sen, G., Kanik Yuksek, S., Kulhas Celik, I., Akca, H., and Dibek Misirlioglu, E. (2021). Evaluation of the Clinical and Laboratory Findings of Asthmatic Children with SARS-CoV-2 Infection. *Int Arch Allergy Immunol 182*, 989–996.

(*206*) Krishnamoorthy, N. et al. (2012). Early infection with respiratory syncytial virus impairs regulatory T cell function and increases susceptibility to allergic asthma. *Nat Med 18*, 1525–30.

(*207*) Lieberman, N. A. P. et al. (2020). In vivo antiviral host transcriptional response to SARS-CoV-2 by viral load, sex, and age. *PLoS Biol 18*, e3000849.

(*208*) Rao, S., Hurst, J. H., Zhao, C., Goldstein, B. A., Thomas, L., Lang, J. E., and Kelly, M. S. (2022). Asthma and the Risk of SARS-CoV-2 Infection Among Children and Adolescents. *Pediatrics 149*, DOI: 10.1542/peds.2021-056164.

(*209*) Ng, K. W., Attig, J., Bolland, W., Young, G. R., Major, J., Wrobel, A. G., Gamblin, S., Wack, A., and Kassiotis, G. (2020). Tissue-specific and interferon-inducible expression of nonfunctional ACE2 through endogenous retroelement co-option. *Nat Genet 52*, 1294–1302.

Chapter 8

Publications

8. Publications

1. **Erb, A.**, Zissler, U. M., Oelsner, M., Chaker, A. M., Schmidt-Weber, C.W., Jakwerth, C. A. Genome-Wide Gene Expression Analysis Reveals Unique Genes Signatures of Epithelial Reorganization in Primary Airway Epithelium Induced by Type-I, -II and -III Interferons. *Biosensors (Basel)* 2022 Oct 26;12(11):929. doi: 10.3390/bios12110929.

2. **Erb, A.**, Asoudeh Moghanloo, S., Oelsner, M., Mootz, M., Pfaffl, M.W., Zissler, U. M., Hansen, G., Bahmer, T., Rabe, K.F., Weckmann, M., Brinkmann, F., Kopp, M. V., Schaub, B., von Mutius, E., Chaker, A. M., Schmidt-Weber, C.W., Jakwerth, C. A. and the ALLIANCE Study Group as part of the German Center for Lung Research (DZL). Asthmatics benefit from defects in the interferon-mediated induction of SARS-CoV-2 entry receptor ACE2 via FoxO1 (Submitted to Nature Communications, currently under revision)

Chapter 9

Supplementary Data

9. Supplementary Data

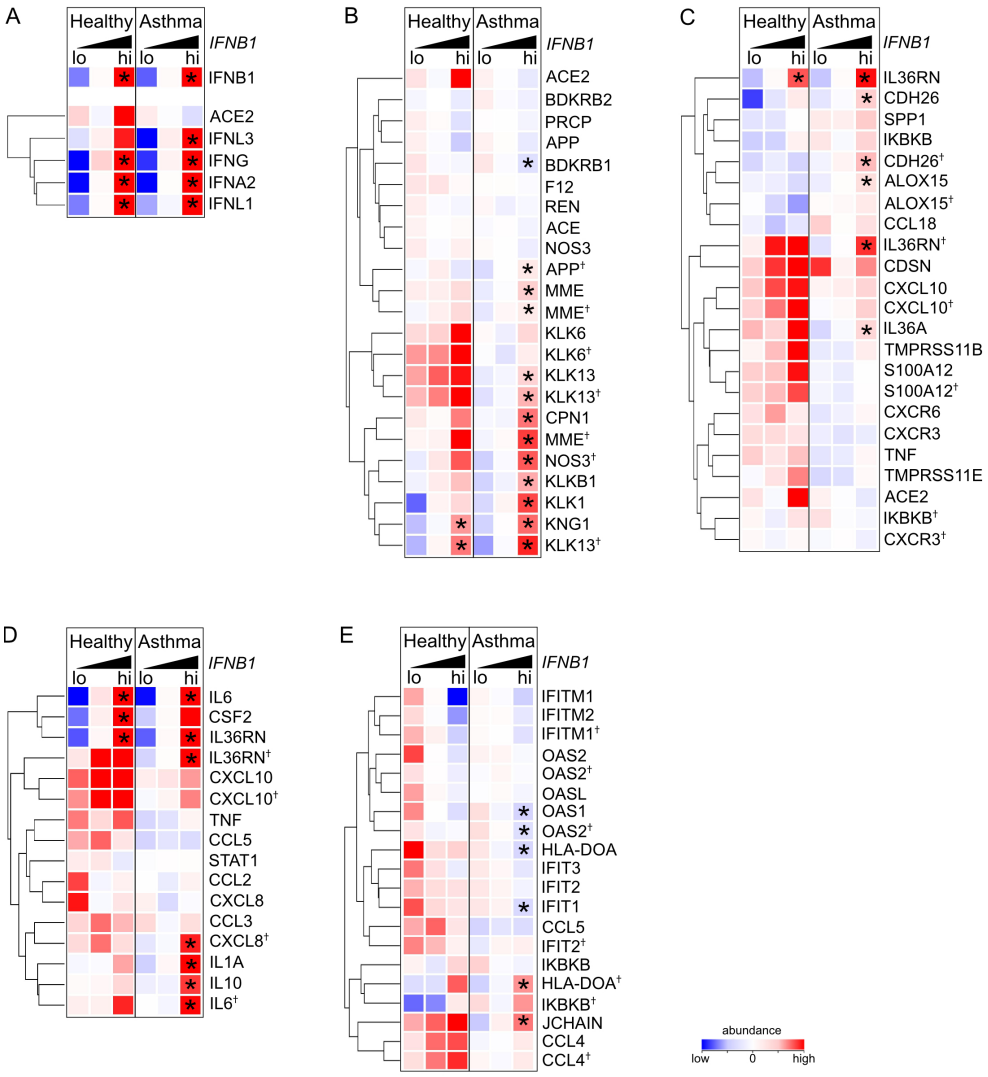

Figure 9.1 Expressed genes associated with SARS-CoV-2 infection demonstrate a *IFNB1* dose-dependent correlation in asthmatics and healthy individuals.
(A) Heat map of induced *IFNs* and *ACE2* in relation to the expression levels of *IFNB1*, categorized as high, intermediate, and low groups of healthy individuals and asthmatic patients. Significantly regulated genes ($P \leq .05$; $FC \geq 1.5$) are indicated with an asterisk in *IFNB1* high expressed samples compared to low in asthmatics and healthy individuals respectively. Benjamin Hochberg (FDR) correction was additionally applied. (B) Heat map of KKS genes in relation to the expression levels of *IFNB1*, categorized as high, intermediate, and low groups of healthy individuals and asthmatic patients. (C) Heat map of induced SARS-CoV-2 infection associated genes in relation to the expression levels of *IFNB1*, categorized as high, intermediate, and low groups of healthy individuals and asthmatic patients. (D) Heat map of acute phase genes in relation to the expression levels of *IFNB1*, categorized as high, intermediate, and low groups of healthy individuals and asthmatic patients. (E) Heat map of induced ISGs in relation to the expression levels of *IFNB1*, categorized as high, intermediate, and low groups of healthy individuals and asthmatic patients. Duplicate gene names are marked with a cross and indicate the occurrence of two or more transcripts of the same gene in the analysis. Grouped genes are represented by similar expression patterns and hierarchical clustering. Their connection was described by dendrograms to the left and each row represents, indicated by the colour, the intensity of their abundance across each group.

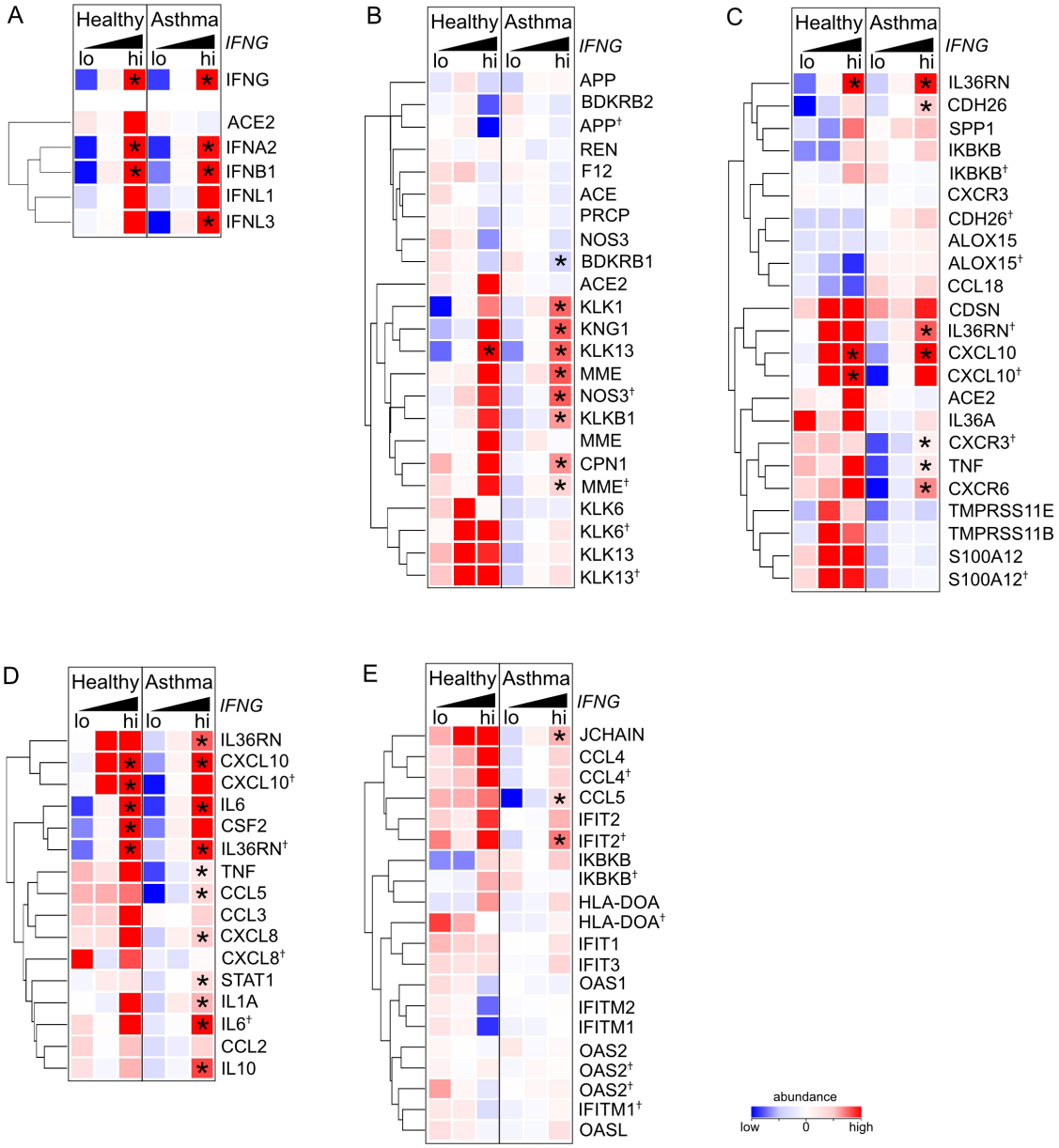

Figure 9.2 Expressed genes associated with SARS-CoV-2 infection demonstrate a *IFNG* dose-dependent correlation in asthmatics and healthy individuals.
(A) Heat map of induced *IFNs* and *ACE2* in relation to the expression levels of *IFNG*, categorized as high, intermediate, and low groups of healthy individuals and asthmatic patients. Significantly regulated genes ($P \leq .05$; $FC \geq 1.5$) are indicated with an asterisk in *IFNG* high expressed samples compared to low in asthmatics and healthy individuals respectively. Benjamin Hochberg (FDR) correction was additionally applied. (B) Heat map of KKS genes in relation to the expression levels of *IFNG*, categorized as high, intermediate, and low groups of healthy individuals and asthmatic patients. (C) Heat map of induced SARS-CoV-2 infection associated genes in relation to the expression levels of *IFNG*, categorized as high, intermediate, and low groups of healthy individuals and asthmatic patients. (D) Heat map of acute phase genes in relation to the expression levels of *IFNG*, categorized as high, intermediate, and low groups of healthy individuals and asthmatic patients. (E) Heat map of induced ISGs in relation to the expression levels of *IFNG*, categorized as high, intermediate, and low groups of healthy individuals and asthmatic patients. Duplicate gene names are marked with a cross and indicate the occurrence of two or more transcripts of the same gene in the analysis. Grouped genes are represented by similar expression patterns and hierarchical clustering. Their connection was described by dendrograms to the left and each row represents, indicated by the colour, the intensity of their abundance across each group.

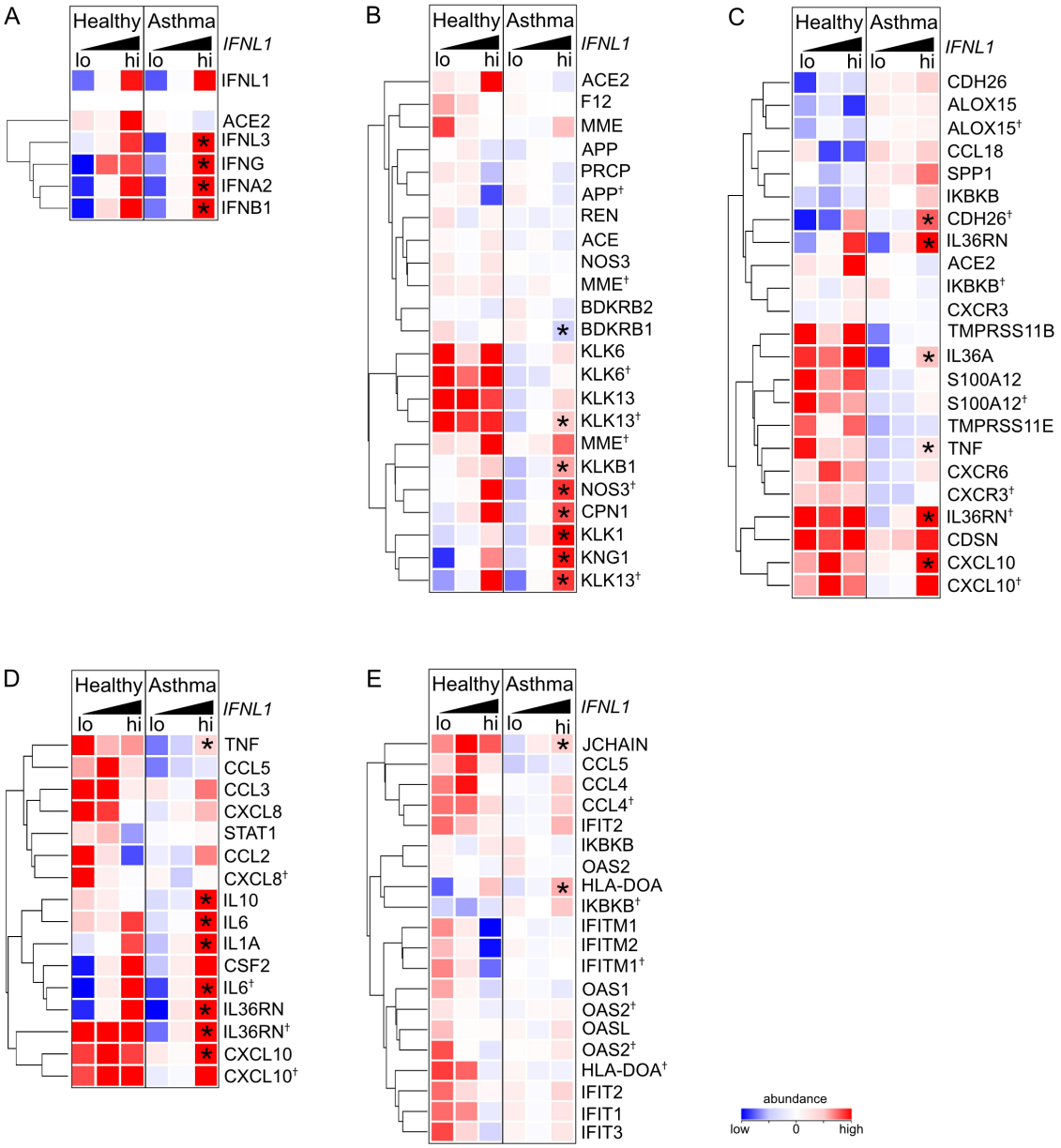

Figure 9.3 Expressed genes associated with SARS-CoV-2 infection demonstrate a *IFNL1* dose-dependent correlation in asthmatics and healthy individuals.
(A) Heat map of induced *IFNs* and *ACE2* in relation to the expression levels of *IFNL1*, categorized as high, intermediate, and low groups of healthy individuals and asthmatic patients. Significantly regulated genes ($P \leq .05$; $FC \geq 1.5$) are indicated with an asterisk in *IFNL1* high expressed samples compared to low in asthmatics and healthy individuals respectively. Benjamin Hochberg (FDR) correction was additionally applied. (B) Heat map of KKS genes in relation to the expression levels of *IFNL1*, categorized as high, intermediate, and low groups of healthy individuals and asthmatic patients. (C) Heat map of induced SARS-CoV-2 infection associated genes in relation to the expression levels of *IFNL1*, categorized as high, intermediate, and low groups of healthy individuals and asthmatic patients. (D) Heat map of acute phase genes in relation to the expression levels of *IFNL1*, categorized as high, intermediate, and low groups of healthy individuals and asthmatic patients. (E) Heat map of induced ISGs in relation to the expression levels of *IFNL1*, categorized as high, intermediate, and low groups of healthy individuals and asthmatic patients. Duplicate gene names are marked with a cross and indicate the occurrence of two or more transcripts of the same gene in the analysis. Grouped genes are represented by similar expression patterns and hierarchical clustering. Their connection was described by dendrograms to the left and each row represents, indicated by the colour, the intensity of their abundance across each group.

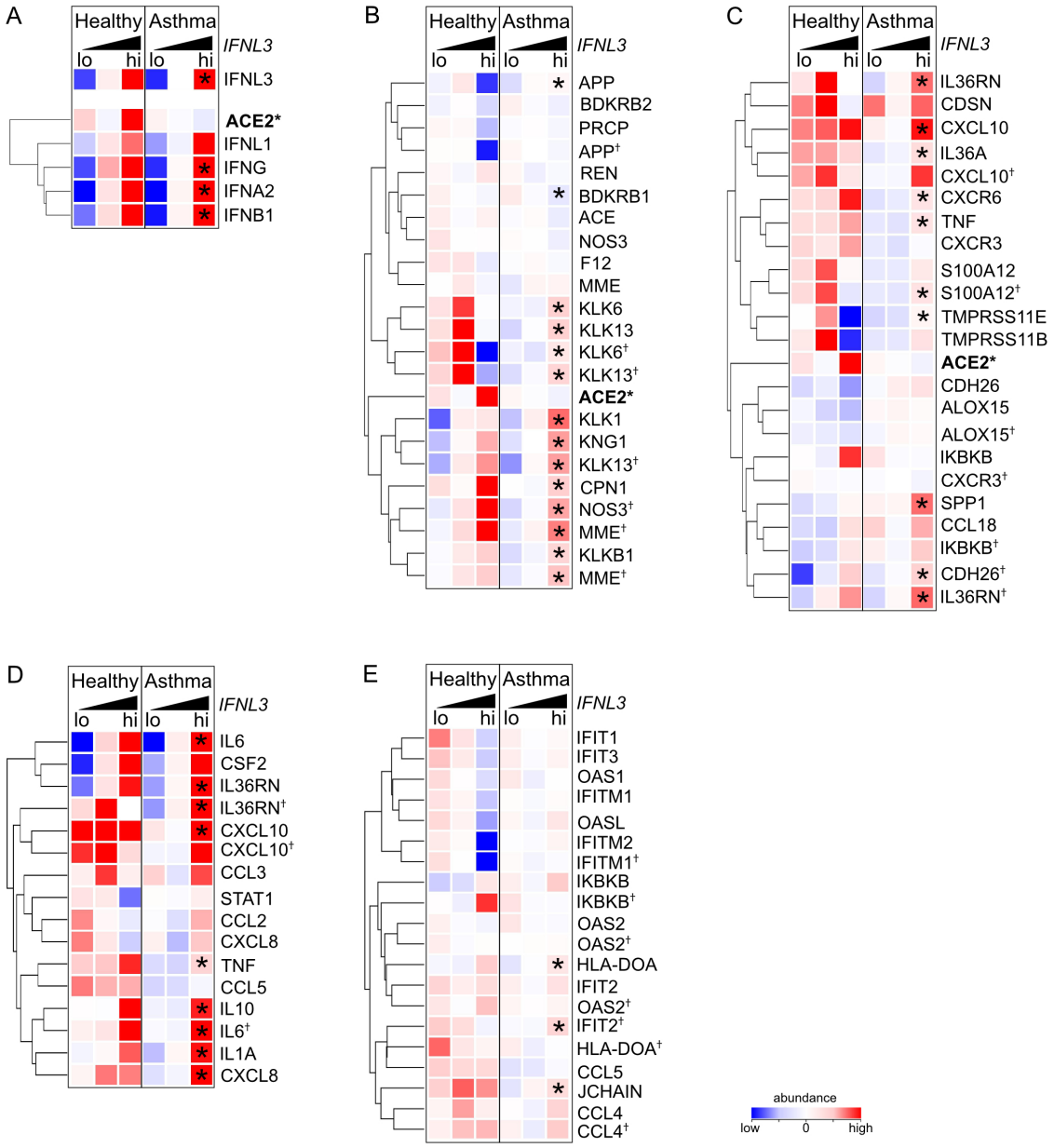

Figure 9.4 Expressed genes associated with SARS-CoV-2 infection demonstrate a *IFNL3* dose-dependent correlation in asthmatics and healthy individuals.
(A) Heat map of induced *IFNs* and *ACE2* in relation to the expression levels of *IFNL3*, categorized as high, intermediate, and low groups of healthy individuals and asthmatic patients. Significantly regulated genes ($P \leq .05$; $FC \geq 1.5$) are indicated with an asterisk in *IFNL3* high expressed samples compared to low in asthmatics and healthy individuals respectively and significantly regulated genes in *IFNL3* high expressed asthmatics compared to high expressed *IFNL3* non-asthmatics. Benjamin Hochberg (FDR) correction was additionally applied. (B) Heat map of KKS genes in relation to the expression levels of *IFNL3*, categorized as high, intermediate, and low groups of healthy individuals and asthmatic patients. (C) Heat map of induced SARS-CoV-2 infection associated genes in relation to the expression levels of *IFNL3*, categorized as high, intermediate, and low groups of healthy individuals and asthmatic patients. (D) Heat map of acute phase genes in relation to the expression levels of *L3*, categorized as high, intermediate, and low groups of healthy individuals and asthmatic patients. (E) Heat map of induced ISGs in relation to the expression levels of *IFNL3*, categorized as high, intermediate, and low groups of healthy individuals and asthmatic patients. Duplicate gene names are marked with a cross and indicate the occurrence of two or more transcripts of the same gene in the analysis. Grouped genes are represented by similar expression patterns and hierarchical clustering. Their connection was described by dendrograms to the left and each row represents, indicated by the colour, the intensity of their abundance across each group.

Table 9.1 DEGs of overlapping induced ISGs by type-I, -II and -III IFNs (normalized)

ProbeName	unstimulated	IFN-α	IFN-β	IFN-γ	IFN-λ1	IFN-λ3	GeneSymbol	Description
A_33_P3225522	-1,9561468	0,5923772	-0,35558686	-0,58024216	-0,062227964	0,13037126	OAS2	Homo sapiens 2´-5´-oligoadenylate synthetase 2 (OAS2), transcript variant 3, mRNA [NM_001032731]
A_24_P30194	-1,7312847	0,67001575	-0,41586718	0,108888626	-0,21739507	0,2190574	IFIT5	Homo sapiens interferon induced protein with tetratricopeptide repeats 5 (IFIT5), mRNA [NM_012420]
A_24_P287043	-2,542518	0,79507595	-0,81094104	-0,006164551	0,14759207	-4,97E-04	IFITM2	Homo sapiens interferon induced transmembrane protein 2 (IFITM2), mRNA [NM_006435]
A_23_P87545	-2,853794	0,8812787	-0,9241107	-0,050669193	0,091745615	-0,078515686	IFITM3	Homo sapiens interferon induced transmembrane protein 3 (IFITM3), transcript variant 1, mRNA [NM_021034]
A_24_P16124	-3,076229	0,7993637	-0,93528223	0,025819778	0,097515106	0,003508886	IFITM4P	Homo sapiens interferon induced transmembrane protein 4 pseudogene (IFITM4P), non-coding RNA [NR_001590]
A_24_P335305	-3,0713136	1,2242434	-1,1515764	-0,29397833	0,26313567	0,24726756	OAS3	Homo sapiens 2´-5´-oligoadenylate synthetase 3 (OAS3), mRNA [NM_006187]
A_23_P64828	-2,9107926	1,0802476	-0,8514719	-0,34537888	-0,011140108	0,31518713	OAS1	Homo sapiens 2´-5´-oligoadenylate synthetase 1 (OAS1), transcript variant 2, mRNA [NM_002534]

A_33_P3225512	-2,553745	1,0747459	-0,771424	-0,31504583	0,06607056	0,44579092	OAS2	Homo sapiens 2´-5´-oligoadenylate synthetase 2 (OAS2), transcript variant 2, mRNA [NM_002535]
A_23_P204087	-2,5860302	1,1788596	-0,7906987	-0,40232325	0,10059786	0,351895	OAS2	Homo sapiens 2´-5´-oligoadenylate synthetase 2 (OAS2), transcript variant 1, mRNA [NM_016817]
A_33_P3283611	-4,022962	1,4585949	-1,0486323	0,03356743	-0,027750969	0,23427264	IFIT3	Homo sapiens interferon induced protein with tetratricopeptide repeats 3 (IFIT3), transcript variant 1, mRNA [NM_001549]
A_23_P72737	-4,0834537	1,063361	-1,0623661	0,019946575	0,0352602	0,04615116	IFITM1	Homo sapiens interferon induced transmembrane protein 1 (IFITM1), mRNA [NM_003641]
A_33_P3423941	-4,016789	1,0813553	-0,99766034	0,20645952	0,106961966	0,06726297	IFITM1	Homo sapiens interferon induced transmembrane protein 1 (IFITM1), mRNA [NM_003641]
A_23_P24004	-3,6393964	2,4704592	-1,8252196	-0,18063688	-0,34579277	0,27567402	IFIT2	Homo sapiens interferon induced protein with tetratricopeptide repeats 2 (IFIT2), mRNA [NM_001547]
A_24_P304071	-3,6050026	2,6666105	-1,6267847	-0,42587042	0,33242583	0,3118539	IFIT2	Homo sapiens interferon induced protein with tetratricopeptide repeats 2 (IFIT2), mRNA [NM_001547]

A_23_P52266	-4,129188	1,8124801	-0,4457725	-1,1010878	0,29395413	0,6926634	IFIT1	Homo sapiens interferon induced protein with tetratricopeptide repeats 1 (IFIT1), transcript variant 1, mRNA [NM_001548]
A_23_P139786	-4,6126957	2,3262177	-1,4168743	-0,759634	0,12619758	0,56437653	OASL	Homo sapiens 2´-5´-oligoadenylate synthetase like (OASL), transcript variant 1, mRNA [NM_003733]

Table 9.2 DEGs of induced pro-inflammatory genes by IFN-α vs unstimulated

ProbeName	GeneSymbol	Description	*P*	FC	Regulation
A_23_P125278	CXCL11	Homo sapiens C-X-C motif chemokine ligand 11 (CXCL11), transcript variant 2, mRNA [NM_001302123]	4,80956E-09	198,46693	up
A_24_P303091	CXCL10	Homo sapiens C-X-C motif chemokine ligand 10 (CXCL10), mRNA [NM_001565]	1,51236E-07	121,668526	up
A_33_P3343175	CXCL10	Homo sapiens C-X-C motif chemokine ligand 10 (CXCL10), mRNA [NM_001565]	9,30642E-10	121,54955	up
A_32_P44394	AIM2	Homo sapiens absent in melanoma 2 (AIM2), transcript variant 1, mRNA [NM_004833]	1,24504E-09	110,805695	up
A_23_P14174	TNFSF13B	Homo sapiens TNF superfamily member 13b (TNFSF13B), transcript variant 1, mRNA [NM_006573]	5,57521E-08	56,008625	up
A_33_P3250443	DUOXA2	dual oxidase maturation factor 2 [Source:HGNC Symbol	2,13195E-08	27,254122	up
A_24_P274270	STAT1	Homo sapiens signal transducer and activator of transcription 1 (STAT1), transcript variant beta, mRNA [NM_139266]	5,39928E-07	13,044019	up
A_23_P167328	CD38	Homo sapiens CD38 molecule (CD38), transcript variant 1, mRNA [NM_001775]	1,81596E-08	10,737364	up
A_23_P18452	CXCL9	C-X-C motif chemokine ligand 9 [Source:HGNC Symbol	2,77834E-05	10,580419	up
A_23_P132159	USP18	ubiquitin specific peptidase 18 [Source:HGNC Symbol	6,83557E-08	9,39189	up
A_24_P227415	CLEC7A	Homo sapiens C-type lectin domain containing 7A (CLEC7A), transcript variant 6, mRNA [NM_197954]	6,2636E-07	9,229906	up
A_23_P252981	ACE2	Homo sapiens angiotensin I converting enzyme 2 (ACE2), mRNA [NM_021804]	7,29514E-07	8,282798	up

A_23_P121695	CXCL13	Homo sapiens C-X-C motif chemokine ligand 13 (CXCL13), mRNA [NM_006419]	8,08138E-05	7,837858	up
A_24_P235988	CLEC7A	Homo sapiens C-type lectin domain containing 7A (CLEC7A), transcript variant 1, mRNA [NM_197947]	2,91985E-05	7,806695	up
A_23_P111000	PSMB9	Homo sapiens proteasome subunit beta 9 (PSMB9), mRNA [NM_002800]	1,96427E-07	7,4464636	up
A_22_P00021230	IL36RN	interleukin 36 receptor antagonist [Source:HGNC Symbol	2,53112E-05	7,387322	up
A_21_P0014047	C4A	Homo sapiens complement C4A (Rodgers blood group) (C4A), transcript variant 2, mRNA [NM_001252204]	3,27689E-06	7,351184	up
A_23_P42282	C4B	Homo sapiens complement C4B (Chido blood group) (C4B), mRNA [NM_001002029]	6,28644E-06	6,932004	up
A_33_P3879161	PIK3AP1	Homo sapiens phosphoinositide-3-kinase adaptor protein 1 (PIK3AP1), mRNA [NM_-152309]	4,84186E-06	6,753397	up
A_23_P154235	NMI	N-myc and STAT interactor [Source:HGNC Symbol	6,83817E-07	6,5186725	up
A_24_P85775	THEMIS2	Homo sapiens thymocyte selection associated family member 2 (THEMIS2), transcript variant 2, mRNA [NM_001039477]	3,16982E-07	6,0220203	up
A_24_P270728	NUPR1	Homo sapiens nuclear protein 1, transcriptional regulator (NUPR1), transcript variant 1, mRNA [NM_001042483]	1,73631E-07	5,9177284	up
A_33_P3389230	CXCR3	Homo sapiens C-X-C motif chemokine receptor 3 (CXCR3), transcript variant 1, mRNA [NM_001504]	0,000556802	5,6277604	up
A_24_P148717	CCR1	Homo sapiens C-C motif chemokine receptor 1 (CCR1), mRNA [NM_001295]	0,000577847	4,768246	up

A_24_P365526	HCK	Homo sapiens HCK proto-oncogene, Src family tyrosine kinase (HCK), transcript variant 1, mRNA [NM_002110]	0,002735959	-4,6934757	down
A_23_P69310	CCRL2	Homo sapiens C-C motif chemokine receptor like 2 (CCRL2), transcript variant 1, mRNA [NM_003965]	5,11399E-05	4,6370835	up
A_23_P250629	PSMB8	Homo sapiens proteasome subunit beta 8 (PSMB8), transcript variant 1, mRNA [NM_004159]	2,25322E-06	4,399743	up
A_23_P206441	FANCA	Homo sapiens FA complementation group A (FANCA), transcript variant 1, mRNA [NM_000135]	1,01021E-07	4,395489	up
A_23_P152838	CCL5	Homo sapiens C-C motif chemokine ligand 5 (CCL5), transcript variant 1, mRNA [NM_002985]	0,000335231	4,307011	up
A_23_P74290	GBP5	Homo sapiens guanylate binding protein 5 (GBP5), transcript variant 1, mRNA [NM_-052942]	2,81275E-06	3,8682363	up
A_23_P215154	NUB1	Homo sapiens negative regulator of ubiquitin like proteins 1 (NUB1), transcript variant 2, mRNA [NM_016118]	1,24915E-06	3,6068823	up
A_24_P416997	APOL3	Homo sapiens apolipoprotein L3 (APOL3), transcript variant beta/a, mRNA [NM_-145641]	2,42328E-06	3,5447066	up
A_23_P160025	IFI16	Homo sapiens interferon gamma inducible protein 16 (IFI16), transcript variant 2, mRNA [NM_005531]	1,1427E-05	3,3995113	up
A_23_P78353	MEP1B	Homo sapiens meprin A subunit beta (MEP1B), transcript variant 2, mRNA [NM_-001308171]	0,015419911	3,2818992	up

A_33_P3288359	PSMB10	Homo sapiens proteasome subunit beta 10 (PSMB10), mRNA [NM_002801]	3,22741E-05	3,2721322	up
A_23_P116557	LGALS9	Homo sapiens galectin 9 (LGALS9), transcript variant 1, mRNA [NM_009587]	0,000219867	3,1431794	up
A_24_P97405	CCRL2	Homo sapiens C-C motif chemokine receptor like 2 (CCRL2), transcript variant 1, mRNA [NM_003965]	0,001043752	3,047805	up
A_23_P152620	TNFSF13	Homo sapiens TNF superfamily member 13 (TNFSF13), transcript variant gamma, mRNA [NM_172088]	2,70117E-05	3,0448825	up
A_33_P3246833	IL1RN	Homo sapiens interleukin 1 receptor antagonist (IL1RN), transcript variant 5, mRNA [NM_001318914]	0,000991929	3,0179389	up
A_21_P0011535	LGALS9	galectin 9 [Source:HGNC Symbol	8,67319E-05	2,9801657	up
A_23_P207564	CCL4	Homo sapiens C-C motif chemokine ligand 4 (CCL4), mRNA [NM_002984]	0,007988034	2,9675875	up
A_33_P3251876	IL18R1	Homo sapiens interleukin 18 receptor 1 (IL18R1), transcript variant 1, mRNA [NM_-003855]	0,016613368	2,953082	up
A_23_P362659	MYD88	Homo sapiens MYD88 innate immune signal transduction adaptor (MYD88), transcript variant 2, mRNA [NM_002468]	1,49833E-05	2,9020975	up
A_21_P0000070	IL1RAP	Homo sapiens interleukin 1 receptor accessory protein (IL1RAP), transcript variant 6, mRNA [NM_001167931]	0,017467685	2,8588443	up
A_33_P3420416	LGALS9	Homo sapiens galectin 9 (LGALS9), transcript variant 4, mRNA [NM_001330163]	0,000119985	2,8405547	up
A_23_P65427	PSME2	Homo sapiens proteasome activator subunit 2 (PSME2), mRNA [NM_002818]	5,6698E-06	2,7937465	up

A_23_P348028	IL36A	interleukin 36 alpha [Source:HGNC Symbol	0,0212123	2,7260356	up
A_33_P3878772	JAK2	Homo sapiens Janus kinase 2 (JAK2), transcript variant 2, mRNA [NM_001322194]	7,80334E-06	2,722643	up
A_23_P310931	CNR2	Homo sapiens cannabinoid receptor 2 (CNR2), mRNA [NM_001841]	0,020695198	2,7174115	up
A_24_P365515	FOXA2	Homo sapiens forkhead box A2 (FOXA2), transcript variant 1, mRNA [NM_021784]	0,005791328	-2,708497	down
A_24_P32935	FOLR2	Homo sapiens folate receptor beta (FOLR2), transcript variant 1, mRNA [NM_000803]	0,006476242	2,7004058	up
A_33_P3212269	MAP2K3	mitogen-activated protein kinase kinase 3 [Source:HGNC Symbol	0,00074325	2,6620166	up
A_23_P213562	F2R	Homo sapiens coagulation factor II thrombin receptor (F2R), transcript variant 1, mRNA [NM_001992]	0,011113957	-2,6562324	down
A_23_P137697	SELP	Homo sapiens selectin P (SELP), mRNA [NM_003005]	0,030771846	-2,6100342	down
A_23_P28334	IL18RAP	Homo sapiens interleukin 18 receptor accessory protein (IL18RAP), mRNA [NM_-003853]	0,042388424	2,5793417	up
A_33_P3284266	CXCL6	C-X-C motif chemokine ligand 6 [Source:HGNC Symbol	0,04977293	2,5776906	up
A_23_P169257	TNFSF8	Homo sapiens TNF superfamily member 8 (TNFSF8), transcript variant 1, mRNA [NM_001244]	0,04140881	2,5718021	up
A_33_P3258046	TAC4	Homo sapiens tachykinin 4 (TAC4), transcript variant alpha, mRNA [NM_170685]	0,021089355	2,4860656	up
A_33_P3503029	TNFSF11	Homo sapiens TNF superfamily member 11 (TNFSF11), transcript variant 1, mRNA [NM_003701]	0,036256775	2,45726	up

A_23_P114299	CXCR3	Homo sapiens C-X-C motif chemokine receptor 3 (CXCR3), transcript variant 1, mRNA [NM_001504]	0,010674125	2,4339871	up
A_33_P3211666	IL18R1	Homo sapiens interleukin 18 receptor 1 (IL18R1), transcript variant 1, mRNA [NM_003855]	0,002139346	2,3723478	up
A_33_P3246829	IL1RN	Homo sapiens interleukin 1 receptor antagonist (IL1RN), transcript variant 5, mRNA [NM_001318914]	0,004432559	2,34952	up
A_33_P3376546	PTGFR	Homo sapiens prostaglandin F receptor (PTGFR), transcript variant 2, mRNA [NM_001039585]	0,024155946	-2,3036528	down
A_23_P127948	ADM	Homo sapiens adrenomedullin (ADM), mRNA [NM_001124]	0,001852063	2,2917843	up
A_24_P62659	TSPAN2	Homo sapiens tetraspanin 2 (TSPAN2), transcript variant 1, mRNA [NM_005725]	0,007465093	2,2805579	up
A_23_P98350	BIRC3	Homo sapiens baculoviral IAP repeat containing 3 (BIRC3), transcript variant 1, mRNA [NM_001165]	0,000540916	2,277504	up
A_33_P3259708	CMA1	Homo sapiens chymase 1 (CMA1), transcript variant 2, mRNA [NM_001308083]	0,003890306	2,248369	up
A_23_P32500	STAB1	Homo sapiens stabilin 1 (STAB1), mRNA [NM_015136]	0,0335545	2,2327397	up
A_24_P208567	IL18R1	Homo sapiens interleukin 18 receptor 1 (IL18R1), transcript variant 1, mRNA [NM_003855]	0,002507854	2,220098	up
A_22_P00022869	PSMF1	proteasome inhibitor subunit 1 [Source:HGNC Symbol	0,03287423	2,2154133	up
A_24_P149704	DAB2IP	Homo sapiens DAB2 interacting protein (DAB2IP), transcript variant 2, mRNA [NM_138709]	0,00438354	2,2151628	up

A_24_P68783	IL36RN	Homo sapiens interleukin 36 receptor antagonist (IL36RN), transcript variant 1, mRNA [NM_012275]	0,011015176	2,1976457	up
A_23_P90925	IL36B	Homo sapiens interleukin 36 beta (IL36B), transcript variant 2, mRNA [NM_173178]	0,03194216	2,17615	up
A_33_P3344423	NCR3	Homo sapiens natural cytotoxicity triggering receptor 3 (NCR3), transcript variant 3, mRNA [NM_001145467]	0,017072132	2,1755116	up
A_33_P3311439	GCH1	Homo sapiens GTP cyclohydrolase 1 (GCH1), transcript variant 4, mRNA [NM_-001024071]	5,65315E-05	2,1611764	up
A_33_P3214035	ADORA2A	Homo sapiens adenosine A2a receptor (ADORA2A), transcript variant 3, mRNA [NM_000675]	0,011950237	2,153515	up
A_23_P47148	NOX4	Homo sapiens NADPH oxidase 4 (NOX4), transcript variant 1, mRNA [NM_016931]	0,025949782	2,1493773	up
A_33_P3292769	NFAM1	Homo sapiens NFAT activating protein with ITAM motif 1 (NFAM1), transcript variant 1, mRNA [NM_145912]	0,006848789	-2,14802	down
A_23_P311632	NLRP6	Homo sapiens NLR family pyrin domain containing 6 (NLRP6), transcript variant 1, mRNA [NM_138329]	0,037582446	2,1371944	up
A_23_P25735	PSMA6	Homo sapiens proteasome subunit alpha 6 (PSMA6), transcript variant 2, mRNA [NM_001282232]	0,001735721	2,1326425	up
A_23_P71855	C5	Homo sapiens complement C5 (C5), transcript variant 1, mRNA [NM_001735]	0,002547465	-2,131948	down
A_33_P3220045	AKNA	Homo sapiens cDNA FLJ44148 fis, clone THYMU2030637. [AK126136]	0,015684625	2,119183	up
A_33_P3415820	THBS1	thrombospondin 1 [Source:HGNC Symbol	0,032301128	2,096251	up

A_33_P3324394	CIITA	Homo sapiens class II major histocompatibility complex transactivator (CIITA), transcript variant 3, mRNA [NM_001286403]	0,021719659	2,0941463	up
A_24_P916496	PRKCA	Homo sapiens protein kinase C alpha (PRKCA), mRNA [NM_002737]	0,038731188	-2,0935864	down
A_23_P50508	PLA2G4C	Homo sapiens phospholipase A2 group IVC (PLA2G4C), transcript variant 1, mRNA [NM_003706]	0,042113036	2,072822	up
A_33_P3243449	CD70	Homo sapiens CD70 molecule (CD70), transcript variant 1, mRNA [NM_001252]	0,035038564	2,0700223	up
A_23_P24469	CSRP3	Homo sapiens cysteine and glycine rich protein 3 (CSRP3), transcript variant 1, mRNA [NM_003476]	0,003612608	2,0590684	up
A_24_P124624	OLR1	Homo sapiens oxidized low density lipoprotein receptor 1 (OLR1), transcript variant 1, mRNA [NM_002543]	0,01550361	2,0393155	up
A_23_P106016	PRKD1	Homo sapiens protein kinase D1 (PRKD1), transcript variant 2, mRNA [NM_002742]	0,030517317	-2,0311153	down
A_32_P209960	CIITA	Homo sapiens class II major histocompatibility complex transactivator (CIITA), transcript variant 2, mRNA [NM_000246]	0,004982785	2,0265503	up
A_23_P71037	IL6	Homo sapiens interleukin 6 (IL6), transcript variant 1, mRNA [NM_000600]	0,041630205	1,9789563	up
A_33_P3265744	PTGER3	Homo sapiens prostaglandin E receptor 3 (PTGER3), transcript variant 5, mRNA [NM_198715]	0,034260232	1,9605243	up
A_33_P3281283	S1PR3	Homo sapiens sphingosine-1-phosphate receptor 3 (S1PR3), mRNA [NM_005226]	0,032766372	1,9586707	up
A_23_P126908	TNFRSF14	Homo sapiens TNF receptor superfamily member 14 (TNFRSF14), transcript variant 1, mRNA [NM_003820]	0,000639808	1,9523147	up

A_33_P3281695	NLRP3	Homo sapiens NLR family pyrin domain containing 3 (NLRP3), transcript variant 6, mRNA [NM_001243133]	0,04157791	1,9438491	up
A_24_P382187	IGFBP4	Homo sapiens insulin like growth factor binding protein 4 (IGFBP4), mRNA [NM_-001552]	0,00789794	1,940885	up
A_23_P92499	TLR2	Homo sapiens toll like receptor 2 (TLR2), transcript variant 3, mRNA [NM_003264]	0,000355408	1,9401038	up
A_33_P3361348	ALOX15	Homo sapiens arachidonate 15-lipoxygenase (ALOX15), mRNA [NM_001140]	0,04676787	-1,9357504	down
A_24_P245298	TNFSF12	Homo sapiens TNF superfamily member 12 (TNFSF12), transcript variant 1, mRNA [NM_003809]	0,003199709	-1,9255168	down
A_24_P303193	HNRNPA0	heterogeneous nuclear ribonucleoprotein A0 [Source:HGNC Symbol	0,005745845	-1,9078555	down
A_32_P193322	RICTOR	Homo sapiens RPTOR independent companion of MTOR complex 2 (RICTOR), transcript variant 1, mRNA [NM_152756]	0,001708047	1,9062043	up
A_23_P29953	IL15	Homo sapiens interleukin 15 (IL15), transcript variant 3, mRNA [NM_000585]	0,044459198	1,9040732	up
A_23_P79931	ATRN	Homo sapiens attractin (ATRN), transcript variant 2, mRNA [NM_139322]	0,003040228	-1,8893961	down
A_24_P36847	DHX9	Homo sapiens DExH-box helicase 9 (DHX9), transcript variant 1, mRNA [NM_001357]	0,007375927	-1,8711134	down
A_23_P251173	EIF2AK1	Homo sapiens eukaryotic translation initiation factor 2 alpha kinase 1 (EIF2AK1), transcript variant 1, mRNA [NM_014413]	0,022077568	-1,8591758	down
A_23_P141035	CHST4	Homo sapiens carbohydrate sulfotransferase 4 (CHST4), transcript variant 1, mRNA [NM_005769]	0,007936569	1,854728	up

A_24_P167642	GCH1	Homo sapiens GTP cyclohydrolase 1 (GCH1), transcript variant 1, mRNA [NM_-000161]	0,011558815	1,8390758	up
A_24_P390495	CX3CL1	Homo sapiens C-X3-C motif chemokine ligand 1 (CX3CL1), transcript variant 1, mRNA [NM_002996]	0,002801295	1,8350171	up
A_23_P91954	ACKR2	Homo sapiens atypical chemokine receptor 2 (ACKR2), mRNA [NM_001296]	0,009875516	1,8200617	up
A_23_P212196	OGG1	Homo sapiens 8-oxoguanine DNA glycosylase (OGG1), transcript variant 2d, mRNA [NM_016828]	0,002954718	-1,8075172	down
A_33_P3322288	AZI2	Homo sapiens 5-azacytidine induced 2 (AZI2), transcript variant 3, mRNA [NM_-001134433]	0,003598729	1,8073945	up
A_33_P3351249	CXCL16	Homo sapiens C-X-C motif chemokine ligand 16 (CXCL16), transcript variant 2, mRNA [NM_001100812]	0,001337373	1,807025	up
A_33_P3245439	CD40	Homo sapiens CD40 molecule (CD40), transcript variant 8, mRNA [NM_001362758]	0,009900363	1,7998384	up
A_33_P3245183	HRH1	Homo sapiens histamine receptor H1 (HRH1), transcript variant 1, mRNA [NM_-001098213]	0,030677153	1,7916778	up
A_23_P112103	GSDMD	Homo sapiens gasdermin D (GSDMD), transcript variant 1, mRNA [NM_024736]	0,021573154	1,7767302	up
A_33_P3256680	MFHAS1	Homo sapiens malignant fibrous histiocytoma amplified sequence 1 (MFHAS1), mRNA [NM_004225]	0,043908104	-1,7727342	down
A_23_P431939	MR1	Homo sapiens major histocompatibility complex, class I-related (MR1), transcript variant 1, mRNA [NM_001531]	0,005525626	1,7726315	up

A_33_P3322283	AZI2	Homo sapiens 5-azacytidine induced 2 (AZI2), transcript variant 4, mRNA [NM_-001271650]	0,0048029	1,7711732	up
A_33_P3281795	MGLL	Homo sapiens monoglyceride lipase (MGLL), transcript variant 1, mRNA [NM_007283]	0,015235945	-1,7400275	down
A_33_P3316539	SLC7A2	Homo sapiens solute carrier family 7 member 2 (SLC7A2), transcript variant 5, mRNA [NM_001370338]	0,008445699	-1,7359629	down
A_24_P129277	NOD1	Homo sapiens nucleotide binding oligomerization domain containing 1 (NOD1), transcript variant 1, mRNA [NM_006092]	0,034648743	1,727478	up
A_23_P74928	MR1	Homo sapiens major histocompatibility complex, class I-related (MR1), transcript variant 1, mRNA [NM_001531]	0,004135493	1,7269909	up
A_23_P151614	PSME1	Homo sapiens proteasome activator subunit 1 (PSME1), transcript variant 1, mRNA [NM_006263]	0,003833243	1,7223362	up
A_33_P3315223	HNRNPA0	heterogeneous nuclear ribonucleoprotein A0 [Source:HGNC Symbol	0,023520144	-1,7170987	down
A_33_P3234697	LXN	Homo sapiens latexin (LXN), mRNA [NM_020169]	0,02903105	-1,7104759	down
A_33_P3262124	MMP25	Homo sapiens matrix metallopeptidase 25 (MMP25), mRNA [NM_022468]	0,014088858	1,7102164	up
A_33_P3354945	CSF1	Homo sapiens colony stimulating factor 1 (CSF1), transcript variant 2, mRNA [NM_-172210]	0,042152002	1,7023019	up
A_23_P345591	PSMA2	Homo sapiens proteasome subunit alpha 2 (PSMA2), mRNA [NM_002787]	0,003654306	1,6695567	up
A_23_P151791	LTB4R	Homo sapiens leukotriene B4 receptor (LTB4R), transcript variant 1, mRNA [NM_-181657]	0,020214127	-1,6636747	down

A_23_P85903	TLR5	Homo sapiens toll like receptor 5 (TLR5), mRNA [NM_003268]	0,013407332	-1,6632558	down
A_23_P5654	IL37	Homo sapiens interleukin 37 (IL37), transcript variant 1, mRNA [NM_014439]	0,01015224	1,6623669	up
A_24_P124992	PSMA4	Homo sapiens proteasome subunit alpha 4 (PSMA4), transcript variant 1, mRNA [NM_002789]	0,011269014	1,6541007	up
A_23_P57036	CD40	Homo sapiens CD40 molecule (CD40), transcript variant 3, mRNA [NM_001302753]	0,015476495	1,6431483	up
A_33_P3279059	RIPK1	Homo sapiens receptor interacting serine/threonine kinase 1 (RIPK1), transcript variant 3, mRNA [NM_001354930]	0,007986327	1,6334586	up
A_33_P3294509	CD44	Homo sapiens CD44 molecule (Indian blood group) (CD44), transcript variant 1, mRNA [NM_000610]	0,015903288	-1,6232344	down
A_24_P300777	ADAM8	Homo sapiens ADAM metallopeptidase domain 8 (ADAM8), transcript variant 1, mRNA [NM_001109]	0,012732982	1,5954155	up
A_24_P125283	HDAC5	Homo sapiens histone deacetylase 5 (HDAC5), transcript variant 3, mRNA [NM_-001015053]	0,020040005	-1,5921069	down
A_24_P79054	TGFB1	transforming growth factor beta 1 [Source:HGNC Symbol	0,040861174	-1,5827398	down
A_23_P94683	NFX1	Homo sapiens nuclear transcription factor, X-box binding 1 (NFX1), transcript variant 1, mRNA [NM_002504]	0,020365098	-1,5799545	down
A_33_P3321657	HSPG2	Homo sapiens heparan sulfate proteoglycan 2 (HSPG2), transcript variant 2, mRNA [NM_005529]	0,015826633	-1,5375807	down

A_23_P86216	PSMA5	Homo sapiens proteasome subunit alpha 5 (PSMA5), transcript variant 1, mRNA [NM_002790]	0,012924188	1,5140365	up
A_23_P35912	CASP4	Homo sapiens caspase 4 (CASP4), transcript variant gamma, mRNA [NM_033306]	0,006587797	1,5083351	up
A_23_P164797	ZNF580	Homo sapiens zinc finger protein 580 (ZNF580), transcript variant 1, mRNA [NM_-016202]	0,037367415	-1,5052494	down
A_23_P90311	TICAM1	Homo sapiens toll like receptor adaptor molecule 1 (TICAM1), mRNA [NM_182919]	0,037218824	1,5051088	up

Table 9.3 DEGs of induced pro-inflammatory genes by IFN-β vs unstimulated

ProbeName	GeneSymbol	Description	*P*	FC	Regulation
A_32_P44394	AIM2	Homo sapiens absent in melanoma 2 (AIM2), transcript variant 1, mRNA [NM_004833]	0,001195282	8,396416	up
A_23_P323823	H2BC1	Homo sapiens histone cluster 1 H2B family member a (HIST1H2BA), mRNA [NM_-170610]	0,04760476	3,5572376	up
A_24_P274270	STAT1	Homo sapiens signal transducer and activator of transcription 1 (STAT1), transcript variant beta, mRNA [NM_139266]	0,018723585	3,437189	up
A_33_P3343175	CXCL10	Homo sapiens C-X-C motif chemokine ligand 10 (CXCL10), mRNA [NM_001565]	0,021988204	3,3313289	up
A_33_P3305243	PSMD5	proteasome 26S subunit, non-ATPase 5 [Source:HGNC Symbol	0,03956273	3,065413	up
A_24_P68783	IL36RN	Homo sapiens interleukin 36 receptor antagonist (IL36RN), transcript variant 1, mRNA [NM_012275]	0,015862998	2,8498673	up
A_33_P3243449	CD70	Homo sapiens CD70 molecule (CD70), transcript variant 1, mRNA [NM_001252]	0,034606494	2,6017787	up
A_23_P426305	AOC3	Homo sapiens amine oxidase copper containing 3 (AOC3), transcript variant 1, mRNA [NM_003734]	0,025483994	2,5278823	up
A_23_P250302	CCR3	Homo sapiens C-C motif chemokine receptor 3 (CCR3), transcript variant 1, mRNA [NM_001837]	0,04159679	2,4443989	up
A_23_P132159	USP18	ubiquitin specific peptidase 18 [Source:HGNC Symbol	0,021988166	2,4142048	up

A_33_P3319905	TREM1	Homo sapiens triggering receptor expressed on myeloid cells 1 (TREM1), transcript variant 1, mRNA [NM_018643]	0,040645182	2,3611996	up
A_33_P3273623	CCL21	Homo sapiens C-C motif chemokine ligand 21 (CCL21), mRNA [NM_002989]	0,048613153	2,263171	up
A_33_P3212274	F2R	coagulation factor II thrombin receptor [Source:HGNC Symbol	0,016203571	2,0971568	up
A_23_P250629	PSMB8	Homo sapiens proteasome subunit beta 8 (PSMB8), transcript variant 1, mRNA [NM_004159]	0,027782155	1,8709359	up
A_24_P270728	NUPR1	Homo sapiens nuclear protein 1, transcriptional regulator (NUPR1), transcript variant 1, mRNA [NM_001042483]	0,030425794	1,6345423	up
A_23_P216966	PTGS1	Homo sapiens prostaglandin-endoperoxide synthase 1 (PTGS1), transcript variant 1, mRNA [NM_000962]	0,025767192	-2,6653693	down

Table 9.4 DEGs of induced pro-inflammatory genes by IFN-λ1 vs unstimulated

ProbeName	GeneSymbol	Description	*P*	FC	Regulation
A_24_P303091	CXCL10	Homo sapiens C-X-C motif chemokine ligand 10 (CXCL10), mRNA [NM_001565]	3,41799E-05	38,32672	up
A_33_P3343175	CXCL10	Homo sapiens C-X-C motif chemokine ligand 10 (CXCL10), mRNA [NM_001565]	4,45514E-07	35,365387	up
A_23_P125278	CXCL11	Homo sapiens C-X-C motif chemokine ligand 11 (CXCL11), transcript variant 2, mRNA [NM_001302123]	1,52521E-05	31,756632	up
A_32_P44394	AIM2	Homo sapiens absent in melanoma 2 (AIM2), transcript variant 1, mRNA [NM_004833]	3,3081E-06	27,773428	up
A_23_P14174	TNFSF13B	Homo sapiens TNF superfamily member 13b (TNFSF13B), transcript variant 1, mRNA [NM_006573]	0,000173624	11,605169	up
A_24_P274270	STAT1	Homo sapiens signal transducer and activator of transcription 1 (STAT1), transcript variant beta, mRNA [NM_139266]	0,000140904	6,929159	up
A_23_P152838	CCL5	Homo sapiens C-C motif chemokine ligand 5 (CCL5), transcript variant 1, mRNA [NM_002985]	0,000904434	4,2394233	up
A_23_P132159	USP18	ubiquitin specific peptidase 18 [Source:HGNC Symbol	0,000207614	4,1353064	up
A_23_P18452	CXCL9	C-X-C motif chemokine ligand 9 [Source:HGNC Symbol	0,010966537	4,0010195	up
A_24_P68783	IL36RN	Homo sapiens interleukin 36 receptor antagonist (IL36RN), transcript variant 1, mRNA [NM_012275]	0,001049758	3,5916095	up

A_33_P3389230	CXCR3	Homo sapiens C-X-C motif chemokine receptor 3 (CXCR3), transcript variant 1, mRNA [NM_001504]	0,000574479	3,3240435	up
A_33_P3250443	DUOXA2	dual oxidase maturation factor 2 [Source:HGNC Symbol	0,006529354	3,1901946	up
A_23_P111000	PSMB9	Homo sapiens proteasome subunit beta 9 (PSMB9), mRNA [NM_002800]	0,000951921	2,8332336	up
A_23_P252981	ACE2	Homo sapiens angiotensin I converting enzyme 2 (ACE2), mRNA [NM_021804]	0,004214379	2,7695415	up
A_21_P0014047	C4A	Homo sapiens complement C4A (Rodgers blood group) (C4A), transcript variant 2, mRNA [NM_001252204]	0,03101198	2,7118797	up
A_22_P00021230	IL36RN	interleukin 36 receptor antagonist [Source:HGNC Symbol	0,013293338	2,708049	up
A_23_P121695	CXCL13	Homo sapiens C-X-C motif chemokine ligand 13 (CXCL13), mRNA [NM_006419]	0,0148905	2,704244	up
A_21_P0011535	LGALS9	galectin 9 [Source:HGNC Symbol	0,003146553	2,663347	up
A_23_P250629	PSMB8	Homo sapiens proteasome subunit beta 8 (PSMB8), transcript variant 1, mRNA [NM_004159]	0,000725181	2,630204	up
A_23_P116557	LGALS9	Homo sapiens galectin 9 (LGALS9), transcript variant 1, mRNA [NM_009587]	0,013954188	2,4895854	up
A_24_P85775	THEMIS2	Homo sapiens thymocyte selection associated family member 2 (THEMIS2), transcript variant 2, mRNA [NM_001039477]	0,002847773	2,4019833	up
A_33_P3243230	CXCL8	C-X-C motif chemokine ligand 8 [Source:HGNC Symbol	0,043112725	2,3465624	up
A_23_P98205	CHST1	Homo sapiens carbohydrate sulfotransferase 1 (CHST1), mRNA [NM_003654]	0,023594666	2,3226292	up

A_23_P169257	TNFSF8	Homo sapiens TNF superfamily member 8 (TNFSF8), transcript variant 1, mRNA [NM_001244]	0,018031914	2,2857323	up
A_19_P00322645	RPS6KA5	Homo sapiens ribosomal protein S6 kinase A5 (RPS6KA5), transcript variant 1, mRNA [NM_004755]	0,041937128	-2,265703	down
A_24_P69538	TLR4	Homo sapiens toll like receptor 4 (TLR4), transcript variant 1, mRNA [NM_138554]	0,038194634	2,25009	up
A_23_P25396	NR1H4	Homo sapiens nuclear receptor subfamily 1 group H member 4 (NR1H4), transcript variant 2, mRNA [NM_005123]	0,017005643	2,2484636	up
A_33_P3420416	LGALS9	Homo sapiens galectin 9 (LGALS9), transcript variant 4, mRNA [NM_001330163]	0,00754448	2,2109463	up
A_23_P154235	NMI	N-myc and STAT interactor [Source:HGNC Symbol	0,03243439	2,1684194	up
A_24_P320410	IL9	interleukin 9 [Source:HGNC Symbol	0,043335572	2,1545959	up
A_23_P78353	MEP1B	Homo sapiens meprin A subunit beta (MEP1B), transcript variant 2, mRNA [NM_001308171]	0,031259034	2,1339095	up
A_33_P3286422	FANCA	Homo sapiens FA complementation group A (FANCA), transcript variant 2, mRNA [NM_001018112]	0,008653687	-2,1271086	down
A_33_P3265749	PTGER3	Homo sapiens prostaglandin E receptor 3 (PTGER3), transcript variant 7, mRNA [NM_198717]	0,01609729	-2,1254554	down
A_23_P71855	C5	Homo sapiens complement C5 (C5), transcript variant 1, mRNA [NM_001735]	0,004244568	-2,1008353	down
A_33_P3256680	MFHAS1	Homo sapiens malignant fibrous histiocytoma amplified sequence 1 (MFHAS1), mRNA [NM_004225]	0,036175005	-2,0786572	down

A_33_P3305250	PSMD5	proteasome 26S subunit, non-ATPase 5 [Source:HGNC Symbol	0,0192146	-2,0365422	down
A_23_P126540	TMIGD3	Homo sapiens transmembrane and immunoglobulin domain containing 3 (TMIGD3), transcript variant 1, mRNA [NM_020683]	0,033951655	2,0017397	up
A_33_P3222069	SPHK1	Homo sapiens sphingosine kinase 1 (SPHK1), transcript variant 2, mRNA [NM_-182965]	0,035616722	1,956149	up
A_23_P19333	TREM1	Homo sapiens triggering receptor expressed on myeloid cells 1 (TREM1), transcript variant 1, mRNA [NM_018643]	0,04622594	1,9433584	up
A_23_P151614	PSME1	Homo sapiens proteasome activator subunit 1 (PSME1), transcript variant 1, mRNA [NM_006263]	0,003861825	1,9318057	up
A_23_P115161	ACKR1	Homo sapiens atypical chemokine receptor 1 (Duffy blood group) (ACKR1), transcript variant 2, mRNA [NM_002036]	0,03860546	1,9202368	up
A_33_P3305571	TNFRSF6B	Homo sapiens TNF receptor superfamily member 6b (TNFRSF6B), mRNA [NM_-003823]	0,03274893	1,8474447	up
A_23_P362659	MYD88	Homo sapiens MYD88 innate immune signal transduction adaptor (MYD88), transcript variant 2, mRNA [NM_002468]	0,014450439	1,8339207	up
A_23_P334173	LY75	Homo sapiens lymphocyte antigen 75 (LY75), mRNA [NM_002349]	0,009471307	-1,800064	down
A_33_P3316539	SLC7A2	Homo sapiens solute carrier family 7 member 2 (SLC7A2), transcript variant 5, mRNA [NM_001370338]	0,01628657	-1,7951075	down
A_33_P3315223	HNRNPA0	heterogeneous nuclear ribonucleoprotein A0 [Source:HGNC Symbol	0,03553062	-1,792397	down

A_23_P34644	FCGR2B	Homo sapiens Fc fragment of IgG receptor IIb (FCGR2B), transcript variant 1, mRNA [NM_004001]	0,049355745	1,7814153	up
A_23_P203665	ACER3	Homo sapiens alkaline ceramidase 3 (ACER3), transcript variant 1, mRNA [NM_-018367]	0,041850083	-1,7586284	down
A_33_P3393537	PTAFR	Homo sapiens platelet activating factor receptor (PTAFR), transcript variant 2, mRNA [NM_001164722]	0,045116637	1,7433258	up
A_33_P3375140	MCPH1	Homo sapiens microcephalin 1 (MCPH1), transcript variant 9, mRNA [NM_001363980]	0,024829047	-1,740886	down
A_23_P29953	IL15	Homo sapiens interleukin 15 (IL15), transcript variant 3, mRNA [NM_000585]	0,034828972	1,7314931	up
A_23_P112103	GSDMD	Homo sapiens gasdermin D (GSDMD), transcript variant 1, mRNA [NM_024736]	0,04110756	1,7283822	up
A_24_P83615	NLRP1	Homo sapiens NLR family pyrin domain containing 1 (NLRP1), transcript variant 5, mRNA [NM_001033053]	0,035158545	1,7155234	up
A_33_P3214550	CXCR2	Homo sapiens C-X-C motif chemokine receptor 2 (CXCR2), transcript variant 1, mRNA [NM_001557]	0,044900894	-1,6883744	down
A_24_P139191	ITCH	Homo sapiens itchy E3 ubiquitin protein ligase (ITCH), transcript variant 2, mRNA [NM_031483]	0,028281048	-1,653237	down
A_24_P270728	NUPR1	Homo sapiens nuclear protein 1, transcriptional regulator (NUPR1), transcript variant 1, mRNA [NM_001042483]	0,024812745	1,6517936	up
A_24_P416997	APOL3	Homo sapiens apolipoprotein L3 (APOL3), transcript variant beta/a, mRNA [NM_-145641]	0,032938723	1,6270928	up

A_23_P37375	RPS6KA5	Homo sapiens ribosomal protein S6 kinase A5 (RPS6KA5), transcript variant 1, mRNA [NM_004755]	0,028630061	-1,623044	down
A_23_P206441	FANCA	Homo sapiens FA complementation group A (FANCA), transcript variant 1, mRNA [NM_000135]	0,01777076	1,6167791	up
A_23_P152620	TNFSF13	Homo sapiens TNF superfamily member 13 (TNFSF13), transcript variant gamma, mRNA [NM_172088]	0,044476084	1,6135417	up
A_24_P125283	HDAC5	Homo sapiens histone deacetylase 5 (HDAC5), transcript variant 3, mRNA [NM_-001015053]	0,044893965	-1,6106997	down
A_23_P150583	SCGB1A1	Homo sapiens secretoglobin family 1A member 1 (SCGB1A1), mRNA [NM_003357]	0,04917339	1,6099755	up

Table 9.5 DEGs of induced pro-inflammatory genes by IFN-λ3 vs unstimulated

ProbeName	GeneSymbol	Description	*P*	FC	Regulation
A_24_P303091	CXCL10	Homo sapiens C-X-C motif chemokine ligand 10 (CXCL10), mRNA [NM_001565]	1,58712E-05	93,695274	up
A_23_P125278	CXCL11	Homo sapiens C-X-C motif chemokine ligand 11 (CXCL11), transcript variant 2, mRNA [NM_001302123]	7,42694E-06	89,1076	up
A_33_P3343175	CXCL10	Homo sapiens C-X-C motif chemokine ligand 10 (CXCL10), mRNA [NM_001565]	4,20379E-07	72,21422	up
A_32_P44394	AIM2	Homo sapiens absent in melanoma 2 (AIM2), transcript variant 1, mRNA [NM_004833]	1,21392E-05	29,89802	up
A_23_P14174	TNFSF13B	Homo sapiens TNF superfamily member 13b (TNFSF13B), transcript variant 1, mRNA [NM_006573]	0,000344219	15,917941	up
A_23_P121695	CXCL13	Homo sapiens C-X-C motif chemokine ligand 13 (CXCL13), mRNA [NM_006419]	6,62901E-06	8,626739	up
A_24_P274270	STAT1	Homo sapiens signal transducer and activator of transcription 1 (STAT1), transcript variant beta, mRNA [NM_139266]	0,000476665	7,6335363	up
A_33_P3250443	DUOXA2	dual oxidase maturation factor 2 [Source:HGNC Symbol	0,00183253	6,251456	up
A_23_P18452	CXCL9	C-X-C motif chemokine ligand 9 [Source:HGNC Symbol	0,00285677	6,105914	up
A_33_P3220045	AKNA	Homo sapiens cDNA FLJ44148 fis, clone THYMU2030637. [AK126136]	0,04000026	4,4678035	up
A_23_P132159	USP18	ubiquitin specific peptidase 18 [Source:HGNC Symbol	0,000732216	4,3340163	up
A_23_P168339	MAS1	Homo sapiens MAS1 proto-oncogene, G protein-coupled receptor (MAS1), transcript variant 1, mRNA [NM_002377]	0,025850676	3,8714952	up

A_23_P1904	MS4A2	Homo sapiens membrane spanning 4-domains A2 (MS4A2), transcript variant 1, mRNA [NM_000139]	0,028512416	3,784655	up
A_23_P152838	CCL5	Homo sapiens C-C motif chemokine ligand 5 (CCL5), transcript variant 1, mRNA [NM_002985]	0,006956873	3,7277532	up
A_24_P227415	CLEC7A	Homo sapiens C-type lectin domain containing 7A (CLEC7A), transcript variant 6, mRNA [NM_197954]	0,004494109	3,6345189	up
A_21_P0000155	PSMC2	Homo sapiens proteasome 26S subunit, ATPase 2 (PSMC2), transcript variant 2, mRNA [NM_001204453]	0,011088803	3,6013997	up
A_23_P154235	NMI	N-myc and STAT interactor [Source:HGNC Symbol	0,001258185	3,5446808	up
A_23_P206806	ITGAL	Homo sapiens integrin subunit alpha L (ITGAL), transcript variant 2, mRNA [NM_-001114380]	0,009260372	-3,4551606	down
A_24_P124624	OLR1	Homo sapiens oxidized low density lipoprotein receptor 1 (OLR1), transcript variant 1, mRNA [NM_002543]	0,029419694	3,3363874	up
A_23_P111000	PSMB9	Homo sapiens proteasome subunit beta 9 (PSMB9), mRNA [NM_002800]	0,000889511	3,3064225	up
A_23_P94230	LY96	Homo sapiens lymphocyte antigen 96 (LY96), transcript variant 2, mRNA [NM_-001195797]	0,04671059	3,2653265	up
A_23_P252981	ACE2	Homo sapiens angiotensin I converting enzyme 2 (ACE2), mRNA [NM_021804]	0,002735071	3,2055185	up
A_24_P85775	THEMIS2	Homo sapiens thymocyte selection associated family member 2 (THEMIS2), transcript variant 2, mRNA [NM_001039477]	0,000439358	3,160906	up

A_24_P68783	IL36RN	Homo sapiens interleukin 36 receptor antagonist (IL36RN), transcript variant 1, mRNA [NM_012275]	0,014129732	3,055497	up
A_33_P3414922	APOL3	apolipoprotein L3 [Source:HGNC Symbol	0,0471484	2,992101	up
A_22_P00000845	CRHBP	corticotropin releasing hormone binding protein [Source:HGNC Symbol	0,012364009	2,741073	up
A_23_P502336	ADGRE2	Homo sapiens adhesion G protein-coupled receptor E2 (ADGRE2), transcript variant 1, mRNA [NM_013447]	0,026913952	2,7340436	up
A_33_P3243449	CD70	Homo sapiens CD70 molecule (CD70), transcript variant 1, mRNA [NM_001252]	0,015416314	2,6600356	up
A_23_P250629	PSMB8	Homo sapiens proteasome subunit beta 8 (PSMB8), transcript variant 1, mRNA [NM_004159]	0,001793553	2,6335993	up
A_24_P54174	TNFRSF1B	Homo sapiens TNF receptor superfamily member 1B (TNFRSF1B), mRNA [NM_-001066]	0,033267632	2,5675566	up
A_23_P164966	NLRP4	NLR family pyrin domain containing 4 [Source:HGNC Symbol	0,04569047	2,5019827	up
A_33_P3250083	NFATC4	Homo sapiens nuclear factor of activated T cells 4 (NFATC4), transcript variant 2, mRNA [NM_004554]	0,008642561	-2,492497	down
A_33_P3319905	TREM1	Homo sapiens triggering receptor expressed on myeloid cells 1 (TREM1), transcript variant 1, mRNA [NM_018643]	0,033184364	2,3837545	up
A_33_P3389230	CXCR3	Homo sapiens C-X-C motif chemokine receptor 3 (CXCR3), transcript variant 1, mRNA [NM_001504]	0,011970643	2,3805401	up
A_23_P300100	PLA2G2D	phospholipase A2 group IID [Source:HGNC Symbol	0,029288419	-2,2971544	down

A_23_P151778	CMA1	Homo sapiens chymase 1 (CMA1), transcript variant 1, mRNA [NM_001836]	0,020392599	2,295212	up
A_23_P137931	ADORA3	Homo sapiens adenosine A3 receptor (ADORA3), transcript variant A, mRNA [NM_-000677]	0,037738964	2,254926	up
A_23_P110473	NAIP	Homo sapiens NLR family apoptosis inhibitory protein (NAIP), transcript variant 1, mRNA [NM_004536]	0,04868632	2,2237003	up
A_21_P0014810	PSMD3	proteasome 26S subunit, non-ATPase 3 [Source:HGNC Symbol	0,038305473	2,1351821	up
A_23_P362659	MYD88	Homo sapiens MYD88 innate immune signal transduction adaptor (MYD88), transcript variant 2, mRNA [NM_002468]	0,008335095	2,05774	up
A_33_P3246833	IL1RN	Homo sapiens interleukin 1 receptor antagonist (IL1RN), transcript variant 5, mRNA [NM_001318914]	0,03890187	2,0516438	up
A_24_P270728	NUPR1	Homo sapiens nuclear protein 1, transcriptional regulator (NUPR1), transcript variant 1, mRNA [NM_001042483]	0,006243372	2,0182953	up
A_23_P501713	IL1F10	Homo sapiens interleukin 1 family member 10 (IL1F10), transcript variant 2, mRNA [NM_173161]	0,047518894	-1,9983101	down
A_24_P374516	TMSB4X	Homo sapiens thymosin beta 4 X-linked (TMSB4X), mRNA [NM_021109]	0,038196415	1,9819475	up
A_23_P160025	IFI16	Homo sapiens interferon gamma inducible protein 16 (IFI16), transcript variant 2, mRNA [NM_005531]	0,023812829	1,9610488	up
A_23_P126735	IL10	Homo sapiens interleukin 10 (IL10), mRNA [NM_000572]	0,02497826	1,8939157	up
A_33_P3420416	LGALS9	Homo sapiens galectin 9 (LGALS9), transcript variant 4, mRNA [NM_001330163]	0,041244317	1,8775862	up

A_33_P3229375	PSMB11	proteasome subunit beta 11 [Source:HGNC Symbol	0,048711326	1,8631315	up
A_24_P416997	APOL3	Homo sapiens apolipoprotein L3 (APOL3), transcript variant beta/a, mRNA [NM_-145641]	0,012298434	1,8523794	up
A_23_P29953	IL15	Homo sapiens interleukin 15 (IL15), transcript variant 3, mRNA [NM_000585]	0,026887393	1,846626	up
A_21_P0011535	LGALS9	galectin 9 [Source:HGNC Symbol	0,04519859	1,8349881	up
A_21_P0000171	IL6R	Homo sapiens interleukin 6 receptor (IL6R), transcript variant 3, mRNA [NM_-001206866]	0,039959107	-1,8247548	down
A_23_P79931	ATRN	Homo sapiens attractin (ATRN), transcript variant 2, mRNA [NM_139322]	0,04644455	-1,8144456	down
A_23_P65427	PSME2	Homo sapiens proteasome activator subunit 2 (PSME2), mRNA [NM_002818]	0,012954407	1,8114257	up
A_23_P25735	PSMA6	Homo sapiens proteasome subunit alpha 6 (PSMA6), transcript variant 2, mRNA [NM_001282232]	0,037919793	1,7935705	up
A_23_P74290	GBP5	Homo sapiens guanylate binding protein 5 (GBP5), transcript variant 1, mRNA [NM_-052942]	0,03558074	1,755531	up
A_23_P215154	NUB1	Homo sapiens negative regulator of ubiquitin like proteins 1 (NUB1), transcript variant 2, mRNA [NM_016118]	0,03086014	1,5804598	up

Table 9.6 DEGs of induced pro-inflammatory genes by IFN-γ vs unstimulated

ProbeName	GeneSymbol	Description	*P*	FC	Regulation
A_23_P18452	CXCL9	C-X-C motif chemokine ligand 9 [Source:HGNC Symbol	4,48318E-12	18053,916	up
A_23_P125278	CXCL11	Homo sapiens C-X-C motif chemokine ligand 11 (CXCL11), transcript variant 2, mRNA [NM_001302123]	2,05344E-09	2483,3115	up
A_24_P303091	CXCL10	Homo sapiens C-X-C motif chemokine ligand 10 (CXCL10), mRNA [NM_001565]	1,47554E-08	1231,2006	up
A_33_P3343175	CXCL10	Homo sapiens C-X-C motif chemokine ligand 10 (CXCL10), mRNA [NM_001565]	5,97279E-10	880,2944	up
A_32_P44394	AIM2	Homo sapiens absent in melanoma 2 (AIM2), transcript variant 1, mRNA [NM_004833]	5,78873E-07	62,164303	up
A_33_P3250443	DUOXA2	dual oxidase maturation factor 2 [Source:HGNC Symbol	2,98122E-06	37,584507	up
A_23_P74290	GBP5	Homo sapiens guanylate binding protein 5 (GBP5), transcript variant 1, mRNA [NM_-052942]	2,86471E-08	36,786858	up
A_23_P14174	TNFSF13B	Homo sapiens TNF superfamily member 13b (TNFSF13B), transcript variant 1, mRNA [NM_006573]	1,18635E-05	32,323044	up
A_23_P111000	PSMB9	Homo sapiens proteasome subunit beta 9 (PSMB9), mRNA [NM_002800]	1,16482E-08	21,906746	up
A_32_P209960	CIITA	Homo sapiens class II major histocompatibility complex transactivator (CIITA), transcript variant 2, mRNA [NM_000246]	6,21397E-08	16,594385	up
A_24_P365526	HCK	Homo sapiens HCK proto-oncogene, Src family tyrosine kinase (HCK), transcript variant 1, mRNA [NM_002110]	3,43377E-06	-14,522271	down

A_23_P152838	CCL5	Homo sapiens C-C motif chemokine ligand 5 (CCL5), transcript variant 1, mRNA [NM_002985]	0,000247173	14,018408	up
A_24_P274270	STAT1	Homo sapiens signal transducer and activator of transcription 1 (STAT1), transcript variant beta, mRNA [NM_139266]	1,2875E-05	12,716562	up
A_23_P94230	LY96	Homo sapiens lymphocyte antigen 96 (LY96), transcript variant 2, mRNA [NM_-001195797]	0,000210004	8,384156	up
A_23_P250629	PSMB8	Homo sapiens proteasome subunit beta 8 (PSMB8), transcript variant 1, mRNA [NM_004159]	4,66517E-07	7,9840136	up
A_23_P42282	C4B	Homo sapiens complement C4B (Chido blood group) (C4B), mRNA [NM_001002029]	1,99751E-05	7,973746	up
A_23_P376557	MMP25	Homo sapiens matrix metallopeptidase 25 (MMP25), mRNA [NM_022468]	7,93866E-06	7,9326267	up
A_24_P416997	APOL3	Homo sapiens apolipoprotein L3 (APOL3), transcript variant beta/a, mRNA [NM_-145641]	5,56759E-07	7,7187634	up
A_21_P0014047	C4A	Homo sapiens complement C4A (Rodgers blood group) (C4A), transcript variant 2, mRNA [NM_001252204]	0,000103405	6,8077097	up
A_23_P55828	CCL25	Homo sapiens C-C motif chemokine ligand 25 (CCL25), transcript variant 1, mRNA [NM_005624]	0,000129288	6,6654983	up
A_23_P29953	IL15	Homo sapiens interleukin 15 (IL15), transcript variant 3, mRNA [NM_000585]	1,05554E-06	6,5455756	up
A_24_P167642	GCH1	Homo sapiens GTP cyclohydrolase 1 (GCH1), transcript variant 1, mRNA [NM_-000161]	7,20131E-07	6,025474	up

A_23_P69310	CCRL2	Homo sapiens C-C motif chemokine receptor like 2 (CCRL2), transcript variant 1, mRNA [NM_003965]	0,000363735	5,4436088	up
A_24_P390495	CX3CL1	Homo sapiens C-X3-C motif chemokine ligand 1 (CX3CL1), transcript variant 1, mRNA [NM_002996]	1,32213E-05	5,3834505	up
A_23_P167328	CD38	Homo sapiens CD38 molecule (CD38), transcript variant 1, mRNA [NM_001775]	2,73687E-05	5,36737	up
A_23_P218646	TNFRSF6B	Homo sapiens TNF receptor superfamily member 6b (TNFRSF6B), mRNA [NM_-003823]	0,000117964	5,282504	up
A_33_P3305571	TNFRSF6B	Homo sapiens TNF receptor superfamily member 6b (TNFRSF6B), mRNA [NM_-003823]	1,23605E-05	5,218821	up
A_33_P3288359	PSMB10	Homo sapiens proteasome subunit beta 10 (PSMB10), mRNA [NM_002801]	1,29975E-05	5,2181478	up
A_23_P65427	PSME2	Homo sapiens proteasome activator subunit 2 (PSME2), mRNA [NM_002818]	9,56221E-07	5,1566687	up
A_23_P154235	NMI	N-myc and STAT interactor [Source:HGNC Symbol	4,38328E-05	5,151972	up
A_23_P24469	CSRP3	Homo sapiens cysteine and glycine rich protein 3 (CSRP3), transcript variant 1, mRNA [NM_003476]	2,47225E-05	5,0730934	up
A_23_P78037	CCL7	C-C motif chemokine ligand 7 [Source:HGNC Symbol	0,000801605	4,7371373	up
A_33_P3311439	GCH1	Homo sapiens GTP cyclohydrolase 1 (GCH1), transcript variant 4, mRNA [NM_-001024071]	1,97945E-05	4,5233736	up
A_33_P3878772	JAK2	Homo sapiens Janus kinase 2 (JAK2), transcript variant 2, mRNA [NM_001322194]	5,55423E-06	4,4320574	up

A_23_P126908	TNFRSF14	Homo sapiens TNF receptor superfamily member 14 (TNFRSF14), transcript variant 1, mRNA [NM_003820]	8,04208E-07	4,3545136	up
A_23_P86975	CARD18	caspase recruitment domain family member 18 [Source:HGNC Symbol	0,001667073	-4,318464	down
A_23_P252981	ACE2	Homo sapiens angiotensin I converting enzyme 2 (ACE2), mRNA [NM_021804]	0,000265573	4,227801	up
A_33_P3879161	PIK3AP1	Homo sapiens phosphoinositide-3-kinase adaptor protein 1 (PIK3AP1), mRNA [NM_-152309]	0,00144879	4,1593246	up
A_33_P3312242	CCL25	Homo sapiens C-C motif chemokine ligand 25 (CCL25), transcript variant 1, mRNA [NM_005624]	0,004460806	3,831968	up
A_23_P207456	CCL8	Homo sapiens C-C motif chemokine ligand 8 (CCL8), mRNA [NM_005623]	0,006919097	3,8256485	up
A_33_P3245439	CD40	Homo sapiens CD40 molecule (CD40), transcript variant 8, mRNA [NM_001362758]	0,000175058	3,7162166	up
A_24_P250922	PTGS2	Homo sapiens prostaglandin-endoperoxide synthase 2 (PTGS2), mRNA [NM_000963]	0,000559145	3,6649647	up
A_23_P127948	ADM	Homo sapiens adrenomedullin (ADM), mRNA [NM_001124]	0,000421865	3,640907	up
A_23_P57036	CD40	Homo sapiens CD40 molecule (CD40), transcript variant 3, mRNA [NM_001302753]	0,000126154	3,5358584	up
A_33_P3414922	APOL3	apolipoprotein L3 [Source:HGNC Symbol	0,025862165	3,4517896	up
A_23_P143994	FANCD2	Homo sapiens FA complementation group D2 (FANCD2), transcript variant 2, mRNA [NM_001018115]	0,002838039	-3,4010487	down
A_33_P3324394	CIITA	Homo sapiens class II major histocompatibility complex transactivator (CIITA), transcript variant 3, mRNA [NM_001286403]	0,000106777	3,3807597	up

A_24_P97405	CCRL2	Homo sapiens C-C motif chemokine receptor like 2 (CCRL2), transcript variant 1, mRNA [NM_003965]	0,005457842	3,3152823	up
A_23_P252106	RIPK2	Homo sapiens receptor interacting serine/threonine kinase 2 (RIPK2), mRNA [NM_-003821]	9,19111E-05	3,2846725	up
A_33_P3286422	FANCA	Homo sapiens FA complementation group A (FANCA), transcript variant 2, mRNA [NM_001018112]	0,000378879	-3,2525175	down
A_33_P3288384	PSMA1	Homo sapiens proteasome subunit alpha 1 (PSMA1), transcript variant 3, mRNA [NM_001143937]	0,015117837	3,2194471	up
A_23_P165624	TNFAIP6	Homo sapiens TNF alpha induced protein 6 (TNFAIP6), mRNA [NM_007115]	0,007945028	3,1728618	up
A_33_P3250083	NFATC4	Homo sapiens nuclear factor of activated T cells 4 (NFATC4), transcript variant 2, mRNA [NM_004554]	0,000473155	-3,161579	down
A_21_P0000155	PSMC2	Homo sapiens proteasome 26S subunit, ATPase 2 (PSMC2), transcript variant 2, mRNA [NM_001204453]	0,008226868	3,1439273	up
A_24_P270728	NUPR1	Homo sapiens nuclear protein 1, transcriptional regulator (NUPR1), transcript variant 1, mRNA [NM_001042483]	0,000126493	3,082599	up
A_23_P123853	CCL19	Homo sapiens C-C motif chemokine ligand 19 (CCL19), mRNA [NM_006274]	0,002024261	-3,0792801	down
A_23_P132159	USP18	ubiquitin specific peptidase 18 [Source:HGNC Symbol	0,003023788	3,0432718	up
A_23_P151614	PSME1	Homo sapiens proteasome activator subunit 1 (PSME1), transcript variant 1, mRNA [NM_006263]	0,000140305	3,0360098	up

A_23_P71530	TNFRSF11B	Homo sapiens TNF receptor superfamily member 11b (TNFRSF11B), mRNA [NM_-002546]	0,005105244	-3,0320866	down
A_33_P3354940	CSF1	Homo sapiens colony stimulating factor 1 (CSF1), transcript variant 1, mRNA [NM_-000757]	0,00038681	2,9860358	up
A_22_P00017060	ADAM8	Homo sapiens ADAM metallopeptidase domain 8 (ADAM8), transcript variant 2, mRNA [NM_001164489]	0,020642113	2,8787022	up
A_33_P3386344	FANCA	Homo sapiens FA complementation group A (FANCA), transcript variant 2, mRNA [NM_001018112]	0,014179152	-2,806199	down
A_23_P206806	ITGAL	Homo sapiens integrin subunit alpha L (ITGAL), transcript variant 2, mRNA [NM_-001114380]	0,008311856	-2,7339065	down
A_23_P79518	IL1B	interleukin 1 beta [Source:HGNC Symbol	0,024047045	-2,634447	down
A_23_P215154	NUB1	Homo sapiens negative regulator of ubiquitin like proteins 1 (NUB1), transcript variant 2, mRNA [NM_016118]	0,00037369	2,62225	up
A_23_P98350	BIRC3	Homo sapiens baculoviral IAP repeat containing 3 (BIRC3), transcript variant 1, mRNA [NM_001165]	0,001283947	2,6072829	up
A_33_P3345816	GPER1	Homo sapiens G protein-coupled estrogen receptor 1 (GPER1), transcript variant 4, mRNA [NM_001098201]	0,009918676	-2,5682487	down
A_23_P345692	IL17D	Homo sapiens interleukin 17D (IL17D), mRNA [NM_138284]	0,011917195	-2,544772	down
A_33_P3281795	MGLL	Homo sapiens monoglyceride lipase (MGLL), transcript variant 1, mRNA [NM_007283]	0,000327424	-2,5382667	down

A_24_P68783	IL36RN	Homo sapiens interleukin 36 receptor antagonist (IL36RN), transcript variant 1, mRNA [NM_012275]	0,007538324	2,5263507	up
A_23_P404162	HDAC9	Homo sapiens histone deacetylase 9 (HDAC9), transcript variant 3, mRNA [NM_-014707]	0,002268475	2,5246727	up
A_22_P00021230	IL36RN	interleukin 36 receptor antagonist [Source:HGNC Symbol	0,031609494	2,4939656	up
A_33_P3389230	CXCR3	Homo sapiens C-X-C motif chemokine receptor 3 (CXCR3), transcript variant 1, mRNA [NM_001504]	0,003813015	2,4857717	up
A_33_P3220047	AKNA	Homo sapiens AT-hook transcription factor (AKNA), transcript variant 1, mRNA [NM_-001317950]	0,035616882	-2,4783955	down
A_23_P25735	PSMA6	Homo sapiens proteasome subunit alpha 6 (PSMA6), transcript variant 2, mRNA [NM_001282232]	0,001550683	2,4721665	up
A_33_P3212269	MAP2K3	mitogen-activated protein kinase kinase 3 [Source:HGNC Symbol	0,00210191	2,4267726	up
A_23_P431939	MR1	Homo sapiens major histocompatibility complex, class I-related (MR1), transcript variant 1, mRNA [NM_001531]	0,001144106	2,404837	up
A_33_P3340769	ADAM9	Homo sapiens ADAM metallopeptidase domain 9 (ADAM9), transcript variant 1, mRNA [NM_003816]	0,025171267	-2,38035	down
A_24_P208567	IL18R1	Homo sapiens interleukin 18 receptor 1 (IL18R1), transcript variant 1, mRNA [NM_-003855]	0,004447163	2,3667467	up

A_24_P85775	THEMIS2	Homo sapiens thymocyte selection associated family member 2 (THEMIS2), transcript variant 2, mRNA [NM_001039477]	0,001319759	2,3551033	up
A_24_P931443	GPR68	Homo sapiens G protein-coupled receptor 68 (GPR68), transcript variant 2, mRNA [NM_003485]	0,03503757	2,3536656	up
A_22_P00011370	P2RX7	Homo sapiens purinergic receptor P2X 7 (P2RX7), transcript variant 1, mRNA [NM_-002562]	0,04160483	2,3516254	up
A_24_P124992	PSMA4	Homo sapiens proteasome subunit alpha 4 (PSMA4), transcript variant 1, mRNA [NM_002789]	0,001734884	2,3435202	up
A_33_P3377151	CCL19	Homo sapiens C-C motif chemokine ligand 19 (CCL19), mRNA [NM_006274]	0,019198181	-2,3171344	down
A_33_P3449417	KARS1	Homo sapiens lysyl-tRNA synthetase (KARS), transcript variant 1, mRNA [NM_-001130089]	0,000815037	2,2740479	up
A_23_P74928	MR1	Homo sapiens major histocompatibility complex, class I-related (MR1), transcript variant 1, mRNA [NM_001531]	0,001736929	2,2735746	up
A_23_P112103	GSDMD	Homo sapiens gasdermin D (GSDMD), transcript variant 1, mRNA [NM_024736]	0,006454958	2,2219229	up
A_24_P129277	NOD1	Homo sapiens nucleotide binding oligomerization domain containing 1 (NOD1), transcript variant 1, mRNA [NM_006092]	0,004076653	2,1840794	up
A_23_P140057	TNFRSF19	Homo sapiens TNF receptor superfamily member 19 (TNFRSF19), transcript variant 1, mRNA [NM_018647]	0,015979132	-2,173614	down
A_24_P365515	FOXA2	Homo sapiens forkhead box A2 (FOXA2), transcript variant 1, mRNA [NM_021784]	0,045509275	-2,1646988	down

A_33_P3305250	PSMD5	proteasome 26S subunit, non-ATPase 5 [Source:HGNC Symbol	0,011404317	-2,120684	down
A_23_P8640	GPER1	Homo sapiens G protein-coupled estrogen receptor 1 (GPER1), transcript variant 3, mRNA [NM_001039966]	0,025177816	-2,110781	down
A_23_P86216	PSMA5	Homo sapiens proteasome subunit alpha 5 (PSMA5), transcript variant 1, mRNA [NM_002790]	0,000838575	2,1024075	up
A_23_P38537	KRT16	Homo sapiens keratin 16 (KRT16), mRNA [NM_005557]	0,014245483	2,0985556	up
A_23_P5654	IL37	Homo sapiens interleukin 37 (IL37), transcript variant 1, mRNA [NM_014439]	0,003557975	2,0948572	up
A_21_P0011535	LGALS9	galectin 9 [Source:HGNC Symbol	0,012899702	2,085774	up
A_23_P35912	CASP4	Homo sapiens caspase 4 (CASP4), transcript variant gamma, mRNA [NM_033306]	0,000935926	2,0759	up
A_23_P145114	GCLC	Homo sapiens glutamate-cysteine ligase catalytic subunit (GCLC), transcript variant 1, mRNA [NM_001498]	0,006355812	-2,0442913	down
A_23_P17053	IL36G	Homo sapiens interleukin 36 gamma (IL36G), transcript variant 1, mRNA [NM_-019618]	0,023416465	2,0345707	up
A_33_P3246833	IL1RN	Homo sapiens interleukin 1 receptor antagonist (IL1RN), transcript variant 5, mRNA [NM_001318914]	0,034363665	2,0188189	up
A_24_P148590	TACR1	Homo sapiens tachykinin receptor 1 (TACR1), transcript variant short, mRNA [NM_-015727]	0,040829606	1,9891534	up
A_23_P345591	PSMA2	Homo sapiens proteasome subunit alpha 2 (PSMA2), mRNA [NM_002787]	0,00157845	1,9888229	up

A_33_P3257808	FANCD2	Homo sapiens FA complementation group D2 (FANCD2), transcript variant 3, mRNA [NM_001319984]	0,015523681	-1,9817924	down
A_33_P3420416	LGALS9	Homo sapiens galectin 9 (LGALS9), transcript variant 4, mRNA [NM_001330163]	0,024612641	1,9764395	up
A_24_P374516	TMSB4X	Homo sapiens thymosin beta 4 X-linked (TMSB4X), mRNA [NM_021109]	0,038309123	1,9721245	up
A_24_P63380	BMPR1B	Homo sapiens bone morphogenetic protein receptor type 1B (BMPR1B), transcript variant 2, mRNA [NM_001203]	0,002745935	-1,9677395	down
A_23_P116557	LGALS9	Homo sapiens galectin 9 (LGALS9), transcript variant 1, mRNA [NM_009587]	0,0431296	1,9665238	up
A_33_P3296479	APP	Homo sapiens amyloid beta precursor protein (APP), transcript variant 10, mRNA [NM_001204303]	0,01703547	-1,9594611	down
A_24_P143189	TMSB4X	Homo sapiens thymosin beta 4 X-linked (TMSB4X), mRNA [NM_021109]	0,03667876	1,9491819	up
A_23_P255869	PLGRKT	Homo sapiens plasminogen receptor with a C-terminal lysine (PLGRKT), mRNA [NM_018465]	0,002600098	1,9391998	up
A_33_P3284266	CXCL6	C-X-C motif chemokine ligand 6 [Source:HGNC Symbol	0,038325097	1,9249294	up
A_33_P3273623	CCL21	Homo sapiens C-C motif chemokine ligand 21 (CCL21), mRNA [NM_002989]	0,043104846	1,9102566	up
A_23_P79931	ATRN	Homo sapiens attractin (ATRN), transcript variant 2, mRNA [NM_139322]	0,00781446	-1,8783094	down
A_23_P49338	TNFRSF12A	Homo sapiens TNF receptor superfamily member 12A (TNFRSF12A), mRNA [NM_-016639]	0,042900596	1,8580667	up

A_23_P56734	HNMT	Homo sapiens histamine N-methyltransferase (HNMT), transcript variant 1, mRNA [NM_006895]	0,025138726	1,8193911	up
A_33_P3315223	HNRNPA0	heterogeneous nuclear ribonucleoprotein A0 [Source:HGNC Symbol	0,024649033	-1,8089725	down
A_33_P3234899	PSMB3	Homo sapiens proteasome subunit beta 3 (PSMB3), transcript variant 1, mRNA [NM_002795]	0,007257387	1,8073184	up
A_33_P3211666	IL18R1	Homo sapiens interleukin 18 receptor 1 (IL18R1), transcript variant 1, mRNA [NM_003855]	0,023021286	1,7707065	up
A_24_P303193	HNRNPA0	heterogeneous nuclear ribonucleoprotein A0 [Source:HGNC Symbol	0,04115043	-1,7580686	down
A_23_P160025	IFI16	Homo sapiens interferon gamma inducible protein 16 (IFI16), transcript variant 2, mRNA [NM_005531]	0,02293824	1,7516944	up
A_24_P382187	IGFBP4	Homo sapiens insulin like growth factor binding protein 4 (IGFBP4), mRNA [NM_001552]	0,04698618	1,7498615	up
A_23_P85903	TLR5	Homo sapiens toll like receptor 5 (TLR5), mRNA [NM_003268]	0,011233333	-1,7423688	down
A_23_P151791	LTB4R	Homo sapiens leukotriene B4 receptor (LTB4R), transcript variant 1, mRNA [NM_181657]	0,03146344	-1,7297573	down
A_23_P156531	PSMB1	Homo sapiens proteasome subunit beta 1 (PSMB1), mRNA [NM_002793]	0,011306197	1,7266426	up
A_33_P3396010	AGER	Homo sapiens advanced glycosylation end-product specific receptor (AGER), transcript variant 9, mRNA [NM_001206966]	0,043459624	-1,7217824	down
A_23_P92499	TLR2	Homo sapiens toll like receptor 2 (TLR2), transcript variant 3, mRNA [NM_003264]	0,014233765	1,7090492	up

A_24_P233570	PSMB1	Homo sapiens proteasome subunit beta 1 (PSMB1), mRNA [NM_002793]	0,011999818	1,7039897	up
A_23_P140301	PSMA3	Homo sapiens proteasome subunit alpha 3 (PSMA3), transcript variant 1, mRNA [NM_002788]	0,009309915	1,6999574	up
A_33_P3298587	SBNO2	Homo sapiens strawberry notch homolog 2 (SBNO2), transcript variant 1, mRNA [NM_014963]	0,016086213	1,6709892	up
A_23_P362659	MYD88	Homo sapiens MYD88 innate immune signal transduction adaptor (MYD88), transcript variant 2, mRNA [NM_002468]	0,03715553	1,6694553	up
A_23_P38505	CXCL16	Homo sapiens C-X-C motif chemokine ligand 16 (CXCL16), transcript variant 1, mRNA [NM_022059]	0,011536107	1,669447	up
A_23_P206441	FANCA	Homo sapiens FA complementation group A (FANCA), transcript variant 1, mRNA [NM_000135]	0,030813394	1,6404985	up
A_33_P6822021	NFATC3	Homo sapiens nuclear factor of activated T cells 3 (NFATC3), transcript variant 1, mRNA [NM_173165]	0,025403498	-1,6387168	down
A_23_P76078	IL23A	Homo sapiens interleukin 23 subunit alpha (IL23A), mRNA [NM_016584]	0,042539258	-1,623701	down
A_22_P00007581	HDAC9	Homo sapiens histone deacetylase 9 (HDAC9), transcript variant 11, mRNA [NM_-001321868]	0,043215577	1,5761733	up
A_23_P207319	MAP3K14	Homo sapiens mitogen-activated protein kinase kinase kinase 14 (MAP3K14), mRNA [NM_003954]	0,019526359	1,5683868	up

A_33_P3351536	PTK2B	Homo sapiens protein tyrosine kinase 2 beta (PTK2B), transcript variant 3, mRNA [NM_173176]	0,043121688	1,5605838	up
A_32_P34552	POLB	Homo sapiens DNA polymerase beta (POLB), mRNA [NM_002690]	0,04704182	1,5491896	up
A_33_P3315355	SETD6	Homo sapiens SET domain containing 6, protein lysine methyltransferase (SETD6), transcript variant 1, mRNA [NM_001160305]	0,04052229	-1,5348529	down
A_33_P3351249	CXCL16	Homo sapiens C-X-C motif chemokine ligand 16 (CXCL16), transcript variant 2, mRNA [NM_001100812]	0,0339535	1,52933	up
A_23_P26629	PYCARD	Homo sapiens PYD and CARD domain containing (PYCARD), transcript variant 1, mRNA [NM_013258]	0,041182503	1,5099634	up
A_23_P212196	OGG1	Homo sapiens 8-oxoguanine DNA glycosylase (OGG1), transcript variant 2d, mRNA [NM_016828]	0,035704352	-1,5028604	down
A_23_P129358	SETD6	Homo sapiens SET domain containing 6, protein lysine methyltransferase (SETD6), transcript variant 2, mRNA [NM_024860]	0,031244267	-1,5010288	down

Table 9.7 DEGs of induced anti-inflammatory genes by IFN-α vs unstimulated

ProbeName	GeneSymbol	Description	*P*	FC	Regulation
A_23_P310931	CNR2	Homo sapiens cannabinoid receptor 2 (CNR2), mRNA [NM_001841]	0,020695198	2,7174115	up
A_24_P354715	NT5E	Homo sapiens 5'-nucleotidase ecto (NT5E), transcript variant 1, mRNA [NM_002526]	0,001752371	2,586492	up
A_23_P208747	PGLYRP1	Homo sapiens peptidoglycan recognition protein 1 (PGLYRP1), mRNA [NM_005091]	0,032002468	2,4330683	up
A_24_P335092	SAA1	Homo sapiens serum amyloid A1 (SAA1), transcript variant 1, mRNA [NM_000331]	0,005250534	2,4323487	up
A_24_P230563	IL2RA	Homo sapiens interleukin 2 receptor subunit alpha (IL2RA), transcript variant 1, mRNA [NM_000417]	0,017909938	2,3027282	up
A_24_P316430	NT5E	Homo sapiens 5'-nucleotidase ecto (NT5E), transcript variant 1, mRNA [NM_002526]	0,001220744	2,2740216	up
A_23_P7560	IL12B	Homo sapiens interleukin 12B (IL12B), mRNA [NM_002187]	0,02695442	2,272247	up
A_33_P3214035	ADORA2A	Homo sapiens adenosine A2a receptor (ADORA2A), transcript variant 3, mRNA [NM_000675]	0,011950237	2,153515	up
A_32_P56713	BCR	Homo sapiens BCR activator of RhoGEF and GTPase (BCR), transcript variant 2, mRNA [NM_021574]	0,001080787	-2,138898	down
A_33_P3276718	HGF	Homo sapiens hepatocyte growth factor (HGF), transcript variant 5, mRNA [NM_-001010934]	0,01039902	2,012407	up
A_23_P16834	FNDC4	Homo sapiens fibronectin type III domain containing 4 (FNDC4), mRNA [NM_022823]	0,04379407	-1,9903374	down

A_33_P3342056	TIGIT	Homo sapiens T cell immunoreceptor with Ig and ITIM domains (TIGIT), mRNA [NM_173799]	0,034138355	1,9860426	up
A_33_P3281695	NLRP3	Homo sapiens NLR family pyrin domain containing 3 (NLRP3), transcript variant 6, mRNA [NM_001243133]	0,04157791	1,9438491	up
A_23_P92499	TLR2	Homo sapiens toll like receptor 2 (TLR2), transcript variant 3, mRNA [NM_003264]	0,000355408	1,9401038	up
A_23_P91850	IL20RB	Homo sapiens interleukin 20 receptor subunit beta (IL20RB), mRNA [NM_144717]	0,006864349	1,870563	up
A_23_P10591	METRNL	Homo sapiens meteorin like, glial cell differentiation regulator (METRNL), transcript variant 1, mRNA [NM_001004431]	0,000795559	1,8405056	up
A_23_P50269	CXCL17	Homo sapiens C-X-C motif chemokine ligand 17 (CXCL17), transcript variant 2, non-coding RNA [NR_133910]	0,002839799	1,7802753	up
A_33_P3256680	MFHAS1	Homo sapiens malignant fibrous histiocytoma amplified sequence 1 (MFHAS1), mRNA [NM_004225]	0,043908104	-1,7727342	down
A_22_P00012743	RABGEF1	Homo sapiens RAB guanine nucleotide exchange factor 1 (RABGEF1), transcript variant 6, mRNA [NM_001367722]	0,032682903	-1,7420006	down
A_21_P0011561	METRNL	meteorin like, glial cell differentiation regulator [Source:HGNC Symbol	0,03577775	1,7260109	up
A_24_P570049	PPARA	Homo sapiens peroxisome proliferator activated receptor alpha (PPARA), transcript variant 5, mRNA [NM_005036]	0,006438012	-1,664367	down
A_24_P873764	BCR	Homo sapiens BCR activator of RhoGEF and GTPase (BCR), transcript variant 2, mRNA [NM_021574]	0,014372252	-1,6557877	down

A_24_P298360	LTBP3	Homo sapiens latent transforming growth factor beta binding protein 3 (LTBP3), transcript variant 2, mRNA [NM_021070]	0,02554592	-1,6209756	down
A_32_P62997	PBK	Homo sapiens PDZ binding kinase (PBK), transcript variant 1, mRNA [NM_018492]	0,032753147	-1,6148638	down
A_23_P210708	SIRPA	Homo sapiens signal regulatory protein alpha (SIRPA), transcript variant 1, mRNA [NM_001040022]	0,01673893	-1,6048037	down
A_23_P142075	ACP5	Homo sapiens acid phosphatase 5, tartrate resistant (ACP5), transcript variant 4, mRNA [NM_001611]	0,006238819	1,5837917	up

Table 9.8 DEGs of induced anti-inflammatory genes by IFN-λ1 vs unstimulated

ProbeName	GeneSymbol	Description	*P*	FC	Regulation
A_24_P69538	TLR4	Homo sapiens toll like receptor 4 (TLR4), transcript variant 1, mRNA [NM_138554]	0,038194634	2,25009	up
A_23_P25396	NR1H4	Homo sapiens nuclear receptor subfamily 1 group H member 4 (NR1H4), transcript variant 2, mRNA [NM_005123]	0,017005643	2,2484636	up
A_33_P3350580	PRKCD	Homo sapiens cDNA FLJ16784 fis, clone CTONG2003764. [AK131548]	0,03758012	2,1491466	up
A_33_P3256680	MFHAS1	Homo sapiens malignant fibrous histiocytoma amplified sequence 1 (MFHAS1), mRNA [NM_004225]	0,036175005	-2,0786572	down
A_33_P3248424	OTULIN	OTU deubiquitinase with linear linkage specificity [Source:HGNC Symbol	0,009007866	-1,9583899	down
A_24_P316430	NT5E	Homo sapiens 5'-nucleotidase ecto (NT5E), transcript variant 1, mRNA [NM_002526]	0,041561972	1,75137	up
A_24_P270769	VPS35	VPS35 retromer complex component [Source:HGNC Symbol	0,049821902	-1,5149858	down

Table 9.9 DEGs of induced anti-inflammatory genes by IFN-λ3 vs unstimulated

ProbeName	GeneSymbol	Description	*P*	FC	Regulation
A_33_P3379396	KRT1	Homo sapiens keratin 1 (KRT1), mRNA [NM_006121]	0,000400509	8,678053	up
A_33_P3422124	IL22RA2	Homo sapiens interleukin 22 receptor subunit alpha 2 (IL22RA2), transcript variant 3, mRNA [NM_181310]	0,004522891	3,3944147	up
A_23_P340019	NLRC3	Homo sapiens NLR family CARD domain containing 3 (NLRC3), transcript variant 1, mRNA [NM_178844]	0,019060135	2,387349	up
A_22_P00012743	RABGEF1	Homo sapiens RAB guanine nucleotide exchange factor 1 (RABGEF1), transcript variant 6, mRNA [NM_001367722]	0,011475356	-2,1470838	down
A_23_P126735	IL10	Homo sapiens interleukin 10 (IL10), mRNA [NM_000572]	0,02497826	1,8939157	up
A_23_P40096	PROC	Homo sapiens protein C, inactivator of coagulation factors Va and VIIIa (PROC), mRNA [NM_000312]	0,04767192	-1,772308	down

Table 9.10 DEGs of induced anti-inflammatory genes by IFN-γ vs unstimulated

ProbeName	GeneSymbol	Description	*P*	FC	Regulation
A_23_P82929	CCN3	Homo sapiens cellular communication network factor 3 (CCN3), mRNA [NM_002514]	0,000345827	-3,9689677	down
A_32_P62997	PBK	Homo sapiens PDZ binding kinase (PBK), transcript variant 1, mRNA [NM_018492]	0,000341482	-3,7252283	down
A_33_P3261957	CALCRL	Homo sapiens calcitonin receptor like receptor (CALCRL), transcript variant 3, mRNA [NM_001369434]	0,000727782	3,6279497	up
A_23_P142075	ACP5	Homo sapiens acid phosphatase 5, tartrate resistant (ACP5), transcript variant 4, mRNA [NM_001611]	3,94115E-05	3,5327504	up
A_23_P165624	TNFAIP6	Homo sapiens TNF alpha induced protein 6 (TNFAIP6), mRNA [NM_007115]	0,007945028	3,1728618	up
A_24_P335092	SAA1	Homo sapiens serum amyloid A1 (SAA1), transcript variant 1, mRNA [NM_000331]	0,001850259	2,9647121	up
A_33_P3306110	CALCRL	Homo sapiens calcitonin receptor like receptor (CALCRL), transcript variant 3, mRNA [NM_001369434]	0,000207679	2,8930366	up
A_33_P3306103	CALCRL	Homo sapiens calcitonin receptor like receptor (CALCRL), transcript variant 3, mRNA [NM_001369434]	6,06647E-05	2,7059715	up
A_24_P12397	TREM2	Homo sapiens triggering receptor expressed on myeloid cells 2 (TREM2), transcript variant 1, mRNA [NM_018965]	0,002985847	-2,6999655	down
A_33_P3345816	GPER1	Homo sapiens G protein-coupled estrogen receptor 1 (GPER1), transcript variant 4, mRNA [NM_001098201]	0,009918676	-2,5682487	down

A_33_P3221783	TSLP	Homo sapiens thymic stromal lymphopoietin (TSLP), transcript variant 2, mRNA [NM_138551]	0,024770781	-2,4019368	down
A_33_P3379922	PROC	Homo sapiens protein C, inactivator of coagulation factors Va and VIIIa (PROC), mRNA [NM_000312]	0,003799794	-2,279098	down
A_23_P54517	TYRO3	Homo sapiens TYRO3 protein tyrosine kinase (TYRO3), transcript variant 1, mRNA [NM_006293]	0,002680668	-2,1884816	down
A_33_P3221084	LTBP3	latent transforming growth factor beta binding protein 3 [Source:HGNC Symbol	0,024178812	2,115041	up
A_23_P8640	GPER1	Homo sapiens G protein-coupled estrogen receptor 1 (GPER1), transcript variant 3, mRNA [NM_001039966]	0,025177816	-2,110781	down
A_23_P40096	PROC	Homo sapiens protein C, inactivator of coagulation factors Va and VIIIa (PROC), mRNA [NM_000312]	0,009713679	-2,0496974	down
A_23_P10591	METRNL	Homo sapiens meteorin like, glial cell differentiation regulator (METRNL), transcript variant 1, mRNA [NM_001004431]	0,000907809	1,95971	up
A_21_P0011561	METRNL	meteorin like, glial cell differentiation regulator [Source:HGNC Symbol	0,015386188	1,9228963	up
A_23_P374695	TEK	Homo sapiens TEK receptor tyrosine kinase (TEK), transcript variant 1, mRNA [NM_-000459]	0,038886894	1,9143898	up
A_33_P3251289	SELENOS	Homo sapiens selenoprotein S (SELENOS), transcript variant 1, mRNA [NM_018445]	0,010541717	1,9017389	up
A_23_P309701	PTPN2	Homo sapiens protein tyrosine phosphatase non-receptor type 2 (PTPN2), transcript variant 1, mRNA [NM_002828]	0,008183401	1,8314859	up

A_32_P56713	BCR	Homo sapiens BCR activator of RhoGEF and GTPase (BCR), transcript variant 2, mRNA [NM_021574]	0,022265507	-1,74745	down
A_23_P92499	TLR2	Homo sapiens toll like receptor 2 (TLR2), transcript variant 3, mRNA [NM_003264]	0,014233765	1,7090492	up
A_32_P1445	PTPN2	Homo sapiens protein tyrosine phosphatase non-receptor type 2 (PTPN2), transcript variant 3, mRNA [NM_080423]	0,0219227	1,6922449	up
A_24_P873764	BCR	Homo sapiens BCR activator of RhoGEF and GTPase (BCR), transcript variant 2, mRNA [NM_021574]	0,03667709	-1,6624783	down
A_23_P207940	PTPN2	Homo sapiens cDNA FLJ34206 fis, clone FCBBF3020140. [AK091525]	0,013064526	1,6621469	up
A_23_P76078	IL23A	Homo sapiens interleukin 23 subunit alpha (IL23A), mRNA [NM_016584]	0,042539258	-1,623701	down
A_32_P75792	C1QTNF12	C1q and TNF related 12 [Source:HGNC Symbol	0,018296337	-1,6161492	down
A_23_P210708	SIRPA	Homo sapiens signal regulatory protein alpha (SIRPA), transcript variant 1, mRNA [NM_001040022]	0,03964822	-1,603094	down
A_24_P244356	NLRX1	Homo sapiens NLR family member X1 (NLRX1), transcript variant 4, mRNA [NM_-001282144]	0,027841514	-1,5496584	down

Table 9.11 DEGs of induced epithelial genes by IFN-α vs unstimulated

ProbeName	GeneSymbol	Description	*P*	FC	Regulation
A_23_P16953	HTR2B	Homo sapiens 5-hydroxytryptamine receptor 2B (HTR2B), transcript variant 1, mRNA [NM_000867]	2,02096E-07	13,197263	up
A_23_P151851	DUOX2	Homo sapiens dual oxidase 2 (DUOX2), transcript variant 1, mRNA [NM_014080]	1,43783E-06	9,35765	up
A_23_P47924	PTPRR	Homo sapiens protein tyrosine phosphatase receptor type R (PTPRR), transcript variant 1, mRNA [NM_002849]	4,05739E-06	8,68389	up
A_21_P0014047	C4A	Homo sapiens complement C4A (Rodgers blood group) (C4A), transcript variant 2, mRNA [NM_001252204]	3,27689E-06	7,351184	up
A_23_P153745	IFI30	Homo sapiens IFI30 lysosomal thiol reductase (IFI30), mRNA [NM_006332]	1,4793E-05	7,168854	up
A_23_P42282	C4B	Homo sapiens complement C4B (Chido blood group) (C4B), mRNA [NM_001002029]	6,28644E-06	6,932004	up
A_24_P382319	CEACAM1	Homo sapiens carcinoembryonic antigen related cell adhesion molecule 1 (CEACAM1), transcript variant 1, mRNA [NM_001712]	1,77756E-05	4,755657	up
A_23_P152655	ICAM2	Homo sapiens intercellular adhesion molecule 2 (ICAM2), transcript variant 5, mRNA [NM_000873]	0,000108417	4,5493717	up
A_23_P115202	CRNN	cornulin [Source:HGNC Symbol	0,036430575	4,481076	up
A_23_P147786	RIMS2	Homo sapiens regulating synaptic membrane exocytosis 2 (RIMS2), transcript variant 2, mRNA [NM_014677]	2,22937E-06	3,8030539	up

A_33_P3408624	IQSEC3	Homo sapiens IQ motif and Sec7 domain 3 (IQSEC3), transcript variant 2, mRNA [NM_015232]	0,003256981	3,325152	up
A_33_P3367850	CHRM4	Homo sapiens cholinergic receptor muscarinic 4 (CHRM4), transcript variant 1, mRNA [NM_000741]	0,041537873	3,2524173	up
A_33_P3825869	CACNA1C	Homo sapiens calcium voltage-gated channel subunit alpha1 C (CACNA1C), transcript variant 1, mRNA [NM_199460]	0,001449274	3,2016602	up
A_32_P136351	SLITRK1	Homo sapiens SLIT and NTRK like family member 1 (SLITRK1), transcript variant 1, mRNA [NM_052910]	0,004846327	3,1475966	up
A_32_P229618	DLG2	Homo sapiens discs large MAGUK scaffold protein 2 (DLG2), transcript variant 2, mRNA [NM_001364]	0,003732252	3,0816195	up
A_33_P3282434	SLC16A1	Homo sapiens solute carrier family 16 member 1 (SLC16A1), transcript variant 2, mRNA [NM_001166496]	9,59744E-05	3,0270991	up
A_33_P3252800	PTPRR	Homo sapiens protein tyrosine phosphatase receptor type R (PTPRR), transcript variant 1, mRNA [NM_002849]	0,003773606	2,9203553	up
A_23_P419503	LRRC4B	Homo sapiens leucine rich repeat containing 4B (LRRC4B), transcript variant 2, mRNA [NM_001080457]	0,009228257	2,9009905	up
A_33_P3297580	CACNA1C	Homo sapiens calcium voltage-gated channel subunit alpha1 C (CACNA1C), transcript variant 1, mRNA [NM_199460]	0,008888299	2,832938	up
A_23_P38864	RABAC1	Homo sapiens Rab acceptor 1 (RABAC1), mRNA [NM_006423]	7,18741E-06	2,8304977	up

A_33_P3319780	PRR7	PREDICTED: Homo sapiens proline rich 7, synaptic (PRR7), transcript variant X1, mRNA [XM_017009896]	0,015716175	2,748395	up
A_33_P3422429	PATJ	PATJ crumbs cell polarity complex component [Source:HGNC Symbol	0,000977395	2,7343943	up
A_33_P3385516	CBLN4	cerebellin 4 precursor [Source:HGNC Symbol	0,04163966	2,688893	up
A_23_P24294	SLC17A6	solute carrier family 17 member 6 [Source:HGNC Symbol	0,001279771	2,6347058	up
A_23_P69617	UNC5C	Homo sapiens unc-5 netrin receptor C (UNC5C), mRNA [NM_003728]	0,03876637	2,631534	up
A_23_P328545	GABRP	Homo sapiens gamma-aminobutyric acid type A receptor pi subunit (GABRP), transcript variant 1, mRNA [NM_014211]	0,003951865	2,6044252	up
A_24_P367410	GABRQ	Homo sapiens gamma-aminobutyric acid type A receptor theta subunit (GABRQ), mRNA [NM_018558]	0,007923308	2,5558465	up
A_33_P3229402	PECAM1	Homo sapiens platelet and endothelial cell adhesion molecule 1 (PECAM1), mRNA [NM_000442]	0,002371973	2,540876	up
A_33_P3268507	CEACAM1	Homo sapiens carcinoembryonic antigen related cell adhesion molecule 1 (CEACAM1), transcript variant 5, mRNA [NM_001184816]	0,002318915	2,5084546	up
A_33_P3405213	PECAM1	Homo sapiens platelet and endothelial cell adhesion molecule 1 (PECAM1), mRNA [NM_000442]	0,001487158	2,5043247	up
A_23_P371215	ICOS	Homo sapiens inducible T cell costimulator (ICOS), mRNA [NM_012092]	0,016584452	2,4934223	up
A_21_P0011917	NRXN1	neurexin 1 [Source:HGNC Symbol	0,03401831	2,4929724	up

A_33_P3358277	KCNK1	potassium two pore domain channel subfamily K member 1 [Source:HGNC Symbol	0,03602107	2,4905782	up
A_24_P393740	FYB1	Homo sapiens FYN binding protein 1 (FYB1), transcript variant 1, mRNA [NM_001465]	0,011118893	2,4754403	up
A_33_P3306624	HCRT	Homo sapiens hypocretin neuropeptide precursor (HCRT), mRNA [NM_001524]	0,04921506	2,451905	up
A_23_P144656	CDH10	Homo sapiens cadherin 10 (CDH10), transcript variant 1, mRNA [NM_006727]	0,046031546	2,405247	up
A_24_P247902	PCLO	Homo sapiens piccolo presynaptic cytomatrix protein (PCLO), transcript variant 2, mRNA [NM_014510]	0,00013701	2,4011607	up
A_33_P3327462	TMEM108	Homo sapiens transmembrane protein 108 (TMEM108), transcript variant 1, mRNA [NM_023943]	0,007653059	2,3834798	up
A_33_P3249976	JAM2	Homo sapiens junctional adhesion molecule 2 (JAM2), transcript variant 1, mRNA [NM_021219]	0,04309566	2,3745139	up
A_33_P3224730	HMCN2	Homo sapiens hemicentin 2 (HMCN2), mRNA [NM_001291815]	0,000876825	2,3610966	up
A_23_P93105	GABRR2	gamma-aminobutyric acid type A receptor rho2 subunit [Source:HGNC Symbol	0,02632793	2,357735	up
A_33_P3235546	RIMS3	Homo sapiens regulating synaptic membrane exocytosis 3 (RIMS3), mRNA [NM_-014747]	0,018352723	2,3392847	up
A_23_P157136	SCIN	Homo sapiens scinderin (SCIN), transcript variant 2, mRNA [NM_033128]	0,000264441	2,3326666	up
A_23_P121480	CD200	Homo sapiens CD200 molecule (CD200), transcript variant 2, mRNA [NM_001004196]	0,003997323	2,2984977	up
A_23_P25503	FNDC3A	Homo sapiens fibronectin type III domain containing 3A (FNDC3A), transcript variant 1, mRNA [NM_001079673]	9,435E-05	2,275111	up

A_23_P125475	GABRQ	Homo sapiens gamma-aminobutyric acid type A receptor theta subunit (GABRQ), mRNA [NM_018558]	0,01856621	2,239265	up
A_23_P252471	PECAM1	Homo sapiens platelet and endothelial cell adhesion molecule 1 (PECAM1), mRNA [NM_000442]	0,026797134	2,2160754	up
A_32_P38645	RIMS4	Homo sapiens regulating synaptic membrane exocytosis 4 (RIMS4), transcript variant 2, mRNA [NM_182970]	0,047630493	2,2005455	up
A_21_P0013605	HMCN2	Homo sapiens hemicentin 2 (HMCN2), mRNA [NM_001291815]	0,02176924	2,191762	up
A_23_P29735	BSN	Homo sapiens bassoon presynaptic cytomatrix protein (BSN), mRNA [NM_003458]	0,049651872	2,1853948	up
A_22_P00024620	CBLL1	Cbl proto-oncogene like 1 [Source:HGNC Symbol	0,048574686	2,1598232	up
A_24_P383523	SAMD4A	Homo sapiens sterile alpha motif domain containing 4A (SAMD4A), transcript variant 1, mRNA [NM_015589]	0,001341247	2,1585908	up
A_23_P355405	CNTNAP4	Homo sapiens contactin associated protein like 4 (CNTNAP4), transcript variant 2, mRNA [NM_138994]	0,026452623	2,148469	up
A_23_P69326	CADPS	Homo sapiens calcium dependent secretion activator (CADPS), transcript variant 3, mRNA [NM_183393]	0,04503907	2,1223836	up
A_33_P3268652	SLC2A11	solute carrier family 2 member 11 [Source:HGNC Symbol	0,04760468	2,1197686	up
A_23_P350396	CDSN	Homo sapiens corneodesmosin (CDSN), mRNA [NM_001264]	0,042261582	2,1174784	up
A_33_P3326217	SHISA6	Homo sapiens shisa family member 6 (SHISA6), transcript variant 3, mRNA [NM_-001173462]	0,046768628	2,1172318	up

A_33_P3325195	IGSF9B	Homo sapiens mRNA for KIAA1030 protein, partial cds. [AB028953]	0,023117764	2,069952	up
A_33_P3226212	JAM2	Homo sapiens junctional adhesion molecule 2 (JAM2), transcript variant 3, mRNA [NM_001270408]	0,018696897	2,0508552	up
A_23_P103617	ANXA9	Homo sapiens annexin A9 (ANXA9), mRNA [NM_003568]	0,031807065	2,027385	up
A_33_P3403162	SLC18A1	Homo sapiens solute carrier family 18 member A1 (SLC18A1), transcript variant 4, mRNA [NM_001142325]	0,012831293	2,0101283	up
A_23_P18649	FAT4	Homo sapiens FAT atypical cadherin 4 (FAT4), transcript variant 1, mRNA [NM_001291303]	0,024237862	2,004799	up
A_22_P00023596	SCIN	Homo sapiens scinderin (SCIN), transcript variant 1, mRNA [NM_001112706]	0,003305362	1,9935211	up
A_33_P3375934	NAMPT	Homo sapiens nicotinamide phosphoribosyltransferase (NAMPT), mRNA [NM_005746]	0,001851261	1,9805418	up
A_23_P303072	GRIA1	Homo sapiens glutamate ionotropic receptor AMPA type subunit 1 (GRIA1), transcript variant 1, mRNA [NM_000827]	0,03351405	1,9792185	up
A_32_P213091	SHISA9	Homo sapiens shisa family member 9 (SHISA9), transcript variant 2, mRNA [NM_001145205]	0,014565554	1,9628971	up
A_21_P0013530	DLGAP2	DLG associated protein 2 [Source:HGNC Symbol	0,046536695	1,9577016	up
A_23_P251443	CHRNA2	Homo sapiens cholinergic receptor nicotinic alpha 2 subunit (CHRNA2), transcript variant 1, mRNA [NM_000742]	0,04755382	1,9092913	up
A_33_P3343573	ABHD17A	abhydrolase domain containing 17A [Source:HGNC Symbol	0,038490225	1,8963628	up

A_33_P3298236	DCHS2	Homo sapiens dachsous cadherin-related 2 (DCHS2), transcript variant 2, mRNA [NM_001142552]	0,03520925	1,8602808	up
A_33_P3217958	FCHSD2	Homo sapiens FCH and double SH3 domains 2 (FCHSD2), mRNA [NM_014824]	0,017855275	1,8194655	up
A_33_P3256391	CRB3	Homo sapiens crumbs cell polarity complex component 3 (CRB3), transcript variant 2, mRNA [NM_139161]	0,01240011	1,7772262	up
A_24_P93967	FMR1	Homo sapiens fragile X mental retardation 1 (FMR1), transcript variant ISO1, mRNA [NM_002024]	0,005716689	1,7701721	up
A_23_P117873	CHRM5	Homo sapiens cholinergic receptor muscarinic 5 (CHRM5), transcript variant 1, mRNA [NM_012125]	0,013035508	1,7535472	up
A_24_P302038	FCHSD2	Homo sapiens FCH and double SH3 domains 2 (FCHSD2), mRNA [NM_014824]	0,03811136	1,7415032	up
A_22_P00000867	AGRN	Homo sapiens agrin (AGRN), transcript variant 1, mRNA [NM_001305275]	0,017270334	1,6798437	up
A_23_P329924	HCAR2	hydroxycarboxylic acid receptor 2 [Source:HGNC Symbol	0,03925321	1,6451162	up
A_23_P64721	HCAR3	hydroxycarboxylic acid receptor 3 [Source:HGNC Symbol	0,008837241	1,6434819	up
A_21_P0000050	DISC1	Homo sapiens DISC1 scaffold protein (DISC1), transcript variant l, mRNA [NM_-001164549]	0,04909253	1,6172572	up
A_24_P300777	ADAM8	Homo sapiens ADAM metallopeptidase domain 8 (ADAM8), transcript variant 1, mRNA [NM_001109]	0,012732982	1,5954155	up
A_24_P161581	SHISA7	Homo sapiens shisa family member 7 (SHISA7), mRNA [NM_001145176]	0,02287945	1,546184	up

A_23_P207106	CHRNB1	Homo sapiens cholinergic receptor nicotinic beta 1 subunit (CHRNB1), mRNA [NM_-000747]	0,018915111	1,5080807	up
A_24_P49214	FAAP20	Homo sapiens FA core complex associated protein 20 (FAAP20), transcript variant 7, mRNA [NM_001282671]	0,009053144	-1,5184857	down
A_23_P132378	CELSR1	Homo sapiens cadherin EGF LAG seven-pass G-type receptor 1 (CELSR1), mRNA [NM_014246]	0,015286986	-1,5262862	down
A_23_P304237	RAPGEF1	Homo sapiens Rap guanine nucleotide exchange factor 1 (RAPGEF1), transcript variant 2, mRNA [NM_198679]	0,023573574	-1,5267081	down
A_24_P194881	SHANK3	Homo sapiens SH3 and multiple ankyrin repeat domains 3 (SHANK3), mRNA [NM_-033517]	0,041468877	-1,5324118	down
A_33_P3377364	ITGB4	Homo sapiens integrin subunit beta 4 (ITGB4), transcript variant 1, mRNA [NM_-000213]	0,01761668	-1,5418597	down
A_33_P3374623	ABCA7	Homo sapiens ATP binding cassette subfamily A member 7 (ABCA7), mRNA [NM_-019112]	0,046025183	-1,5446049	down
A_32_P203515	SPECC1L	Homo sapiens sperm antigen with calponin homology and coiled-coil domains 1 like (SPECC1L), transcript variant 1, mRNA [NM_015330]	0,04985169	-1,573786	down
A_23_P32064	NSMF	Homo sapiens NMDA receptor synaptonuclear signaling and neuronal migration factor (NSMF), transcript variant 2, mRNA [NM_015537]	0,017526977	-1,597004	down
A_24_P88801	NPHP1	Homo sapiens nephrocystin 1 (NPHP1), transcript variant 1, mRNA [NM_000272]	0,009732878	-1,5990181	down

A_33_P3294509	CD44	Homo sapiens CD44 molecule (Indian blood group) (CD44), transcript variant 1, mRNA [NM_000610]	0,015903288	-1,6232344	down
A_32_P24585	SH3PXD2B	Homo sapiens SH3 and PX domains 2B (SH3PXD2B), transcript variant 1, mRNA [NM_001017995]	0,035893872	-1,6520928	down
A_24_P873764	BCR	Homo sapiens BCR activator of RhoGEF and GTPase (BCR), transcript variant 2, mRNA [NM_021574]	0,014372252	-1,6557877	down
A_24_P521994	KLHL24	Homo sapiens kelch like family member 24 (KLHL24), transcript variant 7, mRNA [NM_017644]	0,011069566	-1,6618909	down
A_23_P83110	CDK5RAP2	Homo sapiens CDK5 regulatory subunit associated protein 2 (CDK5RAP2), transcript variant 1, mRNA [NM_018249]	0,008425127	-1,671736	down
A_33_P3307735	OPHN1	Homo sapiens oligophrenin 1 (OPHN1), mRNA [NM_002547]	0,02789738	-1,6752161	down
A_24_P219971	GID8	Homo sapiens GID complex subunit 8 homolog (GID8), mRNA [NM_017896]	0,007397271	-1,67878	down
A_23_P334883	SHANK2	Homo sapiens SH3 and multiple ankyrin repeat domains 2 (SHANK2), transcript variant 1, mRNA [NM_012309]	0,030072745	-1,6927005	down
A_23_P394043	CAMSAP3	Homo sapiens calmodulin regulated spectrin associated protein family member 3 (CAMSAP3), transcript variant 1, mRNA [NM_001080429]	0,033234052	-1,6985283	down
A_33_P3328653	CELSR1	Homo sapiens cadherin EGF LAG seven-pass G-type receptor 1 (CELSR1), mRNA [NM_014246]	0,031352125	-1,700774	down
A_33_P3360426	WDR1	Homo sapiens WD repeat domain 1 (WDR1), transcript variant 1, mRNA [NM_017491]	0,04720626	-1,7008975	down

A_23_P99906	HOMER2	Homo sapiens homer scaffold protein 2 (HOMER2), transcript variant 2, mRNA [NM_-199330]	0,010365476	-1,7110559	down
A_23_P251705	ARHGEF9	Homo sapiens Cdc42 guanine nucleotide exchange factor 9 (ARHGEF9), transcript variant 1, mRNA [NM_015185]	0,011367738	-1,7202693	down
A_23_P16992	PKP4	Homo sapiens plakophilin 4 (PKP4), transcript variant 1, mRNA [NM_003628]	0,005657258	-1,7289432	down
A_24_P62367	DLGAP1	Homo sapiens DLG associated protein 1 (DLGAP1), transcript variant 1, mRNA [NM_004746]	0,013313135	-1,7357167	down
A_33_P3316539	SLC7A2	Homo sapiens solute carrier family 7 member 2 (SLC7A2), transcript variant 5, mRNA [NM_001370338]	0,008445699	-1,7359629	down
A_23_P339773	TPRG1L	Homo sapiens tumor protein p63 regulated 1 like (TPRG1L), mRNA [NM_182752]	0,009281842	-1,744753	down
A_23_P319583	RIMS3	Homo sapiens regulating synaptic membrane exocytosis 3 (RIMS3), mRNA [NM_-014747]	0,024237704	-1,7538623	down
A_24_P344961	AMOT	Homo sapiens angiomotin (AMOT), transcript variant 2, mRNA [NM_133265]	0,015357045	-1,7727904	down
A_23_P152305	CDH11	Homo sapiens cadherin 11 (CDH11), transcript variant 1, mRNA [NM_001797]	0,022071829	-1,7835255	down
A_24_P18146	PSD3	Homo sapiens pleckstrin and Sec7 domain containing 3 (PSD3), transcript variant 1, mRNA [NM_015310]	0,026052002	-1,7862589	down
A_24_P323598	ESCO2	establishment of sister chromatid cohesion N-acetyltransferase 2 [Source:HGNC Symbol	0,036148425	-1,7934244	down

A_33_P3418833	FLRT3	Homo sapiens fibronectin leucine rich transmembrane protein 3 (FLRT3), transcript variant 1, mRNA [NM_013281]	0,049219824	-1,8026942	down
A_24_P193592	CCNF	Homo sapiens cyclin F (CCNF), transcript variant 1, mRNA [NM_001761]	0,035048436	-1,807897	down
A_32_P53524	NTN1	Homo sapiens netrin 1 (NTN1), mRNA [NM_004822]	0,014593937	-1,8085749	down
A_33_P3328609	PKP4	Homo sapiens plakophilin 4 (PKP4), transcript variant 1, mRNA [NM_003628]	0,04456791	-1,8167479	down
A_23_P62967	DISC1	Homo sapiens DISC1 scaffold protein (DISC1), transcript variant L, mRNA [NM_-018662]	0,008029248	-1,8590924	down
A_23_P204998	FARP1	Homo sapiens FERM, ARH/RhoGEF and pleckstrin domain protein 1 (FARP1), transcript variant 3, mRNA [NM_001286839]	0,008174776	-1,8746749	down
A_32_P126375	NHS	Homo sapiens NHS actin remodeling regulator (NHS), transcript variant 1, mRNA [NM_198270]	0,001432643	-1,8777877	down
A_23_P391926	ADGRL1	Homo sapiens adhesion G protein-coupled receptor L1 (ADGRL1), transcript variant 1, mRNA [NM_001008701]	0,016239684	-1,8952749	down
A_33_P3236993	ARVCF	Homo sapiens ARVCF delta catenin family member (ARVCF), mRNA [NM_001670]	0,024966048	-1,9110018	down
A_32_P35969	CHRNA7	Homo sapiens cholinergic receptor nicotinic alpha 7 subunit (CHRNA7), transcript variant 2, mRNA [NM_001190455]	0,001662912	-1,9131806	down
A_33_P3229552	LRFN1	Homo sapiens leucine rich repeat and fibronectin type III domain containing 1 (LRFN1), mRNA [NM_020862]	0,039154563	-1,9589579	down
A_23_P332584	KIAA1107	Homo sapiens KIAA1107 (KIAA1107), mRNA [NM_015237]	0,028381463	-1,9961752	down

A_23_P327361	DMXL2	Homo sapiens Dmx like 2 (DMXL2), transcript variant 2, mRNA [NM_015263]	0,018261088	-2,004038	down
A_24_P34534	PARD3B	Homo sapiens par-3 family cell polarity regulator beta (PARD3B), transcript variant 2, mRNA [NM_152526]	0,037223667	-2,0140564	down
A_33_P3338698	IHH	Homo sapiens Indian hedgehog signaling molecule (IHH), mRNA [NM_002181]	0,000258627	-2,0358562	down
A_24_P64126	CPNE3	Homo sapiens copine 3 (CPNE3), mRNA [NM_003909]	0,012474041	-2,066259	down
A_23_P156284	DBN1	Homo sapiens drebrin 1 (DBN1), transcript variant 2, mRNA [NM_080881]	0,000652268	-2,1251845	down
A_23_P20392	PSD3	Homo sapiens pleckstrin and Sec7 domain containing 3 (PSD3), transcript variant 1, mRNA [NM_015310]	0,005874811	-2,134802	down
A_32_P56713	BCR	Homo sapiens BCR activator of RhoGEF and GTPase (BCR), transcript variant 2, mRNA [NM_021574]	0,001080787	-2,138898	down
A_24_P37253	LYPD6	Homo sapiens LY6/PLAUR domain containing 6 (LYPD6), transcript variant 2, mRNA [NM_194317]	0,011152732	-2,188778	down
A_33_P3268304	LIMS2	Homo sapiens LIM zinc finger domain containing 2 (LIMS2), transcript variant 5, mRNA [NM_001161404]	0,007509677	-2,191964	down
A_23_P144807	SEPTIN8	Homo sapiens septin 8 (SEPTIN8), transcript variant 1, mRNA [NM_001098811]	0,000654919	-2,2239	down
A_23_P47340	DSCAML1	Homo sapiens DS cell adhesion molecule like 1 (DSCAML1), transcript variant 1, mRNA [NM_020693]	0,045390155	-2,259754	down
A_33_P3388331	FARP1	Homo sapiens FERM, ARH/RhoGEF and pleckstrin domain protein 1 (FARP1), transcript variant 3, mRNA [NM_001286839]	0,000852848	-2,2740474	down

A_24_P944049	CEP68	Homo sapiens centrosomal protein 68 (CEP68), transcript variant 1, mRNA [NM_-015147]	0,002108161	-2,4170578	down
A_23_P13885	ATN1	Homo sapiens atrophin 1 (ATN1), transcript variant 1, mRNA [NM_001007026]	0,008990446	-2,4321918	down
A_33_P3309468	PTPRS	Homo sapiens protein tyrosine phosphatase receptor type S (PTPRS), transcript variant 1, mRNA [NM_002850]	0,001084312	-2,4436524	down
A_24_P365515	FOXA2	Homo sapiens forkhead box A2 (FOXA2), transcript variant 1, mRNA [NM_021784]	0,005791328	-2,708497	down
A_33_P3343145	MAP1B	Homo sapiens microtubule associated protein 1B (MAP1B), transcript variant 1, mRNA [NM_005909]	0,01044774	-2,767448	down
A_24_P879740	MAP1B	Homo sapiens microtubule associated protein 1B (MAP1B), transcript variant 1, mRNA [NM_005909]	0,001474955	-2,76922	down
A_23_P167509	CYFIP2	Homo sapiens cytoplasmic FMR1 interacting protein 2 (CYFIP2), transcript variant 1, mRNA [NM_001037333]	0,002641376	-2,8846896	down
A_32_P87568	ENAH	Homo sapiens ENAH actin regulator (ENAH), transcript variant 1, mRNA [NM_-001008493]	0,000134814	-4,474691	down

Table 9.12 DEGs of induced epithelial genes by IFN-β vs unstimulated

ProbeName	GeneSymbol	Description	*P*	FC	Regulation
A_24_P314786	SLC4A10	Homo sapiens solute carrier family 4 member 10 (SLC4A10), transcript variant 2, mRNA [NM_022058]	0,027783567	4,697398	up
A_33_P3522511	NFIA	nuclear factor I A [Source:HGNC Symbol	0,013757064	4,3497357	up
A_22_P00024620	CBLL1	Cbl proto-oncogene like 1 [Source:HGNC Symbol	0,04252063	3,823876	up
A_33_P3217584	CHRNA4	Homo sapiens cholinergic receptor nicotinic alpha 4 subunit (CHRNA4), transcript variant 1, mRNA [NM_000744]	0,010772592	3,355627	up
A_33_P3258003	ANKS1B	Homo sapiens ankyrin repeat and sterile alpha motif domain containing 1B (ANKS1B), transcript variant 20, mRNA [NM_001352196]	0,04518641	3,226583	up
A_23_P309720	GABRD	Homo sapiens gamma-aminobutyric acid type A receptor delta subunit (GABRD), mRNA [NM_000815]	0,046312593	2,8518622	up
A_33_P3215527	TJP2	PREDICTED: Homo sapiens tight junction protein 2 (TJP2), transcript variant X3, mRNA [XM_011519206]	0,027817577	2,7497633	up
A_22_P00002457	HOMER2	homer scaffold protein 2 [Source:HGNC Symbol	0,02242876	2,7280157	up
A_24_P83787	DISC1	Homo sapiens DISC1 scaffold protein (DISC1), transcript variant S, mRNA [NM_-001012959]	0,002429943	2,6582603	up
A_33_P3229402	PECAM1	Homo sapiens platelet and endothelial cell adhesion molecule 1 (PECAM1), mRNA [NM_000442]	0,01862171	2,4964054	up

A_23_P36795	SYT1	Homo sapiens synaptotagmin 1 (SYT1), transcript variant 1, mRNA [NM_005639]	0,025509877	2,4472072	up
A_33_P3252800	PTPRR	Homo sapiens protein tyrosine phosphatase receptor type R (PTPRR), transcript variant 1, mRNA [NM_002849]	0,014037586	2,4372497	up
A_33_P3278664	PDLIM5	Homo sapiens PDZ and LIM domain 5 (PDLIM5), transcript variant 4, mRNA [NM_-001011515]	0,044331763	2,1650605	up
A_23_P430558	CHRND	Homo sapiens cholinergic receptor nicotinic delta subunit (CHRND), transcript variant 1, mRNA [NM_000751]	0,016239088	1,8986375	up
A_24_P47182	VCL	Homo sapiens vinculin (VCL), transcript variant 1, mRNA [NM_014000]	0,048594896	-1,7528193	down
A_33_P3402868	GRIN2D	Homo sapiens glutamate ionotropic receptor NMDA type subunit 2D (GRIN2D), mRNA [NM_000836]	0,04398406	-1,8023696	down
A_33_P3303380	PARD3	par-3 family cell polarity regulator [Source:HGNC Symbol	0,026391061	-2,0215015	down
A_21_P0000196	SVOP	Homo sapiens mRNA	0,039317578	-2,1648822	down

Table 9.13 DEGs of induced epithelial genes by IFN-λ1 vs unstimulated

ProbeName	GeneSymbol	Description	*P*	FC	Regulation
A_23_P151851	DUOX2	Homo sapiens dual oxidase 2 (DUOX2), transcript variant 1, mRNA [NM_014080]	0,002587692	3,160112	up
A_23_P167121	GABRA2	Homo sapiens gamma-aminobutyric acid type A receptor alpha2 subunit (GABRA2), transcript variant 1, mRNA [NM_000807]	0,040144857	2,815075	up
A_21_P0014047	C4A	Homo sapiens complement C4A (Rodgers blood group) (C4A), transcript variant 2, mRNA [NM_001252204]	0,03101198	2,7118797	up
A_24_P153831	CTNNA3	Homo sapiens catenin alpha 3 (CTNNA3), transcript variant 3, mRNA [NM_-001291133]	0,030800577	2,5507252	up
A_23_P47924	PTPRR	Homo sapiens protein tyrosine phosphatase receptor type R (PTPRR), transcript variant 1, mRNA [NM_002849]	0,038484618	2,504023	up
A_33_P3229402	PECAM1	Homo sapiens platelet and endothelial cell adhesion molecule 1 (PECAM1), mRNA [NM_000442]	0,01500933	2,4218612	up
A_33_P3268507	CEACAM1	Homo sapiens carcinoembryonic antigen related cell adhesion molecule 1 (CEA-CAM1), transcript variant 5, mRNA [NM_001184816]	0,025703985	2,2236228	up
A_33_P3422429	PATJ	PATJ crumbs cell polarity complex component [Source:HGNC Symbol	0,017884362	2,1815188	up
A_23_P84736	CTNNA2	Homo sapiens catenin alpha 2 (CTNNA2), transcript variant 1, mRNA [NM_004389]	0,03684994	2,1600661	up
A_23_P256754	GABRR1	Homo sapiens gamma-aminobutyric acid type A receptor rho1 subunit (GABRR1), transcript variant 1, mRNA [NM_002042]	0,046306103	2,1466253	up

A_24_P406601	OLFM1	Homo sapiens olfactomedin 1 (OLFM1), transcript variant 1, mRNA [NM_014279]	0,03192182	2,1106606	up
A_33_P3319780	PRR7	PREDICTED: Homo sapiens proline rich 7, synaptic (PRR7), transcript variant X1, mRNA [XM_017009896]	0,023960153	2,04351	up
A_23_P18152	ATP2B2	Homo sapiens ATPase plasma membrane Ca2+ transporting 2 (ATP2B2), transcript variant 1, mRNA [NM_001001331]	0,03278672	2,0324047	up
A_23_P147786	RIMS2	Homo sapiens regulating synaptic membrane exocytosis 2 (RIMS2), transcript variant 2, mRNA [NM_014677]	0,01446488	2,022675	up
A_33_P3327771	SYT2	Homo sapiens synaptotagmin 2 (SYT2), transcript variant 1, mRNA [NM_177402]	0,03681378	2,0101595	up
A_23_P94902	KCTD8	Homo sapiens potassium channel tetramerization domain containing 8 (KCTD8), mRNA [NM_198353]	0,033493623	1,9869374	up
A_21_P0009377	NLGN2	neuroligin 2 [Source:HGNC Symbol	0,026958479	1,9744006	up
A_33_P3222069	SPHK1	Homo sapiens sphingosine kinase 1 (SPHK1), transcript variant 2, mRNA [NM_-182965]	0,035616722	1,956149	up
A_23_P365738	ARC	Homo sapiens activity regulated cytoskeleton associated protein (ARC), mRNA [NM_-015193]	0,037597056	1,9362539	up
A_23_P373031	CACNA1C	Homo sapiens calcium voltage-gated channel subunit alpha1 C (CACNA1C), transcript variant 18, mRNA [NM_000719]	0,04236487	1,9345921	up
A_33_P3812815	PKD1	Homo sapiens polycystin 1, transient receptor potential channel interacting (PKD1), transcript variant 2, mRNA [NM_000296]	0,018196603	1,8579987	up

A_33_P3209962	RASGRP2	Homo sapiens RAS guanyl releasing protein 2 (RASGRP2), transcript variant 2, mRNA [NM_153819]	0,04624834	1,8266374	up
A_23_P153745	IFI30	Homo sapiens IFI30 lysosomal thiol reductase (IFI30), mRNA [NM_006332]	0,01699572	1,80104	up
A_23_P419503	LRRC4B	Homo sapiens leucine rich repeat containing 4B (LRRC4B), transcript variant 2, mRNA [NM_001080457]	0,011502662	1,7618077	up
A_33_P3234025	KAZN	kazrin, periplakin interacting protein [Source:HGNC Symbol	0,023527367	1,7273299	up
A_23_P152655	ICAM2	Homo sapiens intercellular adhesion molecule 2 (ICAM2), transcript variant 5, mRNA [NM_000873]	0,02012156	1,7020648	up
A_23_P430558	CHRND	Homo sapiens cholinergic receptor nicotinic delta subunit (CHRND), transcript variant 1, mRNA [NM_000751]	0,038746536	1,6529596	up
A_33_P3272553	NCAPH2	Homo sapiens non-SMC condensin II complex subunit H2 (NCAPH2), transcript variant 1, mRNA [NM_014551]	0,031182671	1,5672045	up
A_24_P344961	AMOT	Homo sapiens angiomotin (AMOT), transcript variant 2, mRNA [NM_133265]	0,03788855	-1,5415952	down
A_23_P58877	GOPC	Homo sapiens golgi associated PDZ and coiled-coil motif containing (GOPC), transcript variant 1, mRNA [NM_020399]	0,04923952	-1,5670408	down
A_23_P58647	CTNNA1	Homo sapiens catenin alpha 1 (CTNNA1), transcript variant 1, mRNA [NM_001903]	0,037206177	-1,5907001	down
A_33_P3213772	SRGAP2	Homo sapiens SLIT-ROBO Rho GTPase activating protein 2 (SRGAP2), transcript variant 4, mRNA [NM_001300952]	0,020929404	-1,6027555	down

A_32_P35969	CHRNA7	Homo sapiens cholinergic receptor nicotinic alpha 7 subunit (CHRNA7), transcript variant 2, mRNA [NM_001190455]	0,042631634	-1,6049314	down
A_23_P334883	SHANK2	Homo sapiens SH3 and multiple ankyrin repeat domains 2 (SHANK2), transcript variant 1, mRNA [NM_012309]	0,041005716	-1,6079233	down
A_33_P3414422	GPHN	Homo sapiens gephyrin (GPHN), transcript variant 1, mRNA [NM_020806]	0,04320523	-1,612169	down
A_24_P193435	TJP1	Homo sapiens tight junction protein 1 (TJP1), transcript variant 1, mRNA [NM_003257]	0,042067114	-1,6254888	down
A_32_P126375	NHS	Homo sapiens NHS actin remodeling regulator (NHS), transcript variant 1, mRNA [NM_198270]	0,038700506	-1,6296911	down
A_23_P436353	AFDN	Homo sapiens afadin, adherens junction formation factor (AFDN), transcript variant 4, mRNA [NM_001291964]	0,015052013	-1,6327533	down
A_33_P3275350	NCS1	Homo sapiens neuronal calcium sensor 1 (NCS1), transcript variant 1, mRNA [NM_-014286]	0,035483595	-1,6563724	down
A_23_P144807	SEPTIN8	Homo sapiens septin 8 (SEPTIN8), transcript variant 1, mRNA [NM_001098811]	0,023031695	-1,6670053	down
A_23_P319583	RIMS3	Homo sapiens regulating synaptic membrane exocytosis 3 (RIMS3), mRNA [NM_-014747]	0,042942874	-1,7094431	down
A_23_P51397	ENAH	Homo sapiens ENAH actin regulator (ENAH), transcript variant 1, mRNA [NM_-001008493]	0,016271511	-1,7143546	down
A_23_P206359	CDH1	Homo sapiens cadherin 1 (CDH1), transcript variant 1, mRNA [NM_004360]	0,03042955	-1,7148657	down
A_33_P3405728	PKP2	Homo sapiens plakophilin 2 (PKP2), transcript variant 2b, mRNA [NM_004572]	0,012940494	-1,7299371	down

A_33_P3303380	PARD3	par-3 family cell polarity regulator [Source:HGNC Symbol	0,026130376	-1,7314852	down
A_24_P879740	MAP1B	Homo sapiens microtubule associated protein 1B (MAP1B), transcript variant 1, mRNA [NM_005909]	0,01251363	-1,7359297	down
A_33_P3240512	KCTD12	potassium channel tetramerization domain containing 12 [Source:HGNC Symbol	0,0380478	-1,7483943	down
A_23_P351734	NPHP4	Homo sapiens nephrocystin 4 (NPHP4), transcript variant 1, mRNA [NM_015102]	0,0247995	-1,7515707	down
A_33_P3329974	CGN	Homo sapiens cingulin (CGN), mRNA [NM_020770]	0,012988645	-1,7686033	down
A_33_P3316539	SLC7A2	Homo sapiens solute carrier family 7 member 2 (SLC7A2), transcript variant 5, mRNA [NM_001370338]	0,01628657	-1,7951075	down
A_33_P3338698	IHH	Homo sapiens Indian hedgehog signaling molecule (IHH), mRNA [NM_002181]	0,009938357	-1,8061864	down
A_33_P3268838	CPEB1	Homo sapiens cytoplasmic polyadenylation element binding protein 1 (CPEB1), transcript variant 7, mRNA [NM_001365240]	0,029281756	-1,8225535	down
A_23_P20392	PSD3	Homo sapiens pleckstrin and Sec7 domain containing 3 (PSD3), transcript variant 1, mRNA [NM_015310]	0,034466222	-1,939277	down
A_23_P212126	COLQ	Homo sapiens collagen like tail subunit of asymmetric acetylcholinesterase (COLQ), transcript variant II, mRNA [NM_080538]	0,036593214	-1,9416115	down
A_24_P365975	COL8A2	Homo sapiens collagen type VIII alpha 2 chain (COL8A2), transcript variant 1, mRNA [NM_005202]	0,04363149	-1,9481136	down
A_23_P332584	KIAA1107	Homo sapiens KIAA1107 (KIAA1107), mRNA [NM_015237]	0,028921956	-1,9620205	down

A_32_P194312	SDK2	Homo sapiens sidekick cell adhesion molecule 2 (SDK2), mRNA [NM_001144952]	0,037327595	-2,0082588	down
A_33_P3317618	SYN2	Homo sapiens synapsin II (SYN2), transcript variant IIb, mRNA [NM_003178]	0,020014849	-2,1462097	down
A_33_P3369058	LRRK2	Homo sapiens leucine rich repeat kinase 2 (LRRK2), mRNA [NM_198578]	0,015635734	-2,163894	down
A_23_P152305	CDH11	Homo sapiens cadherin 11 (CDH11), transcript variant 1, mRNA [NM_001797]	0,012840705	-2,2167103	down
A_24_P944049	CEP68	Homo sapiens centrosomal protein 68 (CEP68), transcript variant 1, mRNA [NM_-015147]	0,010402796	-2,2239263	down
A_33_P3359047	LYPD6	Homo sapiens LY6/PLAUR domain containing 6 (LYPD6), transcript variant 2, mRNA [NM_194317]	0,022315906	-2,279138	down
A_32_P87568	ENAH	Homo sapiens ENAH actin regulator (ENAH), transcript variant 1, mRNA [NM_-001008493]	0,023260457	-2,2860718	down
A_32_P85999	CDH13	Homo sapiens cadherin 13 (CDH13), transcript variant 1, mRNA [NM_001257]	0,016372751	-2,3315697	down
A_24_P252364	NRCAM	Homo sapiens neuronal cell adhesion molecule (NRCAM), transcript variant 1, mRNA [NM_001037132]	0,015908863	-2,5470498	down
A_24_P193592	CCNF	Homo sapiens cyclin F (CCNF), transcript variant 1, mRNA [NM_001761]	0,001513646	-2,7848036	down

Table 9.14 DEGs of induced epithelial genes by IFN-λ3 vs unstimulated

ProbeName	GeneSymbol	Description	*P*	FC	Regulation
A_23_P151851	DUOX2	Homo sapiens dual oxidase 2 (DUOX2), transcript variant 1, mRNA [NM_014080]	0,002037346	4,7175407	up
A_23_P340868	GLRA3	Homo sapiens glycine receptor alpha 3 (GLRA3), transcript variant 1, mRNA [NM_-006529]	0,035498284	4,220538	up
A_33_P3210805	GABRG3	Homo sapiens gamma-aminobutyric acid type A receptor gamma3 subunit (GABRG3), transcript variant 1, mRNA [NM_033223]	0,011151509	3,434358	up
A_23_P16953	HTR2B	Homo sapiens 5-hydroxytryptamine receptor 2B (HTR2B), transcript variant 1, mRNA [NM_000867]	0,01094607	3,4068158	up
A_33_P3286362	LRRC4C	PREDICTED: Homo sapiens leucine rich repeat containing 4C (LRRC4C), transcript variant X17, mRNA [XM_017018078]	0,010559005	3,215456	up
A_33_P3497352	GRIA4	Homo sapiens glutamate ionotropic receptor AMPA type subunit 4 (GRIA4), transcript variant 3, mRNA [NM_001077244]	0,031711154	3,1693861	up
A_33_P3522511	NFIA	nuclear factor I A [Source:HGNC Symbol	0,016382044	3,0894341	up
A_32_P98739	IGSF5	Homo sapiens immunoglobulin superfamily member 5 (IGSF5), mRNA [NM_-001080444]	0,025385726	3,0549204	up
A_24_P382319	CEACAM1	Homo sapiens carcinoembryonic antigen related cell adhesion molecule 1 (CEA-CAM1), transcript variant 1, mRNA [NM_001712]	0,008449125	3,0508444	up
A_33_P3322870	SYT9	Homo sapiens synaptotagmin 9 (SYT9), mRNA [NM_175733]	0,03921651	2,899226	up

A_33_P3419032	DLG2	discs large MAGUK scaffold protein 2 [Source:HGNC Symbol	0,012557081	2,819499	up
A_24_P145316	DTNBP1	Homo sapiens dystrobrevin binding protein 1 (DTNBP1), transcript variant 2, mRNA [NM_183040]	0,008965244	2,7835138	up
A_24_P124647	SLC17A8	Homo sapiens solute carrier family 17 member 8 (SLC17A8), transcript variant 2, mRNA [NM_001145288]	0,030611856	2,7785122	up
A_23_P402187	PKHD1	PKHD1 ciliary IPT domain containing fibrocystin/polyductin [Source:HGNC Symbol	0,02889441	2,734033	up
A_33_P3420530	GAD2	Homo sapiens glutamate decarboxylase 2 (GAD2), transcript variant 2, mRNA [NM_-001134366]	0,013752968	2,6119843	up
A_23_P373521	HAND2	heart and neural crest derivatives expressed 2 [Source:HGNC Symbol	0,024404144	2,6038387	up
A_23_P162386	BIN2	Homo sapiens bridging integrator 2 (BIN2), transcript variant 1, mRNA [NM_016293]	0,032904275	2,5830371	up
A_24_P321709	TRIM9	Homo sapiens tripartite motif containing 9 (TRIM9), transcript variant 1, mRNA [NM_-015163]	0,038113065	2,5252445	up
A_32_P538928	DSG4	Homo sapiens desmoglein 4 (DSG4), transcript variant 1, mRNA [NM_001134453]	0,03207687	2,467732	up
A_33_P3283525	ENAH	ENAH actin regulator [Source:HGNC Symbol	0,03389731	2,4580774	up
A_33_P3825869	CACNA1C	Homo sapiens calcium voltage-gated channel subunit alpha1 C (CACNA1C), transcript variant 1, mRNA [NM_199460]	0,03815866	2,3925521	up
A_32_P136351	SLITRK1	Homo sapiens SLIT and NTRK like family member 1 (SLITRK1), transcript variant 1, mRNA [NM_052910]	0,017257698	2,3872132	up

A_23_P147786	RIMS2	Homo sapiens regulating synaptic membrane exocytosis 2 (RIMS2), transcript variant 2, mRNA [NM_014677]	0,004727123	2,3410568	up
A_23_P36795	SYT1	Homo sapiens synaptotagmin 1 (SYT1), transcript variant 1, mRNA [NM_005639]	0,031406358	2,1646123	up
A_33_P3227842	EPB41	Homo sapiens erythrocyte membrane protein band 4.1 (EPB41), transcript variant 3, mRNA [NM_001166006]	0,029973716	2,150705	up
A_23_P331748	CD33	Homo sapiens CD33 molecule (CD33), transcript variant 1, mRNA [NM_001772]	0,028366795	2,1361053	up
A_22_P00015658	SVOP	SV2 related protein [Source:HGNC Symbol	0,024733616	2,122042	up
A_33_P3422429	PATJ	PATJ crumbs cell polarity complex component [Source:HGNC Symbol	0,04083394	2,1198196	up
A_33_P3268507	CEACAM1	Homo sapiens carcinoembryonic antigen related cell adhesion molecule 1 (CEACAM1), transcript variant 5, mRNA [NM_001184816]	0,047315314	2,1171076	up
A_23_P95453	NRXN1	Homo sapiens neurexin 1 (NRXN1), transcript variant alpha1, mRNA [NM_004801]	0,029750006	2,1073744	up
A_33_P3297580	CACNA1C	Homo sapiens calcium voltage-gated channel subunit alpha1 C (CACNA1C), transcript variant 1, mRNA [NM_199460]	0,04627259	2,0480952	up
A_24_P247902	PCLO	Homo sapiens piccolo presynaptic cytomatrix protein (PCLO), transcript variant 2, mRNA [NM_014510]	0,011756865	2,041279	up
A_33_P3252800	PTPRR	Homo sapiens protein tyrosine phosphatase receptor type R (PTPRR), transcript variant 1, mRNA [NM_002849]	0,04272898	2,0380416	up
A_33_P3307836	LRRC7	Homo sapiens leucine rich repeat containing 7 (LRRC7), transcript variant 4, mRNA [NM_001366836]	0,040662378	2,0075788	up

A_23_P24457	LRRC4C	Homo sapiens leucine rich repeat containing 4C (LRRC4C), transcript variant 1, mRNA [NM_020929]	0,045572627	1,9712237	up
A_23_P109286	GRIK1	Homo sapiens glutamate ionotropic receptor kainate type subunit 1 (GRIK1), transcript variant 1, mRNA [NM_000830]	0,047836155	1,9185609	up
A_23_P153745	IFI30	Homo sapiens IFI30 lysosomal thiol reductase (IFI30), mRNA [NM_006332]	0,013094066	1,8911754	up
A_33_P3336925	PDLIM5	Homo sapiens PDZ and LIM domain 5 (PDLIM5), transcript variant 9, mRNA [NM_-001256429]	0,018846085	1,8188062	up
A_23_P46369	RAB13	Homo sapiens RAB13, member RAS oncogene family (RAB13), transcript variant 2, mRNA [NM_001272038]	0,033401348	1,6897448	up
A_33_P3272553	NCAPH2	Homo sapiens non-SMC condensin II complex subunit H2 (NCAPH2), transcript variant 1, mRNA [NM_014551]	0,031490557	1,6453277	up
A_33_P3296499	PTPRK	Homo sapiens protein tyrosine phosphatase receptor type K (PTPRK), transcript variant 5, mRNA [NM_001291983]	0,019433154	1,6349564	up
A_24_P879740	MAP1B	Homo sapiens microtubule associated protein 1B (MAP1B), transcript variant 1, mRNA [NM_005909]	0,045313746	-1,5558475	down
A_24_P34534	PARD3B	Homo sapiens par-3 family cell polarity regulator beta (PARD3B), transcript variant 2, mRNA [NM_152526]	0,04286266	-1,6054515	down
A_24_P160202	PANX2	Homo sapiens pannexin 2 (PANX2), transcript variant 2, mRNA [NM_001160300]	0,043559596	-1,7702668	down
A_33_P3422822	GJC2	Homo sapiens gap junction protein gamma 2 (GJC2), mRNA [NM_020435]	0,04907833	-1,7921596	down

A_24_P42624	UNC5C	Homo sapiens unc-5 netrin receptor C (UNC5C), mRNA [NM_003728]	0,024644347	-1,8137839	down
A_33_P3388331	FARP1	Homo sapiens FERM, ARH/RhoGEF and pleckstrin domain protein 1 (FARP1), transcript variant 3, mRNA [NM_001286839]	0,020829994	-1,9191641	down
A_33_P3317618	SYN2	Homo sapiens synapsin II (SYN2), transcript variant IIb, mRNA [NM_003178]	0,0452353	-1,9499179	down
A_33_P3317613	SYN2	Homo sapiens synapsin II (SYN2), transcript variant IIa, mRNA [NM_133625]	0,006659522	-2,0085557	down
A_24_P193592	CCNF	Homo sapiens cyclin F (CCNF), transcript variant 1, mRNA [NM_001761]	0,03278189	-2,0274422	down
A_33_P3373358	GJC1	Homo sapiens gap junction protein gamma 1 (GJC1), transcript variant 1, mRNA [NM_005497]	0,04236858	-2,0329146	down
A_33_P3326217	SHISA6	Homo sapiens shisa family member 6 (SHISA6), transcript variant 3, mRNA [NM_001173462]	0,027932044	-2,0341122	down
A_33_P3394178	NHS	Homo sapiens NHS actin remodeling regulator (NHS), transcript variant 3, mRNA [NM_001291867]	0,010521363	-2,053714	down
A_23_P67151	OLFM2	Homo sapiens olfactomedin 2 (OLFM2), transcript variant 2, mRNA [NM_058164]	0,031165207	-2,1267912	down
A_23_P133338	CDHR2	Homo sapiens cadherin related family member 2 (CDHR2), transcript variant 2, mRNA [NM_017675]	0,033510756	-2,1662025	down
A_33_P3416376	SHANK1	UI-H-FL1-bgt-o-17-0-UI.s1 NCI_CGAP_FL1 Homo sapiens cDNA clone UI-H-FL1-bgt-o-17-0-UI 3', mRNA sequence [BU633092]	0,04775373	-2,229191	down
A_23_P258088	PACSIN1	Homo sapiens protein kinase C and casein kinase substrate in neurons 1 (PACSIN1), transcript variant 1, mRNA [NM_020804]	0,045917273	-2,2352362	down

A_33_P3268304	LIMS2	Homo sapiens LIM zinc finger domain containing 2 (LIMS2), transcript variant 5, mRNA [NM_001161404]	0,011867906	-2,3032854	down
A_23_P327361	DMXL2	Homo sapiens Dmx like 2 (DMXL2), transcript variant 2, mRNA [NM_015263]	0,016608965	-2,5060966	down
A_33_P3343145	MAP1B	Homo sapiens microtubule associated protein 1B (MAP1B), transcript variant 1, mRNA [NM_005909]	0,02596316	-2,621543	down
A_33_P3214899	SYT2	Homo sapiens synaptotagmin 2 (SYT2), transcript variant 1, mRNA [NM_177402]	0,02016423	-2,7776356	down
A_23_P93727	SDK1	Homo sapiens sidekick cell adhesion molecule 1 (SDK1), transcript variant 2, mRNA [NM_001079653]	0,014645657	-2,787896	down
A_23_P49559	GPR142	Homo sapiens G protein-coupled receptor 142 (GPR142), transcript variant 1, mRNA [NM_181790]	0,016363319	-3,0558083	down
A_23_P206806	ITGAL	Homo sapiens integrin subunit alpha L (ITGAL), transcript variant 2, mRNA [NM_-001114380]	0,009260372	-3,4551606	down
A_33_P3359047	LYPD6	Homo sapiens LY6/PLAUR domain containing 6 (LYPD6), transcript variant 2, mRNA [NM_194317]	4,46E-04	-3,5340557	down

Table 9.15 DEGs of induced epithelial genes by IFN-γ vs unstimulated

ProbeName	GeneSymbol	Description	*P*	FC	Regulation
A_23_P151851	DUOX2	Homo sapiens dual oxidase 2 (DUOX2), transcript variant 1, mRNA [NM_014080]	3,66458E-06	14,953803	up
A_23_P153745	IFI30	Homo sapiens IFI30 lysosomal thiol reductase (IFI30), mRNA [NM_006332]	2,18632E-08	14,108556	up
A_23_P81898	GABBR1	gamma-aminobutyric acid type B receptor subunit 1 [Source:HGNC Symbol	1,34586E-07	12,946273	up
A_24_P247902	PCLO	Homo sapiens piccolo presynaptic cytomatrix protein (PCLO), transcript variant 2, mRNA [NM_014510]	1,77524E-07	10,158711	up
A_24_P71973	KDR	Homo sapiens kinase insert domain receptor (KDR), mRNA [NM_002253]	5,38891E-05	10,079896	up
A_23_P42282	C4B	Homo sapiens complement C4B (Chido blood group) (C4B), mRNA [NM_001002029]	1,99751E-05	7,973746	up
A_23_P47924	PTPRR	Homo sapiens protein tyrosine phosphatase receptor type R (PTPRR), transcript variant 1, mRNA [NM_002849]	0,000924513	7,2578697	up
A_21_P0014047	C4A	Homo sapiens complement C4A (Rodgers blood group) (C4A), transcript variant 2, mRNA [NM_001252204]	0,000103405	6,8077097	up
A_22_P00013159	RNF112	Homo sapiens ring finger protein 112 (RNF112), mRNA [NM_007148]	1,85635E-05	6,387194	up
A_23_P16953	HTR2B	Homo sapiens 5-hydroxytryptamine receptor 2B (HTR2B), transcript variant 1, mRNA [NM_000867]	0,000123368	5,8472443	up
A_24_P382319	CEACAM1	Homo sapiens carcinoembryonic antigen related cell adhesion molecule 1 (CEACAM1), transcript variant 1, mRNA [NM_001712]	8,17503E-05	5,587057	up

A_33_P3522511	NFIA	nuclear factor I A [Source:HGNC Symbol	0,000205451	4,9457574	up
A_33_P3691168	IL31RA	Homo sapiens interleukin 31 receptor A (IL31RA), transcript variant 7, mRNA [NM_-001297572]	0,001698323	4,108009	up
A_33_P3367850	CHRM4	Homo sapiens cholinergic receptor muscarinic 4 (CHRM4), transcript variant 1, mRNA [NM_000741]	0,027710596	3,8890092	up
A_23_P90888	CHRNA1	Homo sapiens cholinergic receptor nicotinic alpha 1 subunit (CHRNA1), transcript variant 1, mRNA [NM_001039523]	0,000281606	3,8524091	up
A_33_P3408624	IQSEC3	Homo sapiens IQ motif and Sec7 domain 3 (IQSEC3), transcript variant 2, mRNA [NM_015232]	0,001817216	3,7036133	up
A_24_P393740	FYB1	Homo sapiens FYN binding protein 1 (FYB1), transcript variant 1, mRNA [NM_001465]	0,00177967	3,6171134	up
A_23_P147786	RIMS2	Homo sapiens regulating synaptic membrane exocytosis 2 (RIMS2), transcript variant 2, mRNA [NM_014677]	0,000939851	3,5487502	up
A_23_P414328	CACNG5	Homo sapiens calcium voltage-gated channel auxiliary subunit gamma 5 (CACNG5), mRNA [NM_145811]	0,015708348	3,3994327	up
A_23_P203920	SSPN	Homo sapiens sarcospan (SSPN), transcript variant 1, mRNA [NM_005086]	0,000458937	3,0207024	up
A_32_P136351	SLITRK1	Homo sapiens SLIT and NTRK like family member 1 (SLITRK1), transcript variant 1, mRNA [NM_052910]	0,001680696	3,0053012	up
A_24_P918907	TCAF2	Homo sapiens TRPM8 channel associated factor 2 (TCAF2), transcript variant 5, mRNA [NM_001365427]	0,005373382	2,9232326	up

A_22_P00017060	ADAM8	Homo sapiens ADAM metallopeptidase domain 8 (ADAM8), transcript variant 2, mRNA [NM_001164489]	0,020642113	2,8787022	up
A_33_P3251024	LRRTM2	Homo sapiens leucine rich repeat transmembrane neuronal 2 (LRRTM2), mRNA [NM_015564]	0,004850307	2,7729878	up
A_23_P152655	ICAM2	Homo sapiens intercellular adhesion molecule 2 (ICAM2), transcript variant 5, mRNA [NM_000873]	0,000220543	2,769751	up
A_24_P237912	TCAF2	Homo sapiens TRPM8 channel associated factor 2 (TCAF2), transcript variant 4, mRNA [NM_001363538]	0,001819862	2,7634723	up
A_32_P89899	GABRG1	Homo sapiens gamma-aminobutyric acid type A receptor gamma1 subunit (GABRG1), mRNA [NM_173536]	0,049765147	2,7105355	up
A_23_P419503	LRRC4B	Homo sapiens leucine rich repeat containing 4B (LRRC4B), transcript variant 2, mRNA [NM_001080457]	0,000259239	2,7048097	up
A_33_P3252800	PTPRR	Homo sapiens protein tyrosine phosphatase receptor type R (PTPRR), transcript variant 1, mRNA [NM_002849]	0,001669895	2,6713839	up
A_33_P3375934	NAMPT	Homo sapiens nicotinamide phosphoribosyltransferase (NAMPT), mRNA [NM_-005746]	0,000664364	2,5971115	up
A_33_P3364864	NAMPT	Homo sapiens nicotinamide phosphoribosyltransferase (NAMPT), mRNA [NM_-005746]	0,03884417	2,3245907	up
A_23_P66017	PRRT2	Homo sapiens proline rich transmembrane protein 2 (PRRT2), transcript variant 1, mRNA [NM_145239]	0,005040602	2,2942724	up

A_32_P15544	PRIMA1	Homo sapiens proline rich membrane anchor 1 (PRIMA1), mRNA [NM_178013]	0,03960926	2,2910473	up
A_32_P229618	DLG2	Homo sapiens discs large MAGUK scaffold protein 2 (DLG2), transcript variant 2, mRNA [NM_001364]	0,03352573	2,2909598	up
A_33_P3224730	HMCN2	Homo sapiens hemicentin 2 (HMCN2), mRNA [NM_001291815]	0,005742016	2,2862313	up
A_23_P24457	LRRC4C	Homo sapiens leucine rich repeat containing 4C (LRRC4C), transcript variant 1, mRNA [NM_020929]	0,018943077	2,2762804	up
A_24_P83787	DISC1	Homo sapiens DISC1 scaffold protein (DISC1), transcript variant S, mRNA [NM_-001012959]	0,01777043	2,2610416	up
A_24_P145316	DTNBP1	Homo sapiens dystrobrevin binding protein 1 (DTNBP1), transcript variant 2, mRNA [NM_183040]	0,017264701	2,2486596	up
A_33_P3209962	RASGRP2	Homo sapiens RAS guanyl releasing protein 2 (RASGRP2), transcript variant 2, mRNA [NM_153819]	0,017643755	2,211986	up
A_33_P3268507	CEACAM1	Homo sapiens carcinoembryonic antigen related cell adhesion molecule 1 (CEA-CAM1), transcript variant 5, mRNA [NM_001184816]	0,015524211	2,2085154	up
A_24_P96897	SYT6	Homo sapiens synaptotagmin 6 (SYT6), transcript variant 2, mRNA [NM_205848]	0,027596582	2,1408732	up
A_33_P3301514	NRCAM	Homo sapiens neuronal cell adhesion molecule (NRCAM), transcript variant 1, mRNA [NM_001037132]	0,01818757	2,1406934	up
A_33_P3249976	JAM2	Homo sapiens junctional adhesion molecule 2 (JAM2), transcript variant 1, mRNA [NM_021219]	0,025864754	2,0599308	up

A_33_P3256391	CRB3	Homo sapiens crumbs cell polarity complex component 3 (CRB3), transcript variant 2, mRNA [NM_139161]	0,007436873	2,047719	up
A_33_P3422429	PATJ	PATJ crumbs cell polarity complex component [Source:HGNC Symbol	0,030119505	2,0189662	up
A_32_P213091	SHISA9	Homo sapiens shisa family member 9 (SHISA9), transcript variant 2, mRNA [NM_-001145205]	0,039404165	2,0022924	up
A_33_P3264926	SAMD4A	Homo sapiens sterile alpha motif domain containing 4A (SAMD4A), transcript variant 1, mRNA [NM_015589]	0,015090156	1,9775187	up
A_23_P64721	HCAR3	hydroxycarboxylic acid receptor 3 [Source:HGNC Symbol	0,003591423	1,9710712	up
A_21_P0013605	HMCN2	Homo sapiens hemicentin 2 (HMCN2), mRNA [NM_001291815]	0,043094028	1,9432424	up
A_24_P383523	SAMD4A	Homo sapiens sterile alpha motif domain containing 4A (SAMD4A), transcript variant 1, mRNA [NM_015589]	0,016173605	1,91907	up
A_32_P10936	CDH12	Homo sapiens cadherin 12 (CDH12), transcript variant 5, mRNA [NM_001364105]	0,017038811	1,9072412	up
A_23_P164341	VAMP2	Homo sapiens vesicle associated membrane protein 2 (VAMP2), transcript variant 1, mRNA [NM_014232]	0,030402603	1,9007465	up
A_23_P124619	S100A14	Homo sapiens S100 calcium binding protein A14 (S100A14), mRNA [NM_020672]	0,005437059	1,8918678	up
A_32_P214925	TCAF2	Homo sapiens TRPM8 channel associated factor 2 (TCAF2), transcript variant 2, mRNA [NM_173678]	0,010297063	1,8914585	up
A_22_P00023596	SCIN	Homo sapiens scinderin (SCIN), transcript variant 1, mRNA [NM_001112706]	0,01635057	1,8784615	up

A_22_P00024620	CBLL1	Cbl proto-oncogene like 1 [Source:HGNC Symbol	0,043260656	1,8768523	up
A_33_P3217958	FCHSD2	Homo sapiens FCH and double SH3 domains 2 (FCHSD2), mRNA [NM_014824]	0,008286154	1,8218371	up
A_23_P329924	HCAR2	hydroxycarboxylic acid receptor 2 [Source:HGNC Symbol	0,026919985	1,8205544	up
A_23_P392317	DLGAP2	Homo sapiens DLG associated protein 2 (DLGAP2), transcript variant 3, mRNA [NM_001346810]	0,04052352	1,8152667	up
A_24_P299685	PDPN	Homo sapiens podoplanin (PDPN), transcript variant 2, mRNA [NM_198389]	0,017275095	1,7990223	up
A_23_P35456	SH3PXD2A	Homo sapiens SH3 and PX domains 2A (SH3PXD2A), transcript variant 1, mRNA [NM_014631]	0,016099986	1,7732731	up
A_24_P161581	SHISA7	Homo sapiens shisa family member 7 (SHISA7), mRNA [NM_001145176]	0,015129384	1,7579408	up
A_33_P3336925	PDLIM5	Homo sapiens PDZ and LIM domain 5 (PDLIM5), transcript variant 9, mRNA [NM_-001256429]	0,0217366	1,6946106	up
A_22_P00008484	KCNB1	Homo sapiens potassium voltage-gated channel subfamily B member 1 (KCNB1), mRNA [NM_004975]	0,03480279	1,657843	up
A_23_P46812	CPEB3	Homo sapiens cytoplasmic polyadenylation element binding protein 3 (CPEB3), transcript variant 1, mRNA [NM_014912]	0,025708716	1,6559296	up
A_33_P3272553	NCAPH2	Homo sapiens non-SMC condensin II complex subunit H2 (NCAPH2), transcript variant 1, mRNA [NM_014551]	0,01955136	1,6441478	up
A_23_P157136	SCIN	Homo sapiens scinderin (SCIN), transcript variant 2, mRNA [NM_033128]	0,03790523	1,5966439	up

A_33_P3364661	RHOA	ras homolog family member A [Source:HGNC Symbol	0,03212313	1,5910858	up
A_33_P3296499	PTPRK	Homo sapiens protein tyrosine phosphatase receptor type K (PTPRK), transcript variant 5, mRNA [NM_001291983]	0,018922634	1,5790296	up
A_23_P502957	CDH26	Homo sapiens cadherin 26 (CDH26), transcript variant b, mRNA [NM_021810]	0,014039554	1,5707216	up
A_23_P93988	ARHGEF5	Homo sapiens Rho guanine nucleotide exchange factor 5 (ARHGEF5), mRNA [NM_-005435]	0,040871825	1,5642239	up
A_23_P368278	FCHSD2	Homo sapiens FCH and double SH3 domains 2 (FCHSD2), mRNA [NM_014824]	0,019816048	1,563704	up
A_33_P3213772	SRGAP2	Homo sapiens SLIT-ROBO Rho GTPase activating protein 2 (SRGAP2), transcript variant 4, mRNA [NM_001300952]	0,037563846	-1,5164857	down
A_23_P304237	RAPGEF1	Homo sapiens Rap guanine nucleotide exchange factor 1 (RAPGEF1), transcript variant 2, mRNA [NM_198679]	0,046998944	-1,5202656	down
A_23_P51397	ENAH	Homo sapiens ENAH actin regulator (ENAH), transcript variant 1, mRNA [NM_-001008493]	0,04057523	-1,5337626	down
A_33_P3329974	CGN	Homo sapiens cingulin (CGN), mRNA [NM_020770]	0,032896817	-1,5494249	down
A_24_P244356	NLRX1	Homo sapiens NLR family member X1 (NLRX1), transcript variant 4, mRNA [NM_-001282144]	0,027841514	-1,5496584	down
A_33_P3249439	NCAPH2	Homo sapiens non-SMC condensin II complex subunit H2 (NCAPH2), transcript variant 3, mRNA [NM_001185011]	0,029703852	-1,5565588	down
A_24_P416961	ARVCF	Homo sapiens ARVCF delta catenin family member (ARVCF), mRNA [NM_001670]	0,04434336	-1,5588889	down

A_33_P3272558	NCAPH2	Homo sapiens non-SMC condensin II complex subunit H2 (NCAPH2), transcript variant 3, mRNA [NM_001185011]	0,027113134	-1,5591936	down
A_33_P3293202	C8orf37	Homo sapiens chromosome 8 open reading frame 37 (C8orf37), transcript variant 1, mRNA [NM_177965]	0,03657634	-1,5697911	down
A_23_P32064	NSMF	Homo sapiens NMDA receptor synaptonuclear signaling and neuronal migration factor (NSMF), transcript variant 2, mRNA [NM_015537]	0,034653496	-1,5986147	down
A_23_P146637	SIGMAR1	Homo sapiens sigma non-opioid intracellular receptor 1 (SIGMAR1), transcript variant 1, mRNA [NM_005866]	0,02028301	-1,6004058	down
A_23_P83939	SYAP1	Homo sapiens synapse associated protein 1 (SYAP1), transcript variant 1, mRNA [NM_032796]	0,04686596	-1,6146489	down
A_24_P374943	CXADR	Homo sapiens CXADR Ig-like cell adhesion molecule (CXADR), transcript variant 1, mRNA [NM_001338]	0,039397284	-1,6194464	down
A_24_P372012	ICA1	Homo sapiens islet cell autoantigen 1 (ICA1), transcript variant 2, mRNA [NM_004968]	0,021723792	-1,6226395	down
A_32_P71943	DSTYK	Homo sapiens dual serine/threonine and tyrosine protein kinase (DSTYK), transcript variant 1, mRNA [NM_015375]	0,032406654	-1,6271439	down
A_23_P83110	CDK5RAP2	Homo sapiens CDK5 regulatory subunit associated protein 2 (CDK5RAP2), transcript variant 1, mRNA [NM_018249]	0,022650769	-1,6276335	down
A_23_P213385	BASP1	Homo sapiens brain abundant membrane attached signal protein 1 (BASP1), transcript variant 1, mRNA [NM_006317]	0,023906741	-1,6446147	down

A_24_P88801	NPHP1	Homo sapiens nephrocystin 1 (NPHP1), transcript variant 1, mRNA [NM_000272]	0,021030042	-1,6448158	down
A_32_P195065	SEMA4F	Homo sapiens ssemaphorin 4F (SEMA4F), transcript variant 1, mRNA [NM_004263]	0,046105433	-1,6588707	down
A_24_P873764	BCR	Homo sapiens BCR activator of RhoGEF and GTPase (BCR), transcript variant 2, mRNA [NM_021574]	0,03667709	-1,6624783	down
A_24_P879740	MAP1B	Homo sapiens microtubule associated protein 1B (MAP1B), transcript variant 1, mRNA [NM_005909]	0,026461422	-1,6659709	down
A_24_P62367	DLGAP1	Homo sapiens DLG associated protein 1 (DLGAP1), transcript variant 1, mRNA [NM_004746]	0,045066312	-1,6788383	down
A_23_P436353	AFDN	Homo sapiens afadin, adherens junction formation factor (AFDN), transcript variant 4, mRNA [NM_001291964]	0,008910642	-1,6980745	down
A_23_P204998	FARP1	Homo sapiens FERM, ARH/RhoGEF and pleckstrin domain protein 1 (FARP1), transcript variant 3, mRNA [NM_001286839]	0,031331718	-1,7080799	down
A_33_P3396010	AGER	Homo sapiens advanced glycosylation end-product specific receptor (AGER), transcript variant 9, mRNA [NM_001206966]	0,043459624	-1,7217824	down
A_24_P915007	NACC1	Homo sapiens nucleus accumbens associated 1 (NACC1), mRNA [NM_052876]	0,013483771	-1,7237916	down
A_24_P16610	ZNRF1	zinc and ring finger 1 [Source:HGNC Symbol	0,009649445	-1,7268947	down
A_23_P332584	KIAA1107	Homo sapiens KIAA1107 (KIAA1107), mRNA [NM_015237]	0,04265545	-1,7358688	down
A_32_P56713	BCR	Homo sapiens BCR activator of RhoGEF and GTPase (BCR), transcript variant 2, mRNA [NM_021574]	0,022265507	-1,74745	down

A_33_P3236993	ARVCF	Homo sapiens ARVCF delta catenin family member (ARVCF), mRNA [NM_001670]	0,047477636	-1,7525777	down
A_33_P3250595	ITSN1	Homo sapiens intersectin 1 (ITSN1), transcript variant 2, mRNA [NM_001001132]	0,017496295	-1,7654272	down
A_23_P144807	SEPTIN8	Homo sapiens septin 8 (SEPTIN8), transcript variant 1, mRNA [NM_001098811]	0,015598139	-1,8041524	down
A_23_P137209	UBA1	Homo sapiens ubiquitin like modifier activating enzyme 1 (UBA1), transcript variant 1, mRNA [NM_003334]	0,04375209	-1,807292	down
A_33_P3221489	KIRREL1	Homo sapiens kirre like nephrin family adhesion molecule 1 (KIRREL1), transcript variant 1, mRNA [NM_018240]	0,032130353	-1,8360727	down
A_23_P20392	PSD3	Homo sapiens pleckstrin and Sec7 domain containing 3 (PSD3), transcript variant 1, mRNA [NM_015310]	0,02567992	-1,8447009	down
A_32_P24585	SH3PXD2B	Homo sapiens SH3 and PX domains 2B (SH3PXD2B), transcript variant 1, mRNA [NM_001017995]	0,02741642	-1,9120244	down
A_23_P152305	CDH11	Homo sapiens cadherin 11 (CDH11), transcript variant 1, mRNA [NM_001797]	0,009080824	-1,9401219	down
A_32_P85999	CDH13	Homo sapiens cadherin 13 (CDH13), transcript variant 1, mRNA [NM_001257]	0,03273146	-1,9634931	down
A_24_P307808	KCTD16	Homo sapiens potassium channel tetramerization domain containing 16 (KCTD16), mRNA [NM_020768]	0,04477735	-1,9750962	down
A_23_P256603	AFDN	Homo sapiens afadin, adherens junction formation factor (AFDN), transcript variant 1, mRNA [NM_001207008]	0,005874145	-1,9882442	down
A_23_P421306	SYT12	Homo sapiens synaptotagmin 12 (SYT12), transcript variant 1, mRNA [NM_177963]	0,003715517	-2,0030982	down

A_23_P99906	HOMER2	Homo sapiens homer scaffold protein 2 (HOMER2), transcript variant 2, mRNA [NM_-199330]	0,001441625	-2,006962	down
A_23_P335495	ANO7	Homo sapiens anoctamin 7 (ANO7), transcript variant NGEP-L, mRNA [NM_-001001891]	0,030993568	-2,0141578	down
A_33_P3414964	PTPRS	protein tyrosine phosphatase receptor type S [Source:HGNC Symbol	0,034130424	-2,034145	down
A_23_P319583	RIMS3	Homo sapiens regulating synaptic membrane exocytosis 3 (RIMS3), mRNA [NM_-014747]	0,009898607	-2,0616257	down
A_33_P3239185	SYT7	Homo sapiens synaptotagmin 7 (SYT7), transcript variant 4, mRNA [NM_001365809]	0,00756977	-2,0720263	down
A_23_P8640	GPER1	Homo sapiens G protein-coupled estrogen receptor 1 (GPER1), transcript variant 3, mRNA [NM_001039966]	0,025177816	-2,110781	down
A_33_P3307144	GRIK2	Homo sapiens glutamate ionotropic receptor kainate type subunit 2 (GRIK2), transcript variant 1, mRNA [NM_021956]	0,034347177	-2,1149888	down
A_23_P167509	CYFIP2	Homo sapiens cytoplasmic FMR1 interacting protein 2 (CYFIP2), transcript variant 1, mRNA [NM_001037333]	0,022910263	-2,1212747	down
A_33_P3413821	KIRREL1	Homo sapiens kirre like nephrin family adhesion molecule 1 (KIRREL1), transcript variant 1, mRNA [NM_018240]	0,00811422	-2,122557	down
A_23_P88691	CHRNA5	Homo sapiens cholinergic receptor nicotinic alpha 5 subunit (CHRNA5), transcript variant 1, mRNA [NM_000745]	0,005636628	-2,1301334	down
A_33_P3307735	OPHN1	Homo sapiens oligophrenin 1 (OPHN1), mRNA [NM_002547]	0,001344996	-2,1545572	down

A_24_P365515	FOXA2	Homo sapiens forkhead box A2 (FOXA2), transcript variant 1, mRNA [NM_021784]	0,045509275	-2,1646988	down
A_33_P3388331	FARP1	Homo sapiens FERM, ARH/RhoGEF and pleckstrin domain protein 1 (FARP1), transcript variant 3, mRNA [NM_001286839]	0,004306705	-2,168677	down
A_23_P341567	SLC9B2	Homo sapiens solute carrier family 9 member B2 (SLC9B2), transcript variant 11, mRNA [NM_001370206]	0,03633956	-2,1779737	down
A_33_P3363355	ICAM4	Homo sapiens intercellular adhesion molecule 4 (Landsteiner-Wiener blood group) (ICAM4), transcript variant 3, mRNA [NM_001039132]	0,020726442	-2,1874375	down
A_23_P59877	FABP5	Homo sapiens fatty acid binding protein 5 (FABP5), mRNA [NM_001444]	0,005267787	-2,216801	down
A_24_P36229	DTNA	Homo sapiens dystrobrevin alpha (DTNA), transcript variant 3, mRNA [NM_001391]	0,007136521	-2,225634	down
A_33_P3252083	GRIP1	Homo sapiens glutamate receptor interacting protein 1 (GRIP1), transcript variant 3, mRNA [NM_001366722]	0,01626034	-2,2392733	down
A_33_P3373358	GJC1	Homo sapiens gap junction protein gamma 1 (GJC1), transcript variant 1, mRNA [NM_005497]	0,010634828	-2,2647507	down
A_24_P409800	KCTD16	Homo sapiens potassium channel tetramerization domain containing 16 (KCTD16), mRNA [NM_020768]	0,039044846	-2,2653146	down
A_33_P3338698	IHH	Homo sapiens Indian hedgehog signaling molecule (IHH), mRNA [NM_002181]	0,001375637	-2,277171	down
A_23_P38732	CDH2	Homo sapiens cadherin 2 (CDH2), transcript variant 1, mRNA [NM_001792]	0,042621743	-2,2801664	down
A_32_P204676	FABP5	Homo sapiens fatty acid binding protein 5 (FABP5), mRNA [NM_001444]	0,002564892	-2,3251011	down

A_24_P944049	CEP68	Homo sapiens centrosomal protein 68 (CEP68), transcript variant 1, mRNA [NM_-015147]	0,003986828	-2,3299613	down
A_32_P35969	CHRNA7	Homo sapiens cholinergic receptor nicotinic alpha 7 subunit (CHRNA7), transcript variant 2, mRNA [NM_001190455]	0,000696146	-2,3749886	down
A_24_P673063	FABP5	Homo sapiens fatty acid binding protein 5 (FABP5), mRNA [NM_001444]	0,002712128	-2,4024856	down
A_32_P87568	ENAH	Homo sapiens ENAH actin regulator (ENAH), transcript variant 1, mRNA [NM_-001008493]	0,03262559	-2,404732	down
A_33_P3268304	LIMS2	Homo sapiens LIM zinc finger domain containing 2 (LIMS2), transcript variant 5, mRNA [NM_001161404]	0,01757703	-2,419941	down
A_23_P134426	GPNMB	Homo sapiens glycoprotein nmb (GPNMB), transcript variant 1, mRNA [NM_-001005340]	0,011783887	-2,4225376	down
A_32_P194312	SDK2	Homo sapiens sidekick cell adhesion molecule 2 (SDK2), mRNA [NM_001144952]	0,034804273	-2,446742	down
A_33_P3345816	GPER1	Homo sapiens G protein-coupled estrogen receptor 1 (GPER1), transcript variant 4, mRNA [NM_001098201]	0,009918676	-2,5682487	down
A_23_P212126	COLQ	Homo sapiens collagen like tail subunit of asymmetric acetylcholinesterase (COLQ), transcript variant II, mRNA [NM_080538]	0,001274031	-2,5814822	down
A_33_P3328653	CELSR1	Homo sapiens cadherin EGF LAG seven-pass G-type receptor 1 (CELSR1), mRNA [NM_014246]	0,006472434	-2,629632	down

A_33_P3343145	MAP1B	Homo sapiens microtubule associated protein 1B (MAP1B), transcript variant 1, mRNA [NM_005909]	0,00886567	-2,633748	down
A_23_P206806	ITGAL	Homo sapiens integrin subunit alpha L (ITGAL), transcript variant 2, mRNA [NM_-001114380]	0,008311856	-2,7339065	down
A_32_P82111	LRFN2	leucine rich repeat and fibronectin type III domain containing 2 [Source:HGNC Symbol	0,000618801	-2,7504306	down
A_24_P34534	PARD3B	Homo sapiens par-3 family cell polarity regulator beta (PARD3B), transcript variant 2, mRNA [NM_152526]	0,000492761	-2,816758	down
A_23_P67151	OLFM2	Homo sapiens olfactomedin 2 (OLFM2), transcript variant 2, mRNA [NM_058164]	0,022541074	-2,9268882	down
A_24_P299474	TENM2	Homo sapiens teneurin transmembrane protein 2 (TENM2), transcript variant 1, mRNA [NM_001122679]	0,000812743	-2,9772754	down
A_33_P3245218	TENM2	Homo sapiens teneurin transmembrane protein 2 (TENM2), transcript variant 1, mRNA [NM_001122679]	0,000610801	-2,9781053	down
A_33_P3422822	GJC2	Homo sapiens gap junction protein gamma 2 (GJC2), mRNA [NM_020435]	0,000336433	-3,0606852	down
A_23_P258088	PACSIN1	Homo sapiens protein kinase C and casein kinase substrate in neurons 1 (PACSIN1), transcript variant 1, mRNA [NM_020804]	0,003026567	-3,2511854	down
A_23_P82929	CCN3	Homo sapiens cellular communication network factor 3 (CCN3), mRNA [NM_002514]	0,000345827	-3,9689677	down
A_33_P3418833	FLRT3	Homo sapiens fibronectin leucine rich transmembrane protein 3 (FLRT3), transcript variant 1, mRNA [NM_013281]	0,000588624	-4,199014	down

A_33_P3280845	THY1	Homo sapiens Thy-1 cell surface antigen (THY1), transcript variant 1, mRNA [NM_-006288]	0,00910191	-4,515882	down
A_24_P323598	ESCO2	establishment of sister chromatid cohesion N-acetyltransferase 2 [Source:HGNC Symbol	0,00219126	-4,669314	down
A_33_P3326210	ESCO2	establishment of sister chromatid cohesion N-acetyltransferase 2 [Source:HGNC Symbol	0,000423389	-4,956261	down

Table 9.16 Cellular process enriched analysis output String network analysis of inflammatory and epithelial DEGs induced by type-I, -II and -III IFNs

term ID	Description	gene count	background gene count	strengsth	false discovery rate	matching proteins in network
GO:1905330	Regulation of morphogenesis of an epithelium	3	180	3,3239	0,0411	CXCL10,STAT1,PSMB8
GO:0032101	Regulation of response to external stimulus	4	1013	4,7119	0,0466	USP18,CXCL10,STAT1,PSMB8
GO:0071944	Cell periphery	49	5432	0,4	1,19E-09	TGFB1,IL12B,NT5E,IL1RN,DAB2IP,RIPK1,THBS1,NOX4,SELP,IL18RAP,FNDC4,HIST1H2BA,TNFSF12,CCR1,FOLR2,CLEC7A,NLRP6,AOC3,STAB1,IL1RAP,F2R,CSF1,IL20RB,PRKD1,NFAM1,ADORA2A,MMP25,NCR3,PTGER3,TSPAN2,PTGFR,CXCR3,CNR2,HSPG2,S1PR3,NFX1,IL2RA,HRH1,TNFSF11,IL6,IL18R1,CD44,PRKCA,ACKR2,TIGIT,CCR3,ADAM8,ALOX15,PLA2G4C
GO:0005886	Plasma membrane	48	5314	0,4	1,40E-09	TGFB1,IL12B,NT5E,IL1RN,DAB2IP,RIPK1,THBS1,NOX4,SELP,IL18RAP,FNDC4,HIST1H2BA,TNFSF12,CCR1,FOLR2,CLEC7A,NLRP6,AOC3,STAB1,IL1RAP,F2R,CSF1,IL20RB,PRKD1,NFAM1,ADORA2A,MMP25,NCR3,PTGER3,TSPAN2,PTGFR,CXCR3,CNR2,HSPG2,S1PR3,NFX1,IL2RA,HRH1,TNFSF11,IL6,IL18R1,CD44,PRKCA,ACKR2,TIGIT,CCR3,ADAM8,ALOX15
GO:0031226	Intrinsic component of plasma membrane	26	1703	0,62	6,08E-08	NOX4,SELP,IL18RAP,TNFSF12,CCR1,FOLR2,STAB1,IL1RAP,F2R,ADORA2A,NCR3,PTGER3,TSPAN2,PTGFR,CXCR3,CNR2,S1PR3,IL2RA,HRH1,TNFSF11,IL6,IL18R1,CD44,ACKR2,CCR3,ADAM8

GO:0005887	Integral component of plasma membrane	25	1623	0,63	9,95E-08	NOX4,SELP,IL18RAP,TNFSF12,CCR1,STAB1,IL1RAP,F2R,ADORA2A,NCR3,PTGER3,TSPAN2,PTGFR,CXCR3,CNR2,S1PR3,IL2RA,HRH1,TNFSF11,IL6,IL18R1,CD44,ACKR2,CCR3,ADAM8
GO:0009986	Cell surface	17	824	0,75	1,87E-06	TGFB1,IL12B,NT5E,THBS1,SELP,CCR1,FOLR2,CLEC7A,AOC3,F2R,CXCR3,IL2RA,CD44,ACKR2,TIGIT,CCR3,ADAM8
GO:0016020	Membrane	56	9072	0,23	6,25E-06	TGFB1,HGF,IL12B,TICAM1,NT5E,IL1RN,DAB2IP,RIPK1,THBS1,NOX4,SELP,IL18RAP,FNDC4,HIST1H2BA,TNFSF12,CCR1,FOLR2,CLEC7A,NLRP6,AOC3,STAB1,IL1RAP,F2R,CSF1,IL20RB,PRKD1,NFAM1,ADORA2A,NLRP3,MMP25,PSMF1,CHST4,NCR3,PTGER3,PTGS1,DHX9,TSPAN2,PTGFR,CXCR3,CNR2,HSPG2,S1PR3,NFX1,IL2RA,HRH1,TNFSF11,IL6,IL18R1,CD44,PRKCA,ACKR2,TIGIT,CCR3,ADAM8,ALOX15,PLA2G4C
GO:0009897	External side of plasma membrane	9	331	0,87	0,00088	IL12B,THBS1,SELP,CCR1,FOLR2,CXCR3,IL2RA,ACKR2,CCR3
GO:0098552	Side of membrane	11	531	0,76	0,00088	IL12B,THBS1,SELP,CCR1,FOLR2,CXCR3,CNR2,IL2RA,ACKR2,CCR3,ALOX15
GO:0005576	Extracellular region	31	4166	0,31	0,0039	PGLYRP1,TGFB1,HGF,IL12B,CMA1,NT5E,IL1RN,IL36A,IL36B,THBS1,SELP,LXN,FNDC4,TNFSF12,FOLR2,LTBP3,IL1RAP,F2R,CSF1,TAC4,NLRP3,MMP25,PTGS1,PTGFR,HSPG2,TNFSF11,IL6,CD44,PRKCA,CXCL17,CCL4
GO:0031224	Intrinsic component of membrane	36	5345	0,27	0,0043	NT5E,NOX4,SELP,IL18RAP,FNDC4,TNFSF12,CCR1,FOLR2,CLEC7A,AOC3,STAB1,IL1RAP,F2R,CSF1,IL20RB,NFAM1,ADORA2A,MMP25,CHST4,NCR3,PTGER3,TSPAN2,PTGFR,CXCR3,CNR2,S1PR3,IL2RA,HRH1,TNFSF11,IL6,IL18R1,CD44,ACKR2,TIGIT,CCR3,ADAM8

GO:0005615	Extracellular space	26	3195	0,35	0,0047	PGLYRP1,TGFB1,HGF,IL12B,CMA1,NT5E,IL1RN,IL36A,IL36B,THBS1,SELP,LXN,FNDC4,TNFSF12,LTBP3,CSF1,TAC4,MMP25,PTGS1,HSPG2,TNFSF11,IL6,CD44,PRKCA,CXCL17,CCL4
GO:0012505	Endomembrane system	32	4542	0,29	0,0061	PGLYRP1,TGFB1,HGF,IL12B,TICAM1,CMA1,RIPK1,THBS1,NOX4,SELP,FNDC4,NLRP6,AOC3,F2R,CSF1,PRKD1,NFAM1,ADORA2A,NLRP3,MMP25,PSMF1,CHST4,PTGER3,PTGS1,CNR2,HSPG2,IL6,CD44,PRKCA,ACKR2,ADAM8,PLA2G4C
GO:0045092	interleukin-18 receptor complex	2	2	1,6103	0,0101	IL18RAP,IL18R1
GO:0016021	Integral component of membrane	34	5181	0,26	0,0114	NOX4,SELP,IL18RAP,FNDC4,TNFSF12,CCR1,CLEC7A,AOC3,STAB1,IL1RAP,F2R,CSF1,IL20RB,NFAM1,ADORA2A,MMP25,CHST4,NCR3,PTGER3,TSPAN2,PTGFR,CXCR3,CNR2,S1PR3,IL2RA,HRH1,TNFSF11,IL6,IL18R1,CD44,ACKR2,TIGIT,CCR3,ADAM8
GO:0098797	Plasma membrane protein complex	9	547	0,66	0,0194	RIPK1,NOX4,IL18RAP,HSPG2,IL2RA,IL6,IL18R1,PRKCA,ADAM8
GO:0097342	Ripoptosome	2	6	3,5065	0,0378	TICAM1,RIPK1
GO:0031091	Platelet alpha granule	4	91	4,4774	0,039	TGFB1,HGF,THBS1,SELP
GO:0043235	Receptor complex	7	381	0,7	0,0472	IL12B,RIPK1,IL18RAP,IL2RA,IL6,IL18R1,CD44
GO:0005576	Extracellular region	34	4166	0,42	8,14E-06	PSMA3,IL23A,PROC,TNFAIP6,PYCARD,IL36G,NOV,PSMB1,IL1B,HNMT,APP,CXCL16,TNFRSF11B,KRT16,LTBP3,IL17D,CCL19,KARS,CSF1,FAM132A,MMP25,TSLP,TNFRSF6B,TREM2,AGER,CCL7,TEK,TMSB4X,CCL25,CCL8,VIMP,PSMA1,ADAM9,PSMB3

GO:0005615	Extracellular space	28	3195	0,45	5,69E-05	PSMA3,IL23A,PROC,TNFAIP6,IL36G,PSMB1,IL1B,HNMT,APP,CXCL16,TNFRSF11B,KRT16,LTBP3,IL17D,CCL19,KARS,CSF1,FAM132A,MMP25,TSLP,TNFRSF6B,CCL7,CCL25,CCL8,VIMP,PSMA1,ADAM9,PSMB3
GO:0005839	Proteasome core complex	4	20	2,9587	0,00048	PSMA3,PSMB1,PSMA1,PSMB3
GO:0038023	Signaling receptor activity	17	1453	0,76	3,72E-06	TREM1,KRT1,MAS1,LY75,IL22RA2,SPHK1,CXCR2,EMR2,PTGER3,FCGR2B,ACKR1,IL6R,ADORA3,PTAFR,TLR4,TNFRSF1B,NR1H4
GO:0004888	Transmembrane signaling receptor activity	13	1240	0,71	0,00071	MAS1,IL22RA2,SPHK1,CXCR2,EMR2,PTGER3,FCGR2B,ACKR1,IL6R,ADORA3,PTAFR,TLR4,TNFRSF1B
GO:0019955	Cytokine binding	5	134	4,6023	0,0073	IL22RA2,CXCR2,ACKR1,IL6R,TNFRSF1B
GO:0030054	Cell junction	66	2075	0,92	9,50E-51	CBLN4,ITGB4,VCL,RABAC1,LRFN1,ABHD17A,ARHGEF9,ABCA7,SLC17A6,GRIN2D,CDH10,GID8,DBN1,HCRT,BSN,CHRNB1,HOMER2,DSCAML1,PSD3,TMEM108,SPECC1L,LYPD6,LPHN1,ATN1,PTPRS,KCNK1,DISC1,ANXA9,CHRNA4,FMR1,RIMS3,CDSN,TPRG1L,GABRD,AGRN,CHRM5,CADPS,PKP4,JAM2,C1orf86,CHRNA2,NRXN1,GABRR2,FCHSD2,SLC18A1,SLC4A10,KLHL24,CD44,DLGAP2,UNC5C,CAMSAP3,WDR1,GRIA1,GABRP,IGSF9B,TJP2,RIMS4,SLC16A1,ANKS1B,PECAM1,GABRQ,CPNE3,SVOP,CNTNAP4,PDLIM5,SLC2A11
GO:0045202	Synapse	49	1351	0,98	3,94E-35	CBLN4,RABAC1,LRFN1,ABHD17A,ARHGEF9,SLC17A6,GRIN2D,CDH10,DBN1,HCRT,BSN,CHRNB1,HOMER2,DSCAML1,PSD3,TMEM108,LYPD6,LPHN1,PTPRS,KCNK1,DISC1,ANXA9,CHRNA4,FMR1,RIMS3,TPRG1L,GABRD,AGRN,CHRM5,CADPS,PKP4,CHRNA2,NRXN1,GABRR2,FCHSD2,SLC18A1,SLC4A10,DLGAP2,UNC5C,GRIA1,GABRP,IGSF9B,RIMS4,SLC16A1,ANKS1B,GABRQ,SVOP,CNTNAP4,PDLIM5

GO:0098794	Postsynapse	30	643	4,4805	6,11E-22	LRFN1,ABHD17A,ARHGEF9,GRIN2D,CDH10,DBN1,HCRT,BSN,CHRNB1,HOMER2,PSD3,TMEM108,LPHN1,PTPRS,DISC1,CHRNA4,FMR1,GABRD,CHRM5,PKP4,CHRNA2,GABRR2,SLC4A10,DLGAP2,GRIA1,GABRP,IGSF9B,ANKS1B,GABRQ,PDLIM5
GO:0097060	Synaptic membrane	23	387	4,3466	2,27E-18	LRFN1,ABHD17A,GRIN2D,CDH10,DBN1,CHRNB1,LPHN1,PTPRS,KCNK1,CHRNA4,FMR1,RIMS3,GABRD,CHRM5,CHRNA2,NRXN1,GABRR2,GRIA1,GABRP,IGSF9B,RIMS4,GABRQ,CNTNAP4
GO:0099572	Postsynaptic specialization	21	369	4,2736	2,83E-16	LRFN1,ABHD17A,ARHGEF9,GRIN2D,CDH10,DBN1,BSN,CHRNB1,HOMER2,PSD3,TMEM108,LPHN1,PTPRS,DISC1,FMR1,PKP4,DLGAP2,GRIA1,IGSF9B,ANKS1B,PDLIM5
GO:0043005	Neuron projection	32	1366	0,79	2,95E-15	ABHD17A,SLC17A6,DBN1,BSN,CHRNB1,HOMER2,DSCAML1,TMEM108,LYPD6,LPHN1,PTPRS,KCNK1,DISC1,CHRNA4,FMR1,TPRG1L,GABRD,CHRM5,CHRNA2,NRXN1,GABRR2,FCHSD2,SLC18A1,SLC4A10,KLHL24,UNC5C,CD200,GRIA1,GABRP,IGSF9B,ANKS1B,GABRQ
GO:0014069	Postsynaptic density	19	344	4,2370	1,99E-14	LRFN1,ABHD17A,ARHGEF9,GRIN2D,DBN1,BSN,HOMER2,PSD3,TMEM108,LPHN1,PTPRS,DISC1,FMR1,PKP4,DLGAP2,GRIA1,IGSF9B,ANKS1B,PDLIM5
GO:0042995	Cell projection	38	2287	0,64	3,49E-14	ABHD17A,ABCA7,SLC17A6,DBN1,BSN,CHRNB1,HOMER2,DSCAML1,PSD3,TMEM108,LYPD6,LPHN1,PTPRS,KCNK1,DISC1,CHRNA4,FMR1,TPRG1L,GABRD,CHRM5,CHRNA2,NRXN1,GABRR2,FCHSD2,SLC18A1,SLC4A10,KLHL24,CD44,UNC5C,CD200,WDR1,GRIA1,GABRP,IGSF9B,ANKS1B,GABRQ,CNTNAP4,PDLIM5

GO:0071944	Cell periphery	55	5432	0,42	6,14E-14	ITGB4,VCL,RABAC1,LRFN1,ABHD17A,CELSR1,ABCA7,GRIN2D,CDH10,DBN1,BSN,CHRNB1,HOMER2,DSCAML1,ICOS,PSD3,LYPD6,LPHN1,PTPRS,KCNK1,ANXA9,CHRNA4,FMR1,RIMS3,CDSN,GABRD,AGRN,CHRM5,PKP4,FAT4,JAM2,CHRNA2,NRXN1,GABRR2,FCHSD2,SLC4A10,CD44,DLGAP2,UNC5C,CD200,WDR1,GRIA1,GABRP,IGSF9B,TJP2,RIMS4,SLC16A1,ANKS1B,ADAM8,PECAM1,GABRQ,CPNE3,CNTNAP4,SLC2A11,DCHS2
GO:0098590	Plasma membrane region	29	1219	0,79	6,14E-14	LRFN1,ABHD17A,ABCA7,GRIN2D,CDH10,DBN1,CHRNB1,PSD3,LPHN1,PTPRS,KCNK1,CHRNA4,FMR1,RIMS3,GABRD,CHRM5,CHRNA2,NRXN1,GABRR2,FCHSD2,SLC4A10,CD44,GRIA1,GABRP,IGSF9B,RIMS4,SLC16A1,GABRQ,CNTNAP4
GO:0098793	Presynapse	21	526	4,4593	1,02E-13	RABAC1,SLC17A6,CDH10,HCRT,BSN,LPHN1,PTPRS,DISC1,CHRNA4,FMR1,RIMS3,TPRG1L,CADPS,NRXN1,SLC18A1,SLC4A10,GRIA1,RIMS4,SVOP,CNTNAP4,PDLIM5
GO:0005886	Plasma membrane	54	5314	0,42	1,20E-13	ITGB4,VCL,RABAC1,LRFN1,ABHD17A,CELSR1,ABCA7,GRIN2D,CDH10,DBN1,CHRNB1,HOMER2,DSCAML1,ICOS,PSD3,LYPD6,LPHN1,PTPRS,KCNK1,ANXA9,CHRNA4,FMR1,RIMS3,CDSN,GABRD,AGRN,CHRM5,PKP4,FAT4,JAM2,CHRNA2,NRXN1,GABRR2,FCHSD2,SLC4A10,CD44,DLGAP2,UNC5C,CD200,WDR1,GRIA1,GABRP,IGSF9B,TJP2,RIMS4,SLC16A1,ANKS1B,ADAM8,PECAM1,GABRQ,CPNE3,CNTNAP4,SLC2A11,DCHS2
GO:0045211	Postsynaptic membrane	17	281	4,4593	1,20E-13	LRFN1,ABHD17A,GRIN2D,CDH10,DBN1,CHRNB1,PTPRS,CHRNA4,FMR1,GABRD,CHRM5,CHRNA2,GABRR2,GRIA1,GABRP,IGSF9B,GABRQ
GO:0120025	Plasma membrane bounded cell projection	35	2193	0,62	2,04E-12	ABHD17A,ABCA7,SLC17A6,DBN1,BSN,CHRNB1,HOMER2,DSCAML1,PSD3,TMEM108,LYPD6,LPHN1,PTPRS,KCNK1,DISC1,CHRNA4,FMR1,TPRG1L,GABRD,CHRM5,CHRNA2,NRXN1,GABRR2,FCHSD2,SLC18A1,SLC4A10,KLHL24,CD44,UNC5C,CD200,GRIA1,GABRP,IGSF9B,ANKS1B,GABRQ

GO:0016020	Membrane	64	9072	0,26	2,86E-10	ITGB4,VCL,RABAC1,LRFN1,ABHD17A,CELSR1,ABCA7,SLC17A6,GRIN2D,CDH10,CRNN,DBN1,BSN,CHRNB1,HOMER2,DSCAML1,ICOS,PSD3,TMEM108,LYPD6,LPHN1,PTPRS,KCNK1,ANXA9,CHRNA4,FMR1,RIMS3,CDSN,TPRG1L,GABRD,AGRN,CHRM5,CADPS,PKP4,FAT4,JAM2,CHRNA2,NRXN1,GABRR2,FCHSD2,SLC18A1,SLC4A10,CD44,DLGAP2,UNC5C,CD200,WDR1,GRIA1,GABRP,IGSF9B,TJP2,RIMS4,SLC16A1,FNDC3A,ANKS1B,ADAM8,PECAM1,GABRQ,CPNE3,SVOP,CNTNAP4,PDLIM5,SLC2A11,DCHS2
GO:0036477	Somatodendritic compartment	20	852	0,79	5,35E-09	ABHD17A,DBN1,BSN,HOMER2,TMEM108,PTPRS,KCNK1,CHRNA4,FMR1,GABRD,CHRM5,JAM2,NRXN1,SLC4A10,KLHL24,UNC5C,CD200,GRIA1,IGSF9B,ANKS1B
GO:0030424	Axon	17	646	0,84	3,35E-08	DBN1,BSN,DSCAML1,TMEM108,LPHN1,PTPRS,DISC1,FMR1,TPRG1L,GABRD,NRXN1,SLC18A1,SLC4A10,KLHL24,UNC5C,CD200,GRIA1
GO:0031226	Intrinsic component of plasma membrane	25	1703	0,58	2,01E-07	ITGB4,LRFN1,ABHD17A,GRIN2D,CDH10,CHRNB1,ICOS,LPHN1,PTPRS,KCNK1,CHRNA4,GABRD,CHRM5,JAM2,CHRNA2,NRXN1,GABRR2,CD44,CD200,GRIA1,GABRP,SLC16A1,ADAM8,PECAM1,GABRQ
GO:0005887	Integral component of plasma membrane	24	1623	0,59	3,88E-07	ITGB4,LRFN1,GRIN2D,CDH10,CHRNB1,ICOS,LPHN1,PTPRS,KCNK1,CHRNA4,GABRD,CHRM5,JAM2,CHRNA2,NRXN1,GABRR2,CD44,CD200,GRIA1,GABRP,SLC16A1,ADAM8,PECAM1,GABRQ
GO:0008021	Synaptic vesicle	10	203	4,4866	6,31E-07	RABAC1,SLC17A6,HCRT,BSN,PTPRS,DISC1,TPRG1L,SLC18A1,GRIA1,SVOP
GO:0030425	Dendrite	15	612	0,81	8,82E-07	ABHD17A,DBN1,BSN,HOMER2,TMEM108,KCNK1,CHRNA4,FMR1,GABRD,CHRM5,SLC4A10,UNC5C,GRIA1,IGSF9B,ANKS1B
GO:0042734	Presynaptic membrane	9	158	4,2736	9,88E-07	CDH10,LPHN1,PTPRS,CHRNA4,FMR1,RIMS3,NRXN1,RIMS4,CNTNAP4

GO:0098982	GABA-ergic synapse	7	74	1,4246	1,55E-06	CBLN4,CDH10,BSN,GABRD,NRXN1,GABRR2,IGSF9B
GO:0099240	Intrinsic component of synaptic membrane	9	169	4,1640	1,55E-06	LRFN1,ABHD17A,CDH10,CHRNB1,PTPRS,CHRNA4,GABRD,NRXN1,GRIA1
GO:0031224	Intrinsic component of membrane	43	5345	0,32	2,88E-06	ITGB4,RABAC1,LRFN1,ABHD17A,CELSR1,ABCA7,SLC17A6,GRIN2D,CDH10,CHRNB1,DSCAML1,ICOS,TMEM108,LYPD6,LPHN1,PTPRS,KCNK1,CHRNA4,GABRD,AGRN,CHRM5,FAT4,JAM2,CHRNA2,NRXN1,GABRR2,SLC18A1,SLC4A10,CD44,UNC5C,CD200,GRIA1,GABRP,IGSF9B,SLC16A1,FNDC3A,ADAM8,PECAM1,GABRQ,SVOP,CNTNAP4,SLC2A11,DCHS2
GO:0005911	Cell-cell junction	13	490	0,84	2,94E-06	VCL,CDH10,DBN1,SPECC1L,CDSN,PKP4,JAM2,KLHL24,CAMSAP3,WDR1,TJP2,PECAM1,PDLIM5
GO:0044297	Cell body	14	588	0,79	3,05E-06	HOMER2,PTPRS,KCNK1,DISC1,CHRNA4,FMR1,GABRD,NRXN1,SLC4A10,KLHL24,UNC5C,CD200,GRIA1,IGSF9B
GO:0070161	Anchoring junction	16	820	0,71	4,33E-06	ITGB4,VCL,CDH10,DBN1,SPECC1L,CDSN,PKP4,JAM2,KLHL24,CD44,CAMSAP3,WDR1,TJP2,PECAM1,CPNE3,PDLIM5
GO:0009986	Cell surface	16	824	0,7	4,49E-06	ITGB4,LRFN1,ABCA7,BSN,DSCAML1,ICOS,ANXA9,CHRNA4,JAM2,NRXN1,CD44,UNC5C,CD200,GRIA1,ADAM8,PECAM1
GO:0043025	Neuronal cell body	13	518	0,82	4,87E-06	HOMER2,PTPRS,KCNK1,CHRNA4,FMR1,GABRD,NRXN1,SLC4A10,KLHL24,UNC5C,CD200,GRIA1,IGSF9B
GO:0034702	Ion channel complex	10	289	0,96	9,66E-06	GRIN2D,CHRNB1,KCNK1,CHRNA4,GABRD,CHRNA2,GABRR2,GRIA1,GABRP,GABRQ

GO:0099699	Integral component of synaptic membrane	8	157	4,4896	1,03E-05	LRFN1,CDH10,CHRNB1,PTPRS,CHRNA4,GABRD,NRXN1,GRIA1
GO:0016021	Integral component of membrane	41	5181	0,31	1,08E-05	ITGB4,RABAC1,LRFN1,CELSR1,ABCA7,SLC17A6,GRIN2D,CDH10,CHRNB1,DSCAML1,ICOS,TMEM108,LPHN1,PTPRS,KCNK1,CHRNA4,GABRD,AGRN,CHRM5,FAT4,JAM2,CHRNA2,NRXN1,GABRR2,SLC18A1,SLC4A10,CD44,UNC5C,CD200,GRIA1,GABRP,IGSF9B,SLC16A1,FNDC3A,ADAM8,PECAM1,GABRQ,SVOP,CNTNAP4,SLC2A11,DCHS2
GO:0099503	Secretory vesicle	17	1010	0,64	1,08E-05	VCL,RABAC1,SLC17A6,HCRT,BSN,PTPRS,DISC1,TPRG1L,CADPS,SLC18A1,CD44,GRIA1,FNDC3A,ADAM8,PECAM1,CPNE3,SVOP
GO:0150034	Distal axon	10	310	0,93	1,62E-05	DBN1,LPHN1,PTPRS,DISC1,FMR1,TPRG1L,NRXN1,SLC18A1,SLC4A10,UNC5C
GO:0098936	Intrinsic component of postsynaptic membrane	7	124	4,2736	2,75E-05	LRFN1,ABHD17A,CDH10,CHRNB1,PTPRS,GABRD,GRIA1
GO:0099634	Postsynaptic specialization membrane	7	126	4,2370	2,98E-05	LRFN1,ABHD17A,GRIN2D,CDH10,CHRNB1,PTPRS,GRIA1
GO:0048786	Presynaptic active zone	6	78	4,4621	3,14E-05	CDH10,BSN,RIMS3,TPRG1L,NRXN1,RIMS4
GO:0098948	Intrinsic component of postsynaptic specialization membrane	6	78	4,4621	3,14E-05	LRFN1,ABHD17A,CDH10,CHRNB1,PTPRS,GRIA1

GO:0098978	Glutamatergic synapse	10	361	0,86	5,27E-05	ABHD17A,CDH10,DBN1,BSN,HOMER2,PTPRS,GABRD,CADPS,NRXN1,GRIA1
GO:0030863	Cortical cytoskeleton	6	96	4,4197	9,21E-05	VCL,DBN1,BSN,RIMS3,WDR1,RIMS4
GO:0030057	Desmosome	4	25	2,2647	0,00014	VCL,CDSN,PKP4,KLHL24
GO:0030672	Synaptic vesicle membrane	6	105	4,2736	0,00014	SLC17A6,BSN,PTPRS,TPRG1L,SLC18A1,SVOP
GO:0048788	Cytoskeleton of presynaptic active zone	3	6	4,4897	0,00014	BSN,RIMS3,RIMS4
GO:0005912	Adherens junction	7	170	4,4621	0,00016	VCL,CDH10,PKP4,KLHL24,CAMSAP3,TJP2,PDLIM5
GO:0099055	Integral component of postsynaptic membrane	6	119	4,4896	0,00026	LRFN1,CDH10,CHRNB1,PTPRS,GABRD,GRIA1
GO:0030426	Growth cone	7	186	0,99	0,00027	DBN1,LPHN1,PTPRS,DISC1,FMR1,NRXN1,UNC5C
GO:0012506	Vesicle membrane	13	793	0,63	0,0003	SLC17A6,BSN,PTPRS,TPRG1L,CADPS,SLC18A1,CD44,GRIA1,FNDC3A,ADAM8,PECAM1,CPNE3,SVOP
GO:0099060	Integral component of postsynaptic specialization membrane	5	75	4,5292	0,00039	LRFN1,CDH10,CHRNB1,PTPRS,GRIA1

GO:0030658	Transport vesicle membrane	7	204	0,95	0,00045	SLC17A6,BSN,PTPRS,TPRG1L,SLC18A1,GRIA1,SVOP
GO:0031410	Cytoplasmic vesicle	23	2386	0,4	0,00055	VCL,RABAC1,ABHD17A,ABCA7,SLC17A6,HCRT,BSN,TMEM108,PTPRS,KCNK1,DISC1,TPRG1L,CADPS,NRXN1,FCHSD2,SLC18A1,CD44,GRIA1,FNDC3A,ADAM8,PECAM1,CPNE3,SVOP
GO:0030659	Cytoplasmic vesicle membrane	12	770	0,61	0,001	SLC17A6,BSN,PTPRS,TPRG1L,CADPS,SLC18A1,CD44,GRIA1,ADAM8,PECAM1,CPNE3,SVOP
GO:0031982	Vesicle	30	3879	0,3	0,0013	ITGB4,VCL,RABAC1,ABHD17A,ABCA7,SLC17A6,CRNN,HCRT,BSN,TMEM108,PTPRS,KCNK1,DISC1,ANXA9,TPRG1L,AGRN,CADPS,FAT4,NRXN1,FCHSD2,SLC18A1,CD44,WDR1,GRIA1,SLC16A1,FNDC3A,ADAM8,PECAM1,CPNE3,SVOP
GO:0034707	Chloride channel complex	4	49	1,2055	0,0013	GABRD,GABRR2,GABRP,GABRQ
GO:0098839	Postsynaptic density membrane	5	100	4,4896	0,0013	LRFN1,ABHD17A,GRIN2D,PTPRS,GRIA1
GO:0005892	Acetylcholine-gated channel complex	3	17	2,4108	0,0014	CHRNB1,CHRNA4,CHRNA2
GO:0098802	Plasma membrane signaling receptor complex	6	169	0,97	0,0014	ITGB4,GRIN2D,CHRNB1,CHRNA4,CHRNA2,GRIA1

GO:0099146	Intrinsic component of postsynaptic density membrane	4	55	4,6753	0,0018	LRFN1,ABHD17A,PTPRS,GRIA1
GO:0043235	Receptor complex	8	381	0,74	0,0028	ITGB4,GRIN2D,CHRNB1,CHRNA4,CHRNA2,CD44,GRIA1,GABRQ
GO:0044291	Cell-cell contact zone	4	72	4,2370	0,0048	VCL,JAM2,TJP2,PECAM1
GO:0098805	Whole membrane	17	1715	0,41	0,0053	VCL,ABHD17A,ABCA7,SLC17A6,BSN,TMEM108,LYPD6,PTPRS,TPRG1L,CADPS,SLC18A1,CD44,GRIA1,ADAM8,PECAM1,CPNE3,SVOP
GO:0002102	Podosome	3	29	1,5707	0,0056	VCL,WDR1,ADAM8
GO:0098797	Plasma membrane protein complex	9	547	0,63	0,0059	ITGB4,GRIN2D,CDH10,CHRNB1,KCNK1,CHRNA4,CHRNA2,GRIA1,ADAM8
GO:0099056	Integral component of presynaptic membrane	4	77	4,1275	0,0059	CDH10,PTPRS,CHRNA4,NRXN1
GO:0044306	Neuron projection terminus	5	147	0,95	0,0064	BSN,FMR1,TPRG1L,SLC18A1,SLC4A10
GO:0032127	Dense core granule membrane	2	6	3,4335	0,0085	CADPS,ADAM8
GO:0043204	Perikaryon	5	157	0,92	0,0085	PTPRS,KCNK1,FMR1,SLC4A10,KLHL24

GO:0098796	Membrane protein complex	13	1141	0,47	0,0085	ITGB4,GRIN2D,CDH10,CHRNB1,KCNK1,CHRNA4,GABRD,CHRNA2,GABRR2,GRIA1,GABRP,ADAM8,GABRQ
GO:0005915	Zonula adherens	2	9	2,7760	0,0159	VCL,CAMSAP3
GO:0110165	Cellular anatomical entity	75	17788	0,04	0,0162	CBLN4,NTN1,ITGB4,VCL,RABAC1,LRFN1,ABHD17A,ARHGEF9,CELSR1,ABCA7,SLC17A6,GRIN2D,CDH10,GID8,CRNN,DBN1,HCRT,BSN,CHRNB1,HOMER2,DSCAML1,ICOS,PSD3,TMEM108,SPECC1L,LYPD6,LPHN1,ATN1,PTPRS,KCNK1,DISC1,ANXA9,CHRNA4,FMR1,RIMS3,CDSN,TPRG1L,GABRD,AGRN,CHRM5,CADPS,PKP4,FAT4,JAM2,C1orf86,CHRNA2,NRXN1,GABRR2,FCHSD2,SLC18A1,SLC4A10,KLHL24,CD44,DLGAP2,UNC5C,CAMSAP3,CD200,WDR1,GRIA1,GABRP,IGSF9B,TJP2,RIMS4,SLC16A1,FNDC3A,ANKS1B,ADAM8,PECAM1,GABRQ,CPNE3,SVOP,CNTNAP4,PDLIM5,SLC2A11,DCHS2
GO:0060076	Excitatory synapse	3	51	4,3466	0,0228	SLC17A6,BSN,GRIA1
GO:0099061	Integral component of postsynaptic density membrane	3	52	4,3101	0,0238	LRFN1,PTPRS,GRIA1
GO:0031252	Cell leading edge	7	425	0,63	0,0251	ITGB4,ABCA7,DBN1,PSD3,CD44,UNC5C,GRIA1
GO:0098858	Actin-based cell projection	5	214	0,78	0,0288	HOMER2,FMR1,FCHSD2,CD44,UNC5C
GO:0043679	Axon terminus	4	128	0,91	0,0309	FMR1,TPRG1L,SLC18A1,SLC4A10
GO:0099059	Integral component of presynaptic active zone membrane	2	16	1,8629	0,0395	CDH10,NRXN1

GO:0043296	Apical junction complex	4	143	0,86	0,0448	VCL,JAM2,CAMSAP3,TJP2
GO:0030864	Cortical actin cytoskeleton	3	68	4,4713	0,0463	VCL,DBN1,WDR1
GO:0030054	Cell junction	62	2075	0,94	8,17E-51	ARHGEF5,NAMPT,SSPN,NOV,CHRNA1,ARVCF,KDR,CDH2,LRRTM2,ANO7,SIGMAR1,THY1,CXADR,C8orf37,NACC1,PDPN,GABRG1,FABP5,CHRNA5,NCAPH2,ESCO2,VAMP2,BASP1,ZNRF1,CDH26,LRFN2,SH3PXD2A,PTPRS,SEMA4F,KIRREL,DSTYK,KCNB1,AGER,GABBR1,NRCAM,SYAP1,ITSN1,CDH12,SAMD4A,MLLT4,PRIMA1,SYT12,SLC9B2,GPER1,GRIP1,ICA1,FCHSD2,NLRX1,GRIK2,RHOA,DLGAP2,FAM115C,IL31RA,KCTD16,TENM2,CACNG5,SYT7,RNF112,PRRT2,DTNA,SYT6,CPEB3
GO:0045202	Synapse	41	1351	0,95	1,62E-27	SSPN,CHRNA1,CDH2,LRRTM2,SIGMAR1,CXADR,GABRG1,FABP5,CHRNA5,VAMP2,ZNRF1,LRFN2,PTPRS,SEMA4F,KCNB1,AGER,GABBR1,NRCAM,SYAP1,ITSN1,SAMD4A,PRIMA1,SYT12,SLC9B2,GPER1,GRIP1,ICA1,FCHSD2,GRIK2,RHOA,DLGAP2,IL31RA,KCTD16,TENM2,CACNG5,SYT7,RNF112,PRRT2,DTNA,SYT6,CPEB3
GO:0097060	Synaptic membrane	24	387	4,6023	4,80E-21	SSPN,CHRNA1,CDH2,LRRTM2,SIGMAR1,GABRG1,CHRNA5,LRFN2,PTPRS,SEMA4F,KCNB1,GABBR1,NRCAM,SYAP1,GPER1,GRIP1,GRIK2,IL31RA,KCTD16,TENM2,CACNG5,SYT7,PRRT2,SYT6
GO:0098794	Postsynapse	28	643	4,4562	4,80E-21	SSPN,CHRNA1,CDH2,LRRTM2,SIGMAR1,GABRG1,FABP5,CHRNA5,LRFN2,PTPRS,SEMA4F,KCNB1,AGER,GABBR1,NRCAM,SYAP1,ITSN1,GPER1,GRIP1,GRIK2,RHOA,DLGAP2,KCTD16,TENM2,CACNG5,RNF112,PRRT2,CPEB3

GO:0098590	Plasma membrane region	34	1219	0,91	9,47E-21	SSPN,CHRNA1,CDH2,LRRTM2,SIGMAR1,THY1,CXADR,PDPN,GABRG1,CHRNA5,LRFN2,PTPRS,SEMA4F,KIRREL,DSTYK,KCNB1,AGER,GABBR1,NRCAM,SYAP1,ITSN1,SLC9B2,GPER1,GRIP1,FCHSD2,GRIK2,RHOA,IL31RA,KCTD16,TENM2,CACNG5,SYT7,PRRT2,SYT6
GO:0045211	Postsynaptic membrane	20	281	1,1689	2,35E-18	SSPN,CHRNA1,CDH2,LRRTM2,SIGMAR1,GABRG1,CHRNA5,LRFN2,PTPRS,SEMA4F,KCNB1,GABBR1,NRCAM,SYAP1,GRIP1,GRIK2,KCTD16,TENM2,CACNG5,PRRT2
GO:0005886	Plasma membrane	55	5314	0,48	3,09E-18	ARHGEF5,NAMPT,SSPN,CHRNA1,ARVCF,KDR,CDH2,LRRTM2,ANO7,SIGMAR1,THY1,CXADR,C8orf37,PDPN,GABRG1,FABP5,CHRNA5,VAMP2,BASP1,CDH26,ICAM4,LRFN2,PTPRS,SEMA4F,KIRREL,DSTYK,KCNB1,AGER,GABBR1,NRCAM,SYAP1,ITSN1,GPNMB,CDH12,MLLT4,PRIMA1,SYT12,SLC9B2,GPER1,GRIP1,FCHSD2,NLRX1,GRIK2,RHOA,DLGAP2,FAM115C,IL31RA,KCTD16,TENM2,CACNG5,SYT7,ADAM8,PRRT2,DTNA,SYT6
GO:0043005	Neuron projection	31	1366	0,82	3,49E-16	NOV,CHRNA1,CDH2,SIGMAR1,THY1,CXADR,GABRG1,CHRNA5,VAMP2,BASP1,PTPRS,SEMA4F,KIRREL,KCNB1,GABBR1,NRCAM,SYAP1,ITSN1,SAMD4A,GPER1,GRIP1,FCHSD2,GRIK2,RHOA,IL31RA,TENM2,SYT7,RNF112,PRRT2,DTNA,CPEB3
GO:0042995	Cell projection	37	2287	0,67	1,82E-15	ARHGEF5,NOV,CHRNA1,CDH2,SIGMAR1,THY1,CXADR,C8orf37,PDPN,GABRG1,CHRNA5,VAMP2,BASP1,SH3PXD2A,PTPRS,SEMA4F,KIRREL,KCNB1,GABBR1,NRCAM,SYAP1,ITSN1,SAMD4A,SLC9B2,GPER1,GRIP1,FCHSD2,GRIK2,RHOA,IL31RA,KCTD16,TENM2,SYT7,RNF112,PRRT2,DTNA,CPEB3
GO:0098984	Neuron to neuron synapse	18	374	4,2005	1,02E-13	CDH2,LRRTM2,SIGMAR1,FABP5,LRFN2,PTPRS,SEMA4F,NRCAM,SYT12,GPER1,GRIP1,GRIK2,DLGAP2,CACNG5,SYT7,RNF112,PRRT2,CPEB3

GO:0120025	Plasma membrane bounded cell projection	34	2193	0,66	2,63E-13	NOV,CHRNA1,CDH2,SIGMAR1,THY1,CXADR,C8orf37,PDPN,GABRG1,CHRNA5,VAMP2,BASP1,PTPRS,SEMA4F,KIRREL,KCNB1,GABBR1,NRCAM,SYAP1,ITSN1,SAMD4A,SLC9B2,GPER1,GRIP1,FCHSD2,GRIK2,RHOA,IL31RA,TENM2,SYT7,RNF112,PRRT2,DTNA,CPEB3
GO:0099572	Postsynaptic specialization	17	369	4,1275	1,24E-12	CHRNA1,CDH2,LRRTM2,SIGMAR1,FABP5,LRFN2,PTPRS,SEMA4F,NRCAM,GPER1,GRIP1,GRIK2,DLGAP2,CACNG5,RNF112,PRRT2,CPEB3
GO:0005887	Integral component of plasma membrane	29	1623	0,72	2,15E-12	SSPN,CHRNA1,KDR,CDH2,LRRTM2,SIGMAR1,THY1,CXADR,PDPN,GABRG1,CHRNA5,VAMP2,ICAM4,LRFN2,PTPRS,SEMA4F,KCNB1,AGER,GABBR1,NRCAM,GPNMB,GPER1,GRIK2,TENM2,CACNG5,SYT7,ADAM8,PRRT2,SYT6
GO:0014069	Postsynaptic density	16	344	4,1275	6,38E-12	CDH2,LRRTM2,SIGMAR1,FABP5,LRFN2,PTPRS,SEMA4F,NRCAM,GPER1,GRIP1,GRIK2,DLGAP2,CACNG5,RNF112,PRRT2,CPEB3
GO:0098793	Presynapse	18	526	1	1,76E-11	CDH2,VAMP2,ZNRF1,PTPRS,GABBR1,SYAP1,ITSN1,SYT12,SLC9B2,GPER1,ICA1,GRIK2,IL31RA,KCTD16,SYT7,RNF112,PRRT2,SYT6
GO:0016020	Membrane	59	9072	0,28	9,88E-11	ARHGEF5,NAMPT,SSPN,CHRNA1,ARVCF,KDR,CDH2,LRRTM2,ANO7,SIGMAR1,THY1,CXADR,C8orf37,PDPN,GABRG1,FABP5,CHRNA5,NCAPH2,VAMP2,BASP1,ZNRF1,CDH26,ICAM4,LRFN2,PTPRS,SEMA4F,KIRREL,DSTYK,KCNB1,AGER,GABBR1,NRCAM,SYAP1,ITSN1,GPNMB,CDH12,MLLT4,PRIMA1,SYT12,SLC9B2,GPER1,GRIP1,ICA1,FCHSD2,NLRX1,GRIK2,RHOA,DLGAP2,FAM115C,IL31RA,KCTD16,TENM2,CACNG5,SYT7,ADAM8,RNF112,PRRT2,DTNA,SYT6
GO:0030424	Axon	18	646	0,91	4,51E-10	NOV,SIGMAR1,THY1,CXADR,BASP1,PTPRS,KCNB1,NRCAM,SYAP1,ITSN1,GPER1,GRIK2,RHOA,IL31RA,TENM2,SYT7,PRRT2,DTNA

GO:0030425	Dendrite	17	612	0,91	1,96E-09	NOV,THY1,SEMA4F,KIRREL,KCNB1,GABBR1,SYAP1,ITSN1,SAMD4A,GPER1,GRIP1,GRIK2,RHOA,TENM2,SYT7,PRRT2,CPEB3
GO:0099634	Postsynaptic specialization membrane	10	126	1,3516	2,38E-09	CHRNA1,CDH2,LRRTM2,SIGMAR1,LRFN2,PTPRS,NRCAM,GRIK2,CACNG5,PRRT2
GO:0036477	Somatodendritic compartment	19	852	0,81	3,69E-09	NOV,THY1,PTPRS,SEMA4F,KIRREL,KCNB1,GABBR1,SYAP1,ITSN1,SAMD4A,GPER1,GRIP1,GRIK2,RHOA,TENM2,SYT7,RNF112,PRRT2,CPEB3
GO:0030672	Synaptic vesicle membrane	9	105	4,4652	1,19E-08	VAMP2,ZNRF1,PTPRS,SYT12,SLC9B2,ICA1,SYT7,PRRT2,SYT6
GO:0099699	Integral component of synaptic membrane	10	157	4,6388	1,55E-08	CHRNA1,CDH2,LRRTM2,LRFN2,PTPRS,NRCAM,CACNG5,SYT7,PRRT2,SYT6
GO:0042734	Presynaptic membrane	10	158	4,6388	1,59E-08	CDH2,PTPRS,GABBR1,SYAP1,GPER1,GRIK2,IL31RA,KCTD16,SYT7,PRRT2
GO:0150034	Distal axon	12	310	4,4682	4,68E-08	SIGMAR1,THY1,CXADR,BASP1,PTPRS,SYAP1,ITSN1,GPER1,GRIK2,TENM2,SYT7,PRRT2
GO:0008021	Synaptic vesicle	10	203	4,2370	1,45E-07	VAMP2,ZNRF1,PTPRS,SYT12,SLC9B2,ICA1,SYT7,RNF112,PRRT2,SYT6
GO:0098839	Postsynaptic density membrane	8	100	1,3516	1,71E-07	LRRTM2,SIGMAR1,LRFN2,PTPRS,NRCAM,GRIK2,CACNG5,PRRT2
GO:0098805	Whole membrane	22	1715	0,57	1,61E-06	KDR,CDH2,SIGMAR1,THY1,CXADR,PDPN,FABP5,VAMP2,ZNRF1,PTPRS,KIRREL,GPNMB,SYT12,SLC9B2,GRIP1,ICA1,NLRX1,RHOA,SYT7,ADAM8,PRRT2,SYT6

GO:0016021	Integral component of membrane	39	5181	0,34	2,22E-06	SSPN,CHRNA1,KDR,CDH2,LRRTM2,ANO7,SIGMAR1,THY1,CXADR,PDPN,GABRG1,CHRNA5,VAMP2,CDH26,ICAM4,LRFN2,PTPRS,SEMA4F,KIRREL,KCNB1,AGER,GABBR1,NRCAM,GPNMB,CDH12,MLLT4,PRIMA1,SYT12,SLC9B2,GPER1,GRIK2,IL31RA,TENM2,CACNG5,SYT7,ADAM8,RNF112,PRRT2,SYT6
GO:0098978	Glutamatergic synapse	11	361	0,95	2,23E-06	LRRTM2,PTPRS,NRCAM,ITSN1,GRIP1,GRIK2,RHOA,CACNG5,SYT7,PRRT2,SYT6
GO:0030133	Transport vesicle	11	407	0,9	6,86E-06	SSPN,VAMP2,ZNRF1,PTPRS,SYT12,SLC9B2,ICA1,SYT7,RNF112,PRRT2,SYT6
GO:0098686	Hippocampal mossy fiber to ca3 synapse	5	34	2,3012	8,89E-06	LRRTM2,SYT12,GPER1,GRIK2,SYT7
GO:0099055	Integral component of postsynaptic membrane	7	119	4,4927	9,93E-06	CHRNA1,CDH2,LRRTM2,LRFN2,PTPRS,NRCAM,CACNG5
GO:0030659	Cytoplasmic vesicle membrane	14	770	0,73	1,26E-05	FABP5,VAMP2,ZNRF1,PTPRS,GPNMB,SYT12,SLC9B2,GPER1,ICA1,RHOA,SYT7,ADAM8,PRRT2,SYT6
GO:0099060	Integral component of postsynaptic specialization membrane	6	75	1,3516	1,29E-05	CHRNA1,CDH2,LRRTM2,LRFN2,PTPRS,NRCAM
GO:0044297	Cell body	12	588	0,78	2,78E-05	NOV,THY1,CXADR,PTPRS,SEMA4F,KCNB1,SYAP1,ITSN1,GRIP1,GRIK2,SYT7,RNF112
GO:0043204	Perikaryon	7	157	4,4866	5,04E-05	PTPRS,SEMA4F,KCNB1,SYAP1,GRIP1,GRIK2,RNF112
GO:0043025	Neuronal cell body	11	518	0,79	5,58E-05	NOV,THY1,PTPRS,SEMA4F,KCNB1,SYAP1,ITSN1,GRIP1,GRIK2,SYT7,RNF112

GO:0031410	Cytoplasmic vesicle	23	2386	0,45	7,98E-05	SSPN,KDR,SIGMAR1,CXADR,PDPN,FABP5,VAMP2,ZNRF1,PTPRS,ITSN1,GPNMB,SYT12,SLC9B2,GPER1,GRIP1,ICA1,FCHSD2,RHOA,SYT7,ADAM8,RNF112,PRRT2,SYT6
GO:0098797	Plasma membrane protein complex	11	547	0,77	8,80E-05	SSPN,CHRNA1,CDH2,CHRNA5,CDH26,KCNB1,GABBR1,CDH12,GRIK2,CACNG5,ADAM8
GO:0030426	Growth cone	7	186	4,4652	0,00013	SIGMAR1,THY1,CXADR,BASP1,PTPRS,SYAP1,TENM2
GO:0005911	Cell-cell junction	10	490	0,78	0,00021	NOV,ARVCF,CDH2,CXADR,CDH26,KIRREL,CDH12,MLLT4,RHOA,TENM2
GO:0043235	Receptor complex	9	381	0,84	0,00021	CHRNA1,KDR,GABRG1,CHRNA5,GABBR1,GRIK2,IL31RA,KCTD16,CACNG5
GO:0099503	Secretory vesicle	14	1010	0,61	0,00022	CXADR,FABP5,VAMP2,ZNRF1,PTPRS,SYT12,SLC9B2,ICA1,RHOA,SYT7,ADAM8,RNF112,PRRT2,SYT6
GO:0019898	Extrinsic component of membrane	8	298	0,89	0,00027	CDH2,CDH26,SYAP1,CDH12,RHOA,RNF112,DTNA,SYT6
GO:0031982	Vesicle	29	3879	0,34	0,00032	NAMPT,SSPN,KDR,SIGMAR1,THY1,CXADR,PDPN,FABP5,VAMP2,BASP1,ZNRF1,UBA1,PTPRS,S100A14,SYAP1,ITSN1,GPNMB,SYT12,SLC9B2,GPER1,GRIP1,ICA1,FCHSD2,RHOA,SYT7,ADAM8,RNF112,PRRT2,SYT6
GO:0044306	Neuron projection terminus	6	147	4,4774	0,00039	VAMP2,ITSN1,GPER1,GRIK2,SYT7,PRRT2
GO:0032590	Dendrite membrane	4	44	1,5342	0,0006	THY1,GABRG1,KCNB1,GPER1
GO:0019897	Extrinsic component of plasma membrane	6	166	4,4593	0,00073	CDH2,CDH26,SYAP1,CDH12,RHOA,DTNA

GO:0098796	Membrane protein complex	14	1141	0,55	0,00077	SSPN,CHRNA1,CDH2,GABRG1,CHRNA5,VAMP2,CDH26,KCNB1,GABBR1,CDH12,MLLT4,GRIK2,CACNG5,ADAM8
GO:0005912	Adherens junction	6	170	4,4562	0,0008	ARVCF,CDH2,CXADR,CDH26,CDH12,MLLT4
GO:0031256	Leading edge membrane	6	174	1	0,0009	THY1,PDPN,GABRG1,KCNB1,GPER1,RHOA
GO:0099061	Integral component of postsynaptic density membrane	4	52	1,2785	0,001	LRRTM2,LRFN2,PTPRS,NRCAM
GO:0043679	Axon terminus	5	128	4,4713	0,0022	ITSN1,GPER1,GRIK2,SYT7,PRRT2
GO:0031252	Cell leading edge	8	425	0,74	0,0026	CDH2,THY1,PDPN,GABRG1,KCNB1,ITSN1,GPER1,RHOA
GO:0070161	Anchoring junction	11	820	0,59	0,0026	NOV,ARVCF,CDH2,THY1,CXADR,CDH26,KIRREL,CDH12,MLLT4,RHOA,TENM2
GO:0045121	Membrane raft	7	324	0,8	0,0031	KDR,CDH2,THY1,CXADR,PDPN,KIRREL,GRIP1
GO:0002102	Podosome	3	29	1,7533	0,0039	ARHGEF5,SH3PXD2A,ADAM8
GO:0031253	Cell projection membrane	7	338	0,78	0,0039	THY1,PDPN,GABRG1,KIRREL,KCNB1,GPER1,RHOA
GO:0099056	Integral component of presynaptic membrane	4	77	4,3101	0,0039	CDH2,PTPRS,SYT7,PRRT2
GO:0016342	Catenin complex	3	30	1,7168	0,0042	CDH2,CDH26,CDH12

GO:0012505	Endomembrane system	29	4542	0,27	0,0049	SSPN,KDR,CDH2,ANO7,SIGMAR1,THY1,CXADR,FABP5,ESCO2,VAMP2,ZNRF1,PTPRS,SEMA4F,SYAP1,ITSN1,GPNMB,SYT12,SLC9B2,GPER1,GRIP1,ICA1,FCHSD2,RHOA,TENM2,SYT7,ADAM8,RNF112,PRRT2,SYT6
GO:0098685	Schaffer collateral - CA1 synapse	4	84	4,1640	0,0049	LRRTM2,LRFN2,PTPRS,GABBR1
GO:0098802	Plasma membrane signaling receptor complex	5	169	0,94	0,0066	CHRNA1,CHRNA5,GABBR1,GRIK2,CACNG5
GO:0043197	Dendritic spine	5	173	0,93	0,0073	ITSN1,GPER1,RHOA,TENM2,PRRT2
GO:0034702	Ion channel complex	6	289	0,78	0,0101	CHRNA1,GABRG1,CHRNA5,KCNB1,GRIK2,CACNG5
GO:0042383	Sarcolemma	4	132	0,95	0,0233	SSPN,CDH2,KCNB1,DTNA
GO:0016324	Apical plasma membrane	6	350	0,7	0,0256	CDH2,THY1,PDPN,DSTYK,AGER,SLC9B2
GO:0016323	Basolateral plasma membrane	5	237	0,79	0,0267	CDH2,CXADR,PDPN,DSTYK,SLC9B2

GO:0110165	Cellular anatomical entity	67	17788	0,04	0,0319	ARHGEF5,NAMPT,SSPN,NOV,CHRNA1,ARVCF,KDR,CDH2,LRRTM2,ANO7,SIGMAR1,THY1,CXADR,C8orf37,NACC1,PDPN,GABRG1,FABP5,CHRNA5,NCAPH2,ESCO2,VAMP2,BASP1,ZNRF1,UBA1,CDH26,ICAM4,LRFN2,SH3PXD2A,PTPRS,SEMA4F,KIRREL,DSTYK,S100A14,KCNB1,AGER,GABBR1,NRCAM,SYAP1,ITSN1,GPNMB,CDH12,SAMD4A,MLLT4,PRIMA1,SYT12,SLC9B2,GPER1,GRIP1,ICA1,FCHSD2,NLRX1,GRIK2,RHOA,DLGAP2,FAM115C,IL31RA,KCTD16,TENM2,CACNG5,SYT7,ADAM8,RNF112,PRRT2,DTNA,SYT6,CPEB3
GO:0098588	Bounding membrane of organelle	16	2107	0,35	0,032	SIGMAR1,FABP5,VAMP2,ZNRF1,PTPRS,GPNMB,SYT12,SLC9B2,GPER1,ICA1,NLRX1,RHOA,SYT7,ADAM8,PRRT2,SYT6
GO:0005892	Acetylcholine-gated channel complex	2	17	1,9725	0,0345	CHRNA1,CHRNA5
GO:0097440	Apical dendrite	2	18	1,8629	0,0379	ITSN1,CPEB3
GO:0044291	Cell-cell contact zone	3	72	4,4805	0,0385	CDH2,CXADR,MLLT4
GO:0098982	GABA-ergic synapse	3	74	4,4743	0,0411	LRRTM2,GABBR1,SYT7
GO:0031594	Neuromuscular junction	3	77	4,4713	0,0453	CHRNA1,CXADR,FCHSD2
GO:0030054	Cell junction	52	2075	0,93	1,55E-41	LRRC7,PKP2,CDH1,CACNA1C,BIN2,GLRA3,LRRC4C,TJP1,GRIA4,SHANK1,TRIM9,LRRK2,CTNNA1,NLGN2,SPHK1,SLC17A8,SYT9,GPR142,EPB41,ARC,DSG4,KCTD8,ATP2B2,ENAH,SYT2,GOPC,RAB13,OLFM1,NCS1,KAZN,DLG2,GAD2,KCTD12,NPHP4,NRCAM,NHS,IGSF5,PANX2,GRIK1,CTNNA2,NRXN1,SDK1,CTNNA3,UNC5C,GABRR1,GPHN,GABRA2,CDHR2,CPEB1,SVOP,GABRG3,SYN2

GO:0045202	Synapse	40	1351	4,4562	2,26E-30	LRRC7,CDH1,CACNA1C,GLRA3,LRRC4C,GRIA4,SHANK1,TRIM9,LRRK2,NLGN2,SPHK1,SLC17A8,SYT9,EPB41,ARC,KCTD8,ATP2B2,ENAH,SYT2,GOPC,RAB13,OLFM1,NCS1,DLG2,GAD2,KCTD12,NPHP4,NRCAM,GRIK1,CTNNA2,NRXN1,SDK1,UNC5C,GABRR1,GPHN,GABRA2,CPEB1,SVOP,GABRG3,SYN2
GO:0098590	Plasma membrane region	32	1219	0,95	4,52E-21	LRRC7,CDH1,PKD1,CACNA1C,GLRA3,LRRC4C,TJP1,GRIA4,SHANK1,LRRK2,CTNNA1,NLGN2,SPHK1,EPB41,ARC,KCTD8,ATP2B2,PKHD1,DLG2,GAD2,KCTD12,NRCAM,NHS,IGSF5,GRIK1,CTNNA2,NRXN1,GABRR1,GPHN,GABRA2,CDHR2,GABRG3
GO:0042995	Cell projection	39	2287	0,77	8,43E-21	LRRC7,CDH1,PKD1,CACNA1C,BIN2,GLRA3,TJP1,GRIA4,SHANK1,TRIM9,LRRK2,CTNNA1,NLGN2,SLC17A8,ARC,KCTD8,ENAH,SYT2,GOPC,RAB13,PKHD1,OLFM1,NCS1,DLG2,GAD2,KCTD12,NPHP4,NRCAM,NHS,CTNNA2,NRXN1,CTNNA3,UNC5C,GABRR1,GPHN,GABRA2,CDHR2,CPEB1,GABRG3
GO:0098794	Postsynapse	26	643	4,1640	8,43E-21	LRRC7,CDH1,CACNA1C,GLRA3,LRRC4C,GRIA4,SHANK1,LRRK2,NLGN2,EPB41,ARC,KCTD8,ATP2B2,GOPC,NCS1,DLG2,KCTD12,NRCAM,GRIK1,CTNNA2,GABRR1,GPHN,GABRA2,CPEB1,GABRG3,SYN2
GO:0097060	Synaptic membrane	20	387	4,5658	2,32E-17	CACNA1C,GLRA3,LRRC4C,GRIA4,SHANK1,NLGN2,ARC,KCTD8,ATP2B2,DLG2,GAD2,KCTD12,NRCAM,GRIK1,CTNNA2,NRXN1,GABRR1,GPHN,GABRA2,GABRG3
GO:0045211	Postsynaptic membrane	18	281	1,2420	5,18E-17	CACNA1C,GLRA3,LRRC4C,GRIA4,SHANK1,NLGN2,ARC,KCTD8,ATP2B2,DLG2,KCTD12,NRCAM,GRIK1,CTNNA2,GABRR1,GPHN,GABRA2,GABRG3
GO:0005886	Plasma membrane	48	5314	0,49	9,16E-17	LRRC7,PKP2,CDH1,CD33,PKD1,CACNA1C,BIN2,GLRA3,LRRC4C,TJP1,GRIA4,SHANK1,LRRK2,CTNNA1,NLGN2,SPHK1,SYT9,GPR142,EPB41,ARC,DSG4,KCTD8,ATP2B2,ENAH,SYT2,GOPC,RAB13,PKHD1,NCS1,KAZN,DLG2,GAD2,KCTD12,NRCAM,NHS,IGSF5,PANX2,GRIK1,CTNNA2,NRXN1,SDK1,UNC5C,GABRR1,GPHN,GABRA2,CDHR2,GABRG3,SYN2

GO:0098984	Neuron to neuron synapse	19	374	4,5292	2,09E-16	LRRC7,CACNA1C,LRRC4C,GRIA4,SHANK1,NLGN2,SYT9,EPB41,ARC,ATP2B2,GOPC,NCS1,DLG2,NRCAM,GRIK1,CTNNA2,GPHN,CPEB1,SYN2
GO:0120025	Plasma membrane bounded cell projection	34	2193	0,73	3,43E-16	LRRC7,CDH1,PKD1,CACNA1C,GLRA3,GRIA4,SHANK1,TRIM9,LRRK2,CTNNA1,SLC17A8,ARC,ENAH,SYT2,GOPC,RAB13,PKHD1,OLFM1,NCS1,DLG2,GAD2,NPHP4,NRCAM,NHS,CTNNA2,NRXN1,CTNNA3,UNC5C,GABRR1,GPHN,GABRA2,CDHR2,CPEB1,GABRG3
GO:0099572	Postsynaptic specialization	18	369	4,4562	2,99E-15	LRRC7,CACNA1C,LRRC4C,GRIA4,SHANK1,NLGN2,EPB41,ARC,ATP2B2,GOPC,NCS1,DLG2,NRCAM,GRIK1,CTNNA2,GPHN,CPEB1,SYN2
GO:0014069	Postsynaptic density	17	344	4,4927	2,03E-14	LRRC7,CACNA1C,LRRC4C,GRIA4,SHANK1,EPB41,ARC,ATP2B2,GOPC,NCS1,DLG2,NRCAM,GRIK1,CTNNA2,GPHN,CPEB1,SYN2
GO:0098793	Presynapse	19	526	4,4805	5,34E-14	TRIM9,LRRK2,NLGN2,SPHK1,SLC17A8,SYT9,KCTD8,ATP2B2,SYT2,RAB13,NCS1,GAD2,KCTD12,GRIK1,CTNNA2,NRXN1,GABRA2,SVOP,SYN2
GO:0043005	Neuron projection	25	1366	0,8	1,72E-12	LRRC7,CACNA1C,GLRA3,GRIA4,SHANK1,TRIM9,LRRK2,SLC17A8,ARC,SYT2,GOPC,RAB13,OLFM1,NCS1,DLG2,GAD2,NRCAM,CTNNA2,NRXN1,UNC5C,GABRR1,GPHN,GABRA2,CPEB1,GABRG3
GO:0099634	Postsynaptic specialization membrane	10	126	1,6072	5,99E-10	CACNA1C,LRRC4C,GRIA4,NLGN2,ARC,ATP2B2,DLG2,NRCAM,GRIK1,GPHN
GO:0016020	Membrane	51	9072	0,29	9,12E-10	LRRC7,PKP2,CDH1,CD33,PKD1,CACNA1C,BIN2,GLRA3,LRRC4C,TJP1,GRIA4,SHANK1,LRRK2,CTNNA1,NLGN2,SPHK1,SLC17A8,SYT9,GPR142,EPB41,ARC,DSG4,KCTD8,ATP2B2,ENAH,SYT2,GOPC,RAB13,PKHD1,NCS1,KAZN,DLG2,GAD2,KCTD12,NRCAM,NHS,IGSF5,PANX2,GRIK1,CTNNA2,NRXN1,SDK1,UNC5C,GABRR1,GPHN,GABRA2,CDHR2,CPEB1,SVOP,GABRG3,SYN2

GO:0005911	Cell-cell junction	14	490	0,99	1,14E-08	LRRC7,PKP2,CDH1,TJP1,CTNNA1,DSG4,RAB13,KAZN,NPHP4,NHS,IGSF5,PANX2,CTNNA2,CTNNA3
GO:0008021	Synaptic vesicle	10	203	4,4927	4,32E-08	TRIM9,LRRK2,SLC17A8,SYT9,SYT2,RAB13,GAD2,GABRA2,SVOP,SYN2
GO:0098978	Glutamatergic synapse	12	361	4,4713	4,95E-08	CDH1,LRRC4C,SHANK1,LRRK2,ARC,ATP2B2,NCS1,DLG2,NRCAM,NRXN1,GABRR1,SYN2
GO:0098839	Postsynaptic density membrane	8	100	1,6072	6,60E-08	CACNA1C,LRRC4C,GRIA4,ARC,ATP2B2,DLG2,NRCAM,GRIK1
GO:0030672	Synaptic vesicle membrane	8	105	1,5342	8,99E-08	LRRK2,SLC17A8,SYT9,SYT2,GAD2,GABRA2,SVOP,SYN2
GO:0036477	Somatodendritic compartment	16	852	0,81	1,29E-07	CACNA1C,GLRA3,GRIA4,SHANK1,TRIM9,LRRK2,SLC17A8,ARC,GOPC,OLFM1,NCS1,DLG2,NRXN1,UNC5C,GPHN,CPEB1
GO:0070161	Anchoring junction	15	820	0,8	6,25E-07	LRRC7,PKP2,CDH1,TJP1,CTNNA1,DSG4,ENAH,RAB13,KAZN,NPHP4,NHS,IGSF5,PANX2,CTNNA2,CTNNA3
GO:0030425	Dendrite	13	612	0,86	1,26E-06	CACNA1C,GLRA3,GRIA4,SHANK1,TRIM9,LRRK2,SLC17A8,ARC,GOPC,NCS1,UNC5C,GPHN,CPEB1
GO:0099503	Secretory vesicle	16	1010	0,74	1,26E-06	LRRC7,CD33,BIN2,TRIM9,LRRK2,CTNNA1,SLC17A8,SYT9,ARC,SYT2,RAB13,NCS1,GAD2,GABRA2,SVOP,SYN2
GO:0030133	Transport vesicle	11	407	0,97	1,51E-06	TRIM9,LRRK2,SLC17A8,SYT9,SYT2,GOPC,RAB13,GAD2,GABRA2,SVOP,SYN2
GO:0030027	Lamellipodium	8	202	4,1275	8,42E-06	CDH1,CTNNA1,ENAH,RAB13,NHS,CTNNA2,CTNNA3,UNC5C
GO:0034702	Ion channel complex	9	289	4,4621	9,04E-06	PKD1,CACNA1C,GLRA3,GRIA4,SHANK1,GRIK1,GABRR1,GABRA2,GABRG3

GO:0043296	Apical junction complex	7	143	4,4927	1,23E-05	CDH1,TJP1,CTNNA1,RAB13,NPHP4,NHS,IGSF5
GO:0030424	Axon	12	646	0,8	1,53E-05	LRRC7,LRRK2,SLC17A8,SYT2,OLFM1,NCS1,DLG2,GAD2,NRCAM,CTNNA2,NRXN1,UNC5C
GO:0031410	Cytoplasmic vesicle	22	2386	0,5	1,73E-05	LRRC7,CDH1,CD33,PKD1,BIN2,GRIA4,TRIM9,LRRK2,CTNNA1,SPHK1,SLC17A8,SYT9,ARC,SYT2,GOPC,RAB13,NCS1,GAD2,NRXN1,GABRA2,SVOP,SYN2
GO:0031252	Cell leading edge	10	425	0,91	1,82E-05	CDH1,CTNNA1,ENAH,RAB13,NHS,CTNNA2,CTNNA3,UNC5C,GABRA2,GABRG3
GO:0042734	Presynaptic membrane	7	158	4,3101	1,96E-05	NLGN2,KCTD8,GAD2,KCTD12,GRIK1,CTNNA2,NRXN1
GO:0005912	Adherens junction	7	170	4,2005	3,08E-05	LRRC7,PKP2,CDH1,TJP1,CTNNA1,CTNNA2,CTNNA3
GO:0043025	Neuronal cell body	10	518	0,82	9,78E-05	CACNA1C,GLRA3,GRIA4,LRRK2,SLC17A8,ARC,OLFM1,DLG2,NRXN1,UNC5C
GO:0098982	GABA-ergic synapse	5	74	1,3516	0,00012	NLGN2,ATP2B2,NRXN1,GABRR1,GABRG3
GO:0098805	Whole membrane	17	1715	0,53	0,00019	CDH1,CD33,PKD1,GRIA4,LRRK2,CTNNA1,SPHK1,SLC17A8,SYT9,ARC,SYT2,GOPC,RAB13,GAD2,GABRA2,SVOP,SYN2
GO:0043204	Perikaryon	6	157	4,4896	0,00028	CACNA1C,GLRA3,LRRK2,SLC17A8,OLFM1,DLG2
GO:0030659	Cytoplasmic vesicle membrane	11	770	0,69	0,00044	CD33,GRIA4,LRRK2,SLC17A8,SYT9,SYT2,RAB13,GAD2,GABRA2,SVOP,SYN2
GO:0099523	Presynaptic cytosol	3	14	3,1778	0,00052	TRIM9,LRRK2,NCS1

GO:0034707	Chloride channel complex	4	49	1,6438	0,00056	GLRA3,GABRR1,GABRA2,GABRG3
GO:0031226	Intrinsic component of plasma membrane	16	1703	0,51	0,00065	CD33,PKD1,CACNA1C,GLRA3,LRRC4C,GRIA4,SHANK1,NLGN2,PKHD1,NRCAM,GRIK1 ,NRXN1,GABRR1,GABRA2,CDHR2,GABRG3
GO:0005923	Bicellular tight junction	5	122	4,2005	0,001	TJP1,RAB13,NPHP4,NHS,IGSF5
GO:0031982	Vesicle	25	3879	0,34	0,001	LRRC7,CDH1,CD33,PKD1,BIN2,GRIA4,TRIM9,LRRK2,CTNNA1,SPHK1,SLC17A8,SYT9, ARC,ATP2B2,SYT2,GOPC,RAB13,PKHD1,NCS1,GAD2,NRXN1,GABRA2,CDHR2,SVOP, SYN2
GO:0005887	Integral component of plasma membrane	15	1623	0,5	0,0014	CD33,PKD1,CACNA1C,GLRA3,LRRC4C,GRIA4,SHANK1,NLGN2,NRCAM,GRIK1,NRXN1 ,GABRR1,GABRA2,CDHR2,GABRG3
GO:0031224	Intrinsic component of membrane	30	5345	0,28	0,0014	PKP2,CDH1,CD33,PKD1,CACNA1C,GLRA3,LRRC4C,GRIA4,SHANK1,NLGN2,SLC17A8, SYT9,GPR142,DSG4,ATP2B2,SYT2,PKHD1,GAD2,NRCAM,IGSF5,PANX2,GRIK1,NRXN 1,SDK1,UNC5C,GABRR1,GABRA2,CDHR2,SVOP,GABRG3
GO:0016021	Integral component of membrane	29	5181	0,28	0,0021	PKP2,CDH1,CD33,PKD1,CACNA1C,GLRA3,LRRC4C,GRIA4,SHANK1,NLGN2,SLC17A8, SYT9,GPR142,DSG4,ATP2B2,SYT2,PKHD1,NRCAM,IGSF5,PANX2,GRIK1,NRXN1,SDK 1,UNC5C,GABRR1,GABRA2,CDHR2,SVOP,GABRG3
GO:0016323	Basolateral plasma membrane	6	237	0,94	0,0021	LRRC7,PKD1,TJP1,EPB41,DLG2,CTNNA2
GO:0030057	Desmosome	3	25	2,2282	0,0021	PKP2,DSG4,KAZN

GO:0031045	Dense core granule	3	26	4,4713	0,0022	SYT9,SYT2,NCS1
GO:0098796	Membrane protein complex	12	1141	0,56	0,0026	CDH1,PKD1,CACNA1C,GLRA3,GRIA4,SHANK1,CTNNA1,GRIK1,GABRR1,GABRA2,GABRG3,SYN2
GO:0099699	Integral component of synaptic membrane	5	157	4,4652	0,0028	LRRC4C,NLGN2,NRCAM,NRXN1,GABRG3
GO:0043235	Receptor complex	7	381	0,8	0,0032	GRIA4,SHANK1,KCTD8,KCTD12,GRIK1,GABRA2,GABRG3
GO:0098685	Schaffer collateral - CA1 synapse	4	84	4,4197	0,0032	LRRC4C,SHANK1,NRXN1,SYN2
GO:0030285	Integral component of synaptic vesicle membrane	3	35	1,7168	0,0045	SLC17A8,SYT9,GABRA2
GO:0030136	Clathrin-coated vesicle	5	191	0,95	0,0063	SYT9,SYT2,GOPC,RAB13,GAD2
GO:0150034	Distal axon	6	310	0,82	0,0072	LRRK2,SLC17A8,OLFM1,NCS1,NRXN1,UNC5C
GO:0008328	Ionotropic glutamate receptor complex	3	43	1,3881	0,0076	GRIA4,SHANK1,GRIK1
GO:0001533	Cornified envelope	3	45	1,3150	0,0085	PKP2,DSG4,KAZN
GO:0016600	Flotillin complex	2	8	3,3970	0,0085	CDH1,CTNNA1

GO:0034703	Cation channel complex	5	214	0,9	0,0097	PKD1,CACNA1C,GRIA4,SHANK1,GRIK1
GO:0005856	Cytoskeleton	16	2221	0,39	0,01	LRRC7,PKP2,CDH1,BIN2,TJP1,TRIM9,CTNNA1,EPB41,ARC,ENAH,PKHD1,KAZN,NPHP4,CTNNA2,CTNNA3,GPHN
GO:0014704	Intercalated disc	3	51	1,1324	0,0112	PKP2,CTNNA1,CTNNA3
GO:0060076	Excitatory synapse	3	51	1,1324	0,0112	SHANK1,SLC17A8,CTNNA2
GO:0030141	Secretory granule	9	845	0,56	0,0155	LRRC7,CD33,BIN2,CTNNA1,SYT9,ARC,SYT2,RAB13,NCS1
GO:0089717	Spanning component of membrane	2	12	2,7760	0,0155	NLGN2,CDHR2
GO:0098588	Bounding membrane of organelle	15	2107	0,39	0,0169	CD33,PKD1,GRIA4,LRRK2,SPHK1,SLC17A8,SYT9,ARC,SYT2,GOPC,RAB13,GAD2,GABRA2,SVOP,SYN2
GO:0016328	Lateral plasma membrane	3	61	4,4927	0,0172	CDH1,PKD1,RAB13
GO:1902711	GABA-A receptor complex	2	13	2,6299	0,0172	GABRA2,GABRG3
GO:0098797	Plasma membrane protein complex	7	547	0,64	0,0209	CDH1,CACNA1C,GLRA3,GRIA4,SHANK1,CTNNA1,GRIK1
GO:0012505	Endomembrane system	24	4542	0,26	0,0236	LRRC7,CDH1,CD33,PKD1,BIN2,TRIM9,LRRK2,CTNNA1,SPHK1,SLC17A8,SYT9,ARC,SYT2,GOPC,RAB13,OLFM1,NCS1,GAD2,NHS,COL8A2,NRXN1,GABRA2,SVOP,SYN2

GO:0044304	Main axon	3	70	4,2736	0,0236	LRRC7,DLG2,NRCAM
GO:0060077	Inhibitory synapse	2	16	2,3012	0,0236	NLGN2,GAD2
GO:0043194	Axon initial segment	2	18	2,1186	0,028	LRRC7,NRCAM
GO:0099060	Integral component of postsynaptic specialization membrane	3	75	4,1640	0,028	LRRC4C,NLGN2,NRCAM
GO:0005901	Caveola	3	78	4,4896	0,0305	CDH1,LRRK2,CTNNA1
GO:0005798	Golgi-associated vesicle	4	178	0,89	0,0338	PKD1,LRRK2,GOPC,RAB13
GO:0030426	Growth cone	4	186	0,87	0,0391	LRRK2,OLFM1,NRXN1,UNC5C
GO:0009986	Cell surface	8	824	0,52	0,0454	CD33,PKD1,NLGN2,PKHD1,NRCAM,IGSF5,NRXN1,UNC5C
GO:0015629	Actin cytoskeleton	6	477	0,64	0,0455	CDH1,BIN2,TJP1,CTNNA1,ARC,CTNNA2

Table 9.17 Significant gene expression changes of SARS-CoV-2 related genes comparing IFN-α-stimulated ALIs vs unstimulated ALIs

ProbeName	GeneSymbol	Description	*P*	FC	Regulation
A_24_P68783	IL36RN	Homo sapiens interleukin 36 receptor antagonist (IL36RN), transcript variant 1, mRNA [NM_012275]	0,011015176	2,1976457	up
A_23_P18751	TMPRSS11E	Homo sapiens transmembrane serine protease 11E (TMPRSS11E), mRNA [NM_-014058]	0,004442317	2,1520252	up
A_24_P303091	CXCL10	Homo sapiens C-X-C motif chemokine ligand 10 (CXCL10), mRNA [NM_001565]	1,51E-07	121,668526	up
A_33_P3389230	CXCR3	Homo sapiens C-X-C motif chemokine receptor 3 (CXCR3), transcript variant 1, mRNA [NM_001504]	5,57E-04	5,6277604	up
A_23_P114299	CXCR3	Homo sapiens C-X-C motif chemokine receptor 3 (CXCR3), transcript variant 1, mRNA [NM_001504]	0,010674125	2,4339871	up
A_23_P252981	ACE2	Homo sapiens angiotensin I converting enzyme 2 (ACE2), mRNA [NM_021804]	7,30E-07	8,282798	up
A_23_P348028	IL36A	interleukin 36 alpha [Source:HGNC Symbol	0,0212123	2,7260356	up
A_23_P350396	CDSN	Homo sapiens corneodesmosin (CDSN), mRNA [NM_001264]	0,042261582	2,1174784	up
A_33_P3361348	ALOX15	Homo sapiens arachidonate 15-lipoxygenase (ALOX15), mRNA [NM_001140]	0,04676787	-1,9357504	down
A_22_P00021230	IL36RN	interleukin 36 receptor antagonist [Source:HGNC Symbol	2,53E-05	7,387322	up
A_33_P3343175	CXCL10	Homo sapiens C-X-C motif chemokine ligand 10 (CXCL10), mRNA [NM_001565]	9,31E-10	121,54955	up

Table 9.18 Significant gene expression changes of SARS-CoV-2 related genes comparing IFN-β-stimulated ALIs vs unstimulated ALIs

ProbeName	GeneSymbol	Description	*P*	FC	Regulation
A_24_P68783	IL36RN	Homo sapiens interleukin 36 receptor antagonist (IL36RN), transcript variant 1, mRNA [NM_012275]	0,015862998	2,8498673	up
A_33_P3343175	CXCL10	Homo sapiens C-X-C motif chemokine ligand 10 (CXCL10), mRNA [NM_001565]	0,021988204	3,3313289	up

Table 9.19 Significant gene expression changes of SARS-CoV-2 related genes comparing IFN-γ-stimulated ALIs vs unstimulated ALIs

ProbeName	GeneSymbol	Description	*P*	FC	Regulation
A_24_P68783	IL36RN	Homo sapiens interleukin 36 receptor antagonist (IL36RN), transcript variant 1, mRNA [NM_012275]	0,007538324	2,5263507	up
A_23_P502957	CDH26	Homo sapiens cadherin 26 (CDH26), transcript variant b, mRNA [NM_021810]	0,014039554	1,5707216	up
A_23_P18751	TMPRSS11E	Homo sapiens transmembrane serine protease 11E (TMPRSS11E), mRNA [NM_-014058]	0,049934905	2,029161	up
A_24_P303091	CXCL10	Homo sapiens C-X-C motif chemokine ligand 10 (CXCL10), mRNA [NM_001565]	1,48E-08	1231,2006	up
A_33_P3389230	CXCR3	Homo sapiens C-X-C motif chemokine receptor 3 (CXCR3), transcript variant 1, mRNA [NM_001504]	0,003813015	2,4857717	up
A_23_P252981	ACE2	Homo sapiens angiotensin I converting enzyme 2 (ACE2), mRNA [NM_021804]	2,66E-04	4,227801	up
A_22_P00021230	IL36RN	interleukin 36 receptor antagonist [Source:HGNC Symbol	0,031609494	2,4939656	up
A_33_P3343175	CXCL10	Homo sapiens C-X-C motif chemokine ligand 10 (CXCL10), mRNA [NM_001565]	5,97E-10	880,2944	up

Table 9.20 Significant gene expression changes of SARS-CoV-2 related genes comparing IFN-λ1-stimulated ALIs vs unstimulated ALIs

ProbeName	GeneSymbol	Description	*P*	FC	Regulation
A_24_P68783	IL36RN	Homo sapiens interleukin 36 receptor antagonist (IL36RN)	0,001049758	3,5916095	up
A_24_P303091	CXCL10	Homo sapiens C-X-C motif chemokine ligand 10 (CXCL10)	3,42E-05	38,32672	up
A_33_P3389230	CXCR3	Homo sapiens C-X-C motif chemokine receptor 3 (CXCR3)	5,74E-04	3,3240435	up
A_23_P252981	ACE2	Homo sapiens angiotensin I converting enzyme 2 (ACE2)	0,004214379	2,7695415	up
A_22_P00021230	IL36RN	interleukin 36 receptor antagonist [Source:HGNC Symbol	0,013293338	2,708049	up
A_33_P3343175	CXCL10	Homo sapiens C-X-C motif chemokine ligand 10 (CXCL10)	4,46E-07	35,365387	up

Table 9.21 Significant gene expression changes of SARS-CoV-2 related genes comparing IFN-λ3-stimulated ALIs vs unstimulated ALIs

ProbeName	GeneSymbol	Description	*P*	FC	Regulation
A_24_P68783	IL36RN	Homo sapiens interleukin 36 receptor antagonist (IL36RN), transcript variant 1, mRNA [NM_012275]	0,014129732	3,055497	up
A_24_P303091	CXCL10	Homo sapiens C-X-C motif chemokine ligand 10 (CXCL10), mRNA [NM_001565]	1,59E-05	93,695274	up
A_33_P3389230	CXCR3	Homo sapiens C-X-C motif chemokine receptor 3 (CXCR3), transcript variant 1, mRNA [NM_001504]	0,011970643	2,3805401	up
A_23_P252981	ACE2	Homo sapiens angiotensin I converting enzyme 2 (ACE2), mRNA [NM_021804]	0,002735071	3,2055185	up
A_33_P3343175	CXCL10	Homo sapiens C-X-C motif chemokine ligand 10 (CXCL10), mRNA [NM_001565]	4,20E-07	72,21422	up

Table 9.22 Significant gene expression changes of IFN, SARS-CoV-2 related genes, KKS genes, acute phase genes, ISGs comparing asthma vs healthy control

ProbeName	GeneSymbol	Description	*P*	FC	Regulation
A_23_P376488	TNF	Homo sapiens tumor necrosis factor (TNF), mRNA [NM_000594]	0,003060047	-1,7183799	down
A_32_P356316	HLA-DOA	Homo sapiens major histocompatibility complex, class II, DO alpha (HLA-DOA), mRNA [NM_002119]	0,003942905	-1,5512874	down
A_23_P7313	SPP1	Homo sapiens secreted phosphoprotein 1 (SPP1), transcript variant 1, mRNA [NM_-001040058]	0,04192459	1,5696558	up
A_24_P68783	IL36RN	Homo sapiens interleukin 36 receptor antagonist (IL36RN), transcript variant 1, mRNA [NM_012275]	0,001118351	-2,155962	down
A_23_P55373	ALOX15	Homo sapiens arachidonate 15-lipoxygenase (ALOX15), mRNA [NM_001140]	0,001451798	1,5743501	up
A_23_P502957	CDH26	Homo sapiens cadherin 26 (CDH26), transcript variant b, mRNA [NM_021810]	0,002395866	1,574427	up
A_23_P152838	CCL5	Homo sapiens C-C motif chemokine ligand 5 (CCL5), transcript variant 1, mRNA [NM_002985]	0,002862293	-1,8725991	down
A_23_P109913	CXCR6	Homo sapiens C-X-C motif chemokine receptor 6 (CXCR6), mRNA [NM_006564]	0,004547741	-1,7970569	down
A_23_P74001	S100A12	Homo sapiens S100 calcium binding protein A12 (S100A12), mRNA [NM_005621]	0,001463726	-2,135935	down
A_24_P236935	KLK6	Homo sapiens kallikrein related peptidase 6 (KLK6), transcript variant B, mRNA [NM_001012964]	0,007871961	-1,9277092	down

A_23_P18751	TMPRSS11E	Homo sapiens transmembrane serine protease 11E (TMPRSS11E), mRNA [NM_-014058]	0,029099412	-1,7427381	down
A_24_P303091	CXCL10	Homo sapiens C-X-C motif chemokine ligand 10 (CXCL10), mRNA [NM_001565]	0,04373732	-1,7980772	down
A_23_P167168	JCHAIN	Homo sapiens joining chain of multimeric IgA and IgM (JCHAIN), mRNA [NM_144646]	0,002812375	-1,8371279	down
A_23_P55270	CCL18	C-C motif chemokine ligand 18 [Source:HGNC Symbol	0,030246304	1,7227612	up
A_23_P207564	CCL4	Homo sapiens C-C motif chemokine ligand 4 (CCL4), mRNA [NM_002984]	0,030234113	-1,5429916	down
A_33_P3318097	TMPRSS11B	Homo sapiens transmembrane serine protease 11B (TMPRSS11B), mRNA [NM_-182502]	0,01373251	-2,0981476	down
A_33_P3417640	KLK14	Homo sapiens kallikrein related peptidase 14 (KLK14), transcript variant 2, mRNA [NM_022046]	0,008145667	-1,769963	down
A_33_P3241756	IKBKB	inhibitor of nuclear factor kappa B kinase subunit beta [Source:HGNC Symbol	0,00354689	1,5193979	up
A_33_P3385785	S100A12	Homo sapiens S100 calcium binding protein A12 (S100A12), mRNA [NM_005621]	0,002317195	-2,1086442	down
A_23_P114299	CXCR3	Homo sapiens C-X-C motif chemokine receptor 3 (CXCR3), transcript variant 1, mRNA [NM_001504]	0,001487521	-1,8035514	down
A_23_P252981	ACE2	Homo sapiens angiotensin I converting enzyme 2 (ACE2), mRNA [NM_021804]	0,003221278	-1,6317257	down
A_23_P348028	IL36A	interleukin 36 alpha [Source:HGNC Symbol	2,36E-04	-1,9185486	down
A_23_P350396	CDSN	Homo sapiens corneodesmosin (CDSN), mRNA [NM_001264]	0,015223812	-1,9827658	down

A_33_P3235940	KLK6	Homo sapiens kallikrein related peptidase 6 (KLK6), transcript variant A, mRNA [NM_002774]	0,003352706	-2,5219223	down
A_24_P416645	KLK13	Homo sapiens kallikrein related peptidase 13 (KLK13), transcript variant 1, mRNA [NM_015596]	0,005287604	-2,2540295	down
A_24_P237036	TNFSF14	Homo sapiens TNF superfamily member 14 (TNFSF14), transcript variant 1, mRNA [NM_003807]	0,042878028	-1,5384884	down
A_33_P3354607	CCL4	Homo sapiens C-C motif chemokine ligand 4 (CCL4), mRNA [NM_002984]	0,045576118	-1,5440998	down
A_24_P333697	KLK13	Homo sapiens kallikrein related peptidase 13 (KLK13), transcript variant 1, mRNA [NM_015596]	0,005273193	-2,116673	down

Table 9.23 Significant gene expression changes of ISGs comparing *FOXO1* high vs *FOXO1* low

ProbeName	GeneSymbol	Description	*P*	FC	Regulation
A_23_P64828	OAS1	Homo sapiens 2'-5'-oligoadenylate synthetase 1 (OAS1), transcript variant 2, mRNA [NM_002534]	3,78E-15	3,0175862	up
A_24_P287043	IFITM2	Homo sapiens interferon induced transmembrane protein 2 (IFITM2), mRNA [NM_-006435]	2,25E-09	2,2561748	up
A_33_P3278968	HLA-DOA	Homo sapiens major histocompatibility complex, class II, DO alpha (HLA-DOA), mRNA [NM_002119]	2,02E-06	-1,832675	down
A_23_P72737	IFITM1	Homo sapiens interferon induced transmembrane protein 1 (IFITM1), mRNA [NM_-003641]	7,89E-09	2,1295063	up
A_23_P207564	CCL4	Homo sapiens C-C motif chemokine ligand 4 (CCL4), mRNA [NM_002984]	0,015580562	1,5762917	up
A_33_P3423941	IFITM1	Homo sapiens interferon induced transmembrane protein 1 (IFITM1), mRNA [NM_-003641]	1,56E-08	2,3593638	up
A_23_P139786	OASL	Homo sapiens 2'-5'-oligoadenylate synthetase like (OASL), transcript variant 1, mRNA [NM_003733]	8,34E-05	1,9965464	up
A_23_P204087	OAS2	Homo sapiens 2'-5'-oligoadenylate synthetase 2 (OAS2), transcript variant 1, mRNA [NM_016817]	1,05E-04	1,5931537	up

Table 9.24 Significant gene expression changes of IFN, SARS-CoV-2 related genes, KKS genes, acute phase genes, ISGs comparing *IFNA2* high vs *IFNA2* low of healthy individuals

ProbeName	GeneSymbol	Description	*P*	FC	Regulation
A_23_P212258	KNG1	Homo sapiens kininogen 1 (KNG1), transcript variant 2, mRNA [NM_000893]	0,004048697	4,661916	up
A_33_P3251065	KLK13	Homo sapiens kallikrein related peptidase 13 (KLK13), transcript variant 6, non-coding RNA [NR_145465]	1,29E-04	7,694752	up
A_33_P3407013	IL6	interleukin 6 [Source:HGNC Symbol	1,35E-04	7,549494	up
A_23_P250251	IFNA2	interferon alpha 2 [Source:HGNC Symbol	2,22E-04	7,928046	up
A_23_P133408	CSF2	Homo sapiens colony stimulating factor 2 (CSF2), mRNA [NM_000758]	7,12E-04	5,9697237	up
A_24_P68783	IL36RN	Homo sapiens interleukin 36 receptor antagonist (IL36RN), transcript variant 1, mRNA [NM_012275]	0,003365281	7,82228	up
A_33_P3324934	CDH26	cadherin 26 [Source:HGNC Symbol	0,005733618	5,1055126	up
A_23_P151294	IFNG	Homo sapiens interferon gamma (IFNG), mRNA [NM_000619]	9,72E-04	6,572457	up
A_23_P72737	IFITM1	Homo sapiens interferon induced transmembrane protein 1 (IFITM1), mRNA [NM_-003641]	0,022176761	-2,8740044	down
A_21_P0000025	NOS3	Homo sapiens nitric oxide synthase 3 (NOS3), transcript variant 2, mRNA [NM_-001160109]	0,008953536	4,466211	up
A_23_P71774	IFNB1	Homo sapiens interferon beta 1 (IFNB1), mRNA [NM_002176]	0,002393098	7,2361546	up

A_23_P337800	IFNL1	Homo sapiens interferon lambda 1 (IFNL1), mRNA [NM_172140]	0,001578472	5,408435	up
A_22_P00021230	IL36RN	interleukin 36 receptor antagonist [Source:HGNC Symbol	4,56E-04	6,1965437	up
A_23_P16252	KLK1	Homo sapiens kallikrein 1 (KLK1), mRNA [NM_002257]	0,005612745	5,648275	up
A_33_P3423941	IFITM1	Homo sapiens interferon induced transmembrane protein 1 (IFITM1), mRNA [NM_-003641]	0,016411236	-4,8621616	down
A_33_P3283611	IFIT3	Homo sapiens interferon induced protein with tetratricopeptide repeats 3 (IFIT3), transcript variant 1, mRNA [NM_001549]	0,01836445	-2,8624449	down

Table 9.25 Significant gene expression changes of IFN, SARS-CoV-2 related genes, KKS genes, acute phase genes, ISGs comparing *IFNA2* high vs *IFNA2* low of asthmatic patients

ProbeName	GeneSymbol	Description	*P*	FC	Regulation
A_23_P212258	KNG1	Homo sapiens kininogen 1 (KNG1), transcript variant 2, mRNA [NM_000893]	2,94E-12	3,0886018	up
A_33_P3251065	KLK13	Homo sapiens kallikrein related peptidase 13 (KLK13), transcript variant 6, non-coding RNA [NR_145465]	1,73E-18	4,888759	up
A_33_P3407013	IL6	interleukin 6 [Source:HGNC Symbol	6,02E-23	6,3118167	up
A_24_P132518	IKBKB	Homo sapiens inhibitor of nuclear factor kappa B kinase subunit beta (IKBKB), transcript variant 1, mRNA [NM_001556]	2,54E-07	-1,5257671	down
A_23_P250251	IFNA2	interferon alpha 2 [Source:HGNC Symbol	2,32E-36	6,9746413	up
A_32_P356316	HLA-DOA	Homo sapiens major histocompatibility complex, class II, DO alpha (HLA-DOA), mRNA [NM_002119]	2,40E-04	-1,7788204	down
A_33_P3225522	OAS2	Homo sapiens 2'-5'-oligoadenylate synthetase 2 (OAS2), transcript variant 3, mRNA [NM_001032731]	4,00E-08	-1,7551374	down
A_23_P24004	IFIT2	Homo sapiens interferon induced protein with tetratricopeptide repeats 2 (IFIT2), mRNA [NM_001547]	4,31E-04	-1,6626337	down
A_33_P3316273	CCL3	Homo sapiens C-C motif chemokine ligand 3 (CCL3), mRNA [NM_002983]	0,015229512	-1,5819223	down
A_24_P68783	IL36RN	Homo sapiens interleukin 36 receptor antagonist (IL36RN), transcript variant 1, mRNA [NM_012275]	2,37E-07	3,6961122	up

A_33_P3324934	CDH26	cadherin 26 [Source:HGNC Symbol	9,36E-08	2,2242854	up
A_23_P126735	IL10	Homo sapiens interleukin 10 (IL10), mRNA [NM_000572]	0,00218331	1,5101075	up
A_23_P502957	CDH26	Homo sapiens cadherin 26 (CDH26), transcript variant b, mRNA [NM_021810]	1,60E-05	1,9654156	up
A_33_P3278968	HLA-DOA	Homo sapiens major histocompatibility complex, class II, DO alpha (HLA-DOA), mRNA [NM_002119]	9,67E-06	1,7820024	up
A_23_P151294	IFNG	Homo sapiens interferon gamma (IFNG), mRNA [NM_000619]	1,80E-13	4,021559	up
A_23_P128744	BDKRB1	Homo sapiens bradykinin receptor B1 (BDKRB1), mRNA [NM_000710]	2,17E-05	-1,5841768	down
A_23_P72096	IL1A	Homo sapiens interleukin 1 alpha (IL1A), mRNA [NM_000575]	8,03E-08	2,6463938	up
A_23_P167168	JCHAIN	Homo sapiens joining chain of multimeric IgA and IgM (JCHAIN), mRNA [NM_144646]	3,02E-05	2,2052329	up
A_23_P52266	IFIT1	Homo sapiens interferon induced protein with tetratricopeptide repeats 1 (IFIT1), transcript variant 1, mRNA [NM_001548]	2,06E-04	-1,9808176	down
A_21_P0000025	NOS3	Homo sapiens nitric oxide synthase 3 (NOS3), transcript variant 2, mRNA [NM_-001160109]	4,65E-12	3,1321626	up
A_23_P71774	IFNB1	Homo sapiens interferon beta 1 (IFNB1), mRNA [NM_002176]	5,06E-24	5,5127935	up
A_23_P337800	IFNL1	Homo sapiens interferon lambda 1 (IFNL1), mRNA [NM_172140]	2,97E-09	2,9391947	up
A_23_P348028	IL36A	interleukin 36 alpha [Source:HGNC Symbol	5,40E-05	2,15116	up
A_33_P3361348	ALOX15	Homo sapiens arachidonate 15-lipoxygenase (ALOX15), mRNA [NM_001140]	0,00199635	1,6330308	up

A_23_P98147	CPN1	carboxypeptidase N subunit 1 [Source:HGNC Symbol	1,42E-05	1,9906176	up
A_22_P00021230	IL36RN	interleukin 36 receptor antagonist [Source:HGNC Symbol	1,01E-19	4,1062765	up
A_23_P16252	KLK1	Homo sapiens kallikrein 1 (KLK1), mRNA [NM_002257]	4,66E-15	4,493133	up
A_33_P3423941	IFITM1	Homo sapiens interferon induced transmembrane protein 1 (IFITM1), mRNA [NM_-003641]	1,35E-04	-1,700065	down
A_23_P252236	KLKB1	Homo sapiens kallikrein B1 (KLKB1), transcript variant 1, mRNA [NM_000892]	1,52E-09	2,4760175	up
A_33_P3370094	MME	Homo sapiens membrane metalloendopeptidase (MME), transcript variant 2b, mRNA [NM_007289]	0,007420292	1,8695168	up
A_33_P3283611	IFIT3	Homo sapiens interferon induced protein with tetratricopeptide repeats 3 (IFIT3), transcript variant 1, mRNA [NM_001549]	4,51E-05	-1,848435	down
A_23_P71037	IL6	Homo sapiens interleukin 6 (IL6), transcript variant 1, mRNA [NM_000600]	0,03308162	1,5145354	up
A_33_P3354607	CCL4	Homo sapiens C-C motif chemokine ligand 4 (CCL4), mRNA [NM_002984]	0,014918437	-1,5437895	down
A_24_P260101	MME	Homo sapiens membrane metalloendopeptidase (MME), transcript variant 2b, mRNA [NM_007289]	4,88E-05	2,4965382	up
A_33_P3290707	MME	Homo sapiens membrane metalloendopeptidase (MME), transcript variant 5, mRNA [NM_001354644]	0,00710586	1,5148816	up
A_24_P333697	KLK13	Homo sapiens kallikrein related peptidase 13 (KLK13), transcript variant 1, mRNA [NM_015596]	0,002079181	2,3567271	up

A_33_P3296479	APP	Homo sapiens amyloid beta precursor protein (APP), transcript variant 10, mRNA [NM_001204303]	1,66E-12	1,83836	up
A_23_P373619	IFNL3	Homo sapiens interferon lambda 3 (IFNL3), transcript variant 1, mRNA [NM_-001346937]	1,20E-12	7,114084	up

Table 9.26 Significant gene expression changes of IFN, SARS-CoV-2 related genes, KKS genes, acute phase genes, ISGs comparing *IFNB1* high vs *IFNB1* low of healthy individuals

ProbeName	GeneSymbol	Description	*P*	FC	Regulation
A_23_P212258	KNG1	Homo sapiens kininogen 1 (KNG1), transcript variant 2, mRNA [NM_000893]	0,013263774	3,3231697	up
A_33_P3251065	KLK13	Homo sapiens kallikrein related peptidase 13 (KLK13), transcript variant 6, non-coding RNA [NR_145465]	0,012497301	3,706571	up
A_33_P3407013	IL6	interleukin 6 [Source:HGNC Symbol	0,002784525	4,4849563	up
A_23_P250251	IFNA2	interferon alpha 2 [Source:HGNC Symbol	0,003938121	4,5900145	up
A_23_P133408	CSF2	Homo sapiens colony stimulating factor 2 (CSF2), mRNA [NM_000758]	0,015573658	3,3133073	up
A_23_P151294	IFNG	Homo sapiens interferon gamma (IFNG), mRNA [NM_000619]	1,11E-04	6,383654	up
A_23_P71774	IFNB1	Homo sapiens interferon beta 1 (IFNB1), mRNA [NM_002176]	2,07E-04	7,7352657	up
A_23_P337800	IFNL1	Homo sapiens interferon lambda 1 (IFNL1), mRNA [NM_172140]	0,005737626	3,768772	up
A_22_P00021230	IL36RN	interleukin 36 receptor antagonist [Source:HGNC Symbol	0,003989669	3,946389	up

Table 9.27 Significant gene expression changes of IFN, SARS-CoV-2 related genes, KKS genes, acute phase genes, ISGs comparing *IFNB1* high vs *IFNB1* low of asthmatic patients

ProbeName	GeneSymbol	Description	*P*	FC	Regulation
A_23_P212258	KNG1	Homo sapiens kininogen 1 (KNG1), transcript variant 2, mRNA [NM_000893]	4,08E-13	3,3691626	up
A_33_P3251065	KLK13	Homo sapiens kallikrein related peptidase 13 (KLK13), transcript variant 6, non-coding RNA [NR_145465]	2,81E-18	4,877687	up
A_33_P3407013	IL6	interleukin 6 [Source:HGNC Symbol	8,98E-23	5,968152	up
A_23_P250251	IFNA2	interferon alpha 2 [Source:HGNC Symbol	3,52E-29	5,9019837	up
A_23_P64828	OAS1	Homo sapiens 2'-5'-oligoadenylate synthetase 1 (OAS1), transcript variant 2, mRNA [NM_002534]	0,001915471	-1,6529486	down
A_32_P356316	HLA-DOA	Homo sapiens major histocompatibility complex, class II, DO alpha (HLA-DOA), mRNA [NM_002119]	0,002423115	-1,5517656	down
A_33_P3225522	OAS2	Homo sapiens 2'-5'-oligoadenylate synthetase 2 (OAS2), transcript variant 3, mRNA [NM_001032731]	4,60E-05	-1,553267	down
A_24_P68783	IL36RN	Homo sapiens interleukin 36 receptor antagonist (IL36RN), transcript variant 1, mRNA [NM_012275]	1,09E-06	3,3312747	up
A_33_P3324934	CDH26	cadherin 26 [Source:HGNC Symbol	2,33E-06	2,1383827	up
A_23_P126735	IL10	Homo sapiens interleukin 10 (IL10), mRNA [NM_000572]	1,43E-06	2,0267882	up
A_23_P502957	CDH26	Homo sapiens cadherin 26 (CDH26), transcript variant b, mRNA [NM_021810]	5,54E-05	1,971116	up

A_33_P3278968	HLA-DOA	Homo sapiens major histocompatibility complex, class II, DO alpha (HLA-DOA), mRNA [NM_002119]	2,06E-08	2,1221132	up
A_23_P151294	IFNG	Homo sapiens interferon gamma (IFNG), mRNA [NM_000619]	3,05E-19	4,8029532	up
A_23_P128744	BDKRB1	Homo sapiens bradykinin receptor B1 (BDKRB1), mRNA [NM_000710]	3,01E-07	-1,7716215	down
A_23_P72096	IL1A	Homo sapiens interleukin 1 alpha (IL1A), mRNA [NM_000575]	6,55E-08	2,7242715	up
A_23_P167168	JCHAIN	Homo sapiens joining chain of multimeric IgA and IgM (JCHAIN), mRNA [NM_144646]	1,53E-06	2,3155715	up
A_23_P52266	IFIT1	Homo sapiens interferon induced protein with tetratricopeptide repeats 1 (IFIT1), transcript variant 1, mRNA [NM_001548]	0,03853991	-1,5223696	down
A_21_P0000025	NOS3	Homo sapiens nitric oxide synthase 3 (NOS3), transcript variant 2, mRNA [NM_-001160109]	3,91E-15	3,6399238	up
A_33_P3243230	CXCL8	C-X-C motif chemokine ligand 8 [Source:HGNC Symbol	0,006061163	2,2361593	up
A_23_P71774	IFNB1	Homo sapiens interferon beta 1 (IFNB1), mRNA [NM_002176]	3,50E-35	7,2700653	up
A_23_P337800	IFNL1	Homo sapiens interferon lambda 1 (IFNL1), mRNA [NM_172140]	3,90E-13	3,4714065	up
A_23_P348028	IL36A	interleukin 36 alpha [Source:HGNC Symbol	5,42E-05	2,2254903	up
A_33_P3361348	ALOX15	Homo sapiens arachidonate 15-lipoxygenase (ALOX15), mRNA [NM_001140]	0,002625476	1,6615373	up
A_24_P416645	KLK13	Homo sapiens kallikrein related peptidase 13 (KLK13), transcript variant 1, mRNA [NM_015596]	0,02945292	1,9235077	up

A_23_P98147	CPN1	carboxypeptidase N subunit 1 [Source:HGNC Symbol	1,03E-06	2,2628334	up
A_22_P00021230	IL36RN	interleukin 36 receptor antagonist [Source:HGNC Symbol	8,89E-23	4,6801147	up
A_23_P16252	KLK1	Homo sapiens kallikrein 1 (KLK1), mRNA [NM_002257]	2,45E-09	3,4925425	up
A_23_P252236	KLKB1	Homo sapiens kallikrein B1 (KLKB1), transcript variant 1, mRNA [NM_000892]	4,95E-12	2,8387582	up
A_33_P3370094	MME	Homo sapiens membrane metalloendopeptidase (MME), transcript variant 2b, mRNA [NM_007289]	0,005074392	1,9495479	up
A_23_P71037	IL6	Homo sapiens interleukin 6 (IL6), transcript variant 1, mRNA [NM_000600]	4,36E-04	1,9704845	up
A_24_P260101	MME	Homo sapiens membrane metalloendopeptidase (MME), transcript variant 2b, mRNA [NM_007289]	1,88E-05	2,7077162	up
A_33_P3290707	MME	Homo sapiens membrane metalloendopeptidase (MME), transcript variant 5, mRNA [NM_001354644]	0,006084633	1,555618	up
A_24_P333697	KLK13	Homo sapiens kallikrein related peptidase 13 (KLK13), transcript variant 1, mRNA [NM_015596]	0,001335491	2,4205382	up
A_33_P3296479	APP	Homo sapiens amyloid beta precursor protein (APP), transcript variant 10, mRNA [NM_001204303]	6,04E-12	1,8069515	up
A_23_P373619	IFNL3	Homo sapiens interferon lambda 3 (IFNL3), transcript variant 1, mRNA [NM_-001346937]	6,99E-20	6,146903	up

Table 9.28 Significant gene expression changes of IFN, SARS-CoV-2 related genes, KKS genes, acute phase genes, ISGs comparing *IFNG* high vs *IFNG* low of healthy individuals

ProbeName	GeneSymbol	Description	*P*	FC	Regulation
A_33_P3251065	KLK13	Homo sapiens kallikrein related peptidase 13 (KLK13), transcript variant 6, non-coding RNA [NR_145465]	0,002649058	4,5497484	up
A_33_P3407013	IL6	interleukin 6 [Source:HGNC Symbol	0,002398077	4,7854056	up
A_23_P250251	IFNA2	interferon alpha 2 [Source:HGNC Symbol	0,00165839	5,314314	up
A_23_P133408	CSF2	Homo sapiens colony stimulating factor 2 (CSF2), mRNA [NM_000758]	0,004297904	4,1159105	up
A_23_P151294	IFNG	Homo sapiens interferon gamma (IFNG), mRNA [NM_000619]	1,00E-06	14,467541	up
A_24_P303091	CXCL10	Homo sapiens C-X-C motif chemokine ligand 10 (CXCL10), mRNA [NM_001565]	6,11E-04	7,3392143	up
A_23_P71774	IFNB1	Homo sapiens interferon beta 1 (IFNB1), mRNA [NM_002176]	0,001266331	7,0107665	up
A_22_P00021230	IL36RN	interleukin 36 receptor antagonist [Source:HGNC Symbol	0,005070508	4,028738	up
A_33_P3343175	CXCL10	Homo sapiens C-X-C motif chemokine ligand 10 (CXCL10), mRNA [NM_001565]	0,001843891	4,9518676	up

Table 9.29 Significant gene expression changes of IFN, SARS-CoV-2 related genes, KKS genes, acute phase genes, ISGs comparing *IFNG* high vs *IFNG* low of asthmatic patients

ProbeName	GeneSymbol	Description	*P*	FC	Regulation
A_23_P212258	KNG1	Homo sapiens kininogen 1 (KNG1), transcript variant 2, mRNA [NM_000893]	1,19E-05	2,2586603	up
A_33_P3251065	KLK13	Homo sapiens kallikrein related peptidase 13 (KLK13), transcript variant 6, non-coding RNA [NR_145465]	7,02E-07	2,6947603	up
A_33_P3407013	IL6	interleukin 6 [Source:HGNC Symbol	1,41E-11	3,9422626	up
A_23_P250251	IFNA2	interferon alpha 2 [Source:HGNC Symbol	3,03E-13	3,671706	up
A_23_P376488	TNF	Homo sapiens tumor necrosis factor (TNF), mRNA [NM_000594]	3,85E-04	2,1094987	up
A_24_P68783	IL36RN	Homo sapiens interleukin 36 receptor antagonist (IL36RN), transcript variant 1, mRNA [NM_012275]	0,001853315	2,2620046	up
A_33_P3324934	CDH26	cadherin 26 [Source:HGNC Symbol	7,40E-04	1,7658217	up
A_23_P126735	IL10	Homo sapiens interleukin 10 (IL10), mRNA [NM_000572]	1,58E-06	2,250299	up
A_23_P151294	IFNG	Homo sapiens interferon gamma (IFNG), mRNA [NM_000619]	1,09E-33	10,021911	up
A_23_P152838	CCL5	Homo sapiens C-C motif chemokine ligand 5 (CCL5), transcript variant 1, mRNA [NM_002985]	1,31E-04	2,7025442	up
A_23_P109913	CXCR6	Homo sapiens C-X-C motif chemokine receptor 6 (CXCR6), mRNA [NM_006564]	8,09E-07	3,1428957	up
A_23_P128744	BDKRB1	Homo sapiens bradykinin receptor B1 (BDKRB1), mRNA [NM_000710]	2,75E-05	-1,6188495	down

A_23_P72096	IL1A	Homo sapiens interleukin 1 alpha (IL1A), mRNA [NM_000575]	2,50E-04	2,0102258	up
A_24_P303091	CXCL10	Homo sapiens C-X-C motif chemokine ligand 10 (CXCL10), mRNA [NM_001565]	4,56E-06	5,335049	up
A_23_P167168	JCHAIN	Homo sapiens joining chain of multimeric IgA and IgM (JCHAIN), mRNA [NM_144646]	2,87E-04	1,8917804	up
A_21_P0000025	NOS3	Homo sapiens nitric oxide synthase 3 (NOS3), transcript variant 2, mRNA [NM_-001160109]	8,76E-06	2,2117722	up
A_24_P304071	IFIT2	Homo sapiens interferon induced protein with tetratricopeptide repeats 2 (IFIT2), mRNA [NM_001547]	5,00E-04	2,1313105	up
A_33_P3243230	CXCL8	C-X-C motif chemokine ligand 8 [Source:HGNC Symbol	0,021215448	1,9324746	up
A_23_P71774	IFNB1	Homo sapiens interferon beta 1 (IFNB1), mRNA [NM_002176]	2,73E-13	3,8178675	up
A_23_P114299	CXCR3	Homo sapiens C-X-C motif chemokine receptor 3 (CXCR3), transcript variant 1, mRNA [NM_001504]	0,002108162	1,9585654	up
A_23_P98147	CPN1	carboxypeptidase N subunit 1 [Source:HGNC Symbol	0,002730148	1,7186602	up
A_22_P00021230	IL36RN	interleukin 36 receptor antagonist [Source:HGNC Symbol	1,12E-08	2,7096856	up
A_23_P16252	KLK1	Homo sapiens kallikrein 1 (KLK1), mRNA [NM_002257]	0,002208981	2,0210931	up
A_23_P252236	KLKB1	Homo sapiens kallikrein B1 (KLKB1), transcript variant 1, mRNA [NM_000892]	4,46E-06	2,0914855	up
A_33_P3370094	MME	Homo sapiens membrane metalloendopeptidase (MME), transcript variant 2b, mRNA [NM_007289]	0,012497134	1,7423285	up

A_23_P71037	IL6	Homo sapiens interleukin 6 (IL6), transcript variant 1, mRNA [NM_000600]	3,83E-04	2,3296661	up
A_24_P274270	STAT1	Homo sapiens signal transducer and activator of transcription 1 (STAT1), transcript variant beta, mRNA [NM_139266]	6,15E-04	1,5946366	up
A_24_P260101	MME	Homo sapiens membrane metalloendopeptidase (MME), transcript variant 2b, mRNA [NM_007289]	0,001102381	2,079889	up
A_23_P373619	IFNL3	Homo sapiens interferon lambda 3 (IFNL3), transcript variant 1, mRNA [NM_-001346937]	2,59E-15	5,6045685	up

Table 9.30 Significant gene expression changes of IFN, SARS-CoV-2 related genes, KKS genes, acute phase genes, ISGs comparing *IFNL1* high vs *IFNL1* low of asthmatic patients

ProbeName	GeneSymbol	Description	*P*	FC	Regulation
A_23_P212258	KNG1	Homo sapiens kininogen 1 (KNG1), transcript variant 2, mRNA [NM_000893]	3,75E-08	2,5530183	up
A_33_P3251065	KLK13	Homo sapiens kallikrein related peptidase 13 (KLK13), transcript variant 6, non-coding RNA [NR_145465]	7,31E-08	2,990746	up
A_33_P3407013	IL6	interleukin 6 [Source:HGNC Symbol	4,54E-08	3,028745	up
A_23_P250251	IFNA2	interferon alpha 2 [Source:HGNC Symbol	5,56E-10	3,0675356	up
A_23_P376488	TNF	Homo sapiens tumor necrosis factor (TNF), mRNA [NM_000594]	0,011630992	1,7215147	up
A_24_P68783	IL36RN	Homo sapiens interleukin 36 receptor antagonist (IL36RN), transcript variant 1, mRNA [NM_012275]	5,46E-05	2,9483502	up
A_33_P3324934	CDH26	cadherin 26 [Source:HGNC Symbol	2,85E-04	1,8437923	up
A_23_P126735	IL10	Homo sapiens interleukin 10 (IL10), mRNA [NM_000572]	7,15E-07	2,2994125	up
A_33_P3278968	HLA-DOA	Homo sapiens major histocompatibility complex, class II, DO alpha (HLA-DOA), mRNA [NM_002119]	4,49E-06	1,8474454	up
A_23_P151294	IFNG	Homo sapiens interferon gamma (IFNG), mRNA [NM_000619]	2,79E-09	3,7656295	up
A_23_P128744	BDKRB1	Homo sapiens bradykinin receptor B1 (BDKRB1), mRNA [NM_000710]	1,27E-04	-1,5286465	down
A_23_P72096	IL1A	Homo sapiens interleukin 1 alpha (IL1A), mRNA [NM_000575]	4,92E-05	2,2892814	up

A_24_P303091	CXCL10	Homo sapiens C-X-C motif chemokine ligand 10 (CXCL10), mRNA [NM_001565]	0,026528051	2,3866463	up
A_23_P167168	JCHAIN	Homo sapiens joining chain of multimeric IgA and IgM (JCHAIN), mRNA [NM_144646]	4,88E-04	1,8201578	up
A_21_P0000025	NOS3	Homo sapiens nitric oxide synthase 3 (NOS3), transcript variant 2, mRNA [NM_-001160109]	6,15E-08	2,6440947	up
A_23_P71774	IFNB1	Homo sapiens interferon beta 1 (IFNB1), mRNA [NM_002176]	2,33E-12	3,6302695	up
A_23_P348028	IL36A	interleukin 36 alpha [Source:HGNC Symbol	4,81E-06	2,5256283	up
A_23_P98147	CPN1	carboxypeptidase N subunit 1 [Source:HGNC Symbol	1,96E-06	2,3821523	up
A_22_P00021230	IL36RN	interleukin 36 receptor antagonist [Source:HGNC Symbol	9,26E-13	3,4828446	up
A_23_P16252	KLK1	Homo sapiens kallikrein 1 (KLK1), mRNA [NM_002257]	3,84E-05	2,727557	up
A_23_P252236	KLKB1	Homo sapiens kallikrein B1 (KLKB1), transcript variant 1, mRNA [NM_000892]	2,30E-06	2,1893542	up
A_23_P71037	IL6	Homo sapiens interleukin 6 (IL6), transcript variant 1, mRNA [NM_000600]	2,82E-04	2,3317387	up
A_24_P333697	KLK13	Homo sapiens kallikrein related peptidase 13 (KLK13), transcript variant 1, mRNA [NM_015596]	0,020932605	1,9768615	up
A_23_P373619	IFNL3	Homo sapiens interferon lambda 3 (IFNL3), transcript variant 1, mRNA [NM_-001346937]	1,54E-11	4,485979	up

Table 9.31 Significant gene expression changes of IFN, SARS-CoV-2 related genes, KKS genes, acute phase genes, ISGs comparing *IFNL3* high vs *IFNL3* low of asthmatic patients

ProbeName	GeneSymbol	Description	*P*	FC	Regulation
A_23_P212258	KNG1	Homo sapiens kininogen 1 (KNG1), transcript variant 2, mRNA [NM_000893]	1,43E-07	2,600287	up
A_33_P3251065	KLK13	Homo sapiens kallikrein related peptidase 13 (KLK13), transcript variant 6, non-coding RNA [NR_145465]	2,74E-12	3,6757245	up
A_33_P3407013	IL6	interleukin 6 [Source:HGNC Symbol	1,05E-17	5,253737	up
A_23_P250251	IFNA2	interferon alpha 2 [Source:HGNC Symbol	1,99E-19	4,7998285	up
A_23_P376488	TNF	Homo sapiens tumor necrosis factor (TNF), mRNA [NM_000594]	0,003091444	1,693701	up
A_23_P7313	SPP1	Homo sapiens secreted phosphoprotein 1 (SPP1), transcript variant 1, mRNA [NM_-001040058]	0,01785524	1,8703346	up
A_24_P68783	IL36RN	Homo sapiens interleukin 36 receptor antagonist (IL36RN), transcript variant 1, mRNA [NM_012275]	4,74E-06	3,3125963	up
A_23_P126735	IL10	Homo sapiens interleukin 10 (IL10), mRNA [NM_000572]	4,74E-06	2,0621407	up
A_33_P3278968	HLA-DOA	Homo sapiens major histocompatibility complex, class II, DO alpha (HLA-DOA), mRNA [NM_002119]	8,93E-05	1,6839054	up
A_23_P151294	IFNG	Homo sapiens interferon gamma (IFNG), mRNA [NM_000619]	7,68E-15	5,2674274	up
A_23_P109913	CXCR6	Homo sapiens C-X-C motif chemokine receptor 6 (CXCR6), mRNA [NM_006564]	0,00689301	1,7725712	up

A_23_P128744	BDKRB1	Homo sapiens bradykinin receptor B1 (BDKRB1), mRNA [NM_000710]	6,76E-05	-1,5612062	down
A_24_P236935	KLK6	Homo sapiens kallikrein related peptidase 6 (KLK6), transcript variant B, mRNA [NM_001012964]	0,015427852	1,7863282	up
A_23_P18751	TMPRSS11E	Homo sapiens transmembrane serine protease 11E (TMPRSS11E), mRNA [NM_-014058]	0,032523423	1,682243	up
A_23_P72096	IL1A	Homo sapiens interleukin 1 alpha (IL1A), mRNA [NM_000575]	6,68E-08	2,8150434	up
A_24_P303091	CXCL10	Homo sapiens C-X-C motif chemokine ligand 10 (CXCL10), mRNA [NM_001565]	0,025495438	2,2890255	up
A_23_P167168	JCHAIN	Homo sapiens joining chain of multimeric IgA and IgM (JCHAIN), mRNA [NM_144646]	3,22E-04	1,873892	up
A_24_P304071	IFIT2	Homo sapiens interferon induced protein with tetratricopeptide repeats 2 (IFIT2), mRNA [NM_001547]	0,023830246	1,594	up
A_23_P71774	IFNB1	Homo sapiens interferon beta 1 (IFNB1), mRNA [NM_002176]	2,74E-19	4,768526	up
A_23_P348028	IL36A	interleukin 36 alpha [Source:HGNC Symbol	0,002644789	1,8107975	up
A_24_P416645	KLK13	Homo sapiens kallikrein related peptidase 13 (KLK13), transcript variant 1, mRNA [NM_015596]	0,005902396	2,1586287	up
A_23_P98147	CPN1	carboxypeptidase N subunit 1 [Source:HGNC Symbol	0,002414796	1,6576564	up
A_22_P00021230	IL36RN	interleukin 36 receptor antagonist [Source:HGNC Symbol	1,17E-12	3,336981	up
A_23_P16252	KLK1	Homo sapiens kallikrein 1 (KLK1), mRNA [NM_002257]	2,24E-11	3,6954892	up

A_23_P252236	KLKB1	Homo sapiens kallikrein B1 (KLKB1), transcript variant 1, mRNA [NM_000892]	6,26E-07	2,1726944	up
A_23_P71037	IL6	Homo sapiens interleukin 6 (IL6), transcript variant 1, mRNA [NM_000600]	4,22E-04	2,105571	up
A_24_P333697	KLK13	Homo sapiens kallikrein related peptidase 13 (KLK13), transcript variant 1, mRNA [NM_015596]	0,001125261	2,4261453	up
A_33_P3296479	APP	Homo sapiens amyloid beta precursor protein (APP), transcript variant 10, mRNA [NM_001204303]	9,40E-07	1,5335402	up
A_23_P373619	IFNL3	Homo sapiens interferon lambda 3 (IFNL3), transcript variant 1, mRNA [NM_-001346937]	1,91E-20	11,561718	up

Acknowledgments

Firstly, I would like to thank Prof Dr. Carsten Schmidt-Weber and Dr. Constanze Jakwerth for giving me the great opportunity to work for more than three years at the Center of Allergy and Environment. Thank you for the possibility and the support to deepen my knowledge in Immunbiology, writing papers and the huge amount of different techniques. I would also like to thank my AGL group with all the current and former members, especially Martine Mootz, Hannah Kitzberger, Dr. Soheila Asoudeh, Dimitri Pogorelov, Dr. Evamaria Stütz and Annika Müller with whom I shared support, tears, fun and a lot of lab-pipetting-sessions. I also want to thank my second supervisor Prof. Dr. Michael Pfaffl and my Mentor Dr. Simon Blank for supporting me during my PhD with their expertise.

My sincere thanks to the members of the ALLIANCE Study Group as part of the German Center for Lung Research (DZL). I am grateful to be part of the ERA Study.

Equally important is the support for the SARS-CoV-2 work from Prof. Dr. Ulrike Protzer and Prof. Dr. Andreas Pichlmair and their lab members Dr. Martin Feuerherd and Dr. Vincent Grass, who helped set up the experiments, conducted the S3 experiments and helped me with my data.

I want to thank Madlen Oelsner, Ferdinant Gürth, Jana Sänger, Myriam Krome-Gissibinger and Stefanie Glocker, who not only guided me with great support and patience through this project, but also embraced me and showed me how to be a better scientist each day.

Thank you to the whole ZAUM. You all welcomed me from day one and we survived some critical times during the COVID-19 pandemic. Thank you all for letting me organize several hiking days, Summer and Christmas Parties and joining those activities. I do not know what I have done without Dr. Sina Bohnacker, Franziska Hartung, Benedikt Spitzlberger, Dr. Manja Jargosch and Jessica Eigemann. Not only the lunch breaks would have been boring but also sharing good and bad moments helped me to continue this journey.

IN ADDITION I want to thank two of my former supervisors. First, Dr. Ariane Böhm my absolute PhD role model who helped me with my writing skills. Second, Dr. Suet-Feung Chin, who guides me with her helpful advises through my career.

I am so thankful for my parents, my grandparents and Max. Thank you for the support and that you always give me the faith in believing and having the strength to push myself into the unknown.

Last but not least, I want to thank my friends, Astrid, Tatjana, Patricia, Christin, Clarissa, Julia and Marie who were there for me throughout this journey and supported me when I felt particularly downbeat. Your support means a lot to me, I am grateful to have you as my friends.

Ì put my heart and my soul into my work, and have lost my mind in the Process.
- Vincent van Gogh.
Thank you to all the people who accompanied and supported me during this challenging, difficult, rewarding, crazy and fun times.